A Facsimile Report

DOE/ID--10183

DE88 015084

ANNUAL PROGRESS REPORT: FY-1987

SUBSURFACE INVESTIGATIONS PROGRAM AT THE RADIOACTIVE WASTE MANAGEMENT COMPLEX OF THE IDAHO NATIONAL ENGINEERING LABORATORY

P. T. Laney
S. C. Minkin

Environmental Monitoring
and Characterization Program

and

R. G. Baca
D. L. McElroy
J. M. Hubbell
L. C. Hull
B. F. Russell
G. J. Stormberg

Environmental and Earth
Sciences, Hydrology Unit

EG&G Idaho, Inc.

and

J. T. Pittman

U.S. Geological Survey
INEL Project Office

April 1988

Idaho National Engineering Laboratory
Idaho Falls, ID 83415

Prepared for the
U.S. Department of Energy
Idaho Operations Office
Under DOE Contract No. DE-AC07-76ID01570

ABSTRACT

The Subsurface Investigations Program made progress in FY-1987 toward obtaining its two program objectives: a field calibration of a model to predict long-term radionuclide migration and measurement of the actual migration to date.

Three deep boreholes were drilled at the Radioactive Waste Management Complex (RWMC) to collect sample material for evaluation of radionuclide content in the interbeds, to determine geologic and hydrologic characteristics of the sediments, and to provide monitoring sites for moisture movement in these sediments. Suction lysimeters and heat dissipation sensors were installed in two deep boreholes to collect moisture data.

Data from the moisture sensing instruments (tensiometers, psychrometers, gypsum blocks, heat dissipation sensors, and neutron logging) installed at the RWMC continued to be collected during FY-1987. Because of the large volume of collected data, the RWMC Data Management System was developed and implemented to facilitate the storage, retrieval, and manipulation of the database.

Analyses of data from the soil-moisture sensing instruments was initiated. Hydraulic gradients indicated downward flow during large portions of the year, in several areas of the RWMC. Matric potential measurements within the SDA suggested the wettest soil-moisture conditions were near drainage and flood control ditches and topographic depressions. A need for statistical analysis of measurement results was identified, due to the variability of data at depths instrumented in triplicate.

Work on the Computer Model Development task focused on three specific areas: (a) a detailed review of previous vadose zone modeling studies at INEL, (b) acquisition and installation of a suite of computer models for unsaturated flow and contaminant transport, and (c) preliminary

applications of computer models using site-specific data. At present, five major computer models have been installed on the INEL CRAY computer for modeling transport through the subsurface pathway. These models are: SEMTRA, FEMTRA, TRACR3D, MAGNUM, and CHAINT. In addition to the major computer models, eight other codes, referred to as support codes and models, have been acquired and implemented.

Sampling of ambient air, air in boreholes, and soil gases was conducted at the RWMC to determine the identity, location, and relative concentrations of selected chlorinated and aromatic volatile organic compounds (VOCs). These sampling efforts indicated that carbon tetrachloride, 1,1,1-trichloroethane, trichloroethylene, and tetrachloroethylene have migrated from a number of the disposal pits where VOCs may have been disposed of. The major sources of VOCs appear to be Pits 4, 5, 6, 9, and 10. Measurable concentrations of VOCs occur in soil gases at distances from 2000 to 3400 ft from the SDA boundary. Analyses of gases collected at various depths beneath the RWMC indicate maximum gas concentrations at around 100 ft below land surface, and measurable concentrations to 576 ft.

Shallow auger hole samples from FY-1985 and FY-1986 were analyzed for radionuclides. Lysimeter water samples and sediment samples collected during FY-1986 and FY-1987 deep drilling were also analyzed for radionuclide parameters.

Results indicated several trends: slight downward migration of background radionuclides from the weathering of the surficial sediments, migration of radionuclides from the buried waste within the surficial sedimentary cover of the RWMC, and downward migration of radionuclides from the buried waste into the 110-ft interbed and possibly into the 240-ft interbed underlying the RWMC.

CONTENTS

FIGURES

TABLES

FACTORS FOR CONVERTING ENGLISH UNITS TO METRIC (SI) UNITS

The following factors can be used to convert English units published herein to the International System of units (SI).

Multiply	By	To obtain
inches (in.)	2.54	centimeters (cm)
inches (in.)	25.4	millimeters (mm)
feet (ft)	0.3048	meters (m)
miles (mi)	1.609	kilometers (km)
acres	0.4047	hectares (ha)
gallons (gal)	3.785	liters (L)
gallons (gal)	3785.434	cubic centimeters (cc)
pounds (lb)	0.4536	kilograms (kg)
micromhos (µmho)	1.00	microsiemens (µS)
pounds per square inch (psi)	6.80	kilopascals (kPa)
pounds per square inch (psi)	0.068	bars
°F - 32	0.556	°C
parts per million (ppm)	1.0	milligrams per liter (mg/L)

ANNUAL PROGRESS REPORT: FY-1987

SUBSURFACE INVESTIGATIONS PROGRAM AT THE RADIOACTIVE WASTE MANAGEMENT COMPLEX OF THE IDAHO NATIONAL ENGINEERING LABORATORY

1. INTRODUCTION

The Subsurface Investigations Program is part of a continuing effort at the Radioactive Waste Management Complex (RWMC) of the Idaho National Engineering Laboratory (INEL) to identify pathways and mechanisms by which radionuclides may eventually migrate through the subsurface environments and present a potential hazard to man. The four methods and fifteen studies to accomplish this objective are presented in A Plan for Studies of Subsurface Radionuclide Migration at the Radioactive Waste Management Complex of the Idaho National Engineering Laboratory (DOE, 1983).

The unsaturated (or vadose) zone encompasses all geologic materials between the ground surface and the water table of the Snake River Plain Aquifer. Included are relatively thin sedimentary units at the surface and at depths of about 30 ft, 110 ft, and 240 ft. (Throughout this report these sedimentary units are referred to as the 30-ft, 110-ft, and 240-ft interbeds. The actual depth of an interbed at a specific location is not necessarily the same as the depth indicated by the interbed name.) Also included in the unsaturated zone are the basalt flows, which compose most of the geologic sequence.

The Snake River Plain Aquifer, whose surface lies at a depth of about 580 ft below the RWMC, consists of basalt flows, volcanic ash, and sedimentary interbeds.

Three of the four methods for collection of data in support of the subsurface investigations were continued in FY-1987. These methods were: Test Trench, Weighing Lysimeter, and Deep Drilling. Five specific studies--Solution Chemistry, Net Downward Flux, Computer Model Development,

Radiochemical Analysis, and Characterization of Geologic Materials--were continued or initiated in FY-1987. In addition, a new study, Organic Vapor Characterization, was implemented in response to the detection of volatile organic compounds (VOCs) at the RWMC during FY-1987. This new study included well water analyses, air sampling for detection of organic vapors, quantitative gas sample analyses, and soil gas survey analyses.

This report summarizes work performed in support of the Subsurface Investigations Program during FY-1987. The work was performed by representatives of EG&G Idaho, Inc. and the U.S. Geological Survey (USGS) INEL Project Office. All work was performed under the direction of the U.S. Department of Energy (DOE), Idaho Operations Office.

2. RATIONALE AND STATEMENT OF OBJECTIVES

The RWMC was established near the southwestern corner of the INEL in 1952 as a controlled area for the management of solid radioactive waste. The RWMC encompasses 144 acres. Radioactive waste is buried in the 88-acre Subsurface Disposal Area (SDA) and temporarily stored above ground in the 56-acre Transuranic Storage Area (TSA). See Figure 1. The closest major population center is Idaho Falls, approximately 50 miles to the east.

The radioactive waste buried at the RWMC is a potential hazard to the environment if its confinement is not maintained. Some radionuclides in the waste are long-lived, so there is a potential of their long-term migration.

The question of subsurface migration of radionuclides is of particular interest for an eventual DOE decision regarding possible retrieval of buried transuranic waste at the RWMC. Evidence of significant migration could be used to argue for retrieval of approximately 2,000,000 ft^3 of this waste or for the development of additional methods to reduce the extent of migration. Conversely, the lack of such evidence could support arguments for leaving the waste in place, at great cost savings.

Therefore, two overall program objectives were established by DOE. These objectives are:

- Field-calibrate a model to predict long-term migration of radionuclides in the unsaturated zone. Achieving this objective will require measuring hydrologic transport properties, accounting for radionuclide behavior and radioactive decay, obtaining or developing a computer program for the model, and field-calibrating the model.

- Measure the actual migration of radionuclides to date, in order to determine whether there is a problem from a public health and safety standpoint. Achieving this objective will require

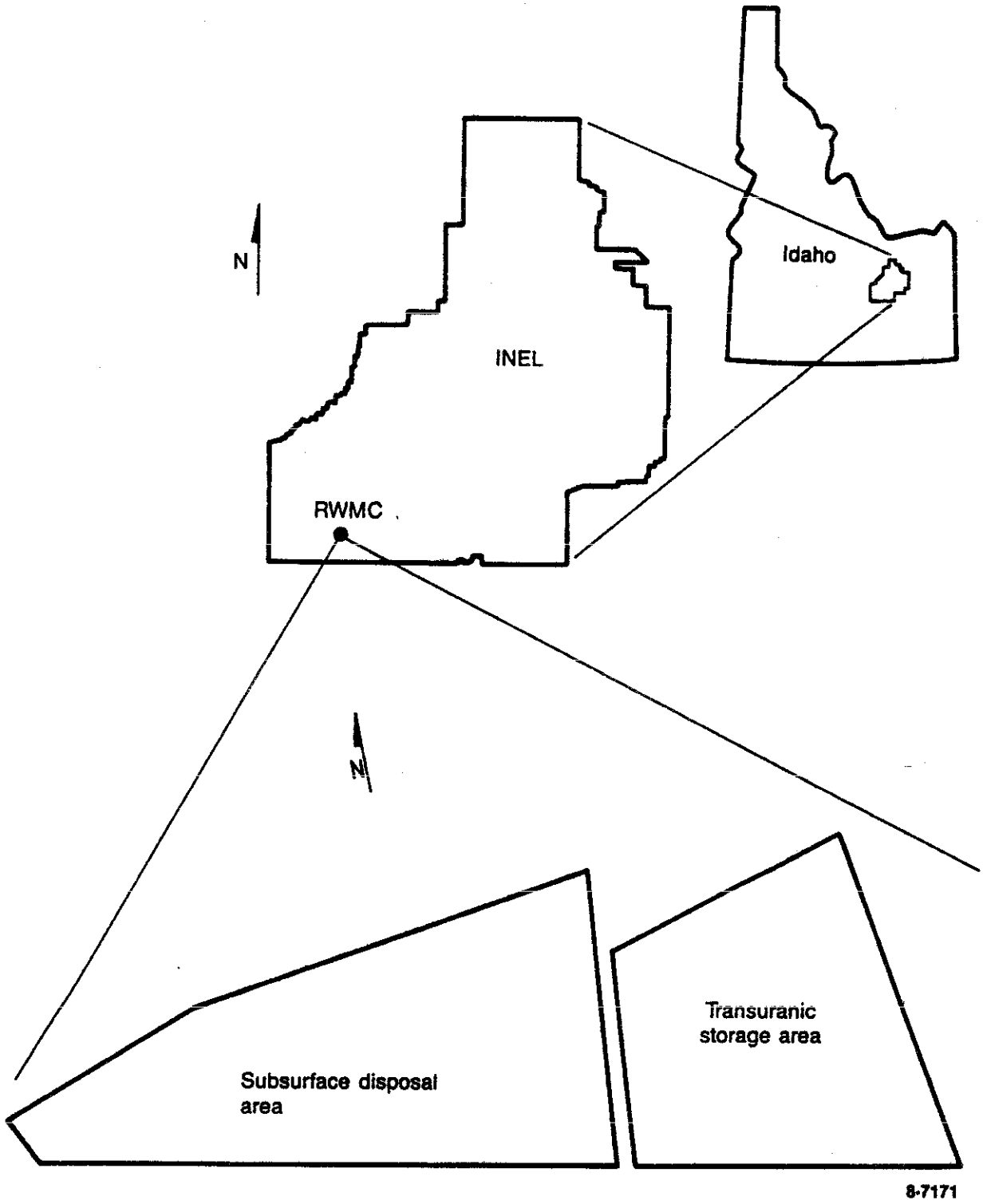

Figure 1. Location of the Radioactive Waste Management Complex.

collection, preparation, and analysis of geologic samples from the unsaturated zone. Strict anticontamination control methods will be followed to ensure the integrity of the analytical results.

The scheduling of Methods and Specific Studies to accomplish the program objectives is shown in Table 1.

The detection of volatile organic compounds (VOCs) has resulted in additional concerns regarding subsurface investigations at the RWMC. These concerns are: safety to the public and the environment, safety to RWMC operational personnel, and the complexing relationship between radionuclides and the VOCs. Therefore, an additional objective of the Subsurface Investigations Program is to characterize (nonradioactive) hazardous constituents at the RWMC and model their potential migration.

TABLE 1. SUBSURFACE INVESTIGATIONS PROGRAM SCHEDULE

Task Description	FY-85	FY-86	FY-87	FY-88	FY-89	FY-90	FY-91
METHODS							
Shallow drilling*	———	———		———			
Test trench	———	———	———	———	———	———	
Weighing lysimeter		———	———	———	———		
Deep drilling**		———	———	———	———	———	———
SPECIFIC STUDIES							
Net downward water flux and interface phenomena	———	———	———	———	———	———	———
Solution chemistry	———	———	———	———	———	———	———
Radionuclide concentrations		———	———	———	———	———	———
Characterization of geologic materials			———	———	———		
Chemical form of radionuclides				———			
Hydrogeology of waste pits				———	———	———	
Model development		———	———	———	———	———	———
Hydrogeologic properties of sediments				———	———	———	
Hydrogeologic properties of basalts			———	———	———		
Chemical mass transfer				———			
Dispersivity				———	———		
Waste leachability				———	———	———	———
Sorption coefficients and kinetics					———	———	
Horizontal and vertical distribution					———	———	———
Model calibration					———	———	———
Organic vapor characterization				———	———	———	———
OTHER							
Program review/support	———	———	———	———	———	———	———

* Fifteen boreholes are planned in FY-88.

** Four boreholes are planned in FY-88, four in FY-89, four in FY-90, and four in FY-91.

3. BRIEF HISTORY OF THE SUBSURFACE INVESTIGATIONS PROGRAM

Studies of possible subsurface migration of radionuclides at the RWMC began in 1960. The most recent study was conducted in 1979. These earlier studies are reported in documents authored by Schmalz (1972), Barraclough et al. (1976), Burgus and Maestas (1976), Humphrey and Tingey (1978), and Humphrey (1980). The results obtained from these previous efforts have provided useful but inconclusive evidence regarding potential migration of radionuclides. The techniques employed in several cases were susceptible to possible cross-contamination during sample collection or handling processes. Also, not all the data required to model radionuclide transport through the subsurface environment have been collected. Therefore, DOE requested EG&G Idaho, Inc. and the USGS INEL Project Office to prepare a comprehensive plan. Specifically, the purpose of the plan was to provide data to determine the extent of subsurface radionuclide migration and to develop and field calibrate a computer model to help project the long-term migration of radionuclides.

The planning effort for this program was initiated in FY-1982 and completed early in FY-1984. The plan integrates data requirements from a variety of technical disciplines to address the program objectives. Specific hydrogeologic and geochemical data requirements were established to field-calibrate a subsurface transport model to predict long-term migration. These data requirements were used to design field and laboratory studies to collect the necessary data.

The activities and studies were then integrated into an overall program and subjected to an external peer review. Details of the review are presented in the 1983 DOE report. The plan was approved in early FY-1984. The remainder of FY-1984 was spent preparing the procedures to drill/sample the surficial sediment overlying the basalt at the RWMC (depth less than 30 ft). This shallow drilling was performed in FY-1985 with 21 auger holes drilled and 19 instrumented.

During 1986, 11 shallow holes were augered and instrumented. Auger hole sample analyses and instrumentation data from the shallow drilling program (1985 and 1986) are described in subsequent sections of this report.

During FY-1986, the deep drilling program began. The deep boreholes were planned to penetrate the 240 ft interbed. Three deep boreholes were drilled during FY-1986. One borehole (D06) was instrumented. Sample analyses and instrumentation data from the 1986 deep drilling program are also presented in subsequent sections of this report.

4. METHODS

The Subsurface Investigation Program (SIP) relies on several methods (or activities) to provide for the collection of data to support the individual specific studies. More detail regarding each method is available in the 1983 DOE report.

During FY-1987, three activities were continued: Deep Drilling Program, Test Trench Installation, and Weighing Lysimeter Modification. These activities are discussed in the following sections.

4.1 Deep Drilling

4.1.1 Introduction

The objectives of the deep drilling activity are to provide representative samples of the main sedimentary interbeds and to prepare boreholes for instrumenting with in situ monitoring instrumentation. The deep drilling activity consists of drilling and sampling the basalt and interbeds inside the SDA and around its periphery. The deep boreholes are drilled to a total depth of approximately 5 ft below the 240-ft interbed. Samples from the 30-ft, 110-ft, and 240-ft interbeds are used to define the geologic and hydrologic characteristics of the sediments and to provide samples for laboratory determination of selected radionuclides.

4.1.2 Summary of Accomplishments

Three deep boreholes were drilled at the RWMC. The locations of these three boreholes, along with the locations of holes augered and drilled during FY-1985 and FY-1986, are shown in Figure 2. The objective for each deep hole was to drill through the 240-ft interbed, obtain samples for radiochemical determinations, determine the locations and thicknesses of the interbeds, and instrument the borehole. Hole TW1, located inside the SDA, was drilled to a depth of 237 ft and subsequently instrumented. Hole D15, lying outside the boundary of the SDA, was drilled to a depth of 243 ft and subsequently instrumented. Hole D10, located inside the SDA,

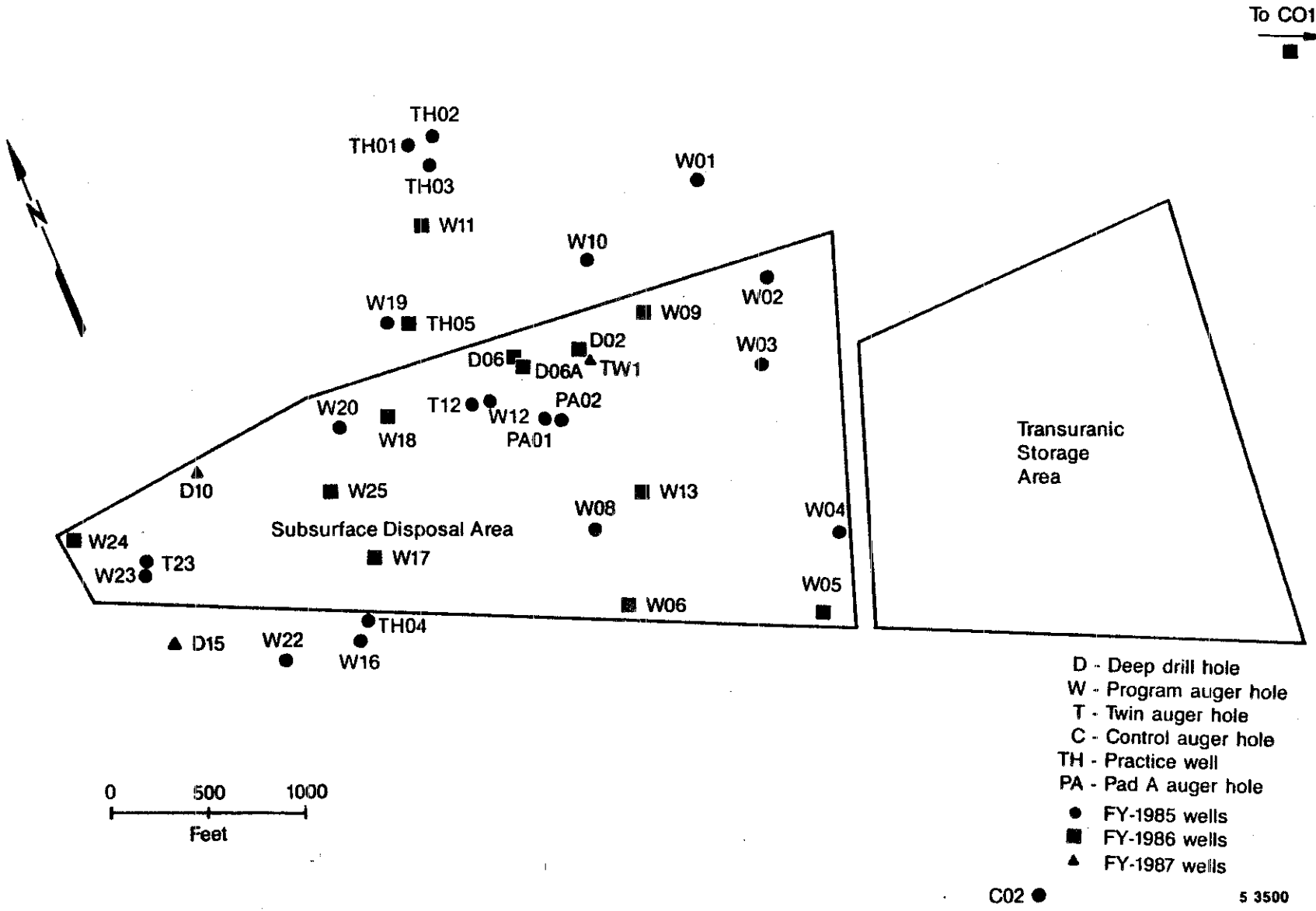

Figure 2. Locations of Subsurface Investigations Program holes drilled during FY-1985, FY-1986, and FY-1987.

was drilled to a depth of 95 ft. Work on D10 was temporarily suspended because of the presence of organic vapors. In addition, work was continued on hole D02, which was drilled during the FY-1986 drilling season. The hole was in the process of being instrumented (during the FY-1987 season) when organic vapors were encountered. Work was temporarily suspended. Both D10 and D02 have been sealed with waterproof locking caps and will be completed and instrumented in FY-1988.

4.1.3 Discussion

4.1.3.1 Deep Drilling Borehole Design. The surficial sediments lying above the uppermost basalt layer are augered by RWMC operations. The thickness of surficial cover to be augered ranges from one ft to approximately 25 ft. A 12-in. auger bit is used.

The SIP drilling rig then cores the first 5 ft of the basalt below the surficial cover using an HXB core barrel. The 5-ft core hole is then reamed using a 12-in. tricone bit. A 10-in.-diameter surface casing is set and cemented into the drill hole from the surface to 5 ft into the underlying basalt.

Drilling into the basalt from beneath the surface casing employs a 7-7/8-in. tricone bit. The basalt is continuously drilled with the tricone bit until an intermediate interbed is reached or the 110-ft interbed is within 5 ft. In each case, the triconing drill string is changed out and an HXB coring drill string is used. Prior to coring, a samarium oxide tracer is placed in the hole to check against mixing of sample material between different rock units down the borehole. The interbed and 5 ft of overlying and underlying basalt are then cored. The core hole is then reamed with the 7-7/8-in. bit. Bentonite is placed at the bottom of the borehole, and 6-in. casing is set into the bentonite layer. The bentonite serves as a seal at the bottom of the casing to prevent moisture and sediment from migrating downward in the borehole when drilling resumes.

Once the 6-in. casing is set, a 5-7/8-in. tricone bit is used to drill out beneath the bottom of the casing into the underlying basalt. The

basalt is continuously drilled with the tricone bit until an intermediate interbed is reached or the 240-ft interbed is within 5 ft. The drill string is changed out and replaced with the coring drill string. The 5 ft of overlying basalt, the interbed, and 5 ft of the underlying basalt are then cored. After coring is complete, the hole is reamed with the 5-7/8-in. tricone bit. This ends the drilling/coring phase of the borehole. The hole is now ready for instrumentation. The instrumentation process is discussed in Section 4.1.3.5.

After borehole D15 was drilled, it was decided that all future holes will be cored in their entirety. Coring the basalt as well as the interbeds will provide more information about the RWMC subsurface. Borehole D10 was continuously cored to the 95-ft depth, at which point drilling was suspended in September 1987. The hole design is basically the same as previously described for boreholes drilled using a tricone bit. Instead of triconing the hole and back-reaming, the borehole was drilled using a 3-1/2-in. rotary diamond core bit and then back-reamed to the standard hole size.

4.1.3.2 Geophysical Logs. Geophysical wireline logs are run in the borehole through the 110-ft interbed before casing is set. The entire hole is logged again after the hole has been drilled to total depth below the 240-ft interbed. Four types of geophysical logs are taken: gamma-ray, gamma-gamma, neutron, and caliper logs. A downhole television log is also run.

Gamma-ray logs indicate the amount of natural gamma radiation emitted from material surrounding the hole. Gamma-ray logs are used to identify sedimentary beds within the basaltic sequence. Sediments at the RWMC emit more gamma radiation than basalt.

Gamma-gamma logs measure the intensity of reflected gamma radiation from a source within the probe after it has been backscattered and attenuated within the hole and surrounding rocks. Gamma-gamma logs measure

the relative density of material surrounding the probe. The logs, therefore, are also used to indicate relative porosity. Basalts show up as high density materials, whereas the sediments have a low density. Therefore, gamma-gamma logs suggest greater relative porosity in sediments.

Neutron logs measure the hydrogen content of material surrounding the hole, thereby reflecting the relative moisture content of the material. Sediment interbeds or fracture zones with sediment infilling within the basalt intervals typically indicate the highest moisture content.

Caliper logs measure the diameter of the borehole.

The geophysical log responses to TW1, D15, and D02 are illustrated in Figures 3, 4, and 5. The figures also show the construction of the boreholes.

4.1.3.3 Health Physics Survey. Health physics surveys are conducted in three specific areas to screen for cross-contamination between the surface and the borehole. These areas are the drill rig location, the decontamination area, and the Subsurface Investigations Field Laboratory (SIFL). Approximately 1350 smears were taken in these locations and counted in the SIFL using an alpha spectrometer and beta/gamma counter. Approximately fifteen percent of these smears were composited and sent to the radiochemical laboratory for wet chemical analysis. Positive radiochemical results (at a 99% confidence level) were detected during the FY-1987 drilling program. These resulted from: (a) contamination inside the SIFL from the prepared laboratory standard and (b) surficial dust accumulating on equipment in the work areas.

Smear samples with positive results are listed in Table 2. Smear samples 6 and 30 showed statistically positive activities of ^{239}Pu, ^{244}Cm, and ^{230}Th. These radionuclides were present in a calibration standard used at the SIFL. The ratios of ^{239}Pu to ^{244}Cm, ^{239}Pu to ^{230}Th, and ^{244}Cm to ^{230}Th in these two smear samples are

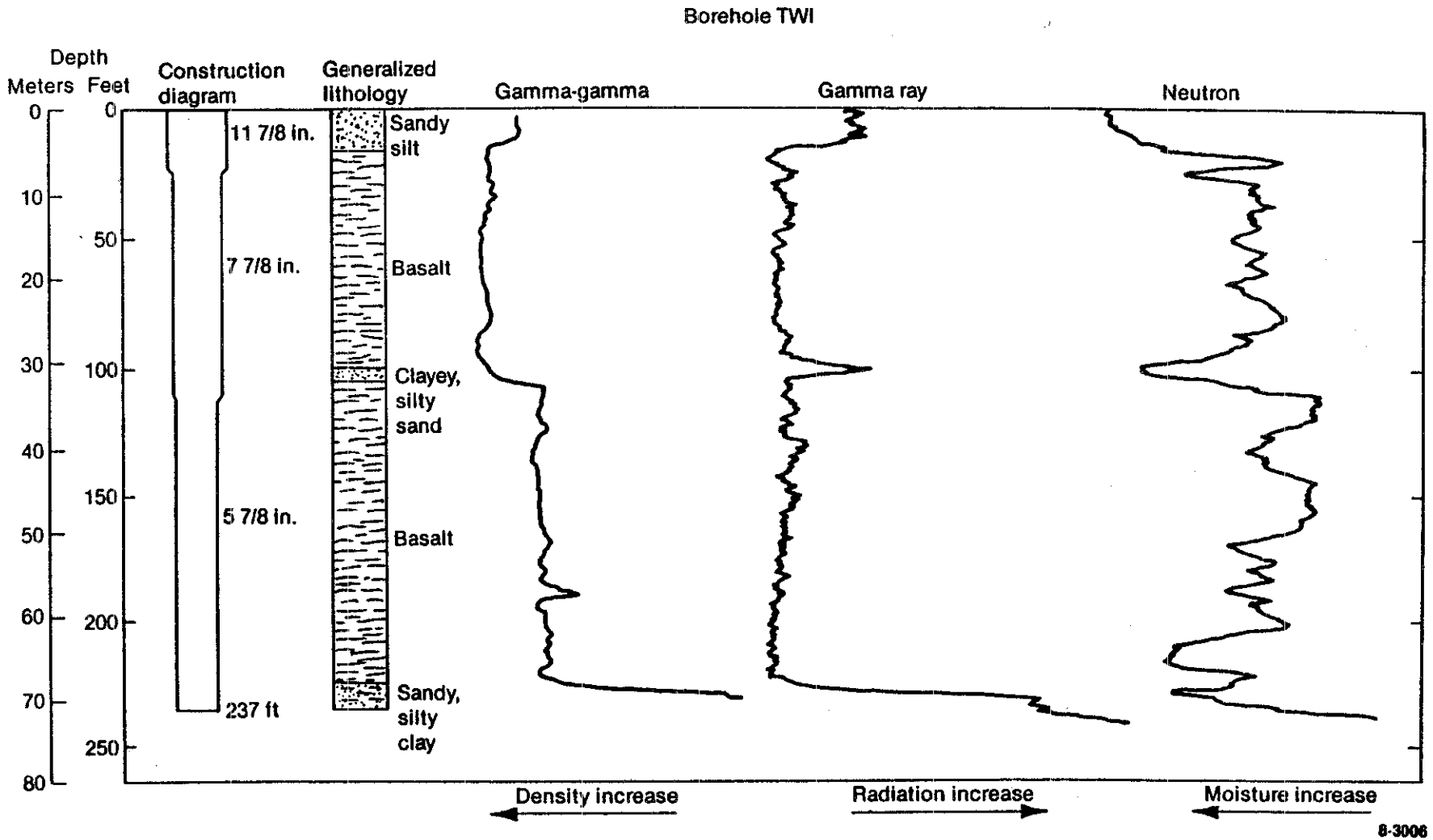

Figure 3. Construction diagram, lithology, and geophysical logs for borehole TW1.

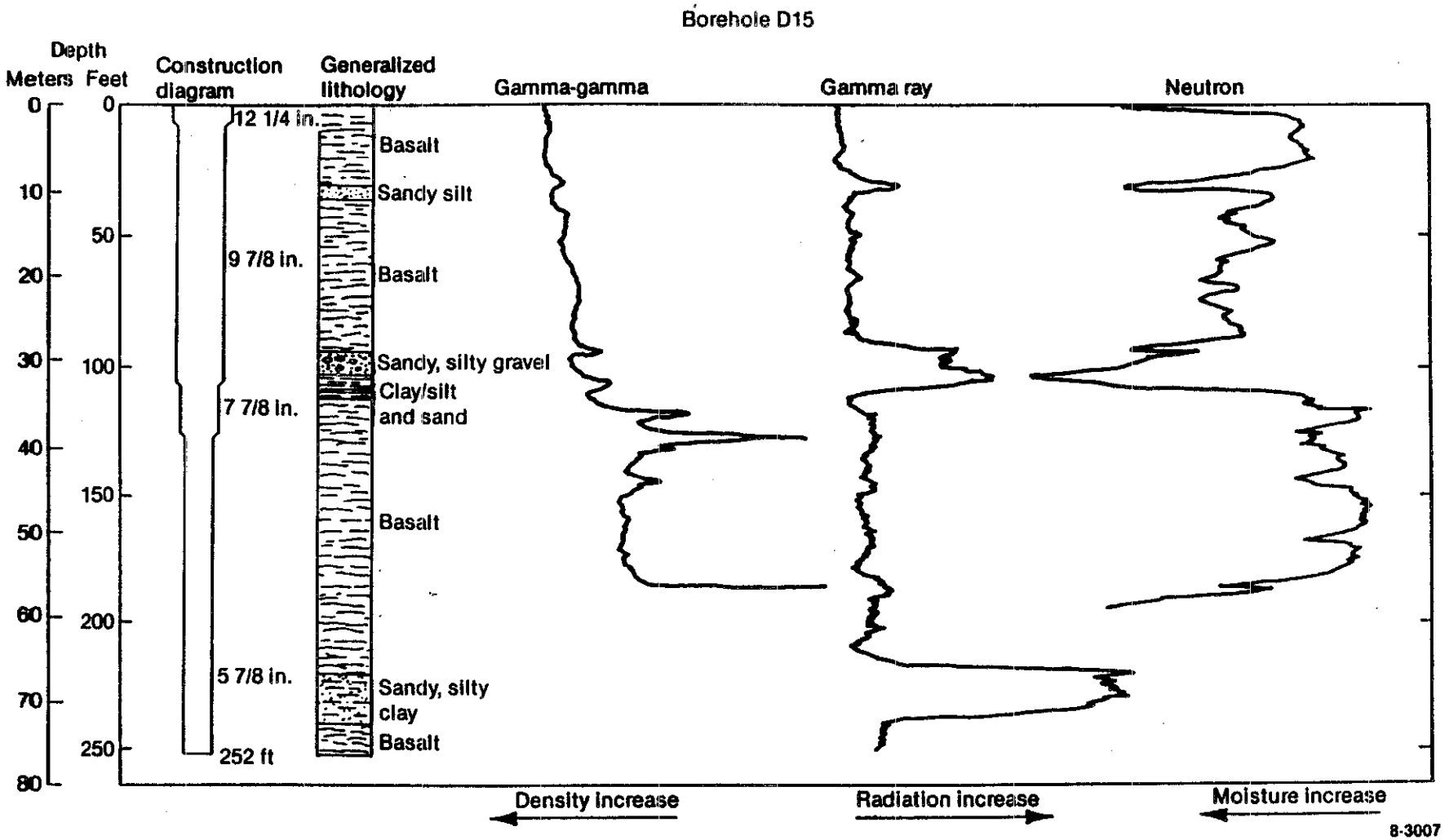

Figure 4. Construction diagram, lithology, and geophysical logs for borehole D15.

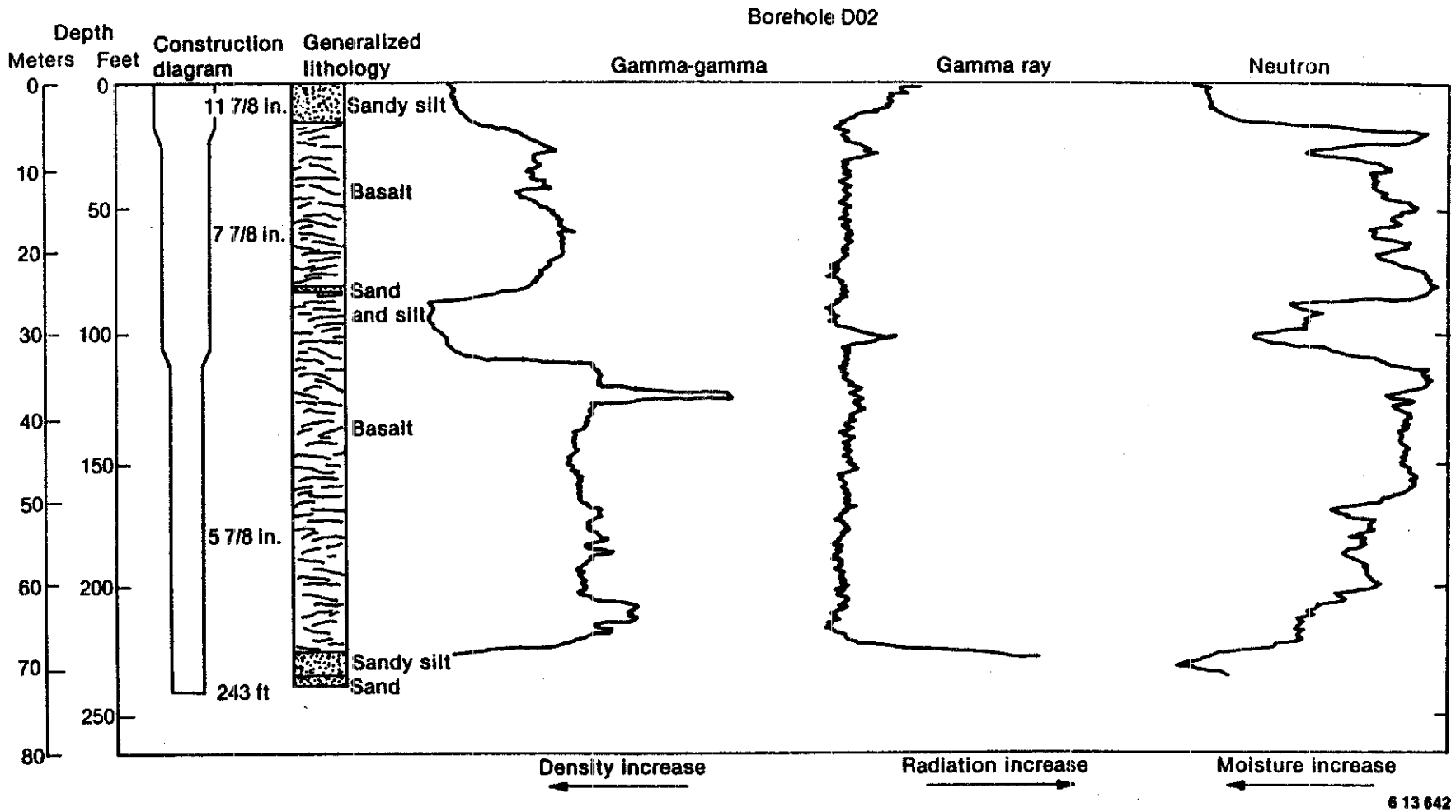

Figure 5. Construction diagram, lithology, and geophysical logs for borehole D02.

TABLE 2. POSITIVE RESULTS FROM SMEAR SAMPLE ANALYSES

Borehole	Smear No.	Date	Nuclide	Activity (μCi)
TW1	6	6-05-87	^{239}Pu	1.32 ± 0.17 E-07
			^{244}Cm	1.35 ± 0.17 E-07
			^{230}Th	3.4 ± 0.9 E-08
TW1	19	5-24-87	^{239}Pu	9.1 ± 1.7 E-08
TW1	20	5-25-87	^{239}Pu	7.3 ± 1.6 E-08
TW1	21	5-26-87	^{239}Pu	1.76 ± 0.20 E-07
TW1	22	5-27-87	^{239}Pu	4.0 ± 1.0 E-08
TW1	24	5-29-87	^{239}Pu	1.13 ± 0.15 E-07
TW1	30	6-04-87	^{239}Pu	8.1 ± 1.4 E-08
			^{244}Cm	8.5 ± 1.4 E-08
			^{230}Th	6.1 ± 1.3 E-08
D15	45	7-23-87	^{239}Pu	1.07 ± 0.17 E-07
D15	46	7-24-87	^{239}Pu	1.09 ± 0.16 E-07
D15	47	7-27-87	^{239}Pu	4.1 ± 1.0 E-08

statistically identical to these same ratios in the calibration standard. Therefore, the ^{239}Pu activity in these two samples is due to contamination from the calibration standard.

Smear samples 19 and 20 show statistically positive ^{239}Pu activity. However, because of the quantity of soil present on the smear, it was not possible to isolate a Cm-Th fraction. Therefore, it is impossible to tell whether or not the ^{239}Pu activity present in these samples came from the calibration standard or from some other source.

Smear samples 21, 22, 24, 45, 46, and 47 showed statistically positive ^{239}Pu activity, but no statistically positive activities of ^{244}Cm or ^{230}Th. This suggests that the activity of ^{239}Pu in these samples is not due to contamination from the calibration standard. Smears 21, 22, and 24 were taken during work on borehole TW1. During the time these smears were taken, work was being done on the 6-in. casing, and basalt was being drilled. Smears 45, 46, and 47 were taken during work on the

surficial cover and surface casing on borehole D15. Sampling of sedimentary interbed material was not taking place during the time these positive smears were taken at these two boreholes. There is no association between these positive smears and positive detections in sedimentary interbed material. Therefore, it is concluded that these positive smear results from borehole TW1 and D15 occurred from contact with contamination from the surficial soil. The surficial soil at the RWMC does have a higher background radionuclide content than the detection limit used for radionuclides sampled for in the subsurface (Arthur, 1982).

Although positive smear samples were detected by radiochemical methods, the positive concentrations were still two orders of magnitude lower than the Health Physics Survey detection limits. Hence, the positive smear values are extremely low.

4.1.3.4 Drilling and Sampling. Borehole TW1 was drilled within 15 ft of borehole D02, which was drilled in the FY-1986 season. The purpose of drilling TW1 was to confirm the presence of migrating radionuclides in the 240-ft interbed of D02.

The 110-ft interbed in borehole TW1 measured about 3 ft thick. Approximately 30% of the interval was recovered using HXB and Shelby tube coring devices. The HXB core barrel, Shelby tube, and thin-wall Shelby tube type coring devices were used to core the 240-ft interbed in TW1. Core recovery in this interval was poor (20%) due to two factors. First, a Shelby tube was lost in the hole. Second, the coarse, noncemented sand in the bottom of the 240-ft interbed would not stay in the core barrel. Repeated attempts to core this material with high pressure air resulted in erosion and caving of the borehole. Hole TW1 was completed at that point and subsequently instrumented.

Borehole D15 was drilled approximately 300 ft south of the SDA for the purpose of providing control samples. The HXB core barrel was used for the 30-ft interbed; 35% core recovery was obtained at this interval. A thick, unconsolidated gravel zone was encountered in the 110-ft interbed. This type of sediment is very difficult to core. Several different coring

techniques were attempted: (a) the HXB core barrel, (b) the standard Shelby tube, (c) a thin-walled Shelby type tube, and (d) a California split-spoon sampler. Each coring device failed to obtain core from this gravel zone. Consequently, the open hole was cased from the surface to the bottom of the gravel interval with an 8-in. casing. HXB coring resumed through the bottom of the casing to the base of the 110-ft interbed. Core recovery in the interbed below the gravel was excellent (78%). The overall core recovery form the entire 110-ft interbed was 26%. Gravel not recovered from the coring was circulated out of the hole by high pressure air and recovered at the surface. These gravel cuttings will aid in the geologic interpretation of the interbed.

The HXB core barrel was the coring device used for the 240-ft interbed in hole D15. Gravel was not encountered in this interbed. Core recovery for this interval was excellent at 74%.

Before work began on borehole D10 in September, it was decided that all subsequent boreholes shall be cored in their entirety (the basalt sections as well as the interbeds). The coring program for borehole D10 was proceeding normally until late September, when volatile organic compounds were detected coming from the borehole. Drilling immediately ceased for the FY-1987 season for safety reasons. The total depth of the borehole at this time was 95 ft 2 in. The 110-ft interbed had just been breached, and the driller was conditioning the hole to core the sediment. No core was obtained from borehole D10 in the 110-ft interbed. Core was taken from the 30-ft interbed, and core recovery was 77%; the HXB core barrel was the coring device used.

Work was discontinued also on borehole D02 because of the detection of organic vapors. Borehole D02 had been drilled to approximately 235 ft during the FY-1986 drilling season. Hole problems were encountered at the 240-ft interbed level, and drilling stopped for FY-1986. The plan for finishing D02 in FY-1987 was to penetrate the base of the 240-ft interbed into the underlying basalt, pull the 6-in. casing, and instrument the hole. Sand (8-ft) was cored in the bottom of the 240-ft interbed; however, no core was recovered because of the lack of cementation in the sand. The unconsolidated sand simply fell out of the bottom of the core barrel. It

was then decided to cease coring and begin the instrumentation process. Volatile organic compounds were detected coming from the borehole during the removal of the 6-in. casing, and the instrumentation of D02 was discontinued.

Interbed samples collected from TW1 and D15 were characterized in terms of texture, type, color, reaction to HCI, and moisture content. This information is presented in Appendix A. Additional discussion is presented in Section 5.1. Results of radiochemical analyses of sediment samples are presented in Section 5.6.

4.1.3.5 Instrumentation and Backfilling. Two deep boreholes, D15 and TW1, were instrumented with heat dissipation sensors to measure soil-water tension within sediments contained in the interbeds. Suction lysimeters, for soil-water extraction, were installed in the interbeds along with the heat dissipation sensors.

Boreholes were instrumented following drilling and sampling. The 6-in. casing, installed to a depth of 5 ft beneath the 110-ft interbed during drilling, was left in place while instruments were placed in the borehole the casing kept materials from falling down the borehole from the 110-ft interbed to the 240-ft interbed. A PVC guide pipe was lowered down the borehole in 10-ft increments while instruments were attached in their respective positions to the guide pipe. The instrument string was lowered into place so that the instruments were placed at depths corresponding to the locations of the interbeds. Borehole completion diagrams in Figure 6 show the placement of instruments and backfill material. The bottom of the borehole was backfilled with bentonite by pouring the bentonite through the center of the guide pipe. The remaining backfill was poured into place using a PVC tremie tube that was lowered down the borehole at the same time the instrument string was lowered. Backfill was placed in the bottom of the borehole and progressed upward to land surface.

Instruments were installed with bentonite beneath them to isolate them from other portions of the borehole. A 6-in. layer of silica sand was poured on top of the bentonite, and 5 gal of distilled water, with a 10-ppm

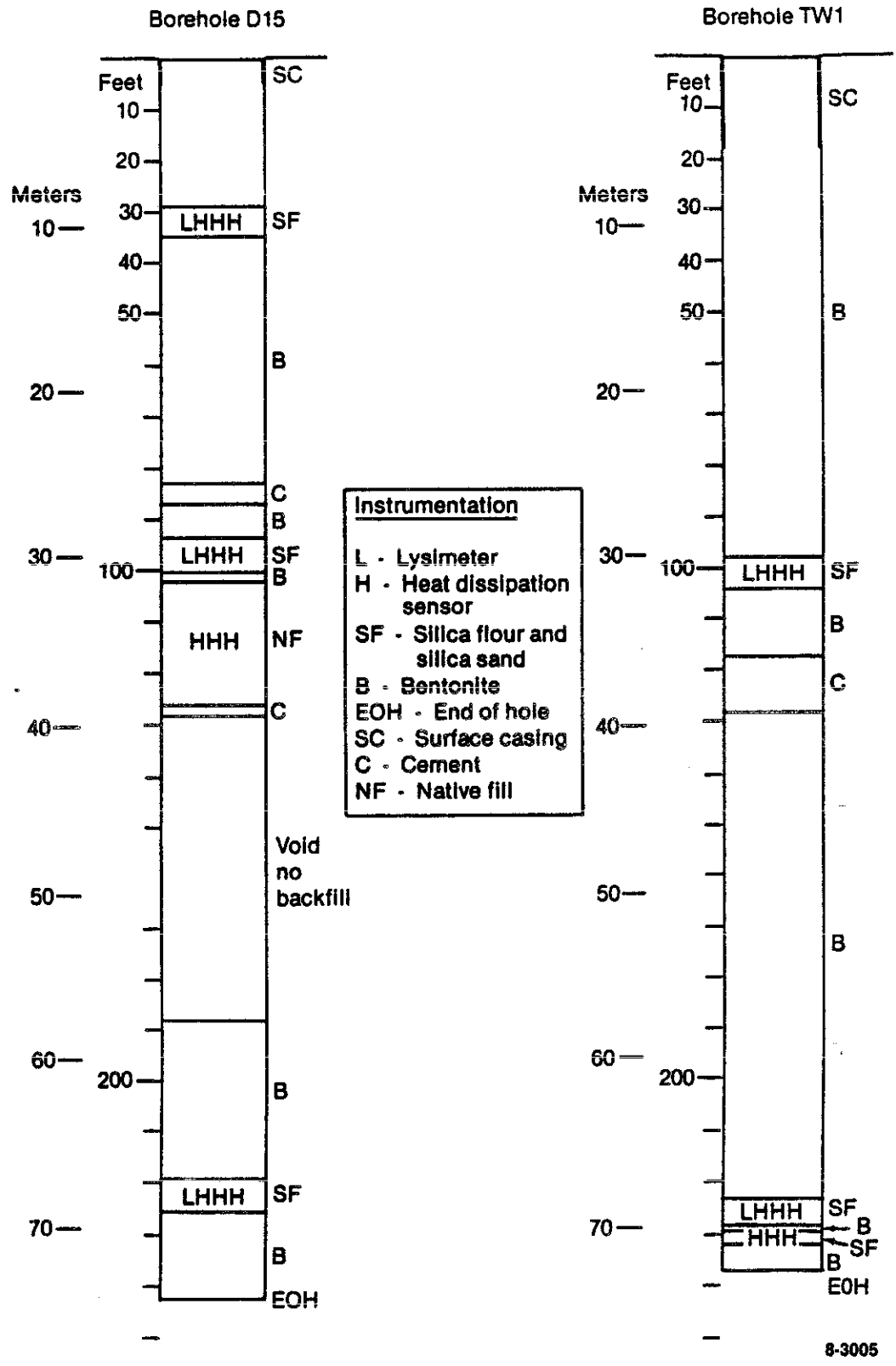

Figure 6. Borehole completion diagrams showing instrumentation and backfilling of boreholes D15 and TW1.

bromide tracer added, was poured on the silica sand. The sand acts as an insulator to dissipate the erosive action of the falling water. Silica flour, a very fine ground silica, was poured down the borehole and mixed with the water to cover the instruments. The silica flour/water mix surrounds the instruments, providing a hydraulic connection between the instruments and the surrounding sediments. The borehole was allowed to sit overnight to allow the silica flour to assimilate the water. Six inches of silica sand was added to complete the backfill around this set of instruments. Bentonite was placed between instrument groupings within the interbeds and adjacent to basalt.

A cement plug was emplaced beneath the 110-ft interbed to act as a support for the remaining backfill. This was done because the bentonite may settle 1 to 2 percent following placement. Without the cement plug, the backfill surrounding the upper interbeds could slip down, placing bentonite adjacent to the instruments. The casing covering the 110-ft interbed was withdrawn from the borehole, and backfilling continued to land surface. Backfilling of D15 was modified due to unusual conditions within the borehole. A large void, encountered at 190 ft below land surface, had to be left open. A plug was installed at 124 ft below land surface so backfilling could continue. Backfilling to cover instruments at 98 ft was not done because native material from within the borehole caved and covered them.

4.2 Weighing Lysimeter

4.2.1 Introduction

The objectives of the weighing lysimeter activity are to provide data that will describe soil moisture content, moisture changes with time, and rates of soil moisture infiltration typical of cover materials at the RWMC. These data will be used to assist in the calibration of a numerical model of soil moisture movement at the RWMC.

Weighing lysimeters are used to determine rates of soil moisture evaporation and plant transpiration in the upper few meters of surficial sediments. Two weighing lysimeters were installed by EG&G north of the SDA in 1979. These instruments did not produce reliable data and consequently were shut down in the latter part of 1982. The weighing lysimeter activity in FY-1987 consisted of making necessary repairs and modifications to bring the lysimeters back into operation such that they produce reliable data.

The weighing lysimeter installation is located 800 ft north of the SDA (Figure 7). This installation is made up of two weighing lysimeters measuring 5 x 5 x 6 ft, a control pit 4.3 ft in diameter, connecting pipe, and an instrument tank. The weighing lysimeters and control pit have identical sets of soil-moisture/temperature blocks (Figure 8) so the instrument data can be compared between the control pit and the weighing lysimeters. In addition, the weighing lysimeters have suction candles in the bottoms of the inner containers to remove any excess water and equilibrate tensions to natural conditions.

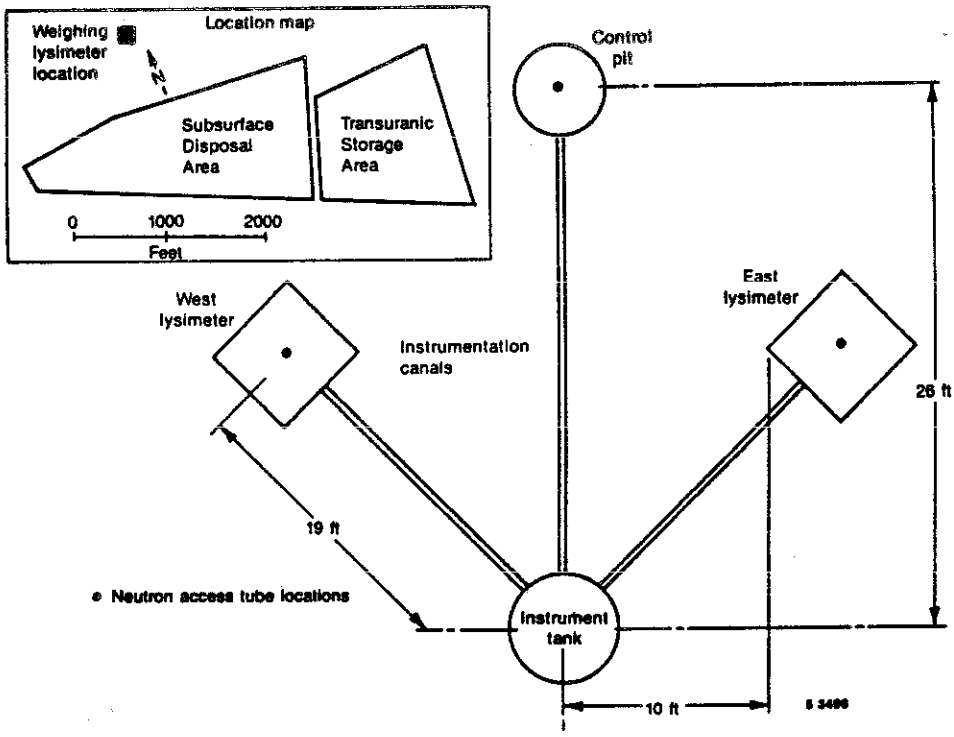

Figure 7. Location and layout of weighing lysimeter installation.

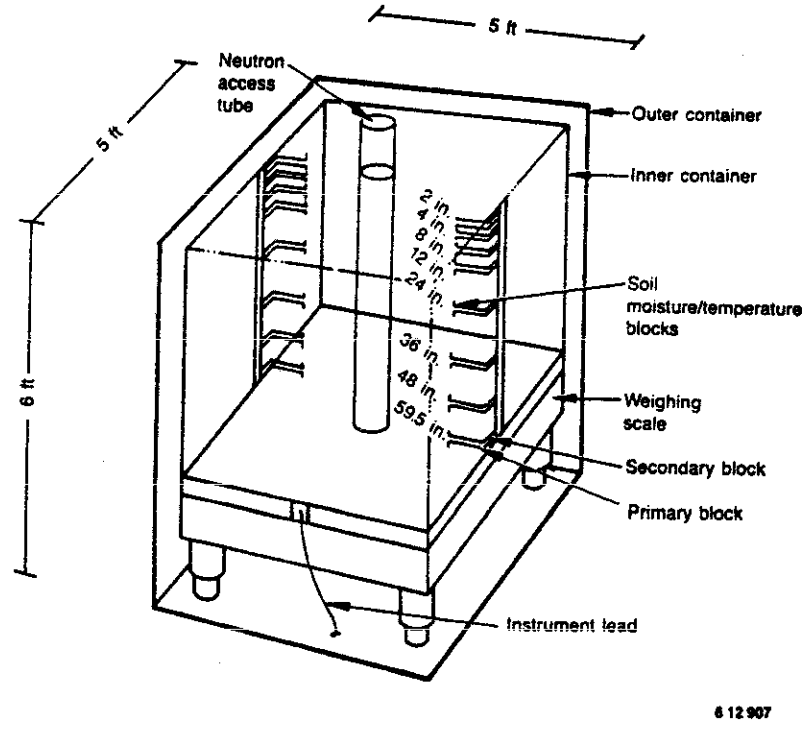

Figure 8. Weighing lysimeter instrumentation diagram showing locations and depths of instrumentation.

4.2.2 Summary of Accomplishments

During FY-1987, east lysimeter core sample analyses were completed. These analyses consisted of sediment characteristics, particle size distribution, and x-ray diffraction of the fine silt and clay fractions. Laboratory calibration of soil moisture/temperature sensors, which are identical to the uncalibrated buried sensors, was completed.

4.2.3 Discussion

Sediment core samples were taken from the weighing lysimeters, which contained soil from the same source areas as the RWMC landfill cover soils. These analyses provide data for the Hydrogeologic Properties of Sediments study, the Characterization of Geologic Materials study, and the Hydrogeology of Waste Pits study.

Particle size analyses of the cores were completed by using the dry sieve method for particles >0.062 mm in diameter, and the pipet method for particles <0.062 mm in diameter. One-and-one-half-in.-diameter core samples were taken at 10-in. depth intervals in both lysimeter boxes. The results of a representative lysimeter soil particle size analysis are shown in Appendix B, Table B-1. The complete east lysimeter soil particle size analyses and sediment characteristics analyses are available to the other study groups and will be included in a USGS Test Trench and Weighing Lysimeter data report currently being prepared.

The laboratory calibration of soil-moisture/temperature sensors showed that laboratory calibration of the in situ sensors was not possible. The sensors used at the lysimeter study area were uncalibrated when they were buried. Eight additional sensors with the same type of construction were purchased from the same manufacturer. These were placed in cells containing soil taken from the east lysimeter and were placed in a pressure plate extractor. The soil was saturated and then allowed to equilibrate at several pressures within the pressure plate extractor. At each equilibrated pressure the cells with the sensors were weighed to determine moisture content changes. At the same, time sensor output was recorded with a data logger identical to the one used at the weighing lysimeter. Multiple regression equations were developed for each laboratory sensor, and a single multiple regression equation was developed for the entire population of laboratory calibrated sensors. Statistical analyses of these calibration equations showed that although an individual calibration equation for each specific sensor would provide an accurate conversion of sensor output to moisture contents, one calibration equation for many sensors would not provide an accurate conversion of sensor output to moisture contents.

The collection of data from the soil-moisture/temperature sensors at the weighing lysimeter was discontinued in FY-1987 because calibration of the in situ sensors is not possible without their retrieval. Lysimeter weight data collection will continue in FY-1988.

4.3 Test Trench

4.3.1 Introduction

The objective of this activity is to obtain detailed information on soil moisture movement in the unsaturated zone at the RWMC. Two test trenches have been installed north of the SDA to determine, under actual and simulated conditions, the typical moisture content unsaturated hydraulic conductivity, matric potential, soil-moisture flux, and soil-moisture velocity. The trenches will also be used to experimentally evaluate the behavior of soil moisture under simulated environmental extremes. Data from the test trenches will be collected using instrumentation located in disturbed and undisturbed soils, adjacent to simulated waste containers, and along the surficial sediment/basalt interface.

The test trench activity is necessary in order to develop an understanding of movement of water (and radionuclides) from the soil surface through the waste pits and into the first sediment/basalt interface. This data will be used to assist in the calibration of a numerical model of moisture movement at the RWMC.

These trenches were instrumented with neutron access holes, tensiometers, and psychrometers to measure temperatures, moisture contents, and tensions in the soil. All instrumentation accessed through the buried test trenches is retrievable so that their calibrations can be verified periodically.

In addition, a micrometeorological station has been installed at this site to determine the effects of atmospheric conditions on subsurface soil moisture and temperature variations. This station will be used to support the Net Downward Flux study and the Weighing Lysimeter activity. Data obtained from the micrometeorological station will be used to develop mass balance equations for input to the numerical model of water movement in the unsaturated zone.

4.3.2 Summary of Accomplishments

The micrometeorological station was modified to provide additional data necessary to determine evapotranspiration rates at the RWMC. The thermocouple psychrometer calibration procedures were modified to improve the accuracy of matric potential determinations. Fifteen additional thermocouple psychrometers were calibrated for sensor rotation and calibration verification. Preliminary preparations were completed in September 1987 for the installation of a simulated waste trench. Laboratory analyses of nine soil cores from a neutron access hole were completed.

4.3.3 Discussion

The test trench installation is located 125 ft north of the SDA boundary (Figure 9). Two test trenches were fabricated and installed in FY-1984. The trenches are made of 6-ft-diameter culvert connected to form a T-shape (Figure 10). A vertical piece of culvert extends from 3 ft above land surface to a depth of 14 ft below land surface. A second culvert joins the vertical culvert at a 90° angle approximately 4 ft below land surface and extends horizontally for 20 ft.

From June to July 1987 the meteorological station was modified to provide additional data necessary for determining the amount of evapotranspiration that occurs at the RWMC. Windspeed, relative humidity, and air temperature sensors were installed at one-meter and two-meter heights above ground to provide data on air moisture fluxes from evaporation and transpiration of soil moisture. Another type of data needed, the air-soil interface temperature, is being measured by the addition of an infrared thermometer gun. Two longwave radiation sensors and two shortwave radiation sensors were installed on the station to determine the net amount of solar radiation available for evaporating soil moisture. One set of longwave and shortwave radiation sensors measures the incoming components of solar and whole sky radiation. The other longwave and shortwave sensor set measures the reflected and emitted longwave and

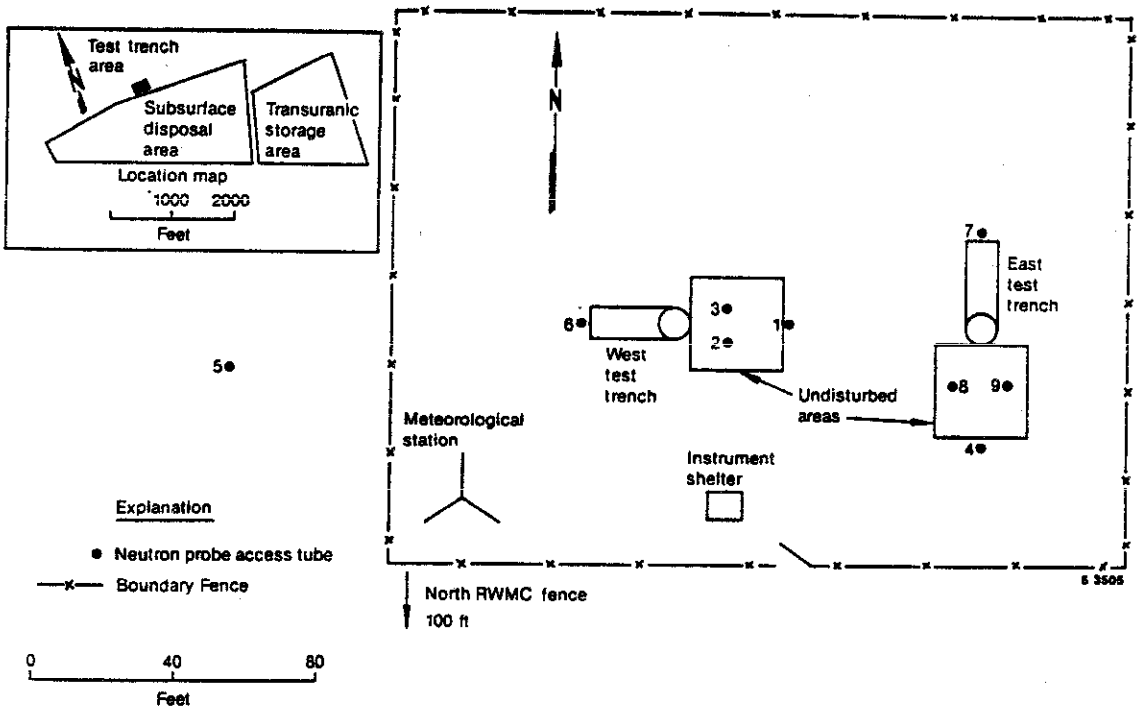

Figure 9. Location of test trench study area and associated neutron probe access tubes at the RWMC.

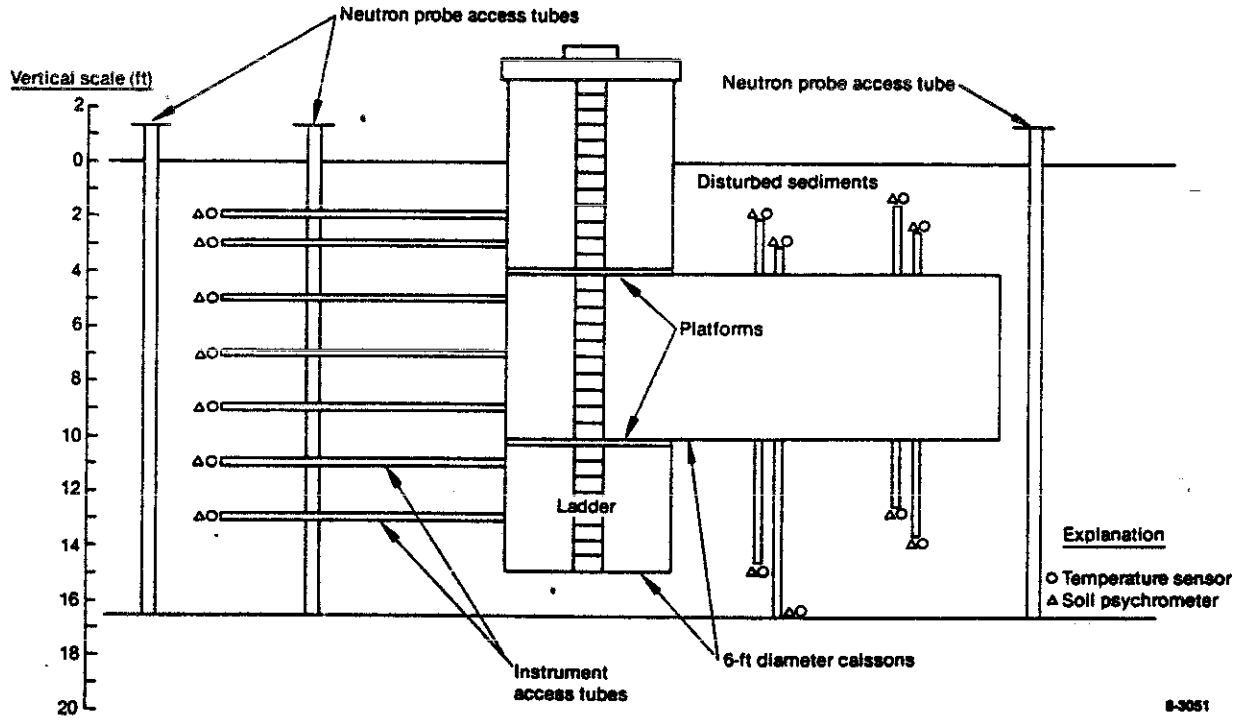

Figure 10. Installation details of the west test trench.

shortwave radiation components. Data from this station will be used in several different mass balance equations to determine the net amount of precipitation available for downward migration through the subsurface.

In FY-1987, the calibration procedures used for the thermocouple psychrometers installed at the test trench were modified to improve the accuracy of matric potential determinations. Matric potential is a calculated value, and accuracy is dependent on the calibration procedures used and the condition of the psychrometer. The accuracy of the calculated matric potential is important because it is used to determine soil moisture content, unsaturated hydraulic conductivity, soil-moisture flux, and soil-moisture velocity. Meyn and White (1972) have shown that the accuracy of the manufacturer-supplied calibration, which is described by Brown (1970), decreases as ambient temperatures deviate from the single calibration temperature of approximately 25°C. The soil temperatures recorded at the test trench during FY-1987 ranged from approximately -1°C to 20°C. Meyn and White also showed that the manufacturer's use of an empirical correction equation that enables their use of a single point calibration method would result in an increasing underestimation of soil moisture content as matric potentials increase from approximately -20 bar (low moisture content) to the psychrometer detection limit of -1 bar (high moisture content).

Because of these accuracy problems with the use of the manufacturer-supplied calibration, a different procedure was used for the test trench thermocouple psychrometers. All of the test trench psychrometers were calibrated using twenty data points that bracket the expected matric potential and soil temperature conditions of the test trench soils. Multiple regression techniques were used to develop a two-term mathematical equation that more accurately converts psychrometer output to matric potential. A separate equation is developed for each thermocouple psychrometer. In FY-1987, the temperature and water potential ranges used in the psychrometer calibration process were narrowed to more closely approximate the observed field conditions and to improve the accuracy of matric potential determinations.

An additional set of fifteen thermocouple psychrometers was calibrated. These psychrometers will be used to rotate the installed psychrometers out for calibration checks to ensure data accuracy. This will be an annual activity for the remainder of the project.

Preliminary preparations were completed for the installation of a simulated waste trench just north of the east test trench. Eight instrument access ports were installed in the east test trench for access to psychrometers that will be located in disturbed soil backfill in the simulated waste trench. Fifteen 55 gal DOT (Department of Transportation) hazardous waste drums were purchased and filled with simulated waste and a potassium bromide tracer. Twenty heat dissipation blocks were purchased; these will be emplaced within the simulated waste trench. These blocks measure soil moisture content in the 0 to 3 bar tension range and will take the place of tensiometers, which generally do not work in the dry soil conditions at the test trench area.

Particle size analyses of nine soil samples from neutron access hole NAH-1 were completed. Particles <0.062 mm in diameter were analyzed by the dry sieve method and particles >0.062 mm in diameter were analyzed by the pipette method. The results of these analyses are shown in Appendix B, Tables B-2 through B-10. Particle size analyses will be conducted on the remaining test trench soil samples.

Analyses of sediment sample characteristics were also completed on the nine NAH-1 soil samples. The results of these analyses are shown in Appendix B, Tables B-11 through B-19. The analyses show that, in this particular area, quartz, plagioclase, and basalt fragments predominate as the most abundant soil components. Analyses of sediment sample characteristics will be conducted on the remaining neutron access hole soil samples.

Soil-water characteristic curves are used to determine the relation between soil tension (matric potential) and soil moisture content by volume, and are also used to determine unsaturated hydraulic conductivity.

Data for these curves are collected by placing soil cores within a pressure plate extractor, saturating the soil cores, and then weighing the soil cores after the soil moisture within the cores equilibrates at several selected pressure settings. At the end of the test, the soil cores are oven-dried, and intermediate masses are converted to volumetric water content values. Soil-water characteristic curve data sets were completed for samples from four neutron access holes (NAH-2, 3, 6, and 9). These data sets are shown in Appendix B, Tables B-20 through B-24. Soil-water characteristic curve work will continue through FY-1988.

Nine neutron access holes were installed in and around the test trench area. The holes were hand-augered to the surficial sediment/basalt interface while undisturbed core samples were collected for bulk density, soil, moisture, and particle size analyses. The holes were cased with 1.5 in. inner diameter stainless steel tubing from 2 ft above land surface to the basalt. Locations of these access holes are shown in Figure 9. Readings were taken from the nine access tubes on a bimonthly basis; these readings show relative soil-moisture content changes. Data from the neutron access holes will be documented in a USGS data report currently under peer review.

Psychrometer data collected at the test trench area show the soil temperature and soil matric potential changes with time and depth. Soil temperature changes with time at six depths in the surficial sediments are shown in Figure 11. Changes in soil tension (matric potential) with time at four depths are shown in Figure 12.

Approximately 65,000 data points collected at the test trench study area in FY-1987 were compiled and are being checked for accuracy.

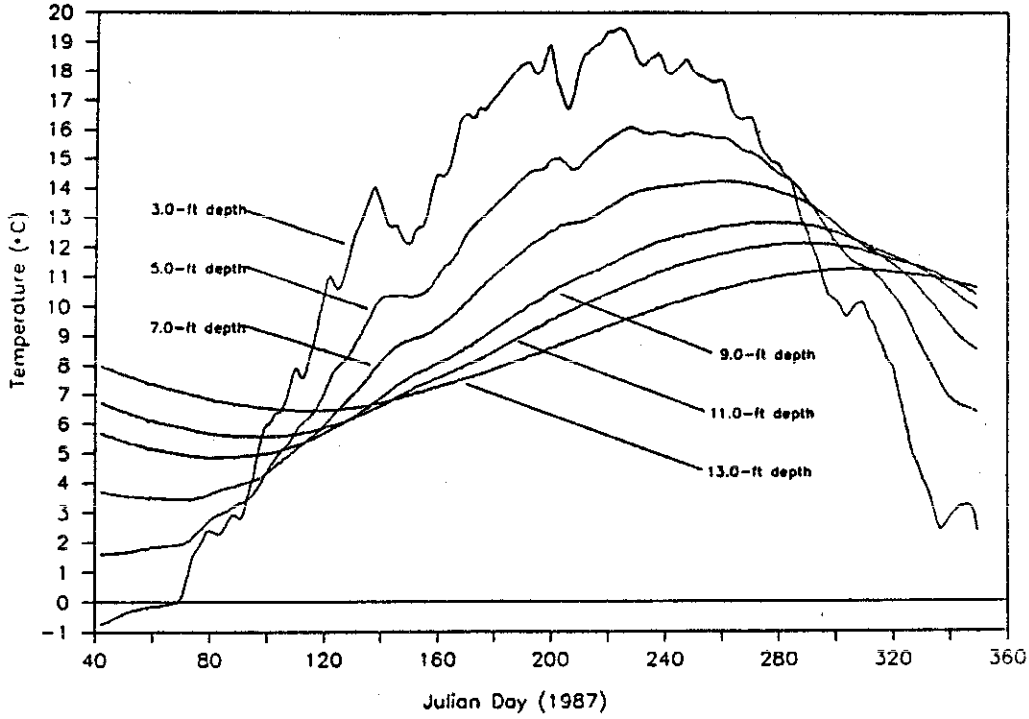

Figure 11. Undisturbed-soil temperatures at six depths at the west test trench.

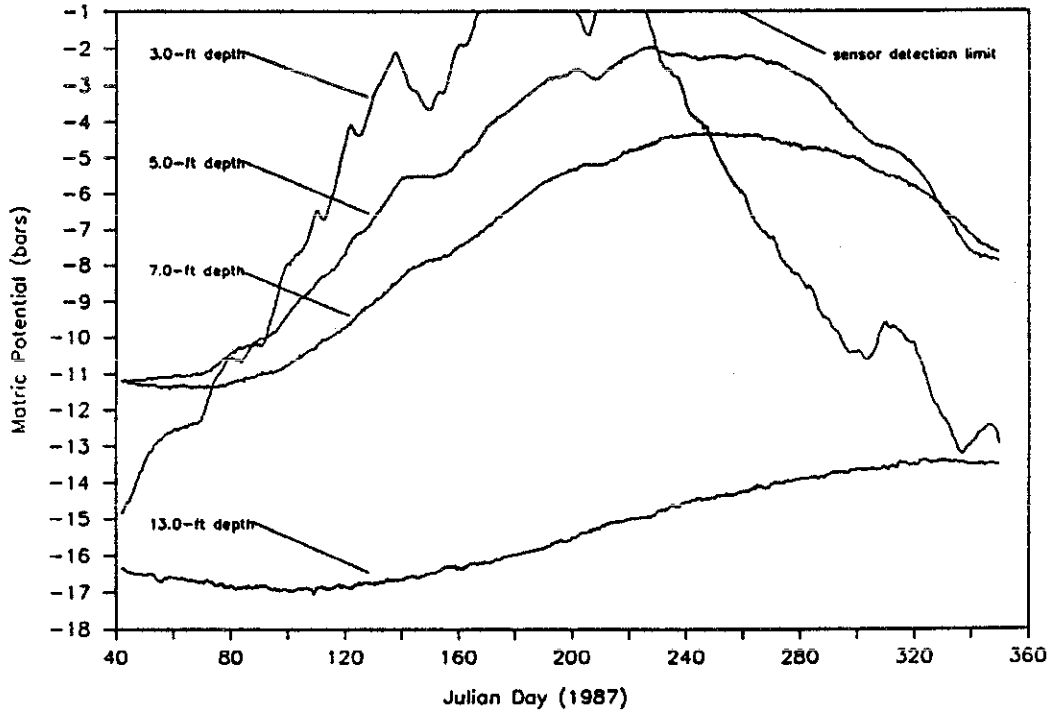

Figure 12. Soil-water potentials at four depths at the west test trench.

5. SPECIFIC STUDIES

Of the specific studies outlined in the 1983 DOE report, five were continued or initiated in FY-1987. These are: Characterization of Geologic Materials, Solution Chemistry, Net Downward Flux, Computer Model Development, and Radionuclide Concentrations. In addition, another study, Organic Vapor Characterization, was initiated at the beginning of FY-1988 in response to the detection of volatile organic compounds during drilling operations at the RWMC.

5.1 Characterization of Geologic Materials

5.1.1 Introduction

The objectives of this specific study are to quantify physical and chemical properties of surficial sediments, basalt, fracture fill material and interbed sediments. These data will ultimately be used to determine the properties of radionuclide sorption and migration within the geologic section of basalts and sedimentary interbeds underlying the RWMC.

5.1.2 Summary of Accomplishments

Sediment samples taken from the interbeds during the deep drilling activities were characterized. Descriptions of these samples are presented in Appendix A. Samples obtained from the surficial sediments near the weighing lysimeter and test trench projects are described in Appendix B. Several cross-sections, a fence diagram, and sand trend maps were constructed in order to gain a greater understanding of the subsurface sedimentary patterns. Analysis of this information will aid in the effort to predict the movement of moisture and migration of radionuclides through the vadose zone.

5.1.3 Discussion

The data obtained from the drilling program are being used in the effort to develop a conceptual model of the sedimentary and basalt layers underlying the RWMC. Borehole construction diagrams, structural cross-sections, fence diagrams, geologic structural maps, and sand thickness maps are useful tools in this effort.

Figures 3, 4, and 5 (see Section 4.1.3.2) are borehole construction diagrams illustrating the geophysical logs and the stratigraphy of boreholes TW1, D15, and D02.

Geologic cross-sections are important in the understanding of lateral and vertical changes between adjacent rock and sediment units. Three structural cross-sections extending through the RWMC have been constructed. Figure 13 is a map showing the locations of the cross-sections relative to the RWMC. The cross-sections are presented in Figures 14, 15, and 16. The thickening and thinning of the interbeds and the slopes of the interfaces are shown in the cross-sections.

Figure 17 presents a fence diagram showing a three-dimensional perspective of the lateral and vertical changes in the interbed strata underlying the RWMC. The fence diagram actually shows how the three cross sections (Figures 14, 15, and 16) are interrelated.

Figures 18 through 23 are structural and sand thickness maps of the 30-ft, 110-ft, and 240-ft interbeds. The structural maps were constructed for the base of each interbed; these represent the topography of the surface of the basalts on which the interbeds were deposited. A structural low depicts a stream channel area, while the high shows an interchannel ridge. The sand thickness maps indicate areas of sedimentary thickness. A comparison of the structural map and sand thickness map for an interbed, shows that the channel areas accumulated the thickest sedimentary units.

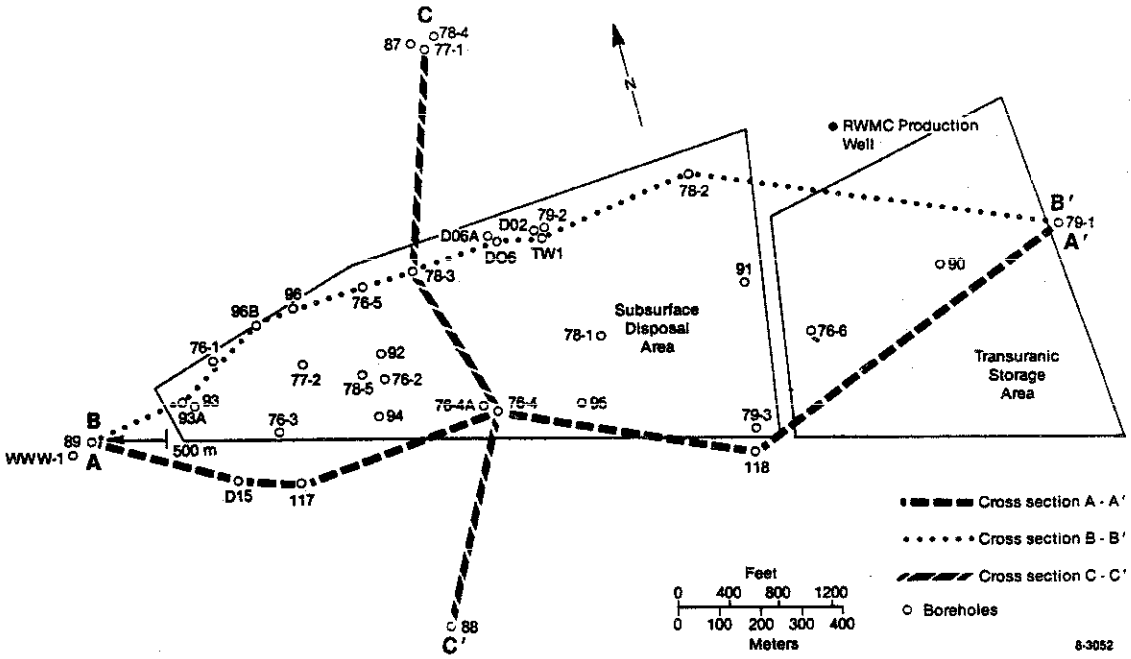

Figure 13. Locations of cross-sections shown in Figures 14, 15, and 16 (locations of deep boreholes at the RWMC are shown also).

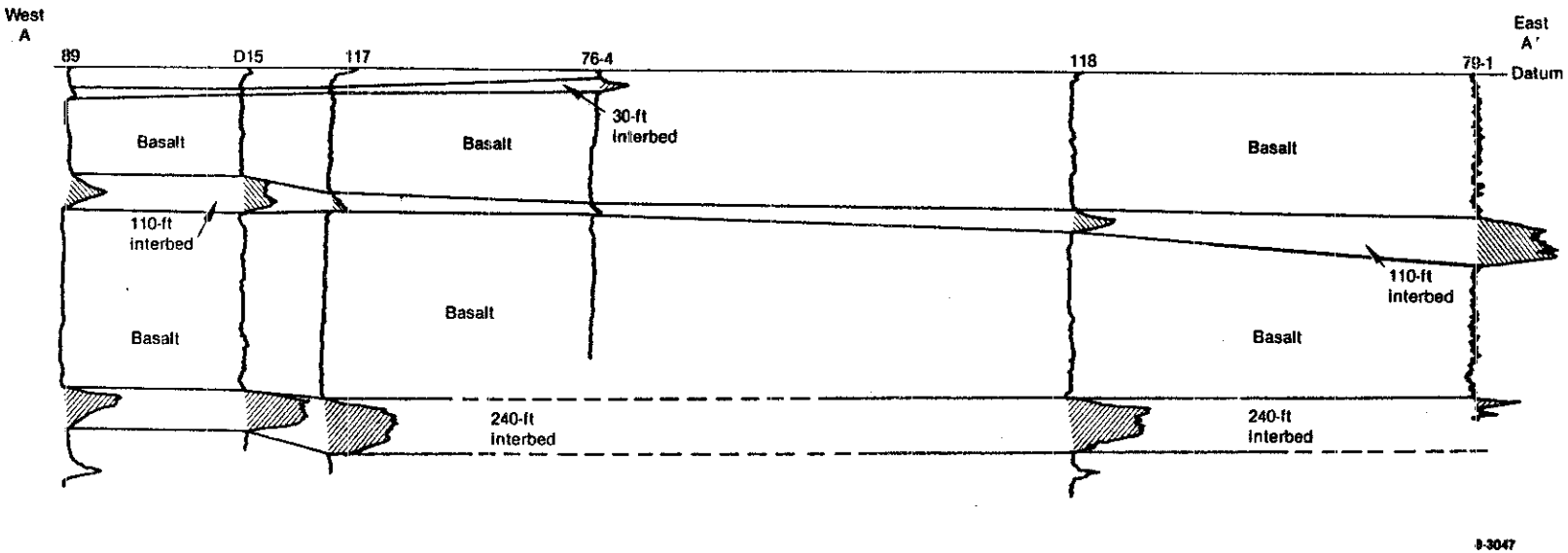

Figure 14. Cross-section A to A' (see Figure 13) based on gamma-ray log correlation.

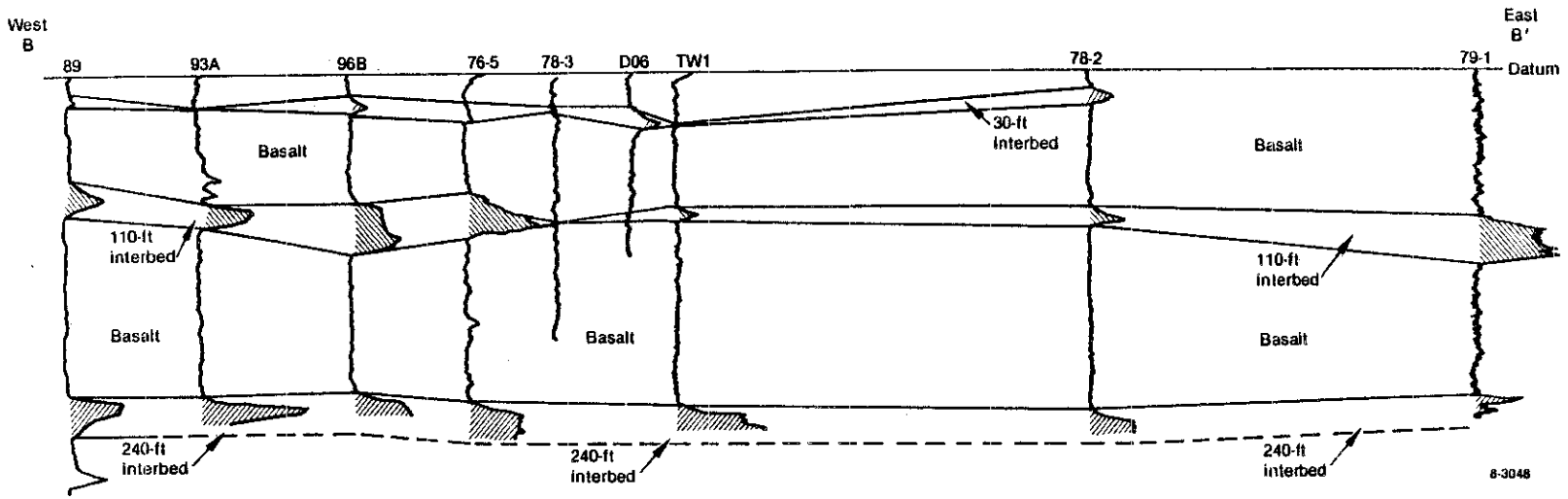

Figure 15. Cross-section B to B' (see Figure 13) based on gamma-ray log correlation.

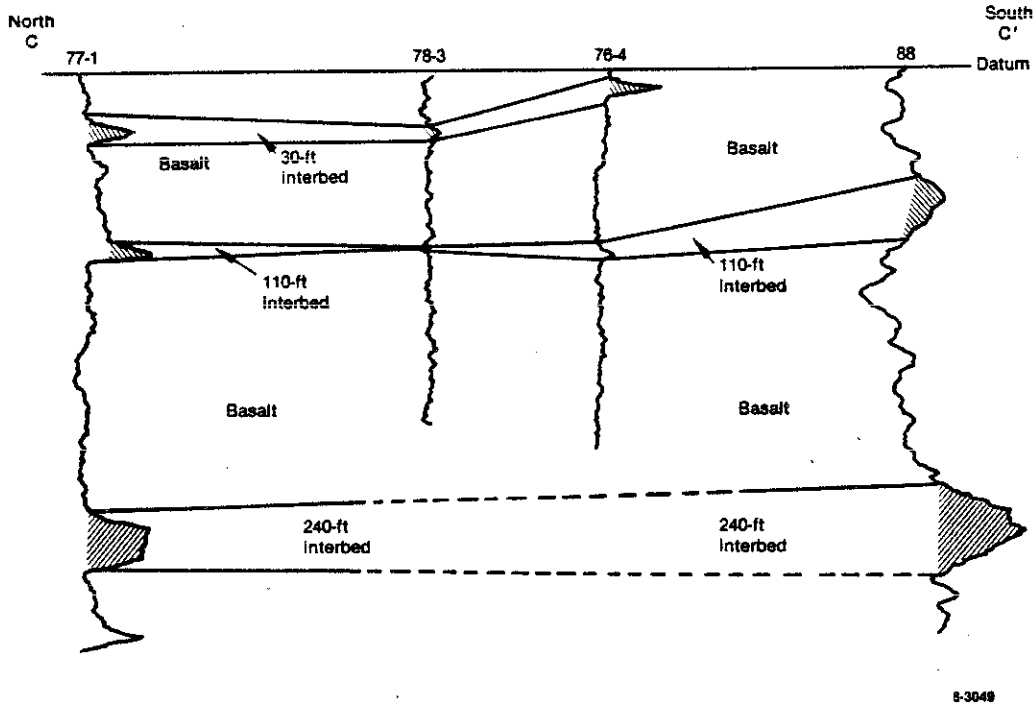

Figure 16. Cross-section C to C' (see Figure 13) based on gamma-ray log correlation.

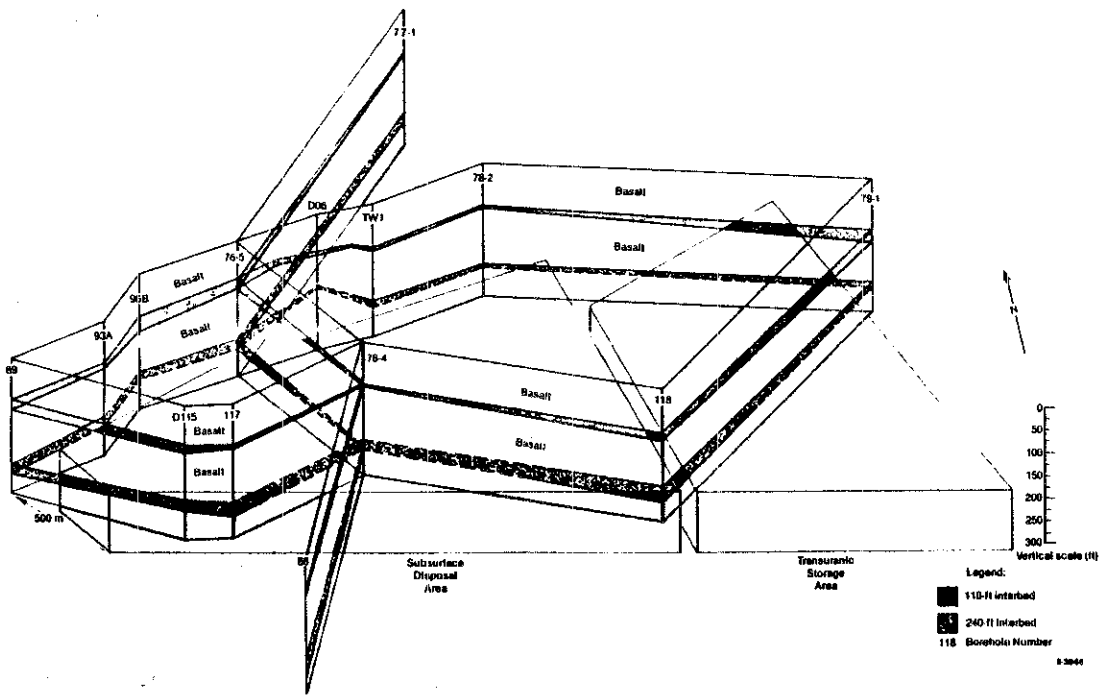

Figure 17. Fence diagram of the geologic structures underlying the RWMC.

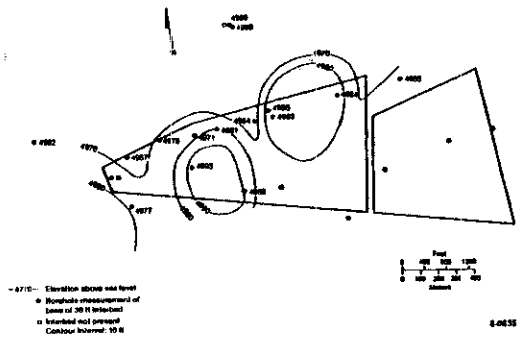

Figure 18. Structural map of the base of the 30-ft interbed.

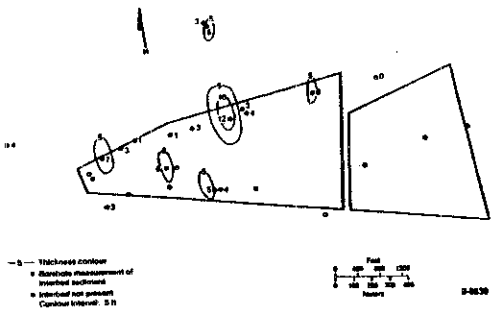

Figure 19. Thickness map of the 30-ft interbed.

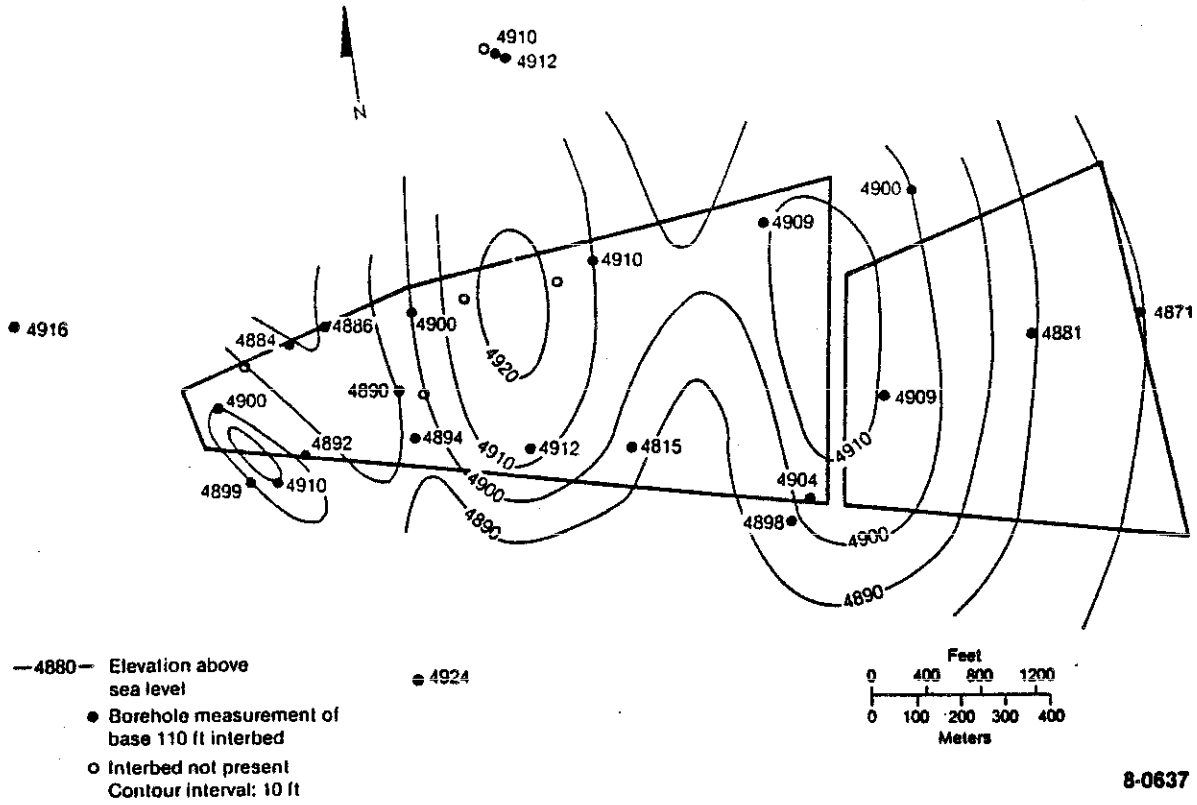

Figure 20. Structural map of the base of the 110-ft interbed.

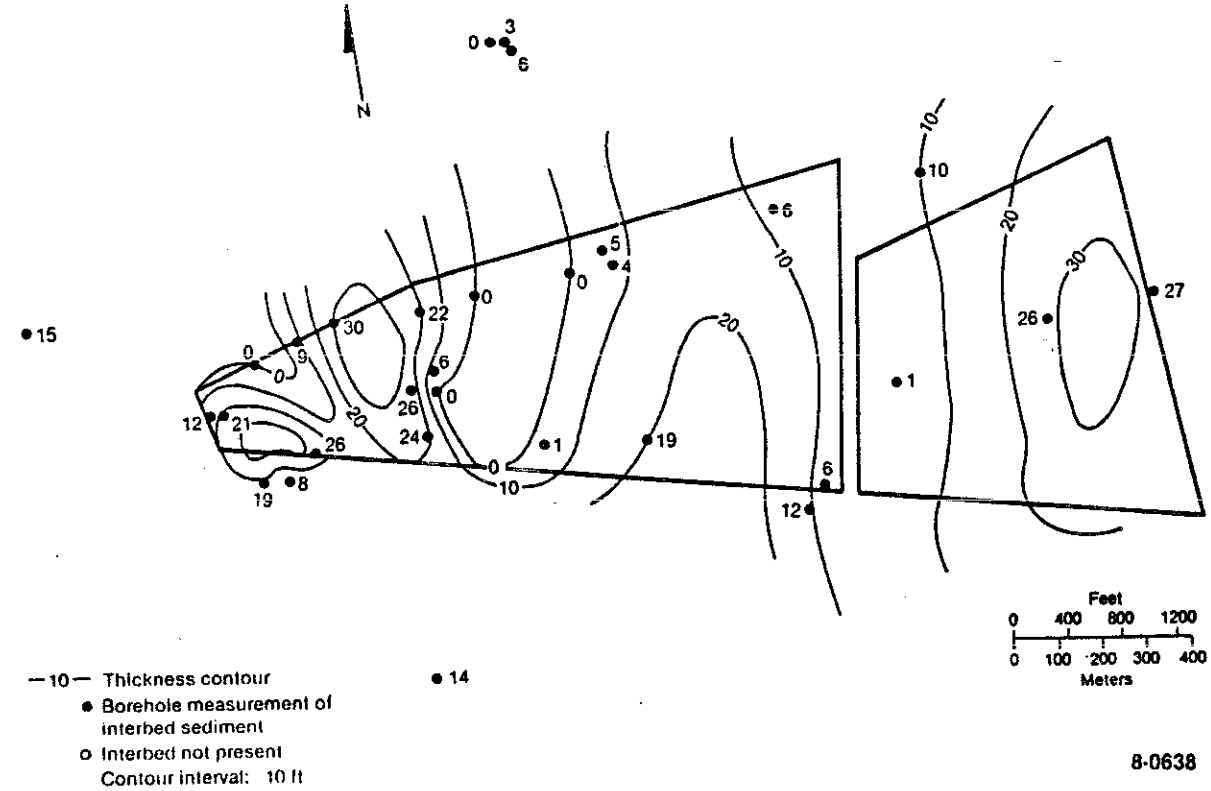

Figure 21. Thickness map of the 110-ft interbed.

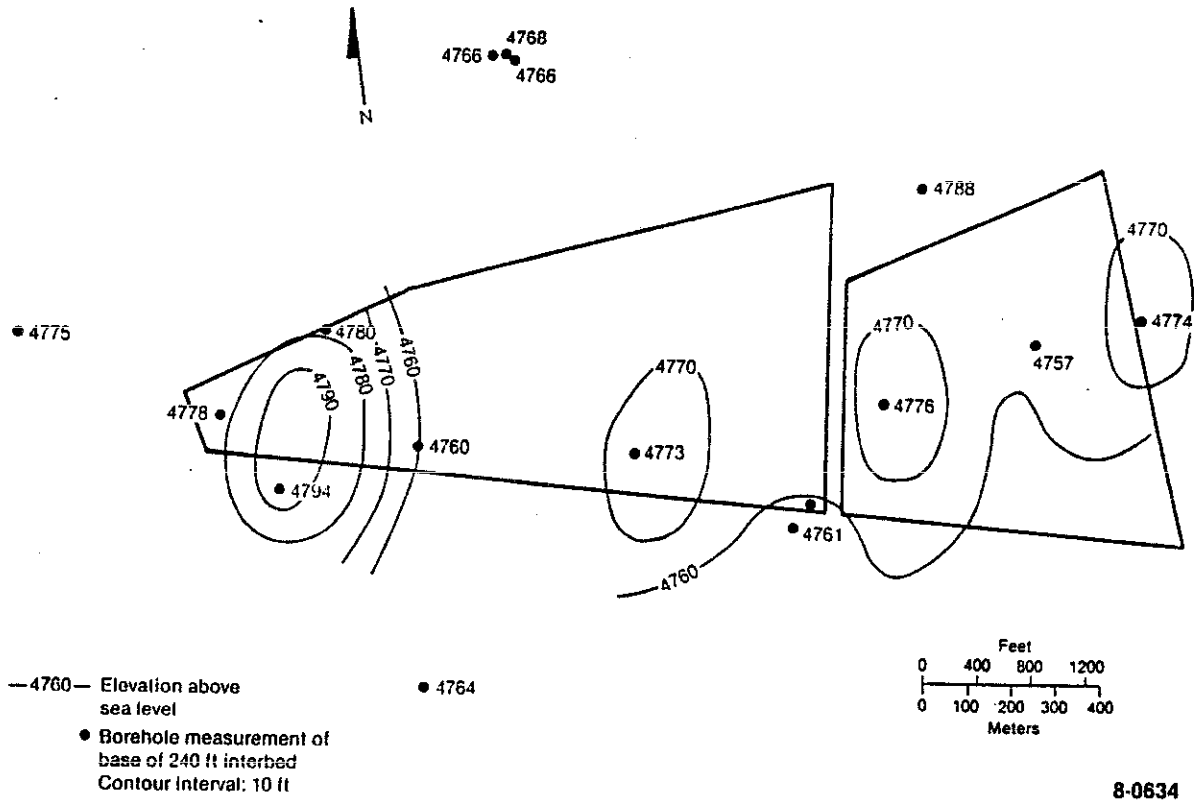

Figure 22. Structural map of the base of the 240-ft interbed.

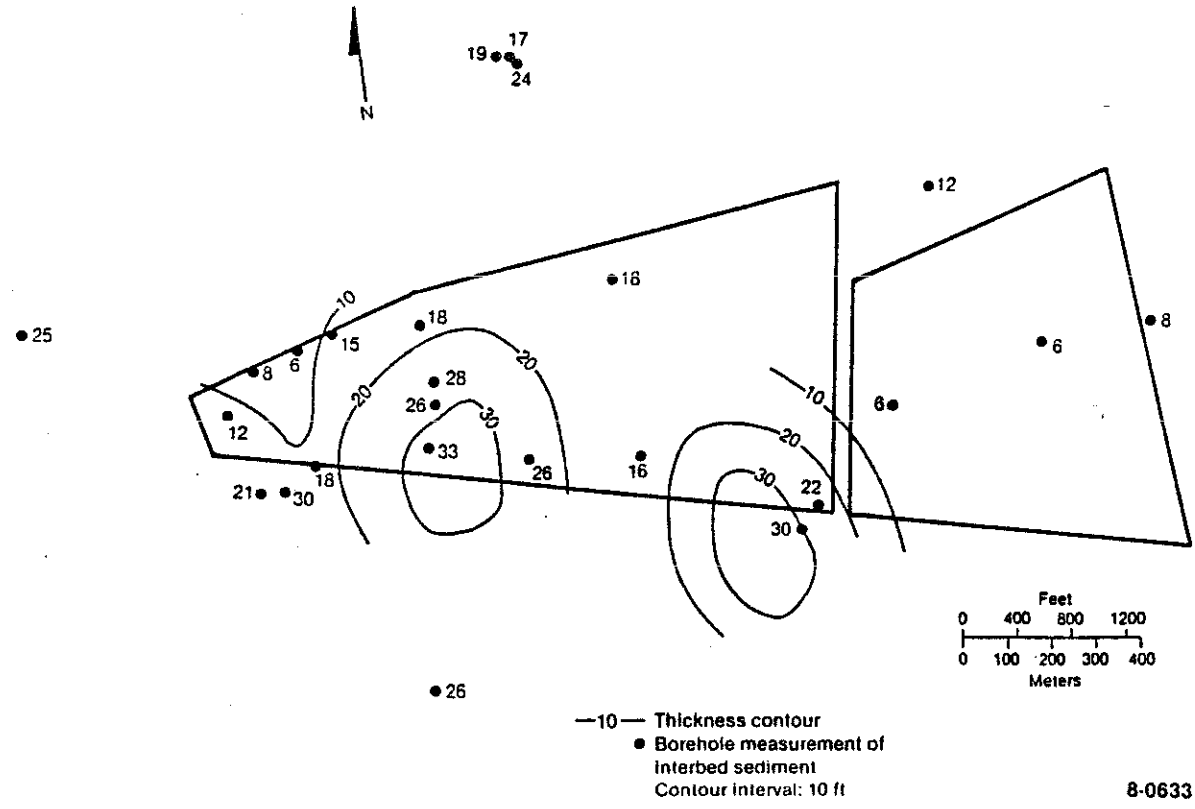

Figure 23. Thickness map of the 240-ft interbed.

The structural and sand thickness maps of the 110-ft interbed best illustrate this stream channel pattern. Refer to Figures 20 and 21. A structural high exists in the central portion of the SDA, trending along the north-south axis of cross-section C to C' (Figure 13). This is also an area of a sedimentary thin, an interchannel ridge. The same pattern of a structural high and a sedimentary thin occurs in the 110-ft interbed below the boundary between the SDA and the TSA. Conversely, the structural low at the western end of the SDA corresponds to a depositional thick, which indicates a stream channel in the 110-ft interbed.

Similar sand trends are also illustrated in the structural and sand thickness maps of the 30-ft and 240-ft interbeds.

A comprehensive interbed study is currently underway. By combining several sources of sedimentological data (i.e., lithologic descriptions, subsurface maps, outcrop investigations), the Subsurface Investigations Program will be able to gain a better understanding of the subsurface at the RWMC.

5.2 Solution Chemistry

5.2.1 Introduction

The first objective of the Solution Chemistry Study is to determine the major ion chemistry, pH, and redox potential of solutions in soil and basalt at the RWMC. This information will be used in the predictive model of radionuclide transport at the RWMC. The second objective is to define the actual radionuclide migration by monitoring for radionuclides in soil waters collected using porous cup lysimeters. The Solution Chemistry Study consists of installing porous cup lysimeters in augered and drilled holes, collecting samples of soil water, analyzing the water samples, and utilizing the resultant data for prediction of radionuclide migration.

5.2.2 Summary of Accomplishments

Five porous cup lysimeters were installed in two deep boreholes at the RWMC during FY-1987. A soil-water sample was collected and analyzed from only one of these lysimeters (DL04). In all, samples from 22 of the 39 lysimeters installed since FY-1985 were collected and analyzed for major ion chemistry. Of the 17 not sampled, three were new installations, four are teflon lysimeters (which are no longer sampled), two require reserve air tanks, and eight had temporarily dry soil.

5.2.3 Discussion

Five porous cup lysimeters were installed during FY-1987. Three of these lysimeters were installed in borehole D15 at depths of 30 ft, 110 ft, and 240 ft. The other two lysimeters were installed in borehole TW1 at the 110 ft and 240 ft interbeds. One of those lysimeters (DL04) yielded a soil-water sample. Figure 2 (see Section 4.1.2) shows the locations of all shallow and deep Subsurface Investigations Program boreholes drilled at the RWMC since FY-1985. Table 3 shows the installation dates, installation depths, and status of all lysimeters installed to date. As described in the FY-1986 annual report (Hubbell et al., 1987), a number of lysimeters leak and thus require the use of a reservoir air tank to increase the effective volume of the lysimeter for samples to be collected. The volume of the air tank used or needed is shown in Table 3.

Details on the procedures used to install the porous cup lysimeters are given in the FY-1985 annual report (Hubbell et al., 1985). Modifications to those procedures are described in the FY-1986 annual report (Hubbell et al., 1987). No significant changes were introduced to lysimeter installation procedures for the current year. Water is still added to the silica flour during installation to ensure that good contact is achieved between the native soil and the lysimeter. A 10 mg/L potassium bromide (KBr) tracer was added to the water to determine when valid samples can be collected.

TABLE 3. STATUS OF POROUS CUP LYSIMETERS INSTALLED AT THE RWMC

Instrument Number	Date Installed	Depth Installed (ft-in.)	Status of Lysimeter
Borehole D06			
DL01	09/12/86	88-0	holds pressure but soil dry
DL02	09/12/86	44-0	uses 5.0-gal air tank
Auger Hole TW1			
DL03	06/25/87	226-11	may be too dry to sample
DL04	06/25/87	101-8	good condition
Auger Hole D15			
DL05	09/15/87	222-11	not sampled yet
DL06	09/15/87	97-11	not sampled yet
DL07	11/04/87	32-2	not sampled yet
Auger Hole W02			
L01	06/14/85	14-0	uses 7.5-gal air tank
Auger Hole W03			
L02	06/17/85	10-6	uses 7.5-gal air tank
Auger Hole W04			
L03	06/19/85	24-6	uses 7.5-gal air tank
L04	06/19/85	15-5	uses 7.5-gal air tank
L05	06/19/85	6-2	holds pressure, but temporarily dry
Auger Hole W20			
L06	06/28/85	6-8	teflon, no sample[a]
Auger Hole W23			
L07	06/28/85	18-10	teflon, no sample[a]
L08	06/28/85	11-10	uses 7.5-gal air tank
L09	06/28/85	7-8	good condition
Auger Hole T23			
L10	07/02/85	19-0	teflon, no sample[a]

TABLE 3. (continued)

Instrument Number	Date Installed	Depth Installed (ft-in.)	Status of Lysimeter
Auger Hole C02			
L11	07/03/85	4-4	teflon, no sample[a]
Auger Hole W08			
L12	07/09/85	22-1	requires 5-gal air tank
L13	07/09/85	11-4	good condition
L14	07/09/85	6-2	uses 7.5-gal air tank
Auger Hole PA01			
L15	07/11/85	14-4	good condition
Auger Hole PA02			
L16	07/11/85	8-8	good condition
Auger Hole TH02			
L17	06/07/85	6-0	good condition--soil temporarily dry
Auger Hole TH04			
L18	04/23/85	4-0	good condition--soil temporarily dry
Auger Hole C01			
L19	08/06/86	17-8	good condition
L20	08/06/86	7-5	good condition
Auger Hole TH05			
L21	09/08/86	15-2	requires air tank, size not determined
L22	09/08/86	5-11	good condition
Auger Hole W09			
L23	09/17/86	14-10	good condition

TABLE 3. (continued)

Instrument Number	Date Installed	Depth Installed (ft-in.)	Status of Lysimeter
Auger Hole W05			
L24	09/22/86	15-11	good condition
L25	09/22/86	10-0	good condition
L26	09/22/86	6-8	good condition
Auger Hole W06			
L27	09/23/86	11-9	good condition
Auger Hole W25			
L28	09/24/86	15-6	requires 2.5-gal air tank
Auger Hole W13			
L29	09/20/86	14-0	requires 2.5- or 5-gal air tank
L30	09/28/86	6-8	good condition
Auger Hole W17			
L31	09/29/86	19-7	good condition--soil temporarily dry
L32	09/29/86	10-11	good condition--soil temporarily dry

a. Teflon lysimeters have low air entry values and therefore will not collect samples except when the soil is nearly saturated.

Table 4 shows the results of the most recent soil-water sample analyses for major ion chemistry from lysimeters installed during FY-1986 and FY-1987. It should be noted that with the exception of DL04, bromide tracer was not detected in any of the samples analyzed. This indicates that water (and KBr) added to the borehole during installation of the silica flour has either dissipated into the surrounding sediments, or has been removed during the previous sampling event. The chemical data shown in Table 4 can thus be considered representative of the sediment water.

TABLE 4. MAJOR ION CHEMISTRY IN SOIL-WATER SAMPLES FROM THE RWMC

Lysimeter Number	Date Sampled	Na (mg/L)	K (mg/L)	Ca (mg/L)	Mg (mg/L)	SiO_2 (mg/L)	B (mg/L)	Li (mg/L)	Sr (mg/L)	Zn (mg/L)	HCO_3 (mg/L)	CL (mg/L)	F (mg/L)	SO_4 (mg/L)	Br (mg/L)	PO_4 (mg/L)	TDS[a] (mg/L)
DL02	9/02/87	1652.10	36.14	488.37	371.98	81.40	0.00	0.10	2.93	0.51	125.00	3150.00	0.50	1430.00	0.00	2.04	7315.00
DL04	9/10/87	63.35	6.65	116.44	26.79	76.94	0.05	0.10	0.75	0.00	297.00	135.00	0.38	131.00	7.70	0.00	686.00
L01	9/03/87	152.62	1.19	34.75	10.53	76.99	0.16	0.00	0.27	0.06	408.00	34.00	1.50	97.00	0.00	0.00	598.00
L02	9/04/87	3920.00	26.35	2434.75	1465.00	79.80	0.00	0.11	16.78	1.06	196.00	12,500.00	0.34	0.00	0.00	0.00	23,128.00
L03	9/05/87	438.83	2.80	61.81	21.47	67.75	0.14	0.06	0.45	0.51	1387.00	5.00	0.72	139.00	0.00	0.00	0.00
L04	9/04/86	381.49	3.64	81.01	45.32	72.03	0.24	0.08	0.81	0.49	1213.00	11.00	1.40	194.00	0.00	0.00	1294.00
L08	9/04/87	1534.76	11.16	416.87	104.87	84.33	0.46	0.07	1.89	0.48	540.00	1465.00	0.35	2063.00	0.00	0.00	6222.00
L09	9/02/87	949.65	5.99	58.16	35.83	87.33	0.62	0.08	0.84	0.31	1184.00	524.00	0.95	658.00	0.00	0.00	3170.00
L13	9/04/87	320.98	18.00	126.15	79.43	78.46	0.28	0.06	1.37	0.32	727.00	75.00	0.75	654.00	0.00	0.00	1848.00
L15	4/08/87	716.75	5.16	77.59	44.88	75.19	1.52	0.00	0.64	0.00	1560.00	153.00	2.00	372.00	0.00	0.00	2392.00
L16	9/03/87	751.40	4.34	69.05	41.75	70.73	1.23	0.00	0.63	0.00	1621.00	173.00	2.10	377.00	0.00	0.00	2388.00
L17	9/03/87	820.82	7.23	215.82	112.23	87.75	0.11	0.16	1.87	0.00	893.00	239.00	0.71	1690.00	0.00	0.00	3818.00
L19	9/03/87	127.25	2.47	69.31	23.29	79.03	0.06	0.00	0.47	0.16	152.00	17.00	0.73	355.00	0.00	0.00	792.00
L20	9/03/87	30.98	2.70	90.58	29.06	91.32	0.06	0.00	0.73	0.00	129.00	5.00	0.48	293.00	0.00	0.00	668.00
L21	9/14/87	106.46	5.10	61.55	16.23	72.82	0.00	0.00	0.35	0.08	388.00	1.40	0.73	150.00	0.00	0.00	0.00
L23	9/08/87	45.34	3.95	108.32	49.72	74.62	0.07	0.00	0.97	0.00	458.00	42.00	0.24	167.00	0.00	0.00	3094.00
L24	9/03/87	335.87	3.16	61.96	39.67	72.97	0.10	0.00	0.41	0.00	478.00	136.00	0.40	467.00	0.00	0.00	1438.00
L25	9/03/87	2862.50	14.18	2060.25	1664.00	74.77	0.56	0.13	15.24	0.44	193.00	10,900.00	0.30	2060.00	0.00	0.00	20,390.00
L26	9/03/87	3785.00	18.70	1258.25	1127.00	84.72	1.37	0.18	14.03	0.84	231.00	9075.00	1.10	2290.00	0.00	0.00	17,670.00
L27	9/04/87	241.19	2.72	34.57	16.87	77.88	0.27	0.00	0.26	0.13	479.00	17.00	0.97	257.00	0.00	0.00	900.00
L28	9/04/87	36.77	4.60	114.86	48.39	76.03	0.08	0.00	1.10	0.07	453.00	34.00	0.35	169.00	0.00	0.00	744.00
L29	8/27/87	173.00	6.50	77.24	67.75	71.96	0.29	0.04	1.00	0.15	213.00	74.00	0.95	348.00	0.00	0.00	1236.00

a. Total dissolved solids.

DL04 was the only FY-1987 installed lysimeter sampled. The presence of bromide in the DL04 chemical data suggests that the water used during borehole construction and instrumentation is still present in the immediate vicinity of the lysimeter.

Overall, the soil waters from the RWMC show a broad range in composition. The only parameter to show consistency is dissolved silica. The recorded concentrations are indicative of equilibration between the soil water and the silica flour emplaced during borehole construction and instrumentation, and not the result of natural soil processes.

Elevated concentrations of Na, K, Ca, Mg, Cl, SO_4, and total dissolved solids were recorded for five soil water samples collected from lysimeters DL02, L02, L08, L25, and L26. The five lysimeters are located randomly over the RWMC. Natural soil exchange processes could account for part of the Na, K, Ca, Sr, and total dissolved solids detected in these lysimeters. It is known that a magnesium chloride solution was used to treat roads for dust suppression at the RWMC. All those lysimeters except DL02 are located in boreholes near treated roads. It is possible that the MgCl treatment has influenced the chemistry of soil waters near these roads. However, it should be pointed out that there are other samples (see Table 4) that show low concentrations of magnesium and chloride, even though they, too, are located in close proximity to these roads.

No apparent trends exist for other ions showing elevated concentrations. At the present time, the number of analyses for individual lysimeters is insufficient to show any trends or indicate whether the above mentioned lysimeters show consistently high specific ion concentrations. Two or three samplings per year would allow for the analysis and detection of trends, as well as the evaluation of seasonal soil water chemistry fluctuations.

Twelve soil water samples collected from lysimeters were subjected to radiochemical analyses. The results of these analyses are presented in Section 5.6.

5.3 Organic Vapor Characterization

5.3.1 Introduction

Organic constituents were detected in water samples collected from RWMC aquifer monitoring wells and by personnel involved in drilling operations during FY-1987. These findings resulted in modifications to the Subsurface Investigations Program and implementation of a new specific study, Organic Vapor Characterization. The work done as a part of this new study has produced a significant set of data that will require further integration with the RWMC Subsurface Investigations Program. The following discussion summarizes the results of the activities initiated late in FY-1987 and early in FY-1988 in response to the detection of organic constituents at the RWMC.

5.3.2 Summary of Accomplishments

Water samples were collected from RWMC aquifer monitoring wells and analyzed for the presence of organic compounds. Organic vapors were detected emanating from boreholes drilled during the deep drilling activity. A survey of organic wastes stored at the RWMC was conducted. A soil gas survey was conducted, and samples collected during the survey were analyzed.

5.3.3 Discussion

In response to a DOE request, groundwater samples were collected in June, July, and August 1987 from wells in and associated with the RWMC. Samples were analyzed for 36 purgeable organic constituents (Table 5). Concentrations of carbon tetrachloride (CBT), chloroform, 1,1,1 trichloroethane (TCA), and trichloroethylene (TCE) were found above detection limits in several RWMC wells (see Table 6), although all samples but one were below proposed EPA maximum concentration levels of 5 µg/L for drinking water. Locations of the RWMC production well, perched water

TABLE 5. PURGEABLE ORGANIC COMPOUNDS FOR WHICH ANALYSES WERE PERFORMED

Benzene	Cis-1,3-Dichloropropene
Bromoform	Trans-1,3-Dichloropropene
Carbon tetrachloride	1,3-Dichloropropene
Chlorobenzene	Ethylbenzene
Chloroethane	Methyl bromide
2-Chloroethyl vinyl ether	Styrene
Chloroform	Methylene chloride
Chloromethane	1,1,2,2-Tetrachloroethane
Dibromochloromethane	Tetrachloroethylene
Dichlorobromomethane	Toluene
1,2-Dichlorobenzene	Trichlorofluoromethane
1,3-Dichlorobenzene	1,1,1-Trichloroethane
1,4-Dichlorobenzene	1,1,2-Trichloroethane
Dichlorodifluromethane	Trichloroethylene
1,2-Dibromoethylene	Vinyl chloride
1,1-Dichloroethane	Xylenes, mixed
1,2-Dichloroethane	
1,1-Dichloroethylene	
1,2-trans-Dichloroethylene	
1,2-Dichloropropane	

well 92, and aquifer wells 87, 88, 89, and 90 are shown in Figure 24. Wells 9, 105, and 109 are located about 2 miles south of the RWMC near the INEL boundary, and well 86 is located about 4 mi west of the RWMC.

Resampling of the RWMC aquifer monitoring wells and the RWMC production well was performed in October 1987 under rigorous sample collection and quality assurance/quality control procedures. Duplicate samples were provided to EG&G Idaho subcontractor laboratories and the USGS Laboratory in Denver.

The analytical results show repeatable detections of organic constituents in water samples from RWMC aquifer wells 87, 88, and 90, and significantly high concentrations in perched well 92 water samples. Well 88, which lies downgradient from the RWMC with respect to aquifer flow, showed the highest concentrations of volatile organic compounds

TABLE 6. RWMC AND VICINITY GROUNDWATER MONITORING RESULTS (μg/L)[a]

Well Number	Date Sampled	Carbon tetra-chloride	Chloroform	1,1,1-Trichloro-ethane	Trichloro-ethylene	Tetrachloro-ethylene	Dichloro-difluoro-methane	Toluene	1,1-Dichloro-ethane	1,1-Dichloro-ethylene	Remarks
87	06/03/1987	3.0	3.0	3.0	3.0	3.0	3.0	3.0	3.0	3.0	--
	08/11/1987	0.3	0.2	0.2	0.2	0.2	0.2	0.2	0.2	0.2	--
	09/23/1987	0.7	0.2	0.2	0.2	0.2	0.2	0.2	0.2	0.2	--
88	06/03/1987	6.6	3.0	3.0	3.0	3.0	3.0	3.0	3.0	3.0	--
	07/08/1987	2.7	0.2	0.6	1.1	0.2	0.3	0.2	0.2	0.2	40 minutes of pumping
		3.2	0.2	0.7	1.2	0.2	0.2	0.2	0.2	0.2	1 hour of pumping
		3.1	0.2	0.7	1.2	0.2	0.2	0.2	0.2	0.2	2 hours of pumping
		2.9	0.2	0.6	1.2	0.2	0.2	0.2	0.2	0.2	3 hours of pumping
		2.8	0.2	0.6	1.2	0.2	0.2	0.2	0.2	0.2	4 hours of pumping
	07/15/1987	4.4	1.0	0.9	1.4	0.2	0.2	0.2	0.2	0.2	--
	08/11/1987	2.1	0.4	0.4	1.2	0.2	0.2	0.2	0.2	0.2	--
	09/22/1987	2.9	0.7	0.5	1.1	0.2	0.2	0.2	0.2	0.2	--
89	06/03/1987	3.0	3.0	3.0	3.0	3.0	3.0	3.0	3.0	3.0	--
	08/12/1987	0.2	0.2	0.2	0.2	0.2	0.2	0.2	0.2	0.2	--
	09/22/1987	0.2	0.2	0.2	0.2	0.2	0.2	0.2	0.3	0.2	
90	06/03/1987	3.0	3.0	3.0	3.0	3.0	3.0	3.0	3.0	3.0	--
	08/11/1987	0.6	0.2	0.2	0.2	0.2	0.2	0.2	0.2	0.2	--
	09/23/1987	0.8	0.2	0.2	0.3	0.2	0.2	0.2	0.2	0.2	--
9	07/30/1987	0.2	0.2	0.2	0.2	0.2	0.2	0.3	0.2	0.2	--
	10/05/1987	0.2	0.2	0.2	0.2	0.2	0.2	0.2	0.2	0.2	--
86	08/04/1987	0.2	0.2	0.2	0.2	0.2	0.2	0.2	0.2	0.2	--
	10/06/1987	0.2	0.2	0.2	0.2	0.2	0.2	0.2	0.2	0.2	--
105	07/30/1987	0.2	0.2	0.2	0.2	0.2	0.2	0.2	0.2	0.2	--
	09/28/1987	0.2	0.2	0.2	0.2	0.2	0.2	0.2	0.2	0.2	--
		0.2	0.2	0.2	0.2	0.2	0.2	0.2	0.2	0.2	QA Replicate
109	07/31/1987	0.2	0.2	0.2	0.2	0.2	0.2	0.7	0.2	0.2	--
	10/05/1987	0.2	0.2	0.2	0.2	0.2	0.2	1.0	0.2	0.2	--
92[b]	10/23/1987	1,200	650	140	860	110	0.2	0.2	13	0.8	1,1,2,2-Tetrachloro-ethane, 1.0 μg/L 1,2-Dichloropropane, 5.9 μg/L
	10/22/1987	0.2	0.2	0.2	0.2	0.2	0.2	0.2	0.2	0.2	Equipment blank for well 92; styrene, 0.5 μg/L

TABLE 6. continued

Well Number	Date Sampled	Carbon tetra-chloride	Chloroform	1,1,1-Trichloro-ethane	Trichloro-ethylene	Tetrachloro-ethylene	Dichloro-difluoro-methane	Toluene	1,1-Dichloro-ethane	1,1-Dichloro-ethylene	Remarks
	06/03/1987	3.0	3.0	3.0	3.0	3.0	3.0	3.0	3.0	3.0	--
	08/11/1987	1.0	0.2	0.2	0.5	0.2	0.2	0.2	0.2	0.2	--
	09/23/1987	1.3	0.2	0.3	0.5	0.2	0.2	0.2	0.2	0.2	--
	10/14/1987	1.5	0.2	0.5	0.6	0.2	0.2	0.2	0.2	0.2	--

a. Analytical results in µg/L (micrograms per liter); indicates the concentration was less than the reporting level.

b. Well 92 taps a perched water body; these samples were not taken from the Snake River Plain Aquifer.

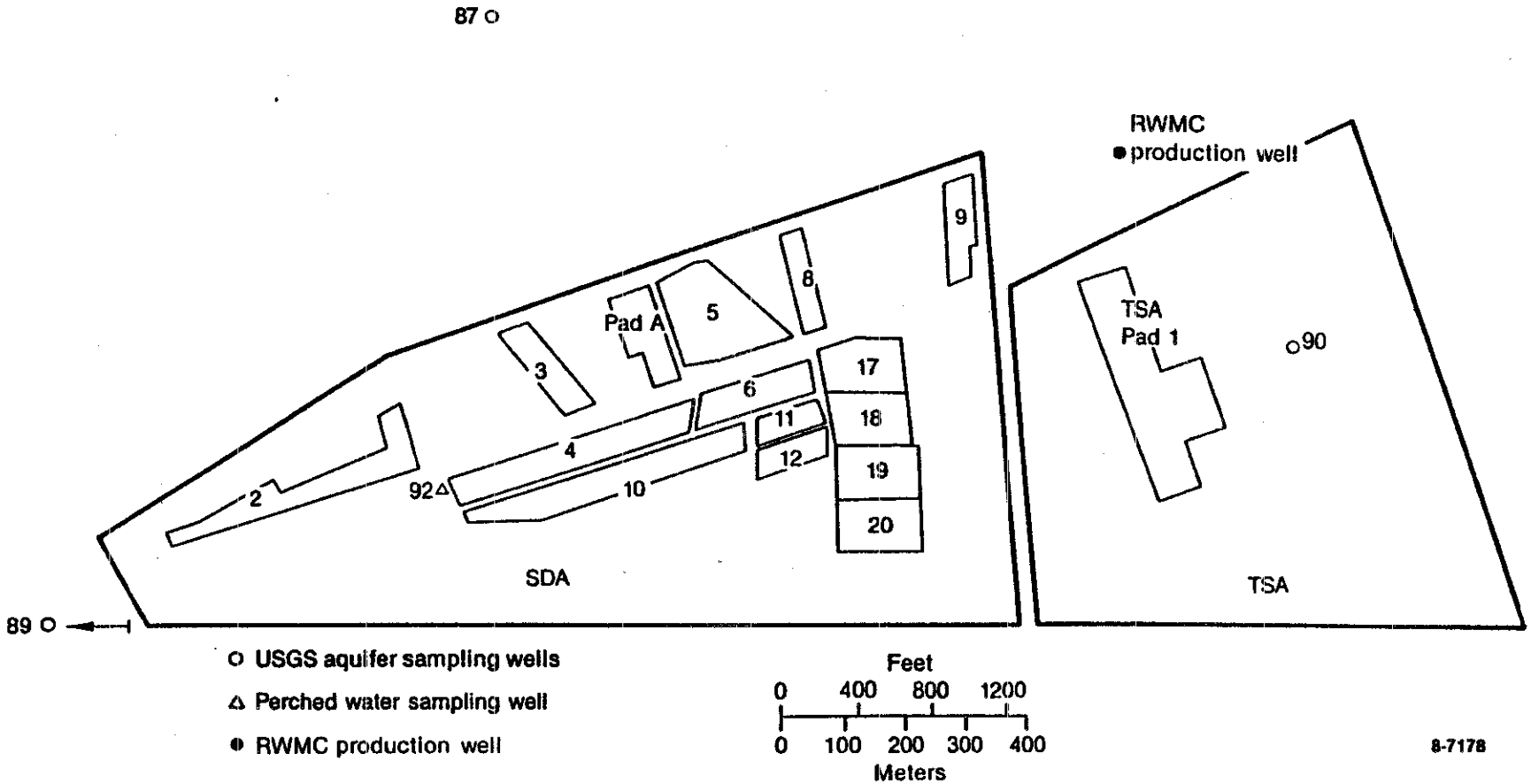

Figure 24. Locations of RWMC aquifer wells and disposal pits.

(VOCs) in the aquifer, primarily carbon tetrachloride, trichloroethylene, and 1,1,1-trichloroethane. RWMC well 89 and well 90 indicated organic concentrations near the detection limit.

The subsurface drilling activities continued, as originally planned, through the summer and into the fall until September 24, 1987, when the casing for borehole D02 was pulled up from the basalt below the 110-ft interbed, exposing several inches of the interbed. At that time, the field crew reported a strong organic odor emanating from the casing at land surface. The following day, organic odors were detected during drilling operations on borehole D10. The vapors were first noticed when the 110-ft interbed was encountered. Gas grab samples were collected on September 25 from boreholes D10 and D02 (Table 7). These samples confirmed the presence of VOCs. Additional gas grab samples were taken on September 29 and 30. Tables 8 and 9 document the results of these sampling efforts. All samples were analyzed with a GC/MS by the Chemical Sciences Laboratory at the INEL.

Well 89 is cased and cemented to 576 ft and has several feet of open hole above the water table. Gas grab samples obtained from this well showed positive results (Table 8), indicating the presence of VOCs as deep as 576 ft in the vadose zone.

These findings in both the groundwater and the vadose zone provided the impetus to further investigate the potential sources of the VOCs and assess the extent of VOC migration. The RWMC waste inventory was thoroughly reviewed so that the source(s) of the VOCs could be identified, and a soil-gas survey was conducted.

5.3.3.1 Examination of Disposal Records. An effort to estimate the types and quantities of hazardous materials disposed of at the RWMC SDA was conducted. The following compilation of data is based on a number of sources. The first, and most extensive, is the Radioactive Waste Management Information System Database. Other sources include responses to

TABLE 7. RESULTS OF ANALYSIS OF GAS SAMPLES FROM BOREHOLES DO2 AND D10 (µg/L) (Groenewold and Pink, 1987)

	DO2	D10		TWA[a]
Chloroform	210	9	12	50[I]
1,1,1-Trichloroethane	95	14	15	45[S,I]
Carbon Tetrachloride	900	130	140	30[S,I]
Trichloroethylene	220	34	38	270[I]
Tetrachloroethylene	20	9	9	335[I]
Toluene	--	--	--	

a. EPA time weighted average values.

S Occupational exposure to skin.

I Occupational exposure for inhalation.

TABLE 8. BOREHOLE GAS SAMPLE ANALYSIS RESULTS (µg/L) (Groenewold and Pink, 1987)

Borehole	DO2	D10	89	DO2[a]	D10[a]	118[a]	Field Blank
Chloroform	230	4	1	0.4	N.D.[b]	N.D.	0.9
1,1,1-Trichloroethane	120	11	0.8	0.4	N.D.	N.D.	2.0
Carbon Tetachloride	1000	200	8	3	N.D.	N.D.	N.D.
Trichloroethyene	380	17	3	0.5	N.D.	N.D.	N.D.
Tetrachloroethene	62	7	0.4	N.D.	N.D.	N.D.	N.D.
Toluene	0.3	--	--	--	--	--	--

a. Working level around hole; sample drawn approximately 3 ft above the opening of the borehole.

b. Not detected.

TABLE 9. SDA GAS SAMPLE ANALYSIS RESULTS[a] (µg/L)

Location	Control	Pad A South	Pad A North	Pit 17 West-Wall	Pit 17 Blasting Area
Chloroform	N.D.[b]	2	N.D.	N.D.	N.D.
1,1,1-Trichloroethane	N.D.	1	0.3	N.D.	N.D.
Carbon Tetrachloride	N.D.	17	N.D.	--[c]	N.D.
Trichloroethene	N.D.	5	N.D.	N.D.	N.D.
Tetrachloroethyene	N.D.	0.5	N.D.	N.D.	N.D.
Tolune	N.D.	1	N.D.	N.D.	N.D.

a. Working levels.

b. Not detected.

c. The sample was cross-contaminated during analysis.

a request by the RWMC for estimates on halogenated solvents disposed of at the RWMC, interviews with waste management personnel familiar with the history of RWMC operations, and estimates of Rocky Flats Plant (RFP) transuranic waste disposed of at the RWMC.

The information presented in Table 10 represents an estimate of the amount and types of hazardous materials disposed of at the RWMC, based primarily on past database records. Based on this estimate, the total volume of potentially hazardous waste buried in the SDA is 49,080 cubic feet. This includes an estimated 11,816 cubic feet of buried TRU organic wastes. Major contributors to this volume, other than the organics from transuranic (TRU) waste, include 23,400 gallons of oils in Oil-Dri, 10,200 gallons of acids in various absorbent materials, 27,600 gallons of sodium (in contaminated pipe), and 6,900 gallons of caustic material. In addition, 53,700 gallons of Santo Wax from the Organic Moderated Reactor

TABLE 10. ESTIMATES OF HAZARDOUS MATERIALS DISPOSED OF IN THE RWMC SUBSURFACE DISPOSAL AREA

Material	Volume (m^3)	Volume (ft^3)	Volume (gal)
Rags[a]	128	4,500	N/A
Oil (in absorbent)	89	3,100	23,400
Lead	170	6,100	N/A
Asbestos/Lagging	100	3,500	N/A
Ethylene Glycol	1.5	50	390
Mercury	8.5	300	2,240
Acids (HF, HCl, etc. in absorbent)	38	1,400	10,200
Organics (Ether, etc.)	25	900	6,700
Santo Wax[b]	200	7,100	53,700
Sodium, Sodium compounds and pipe	105	3,700	27,600
Batteries	0.5	20	N/A
Benzene	0.1	3	20
Animal Carcasses and Feces	71	2,500	N/A
Vehicles[c]	24	860	N/A
Cyanide	<0.01	<0.35	N/A
Meat w/Botulinus	0.05	0.25	N/A
Tritium Vials	2	64	N/A
Zirconium Chips	30	1,100	N/A
Caustic Compounds (NaOH in absorbent, etc.)	26	930	6,900
Paint Chips & Cans	6	210	1,600
Gasoline (absorbed)	5	180	1,300
Ammonia Bottles	0.2	7	N/A
Thallium Oxide	<0.1	<3	N/A
TRU Texaco Regal Oil	148	5,215	39,018
TRU Carbon Tetrachloride	92	3,263	24,413
TRU Other Organics	94	3,338	24,968
Total (approximate)	1,389	49,080	222,450[d]

a. The quality identified assumes 5% of the total rag inventory at the RWMC is oil/solvent soaked.

b. Santo Wax is from the Organic Moderated Reactor Experiment (OMRE); it may not be a hazardous material.

c. Vehicles disposed of at the RWMC were assumed to be driven into the pits with fuel, oil, antifreeze, and batteries left in place. The volume indicated represents 5% of the total vehicle volume.

d. Gallons are not volume equivalent due to some solid materials.

N/A Volume, in gallons, is an inappropriate measure for these materials.

Experiment (OMRE) was disposed of, although it may not be a hazardous material. A complete list of the materials is provided in Table 10.

Most of the TRU-contaminated organic wastes from RFP was received as Organic Setup sludges. These sludges are liquid organic wastes that are mixed with calcium silicate to form a grease or paste-like material. Normally, small amounts of absorbent, such as Oil-Dri, are also mixed with the waste. These organic wastes are mainly lathe coolant [machining oil and carbon tetrachloride, trichloroethylene, and tetrachloroethylene (PCE)]. Of this material, approximately 24,400 gallons are estimated to be carbon tetrachloride. The remaining volume consists of approximately 39,000 gallons of Texaco Regal Oil used in machinery processes and 25,000 gallons of miscellaneous organic wastes (1,1,1-trichloroethane, trichloroethylene, tetrachloroethylene, and lubricating oils). Prior to 1971 or 1972, this mixture was wrapped in plastic bags and placed in 55 gallon drums. Since 1972, 90-mil rigid polyethylene drum liners have been used inside the 55 gallon drums. All TRU waste received prior to 1970 was disposed in the SDA. Receipt of organic wastes from RFP began in August 1966. During 1967-68, the backlog of organic waste (primary lathe coolant) generated during 1953-66 at RFP was processed and shipped to the RWMC for disposal. The RFP organic wastes currently exist in Pits 4, 5, 6, 9, and 10 (Figure 24), although the quantities and exact disposal locations within each pit are uncertain.

Because of the lack of data, some potentially hazardous materials were not included in Table 10. These are:

- Sludges (sewage, evaporator, tank bottom, etc.)
- Resins
- Acid pit contents.

Sludges and resins were not included because of the diversity in sources, and, consequently, the variety in potential constituents. Acid

pit contents were not included because of lack of data. Preliminary interviews indicate that routine disposal of free liquid "cleaning solutions" occurred during the 1960s, but actual volumes and contents are uncertain.

As presented, the table represents a conservative estimate of the hazardous constituents in the SDA. Further efforts to quantify and categorize materials are underway.

5.3.3.2 Soil-Gas Survey. Golder Associates of Redmond, Washington, was contracted to perform the soil-gas survey. The purpose of the survey was to determine the identity, location, and relative concentration of selected chlorinated and aromatic VOCs in the vadose zone at the RWMC and adjacent areas.

To provide a comprehensive analysis of the SDA, a grid with 200-ft spacing in north-south and east-west directions was defined. The grid covered the SDA and the TSA and extended approximately 600 ft beyond the fence of the SDA. All of the grid points inside the SDA were sampled. Sampling of the grid generally stopped one row beyond the SDA fence. In addition to the grid locations, 63 supplemental locations were sampled. Many of these locations were selected to better define areas where high levels of VOCs were detected.

5.3.3.3 Sampling Procedure. Soil gas was extracted by installing a 5/8 in. OD carbon steel pipe into a 1/2 in. hole drilled approximately 30 in. into the ground using a hand-held electric drill. One end of the pipe was fitted with a metal cap to prevent clogging, and the pipe driven into the hole with a sliding hammer. The cap was then displaced using a steel rod inserted through the pipe. A battery operated pump was attached to the top of the probe using a stainless steel quick-connect coupler and surgical rubber tubing. Three to ten pipe volumes were pumped from the probe. An organic vapor analyzer (OVA or HNU) was used to monitor the discharge from the sampling pump. Gas concentrations in the discharge stream stabilized very quickly. The gas sample was collected from just

inside the stainless steel quick-connect by inserting a hypodermic needle on a glass syringe through the surgical tubing. The syringe was then sealed and transported to the field analytical laboratory.

Exceptions to this procedure occurred at the west end of the SDA and where previously installed access tubes existed. At the west end of the SDA, sample probes were driven only 12 in. into the ground because of concern for transuranic waste near the surface. Gas samples were collected from holes 77-1, 78-1, and WWW-1, by pumping through the existing 1/4 in. ID tubing. Samples from neutron access tubes, pits 19 and 20, and within stored transuranic waste in the TSA were collected by lowering a 1/4-in. ID stainless tube down the existing access tube, sealing the top of the access tube, and pumping the sample from the bottom of the access tube.

5.3.3.4 Gas Analysis. Analysis of soil gas samples was performed in a field laboratory set up in a trailer immediately to the north of the SDA. Analyses were performed with an HNU Model 321 field gas chromatograph (GC). The GC was equipped with two silica capillary columns and electron capture and photoionization detectors. Standard mixtures of VOCs were prepared by serial dilution of pure chlorinated and aromatic compounds in dodecane or hexane. Soil gas samples were directly injected into the GC for analysis and the response compared to those of VOC standards. Each sample was screened for 10 chlorinated and two aromatic compounds (Table 11). Chloroform was intended for analysis, but in most chromatograms, the elution of chloroform was obscured by large concentrations of 1,1,1-trichloroethane and carbon tetrachloride. Therefore, no chloroform results are reported from the survey.

A major concern of quality control is to ensure that there is no carry-over of VOCs between samples from contamination of sampling probes, the sampling train, or syringes. All syringes were cleaned using hexane and heated in an oven at 100°C for 10 to 15 minutes before reuse. After cleaning, the syringe was tested by pulling ambient air into the syringe and injecting into the GC. If VOCs were detected by the GC, the syringe was cleaned again. To check for possible cross contamination in the sampling train, blank samples were collected by pulling air through a probe

TABLE 11. TARGET COMPOUNDS FOR THE RWMC SOIL GAS SURVEY

Compound	Detection Limit (µ/L)
1,1,1-Trichloroethane	0.01
Carbon Tetrachloride	0.01
Trichloroethylene	0.01
Tetrachloroethylene	0.01
1,1-Dichloroethylene	0.6
Methylene Chloride	0.6
1,2-Trans-Dichloroethylene	0.6
Trans-1,3-Dichloropropene	0.5
1,2-Dichloropropane	0.6
1,1,2-Trichloroethane	0.6
Benzene	1.0
Toluene	1.0

before installing it in the ground. This sample was then analyzed with the GC. Twenty four such samples were collected and showed that, at most, barely detectable quantities of VOCs were carried over between samples.

In addition, grab air samples were collected during the investigation by INEL personnel and independently analyzed for VOCs. Initial comparisons of the Golder and INEL data are consistent with one another. Further analysis of these data sets is continuing.

5.3.3.5 Results. Of the 12 compounds screened by the survey (Table 11), only four were identified: 1,1,1-trichloroethane, carbon tetrachloride, trichloroethylene, and tetrachloroethylene. As indicated above for chloroform, the GC is not capable of analyzing a complete suite of compounds under all conditions. The numbers generated by the survey give an accurate indication of the relative amounts of VOCs in soil gas at the RWMC, but they do not provide a rigorous quantitative analysis of all the organic compounds. A summary of the soil gas survey data is provided in Appendix C.

An evaluation of the four primary constituents indicated that concentrations of carbon tetrachloride correlate closely with concentrations of trichloroethylene and tetrachloroethylene. Figures 25 and 26 show that most of the samples with high concentrations of carbon tetrachloride also have high concentrations of trichloroethylene and tetrachloroethylene. This relationship suggests that these constituents are mixed together at the source(s). However, the correlation between carbon tetrachloride and 1,1,1-trichloroethane (Figure 27) is substantially different. A significant percentage of the samples high in carbon tetrachloride did not contain detectable levels of 1,1,1-trichloroethane, and vice versa, while some samples contained both constituents in nearly equal proportions. These results suggest that there may be some sources where both constituents occur mixed in near equal proportions and other sources where they occur separately within the SDA. Additional analysis of these data is necessary to address the specific physical and chemical properties of each constituent. This additional effort will be performed in support of the computer modeling activities in FY-1988.

The spatial distribution of carbon tetrachloride is shown in Figure 28. The distributions of trichloroethylene and tetrachloroethylene (see Figures 29 and 30) are similar to the distribution of carbon tetrachloride. Of these three, carbon tetrachloride is the most prevalent and tetrachloroethylene the least prevalent. These compounds exhibit highest concentrations near the southern end of Pit 9, the northern end of Pit 5, the eastern end of Pit 4, and the western end of Pit 10 (compare Figure 24). A lesser area of contamination by these three compounds occurs at and near Pit 2. Whether this area is a source area or just an area where organic vapors accumulate is not clear. Only carbon tetrachloride appears to show movement of plumes away from the pits. There is a concentration of carbon tetrachloride under the drainage ditch along the north boundary of the SDA, and there may be a plume moving to the southwest.

1,1,1-trichloroethane showed a behavior different from that of the other three VOCs (Figure 31). The highest concentrations of 1,1,1-trichloroethane were found in the southern end of Pit 5, the middle

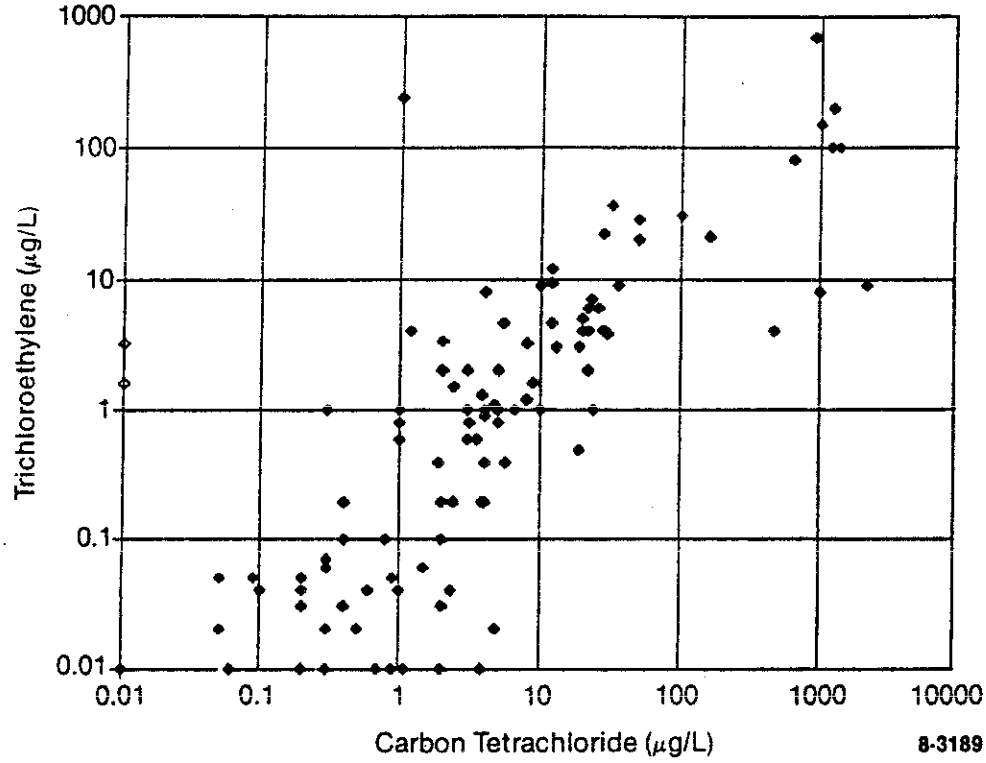

Figure 25. Ratio of carbon tetrachloride to trichloroethylene detected in soil gas survey samples.

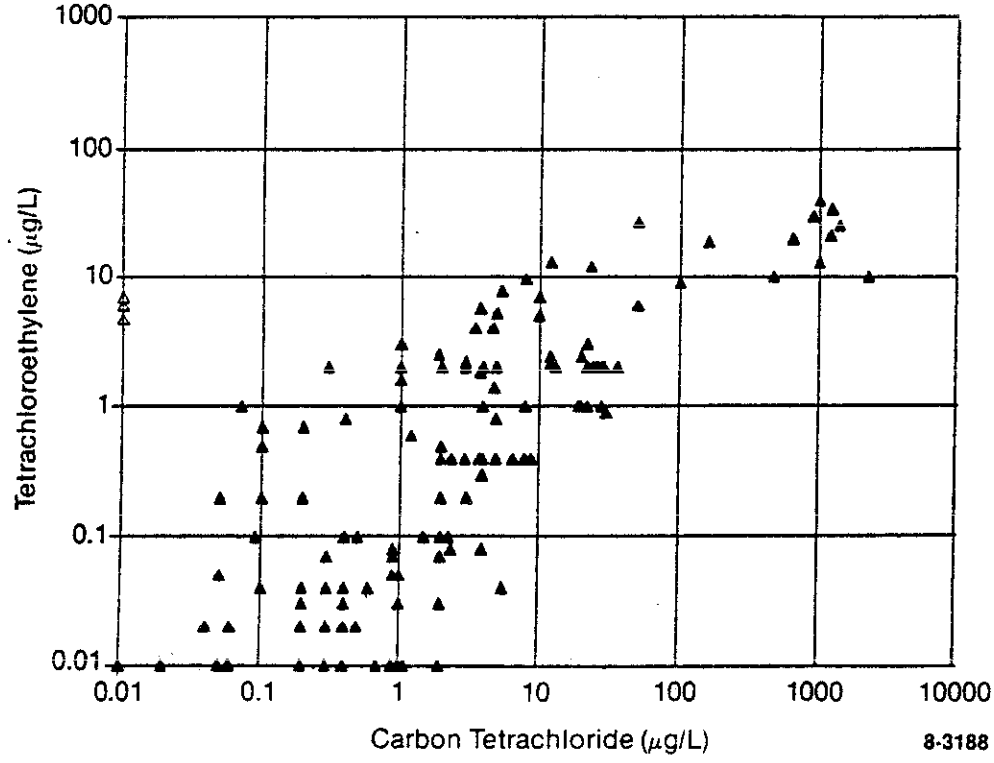

Figure 26. Ratio of carbon tetrachloride to tetrachloroethylene detected in soil gas survey samples.

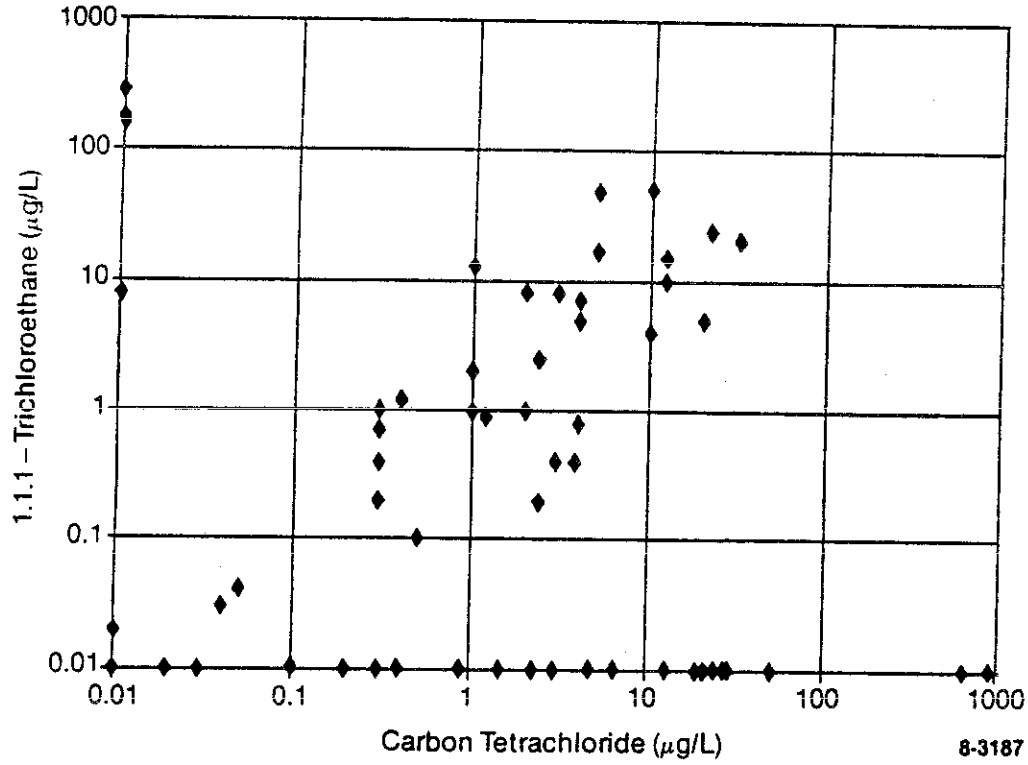

Figure 27. Ratio of carbon tetrachloride to 1,1,1-trichloroethane detected in soil gas survey samples.

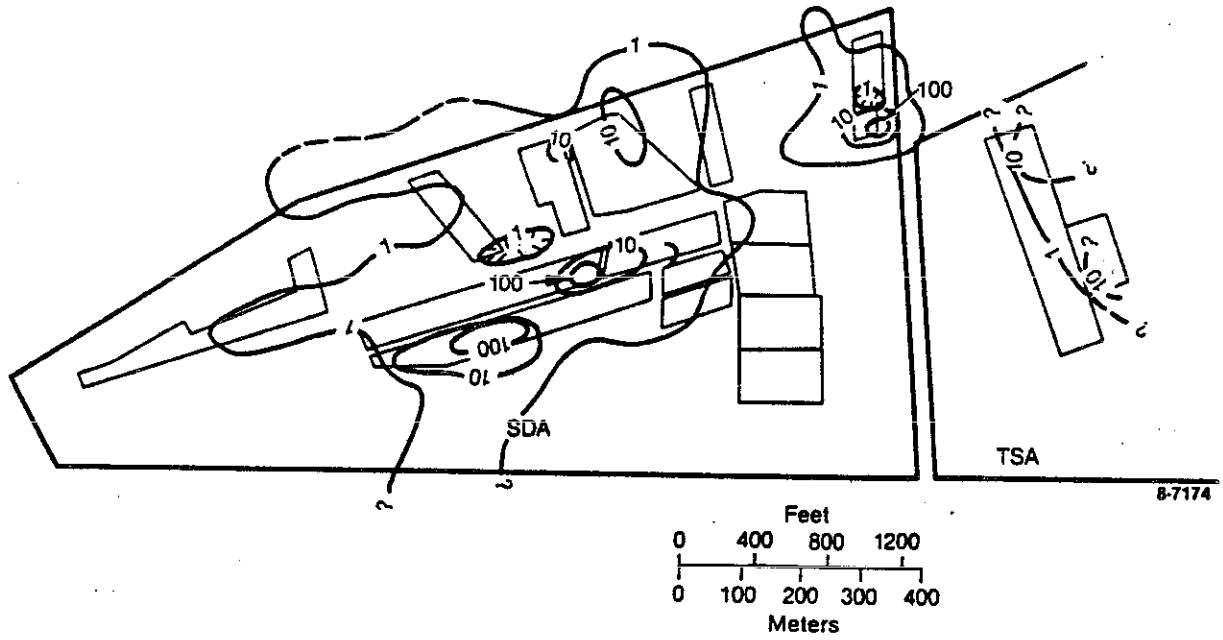

Figure 28. Isopleth map of the concentrations of carbon tetrachloride measured during the soil-gas survey at the RWMC [units of micrograms per liter (μg/L)].

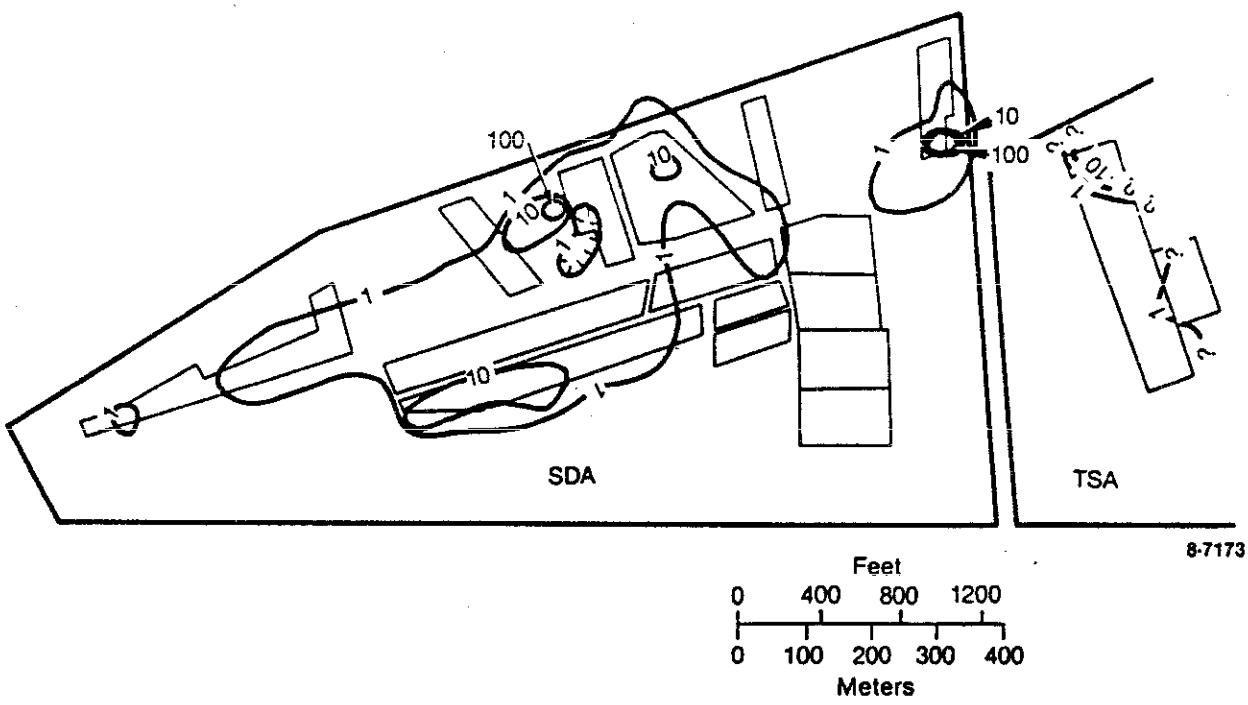

Figure 29. Isopleth map of the concentrations of trichloroethylene measured at the RWMC [units of micrograms per liter (µg/L)].

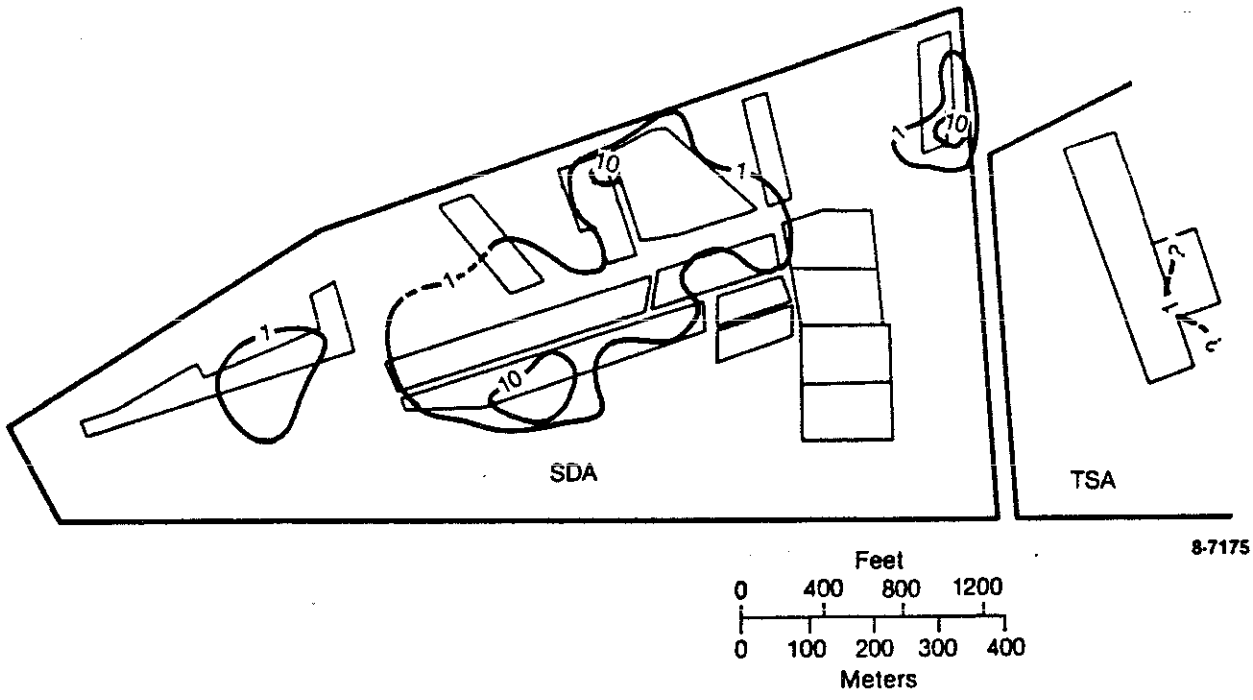

Figure 30. Isopleth map of the concentrations of tetrachloroethylene measured at the RWMC [units of micrograms per liter (µg/L)].

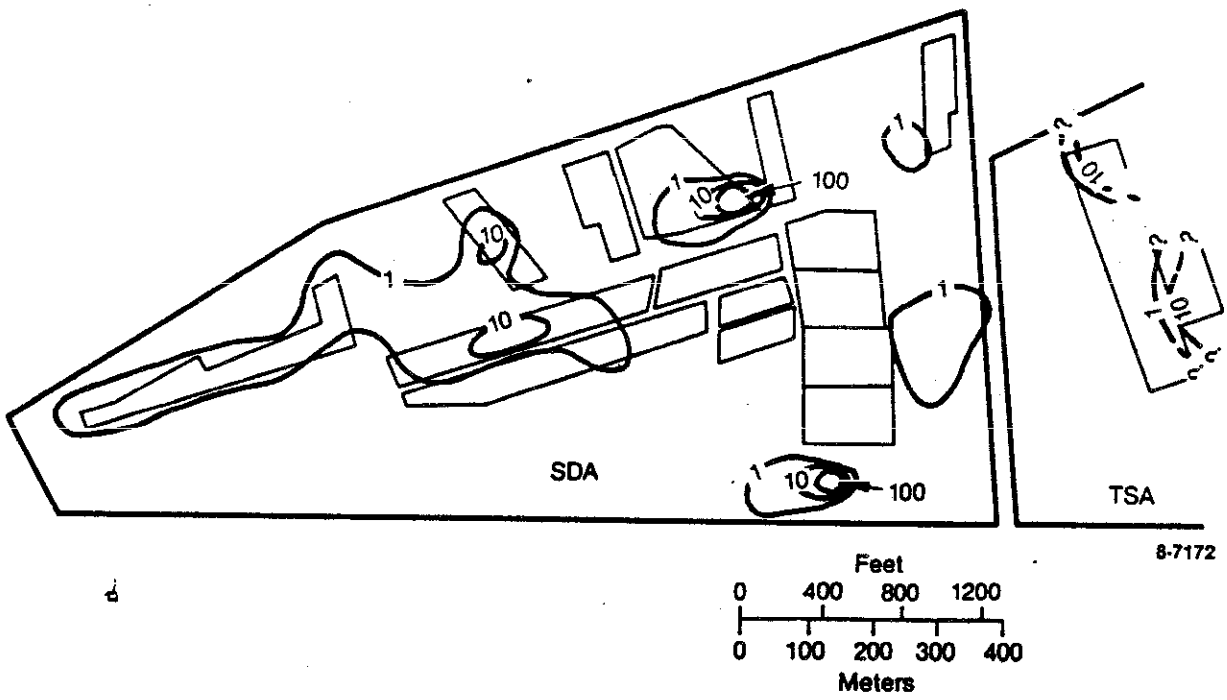

Figure 31. Isopleth map of the concentrations of 1,1,1-trichloroethane measured at the RWMC [units of micrograms per liter (µg/L)].

of Pit 3, and near the southeast corner of the SDA. High concentrations of 1,1,1-trichloroethane were also found associated with Pit 2, Trenches 24, 29, and 32, and Pit 4. (Trenches 24, 29, and 32, not shown on Figure 24, are located east of Pit 2 and north of the west end of Pit 4.) The area of Pit 4 highest in 1,1,1-trichloroethane does not correspond to the area highest in carbon tetrachloride.

Samples were collected from access tubes in the TSA pad and neutron access tubes installed in the SDA. At the TSA pad, moderate concentrations of carbon tetrachloride, trichloroethylene, and 1,1,1-trichloroethane were found. The neutron access tubes are open only just above the basalt; this removes the effects of overlying soil on VOC concentrations. Values measured in the neutron access tubes were generally higher than soil gas concentrations measured nearby but followed the trends shown by the shallower samples.

Soil gas samples were also collected along roads running to the north, east, south, and west of the SDA. Detectable levels of carbon

tetrachloride were found 2500 ft north, 3400 ft east, 1900 ft west, and 2200 ft south of the SDA fence. Only the northernmost sample did not have detectable concentrations of VOCs.

Figure 27 shows that some soil gas samples from the RWMC contained carbon tetrachloride but no 1,1,1-trichloroethane. Other samples contained 1,1,1-trichloroethane but no carbon tetrachloride. A third group of samples showed a near 1:1 ratio of carbon tetrachloride to 1,1,1-trichloroethane. Whether this indicates three distinct source materials, two pure source materials which mix, or some other possibility is not clear. Figure 32 shows the spatial distribution of these samples. The areas of pure 1,1,1-trichloroethane are generally surrounded by areas of gas mixtures. This suggests that samples with both carbon tetrachloride and 1,1,1-trichloroethane are the result of gas mixing in the subsurface. However, the samples from the TSA also show a 1:1 gas mixture. This area is aboveground on an asphalt pad, and all gases sampled from the TSA likely originated in the TSA. Therefore, some of the source material probably contains a mixture of both organic compounds. Additional analysis of the data is necessary to determine the types and extent of sources of VOCs at the RWMC.

The results portrayed in Figures 28 through 32 are not fully consistent with the existing RFP source term data. Therefore, additional identification of source term data is needed. Some of the VOCs may be coming from wastes that originated at the INEL.

Samples collected from three deep boreholes at the RWMC (gas sampling holes 77-1, 78-4, and WWW-1; see Figure 13 for locations of these holes) indicate the VOC concentrations with depth. Each of the three holes is instrumented with gas sampling ports at multiple depths. Table 12 shows that maximum concentrations generally occur at depths near 100 ft (80 to 150 ft). Concentrations drop off at depths greater than about 170 ft, but detectable concentrations were measured in all samples, including a sample

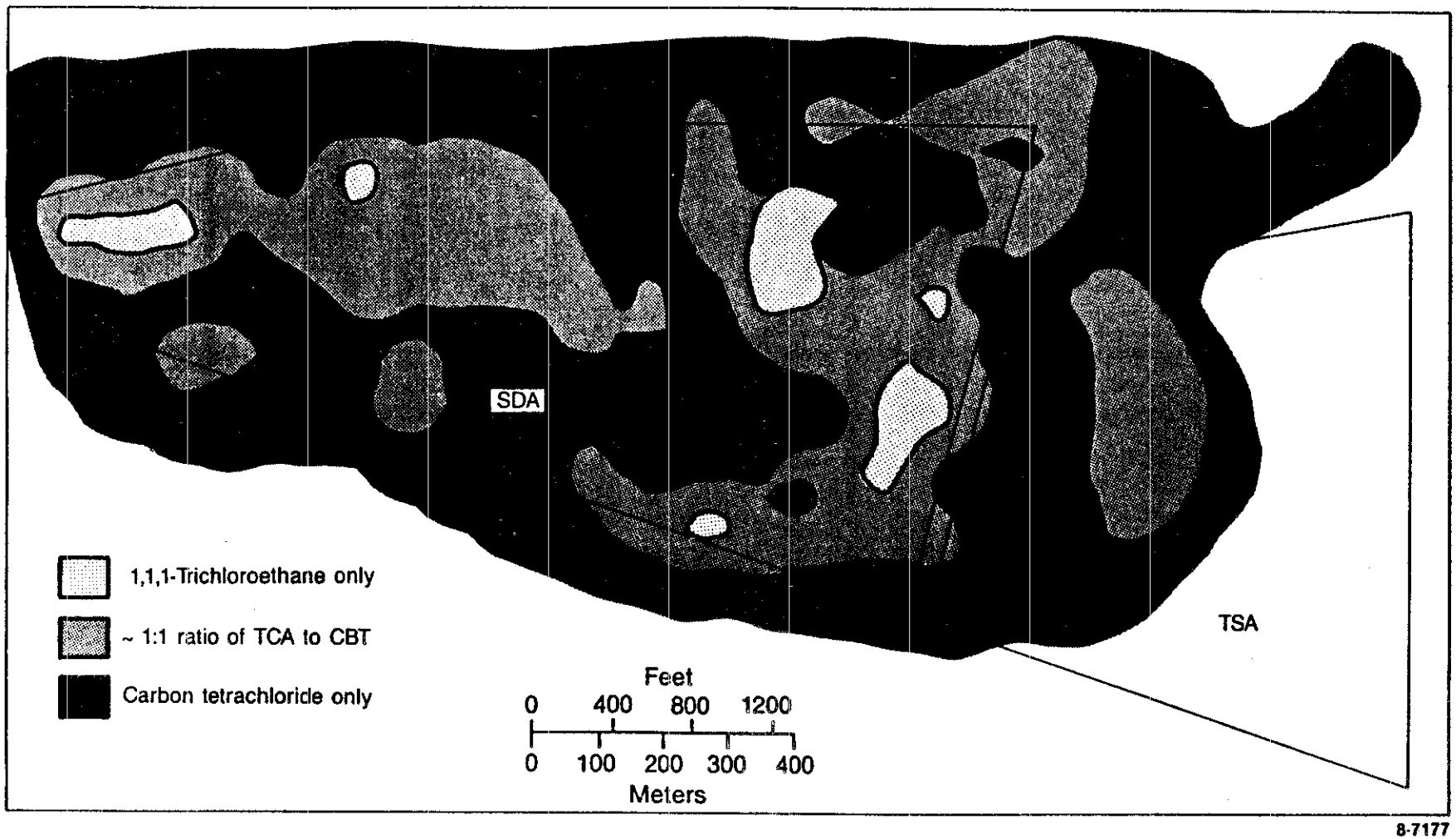

Figure 32. Distribution of carbon tetrachloride (CBT) compared to the distribution of 1,1,1-trichloroethane (TCA) at the RWMC.

TABLE 12. RESULTS OF ANALYSIS OF DEEP BOREHOLE GAS SAMPLES TAKEN DURING SOIL GAS SURVEY (μg/L)

Bore-hole	East	North	Sample Depth (ft)	1,1,1-Trichloroethane	Carbon Tetrachloride	Tri Chloroethylene	Tetra Chloroethylene
WWW1-1	-1600	1800	15	<0.01	8.8	1.6	0.4
WWW1-2	-1600	1800	48	<0.01	8	1.2	0.4
WWW1-3	-1600	1800	74	<0.01	30	3.8	0.9
WWW1-4	-1600	1800	112	P	6.6	1	0.4
WWW1-5	-1600	1800	135	P	28	4	1
WWW1-6	-1600	1800	180	P	3	2	0.4
WWW1-7	-1600	1800	240	<0.01	0.9	P	P
77-1-2	2175	2900	171	P	2.3	0.04	0.1
77-1-3	2175	2900	153	5.0	20.0	5	2.4
77-1-4	2175	2900	112	5.0	20.0	4	1
77-1-5	2175	2900	104	0.8	4.0	0.9	0.4
77-1-6	2175	2900	66	7.0	4.0	8	2
78-4-1	2175	2975	335	<0.01	0.6	0.04	0.04
78-4-2	2175	2975	253	<0.01	2.0	0.03	0.03
78-4-3	2175	2975	227	<0.01	0.1	<0.01	<0.01
78-4-4	2175	2975	118	<0.01	26.0	6	2
78-4-5	2175	2975	78	<0.01	36.0	9	2

Note: P indicates that the constituent was detected at an unquantified level.

collected at 355 ft. The elevated concentrations at depths around 100 ft are consistent with modeling results that suggest the interbed at 110 ft is a major pathway for organic vapor migration.

5.3.3.6 Conclusions. Based on the analysis of VOC concentrations in soil gas at the RWMC, carbon tetrachloride, 1,1,1-trichloroethane, trichloroethylene, and tetrachloroethylene are migrating from a number of the pits. The major sources of organic compounds are Pits 4, 5, 6, 9, and 10. Soil gas concentrations measured immediately adjacent to the pits, but not over the pits, showed markedly lower concentrations, indicating a definite source within the pits. Measurable concentrations of VOCs occur in soil gasses at distances from 2000 to 3400 ft from the SDA fence. Analysis of gasses collected at depth under the SDA indicate maximum gas concentrations around 100 ft, and measurable concentrations down to 576 ft.

5.4 Net Downward Flux

5.4.1 Introduction

The objectives of this study are to determine the volume and rate of moisture inflow through the SDA surface, identify pathways of moisture migration, characterize the effect of lithologic interfaces on moisture movement, and develop data describing moisture entry into the ground and moisture movement through the unsaturated zone for verification of a simulation model.

This study is using in situ field equipment to measure and monitor soil water content at the RWMC. The intent is to define the volume and rate of moisture movement into and through the unsaturated zone and to delineate moisture migration pathways through the unsaturated zone. These data will be used to field calibrate a model to predict long-term migration of radionuclides in the unsaturated zone. The study will require instrumentation throughout the SDA to characterize moisture availability, variability, and movement.

5.4.2 Summary of Accomplishments

Two deep boreholes were instrumented with heat dissipation sensors and suction lysimeters in FY-1987. A suction lysimeter and three heat dissipation sensors were installed in the 110-ft and 240-ft interbeds in borehole TW1 and the 30-ft, 110-ft, and 240-ft interbeds in borehole D15. Three additional heat dissipation sensors were installed in borehole D15 in the lower portion of the 110-ft interbed. Readings were taken from twenty-three instrumented shallow monitor holes, two neutron access tubes, and three deep boreholes on a monthly basis. Approximately 270 readings were taken each month from these instruments. A data base was set up to store the data collected from this program. Data were stored on an IBM-AT using the DBASE III software package. An initial analysis of the existing data was performed. A discussion of the trends and conclusions from this analysis is presented along with recommendations for further work.

5.4.3 Discussion

Data collection from instruments installed for the RWMC Subsurface Investigations Program began in June, 1985. To date, 34 holes have been completed and 266 instruments installed. The instruments include 59 psychrometers, 98 heat dissipation sensors, 50 gypsum blocks, 19 tensiometers, 39 porous cup lysimeters, and 2 neutron access tubes. Data from these instruments (except lysimeters) are collected monthly. In total, more than 10,000 measurements and matric potential values have been collected.

Two days of field time are required to read the instruments. Only the psychrometers are read with a data logger, and these readings may be taken without a person present. Readings from the other instruments are taken visually from meters attached to the instruments. Readings are recorded in the field and entered onto the RWMC database. Readings from the psychrometers are downloaded from the data logger directly into the RWMC database. Each month, 270 readings are taken from instruments within the RWMC.

To accommodate large volume of collected data, the RWMC Data Management System (RWMC-DMS) was established. This database system has program applications and special routines that were constructed using the DBASE III Plus software package. Based on an IBM-AT, the RWMC-DMS may be used to quickly and easily store the collected data, organize and retrieve specific information, and print selected reports to either printer or disk files. Files generated by the RWMC-DMS may also be transferred to other software packages such as LOTUS 1-2-3 or Minitab for analysis.

Separate database files are used to store measured data for each type of instrument. Two more database files contain basic information (dates, coordinates, etc.) for each hole and calibration information for each instrument. The RWMC-DMS is menu driven, providing simple and easy movement from one database to another. Selections from these menus provide basic functions such as adding and deleting information, or editing and viewing specific entries. Searching and organization may be conducted on any of the data fields using the built-in indexing options. Special applications are still permitted using standard DBASE III Plus commands, and new routines and utilities may be easily added to the existing RWMC-DMS directory. Appendix D lists the structure for each major database file utilized by the RWMC-DMS.

The following sections (Sections 5.4.3.1 through 5.4.3.7) present an analysis of field data collected through November 1987 and recommendations for further analysis. As a quality control measure, the data base has been checked against the field record sheets for correct dates and readings. Because of the large volume of data, only selected portions of the data can be presented in this discussion. The bulk of the analyzed data is presented in the appendixes in graphical form.

The data from tensiometers, gypsum blocks, heat dissipation sensors, psychrometers, neutron logging, and porous cup lysimeters are presented and discussed individually. Each instrument section describes the instrument, explains and evaluates its performance, analyzes the measurement data, and discusses the relative quality and usefulness of the data.

The data from the tensiometers, gypsum blocks, heat dissipation sensors, and psychrometers are presented in the form of matric potentials. Matric potential is a negative pressure potential (less than atmospheric pressure) which results from the combination of capillary and adsorptive forces within the soil matrix. The negative pressure potential may be expressed in negative pressure units (as a matric potential) or in positive pressure units (as tension or suction). All three terms are used in the following discussions.

Following the presentation of all the instrument sections, the data from all the instruments are summarized in terms of observed spatial variation. The relative value of the different instruments used in data collection is compared. Finally, general conclusions and recommendations for future work are presented.

5.4.3.1 Tensiometers. Tensiometers measure the matric potential in sediment for the range of 0 to 0.65 bars tension. A porous ceramic cup on the tensiometer allows water within the instrument to equilibrate with the matric potential of the material adjacent to the ceramic cup. The tension within the sediment is measured on a vacuum dial gauge. Further details are given in the FY-1985 annual report (Hubbell et al., 1985).

Nineteen tensiometers were installed in surficial sediments within 10 auger holes as indicated in Table 13. Figure 2 (see Section 4.1.2) shows the locations of the auger holes. Instruments were located in holes having moist to wet sediments, as determined by observation during drilling. All of the instruments except T06 in T23 and T04 in W20 are presently in use. T06 was removed due to maintenance problems and T04 is in a location too dry for the instrument to function.

Matric potentials, total potentials (a combination of matric potential and elevation potential), and hydraulic gradients for tensiometers were plotted versus time for the period of record. The large volume of data requires a short summary be presented in this report with a detailed discussion presented for selected holes. Appendix E contains the graphs of data for all the tensiometers not discussed in this section.

TABLE 13. TENSIOMETER INSTALLATIONS

Hole	Date	Instrument	Depth (m)	Depth (ft)
PA1	07/16/85	T09	0.93	3.05
PA1	07/16/85	T08	1.84	6.03
PA1	07/16/85	T07	2.76	9.05
PA2	07/16/85	T11	0.89	2.92
PA2	07/16/85	T10	1.80	5.90
T23	07/02/85	T06	0.91	2.98
W02	06/14/85	T01	1.83	3.67
W02	06/14/85	T02	2.74	8.62
W06	09/23/86	T17	0.91	2.98
W06	09/23/86	T16	1.83	6.00
W06	09/23/86	T15	2.74	8.98
W17	09/29/86	T19	0.91	2.98
W17	09/29/86	T18	1.83	6.00
W20	06/28/85	T04	0.93	3.05
W20	06/28/85	T03	1.37	4.49
W23	06/28/85	T05	0.93	3.05
W24	09/18/86	T14	0.91	2.98
W24	09/18/86	T13	1.83	6.00
W24	09/18/86	T12	2.74	8.98

Data for three tensiometers in hole W06 are presented in Figure 33 for the period of October 1986 to November 1987. The tensiometers indicate the dryest (lowest matric potential) conditions are present at 3 ft below land surface (BLS) with progressively wetter conditions at 6 and 9 ft below land surface. The instrument at 3-ft depth indicates the largest variation in matric potential, with the instruments at 6- and 9-ft depths showing progressively less variation over the same period of time. Figure 34 presents the total potential energy for the instruments relative to land surface. These total potential data are used to calculate the gradients within the auger hole.

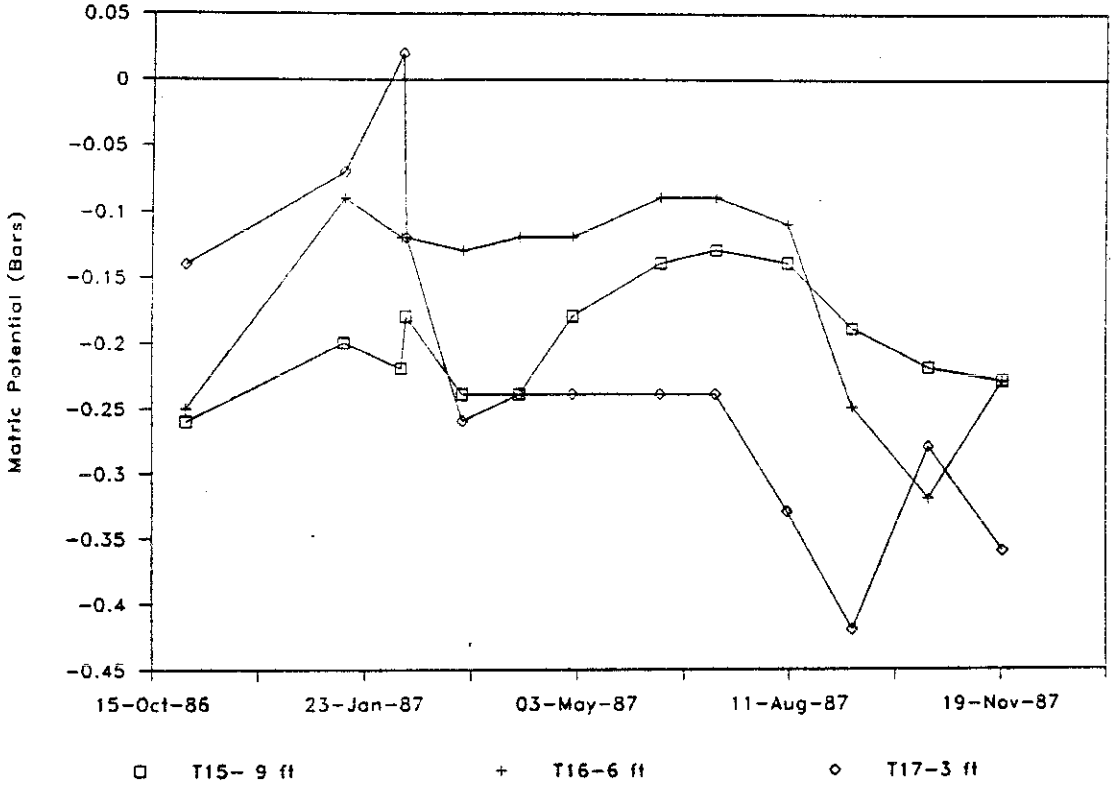

Figure 33. Tensiometer data from auger hole W06 at 3-, 6-, and 9 ft depths.

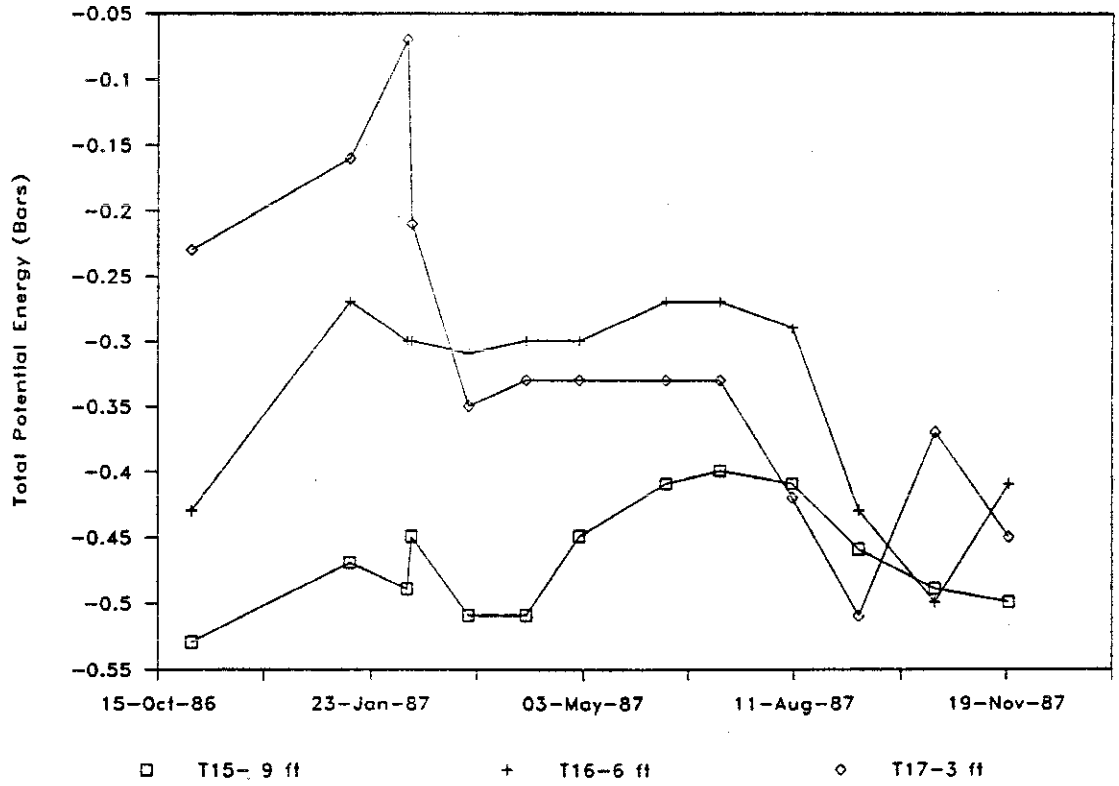

Figure 34. Total potential energy relative to land surface, calculated for auger hole W06 at three depths.

Figure 35 presents the hydraulic gradients between the 3- to 6-ft depth instruments and the 6- to 9-ft instruments. Upward flow is indicated by positive values, and downward flow by negative values. This figure indicates there is a marked difference in direction of water movement between these depths. The upper 6 ft has upward flow from March to October 1987, whereas the interval from 6 to 9 ft shows downward flux the entire time period excepting October 1987. The downward gradient in the lower two instruments is greatest from January through April. The gradient is reversed in October, due to evapotranspiration over the summer months. These data indicate that there is a potential for downward migration of water over a large portion of the year at this monitoring location.

Matric potential data for auger hole W17 are presented in Figure 36 for the period of December 1986 to November 1987. These data indicate that the 3-ft instrument had a lower tension from March 1987 through October 1987 than the 6-ft instrument. The hydraulic gradient presented in Figure 37 indicates a potential for upward movement of moisture in the winter, then the hydraulic gradient reverses from March to October 1987. The influence of water loss due to evapotranspiration is seen in the gradient approaching positive values.

Holes with multiple tensiometers showed the trend of decreasing tensions with increasing depth. For a homogeneous material this would mean that the holes were wetter at the bottom than at land surface. One exception was auger hole W17, where the 3-ft depth had a smaller tension than the 6-ft depth for a large portion of the year. The dryest reading (highest tensions) were usually seen near the land surface. During portions of the year, all of the operating instruments have readings that are in the range of field capacity (<20 bar tension). Field capacity is the point where the sediment will not hold additional water without gravity drainage. Tensiometers in auger holes W02, W06, W23, T23, PA01 and PA02 have had readings at or above 0.0 bar, indicating saturation of the materials around the instrument.

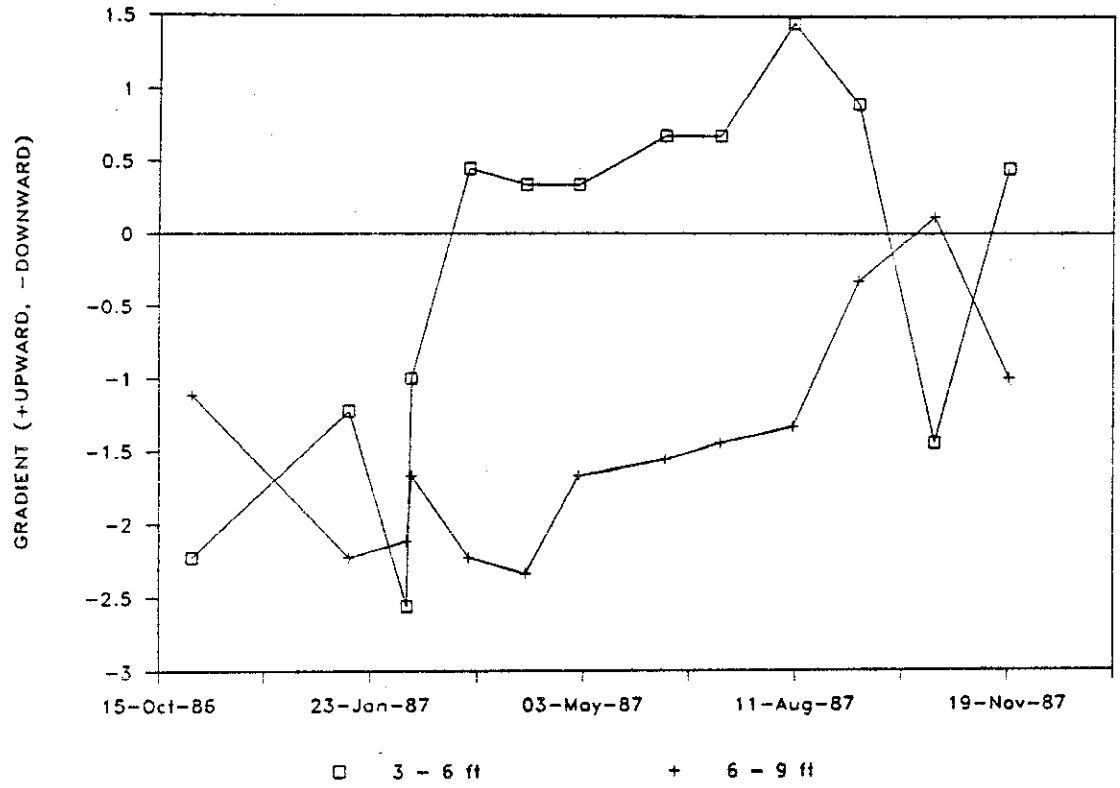

Figure 35. Hydraulic gradient data from tensiometers in auger hole W06.

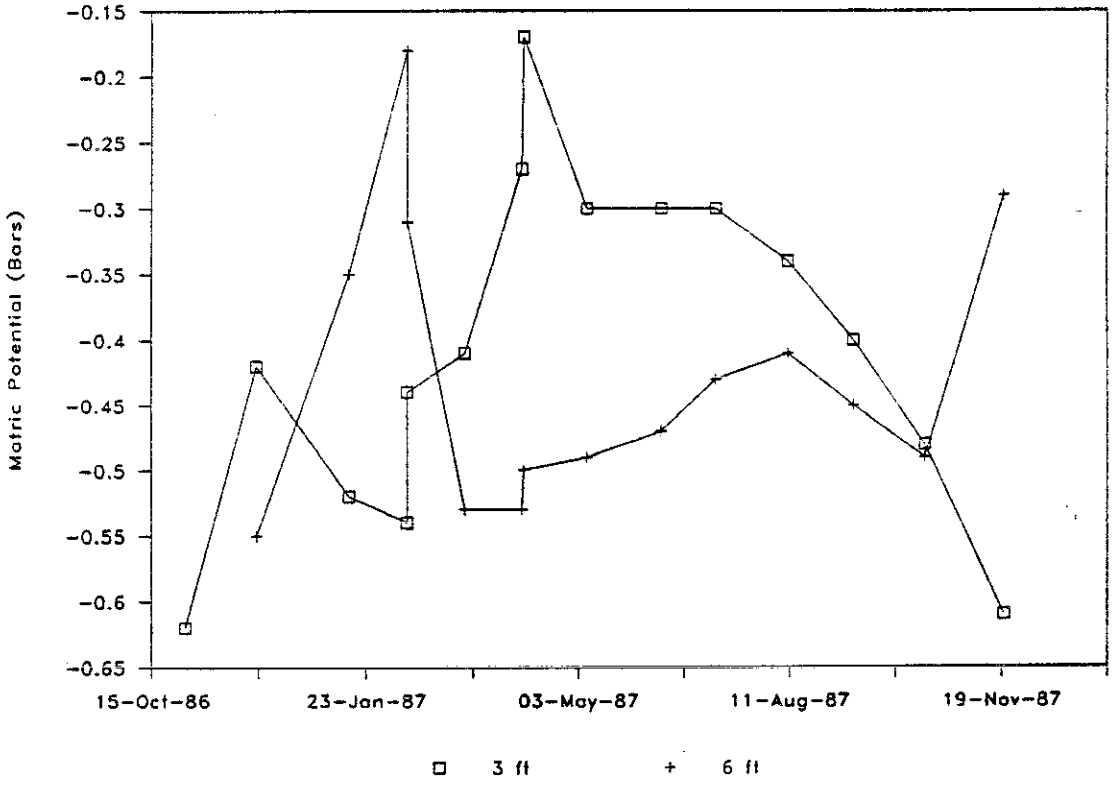

Figure 36. Matric potential data from auger hole W17 at 3- and 6-ft depths.

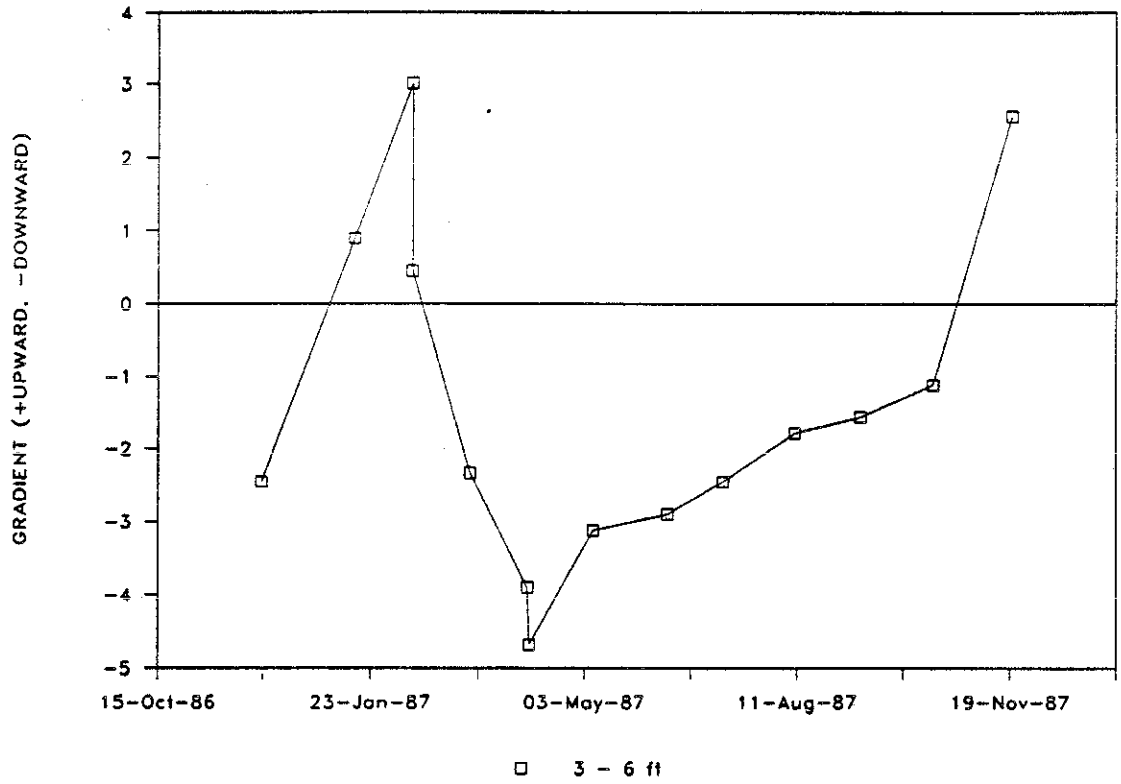

Figure 37. Hydraulic gradient data from auger hole W17.

Total potential energy or hydraulic head (matric potential plus elevation head) were calculated for several of the holes. These data were used to calculate the gradients within several holes. In general, there appeared to be positive gradients (upward flux) in the 3- to 6-ft depths for most of the year and negative gradients (downward flux) in the 6- to 9-ft depths. This suggests that multiple instruments, preferably below 6 ft, should be installed to provide matric potentials and gradients for the sediments below the zone affected by evapotranspiration.

Eighteen of the nineteen instruments are located in areas where tensions are within the instruments' operating range (0 to 0.65 bar). Most of these installations are located in or near topographic lows (W02, W06, T23, W23, W24, PA01 and PA02) where water has the opportunity to collect in periods of high precipitation or runoff. Holes W17 and W20 are not located near low spots or other water sources. The topographic depressions are usually very slight since there is only approximately 10 ft of relief

throughout the SDA, excepting the active pit. Several of these locations (underlined above) had standing water around them during spring runoff.

Tensiometers are accurate in their operating range (±0.02 bar tension). They require little or no initial calibration, and replacement parts are easily accessible. Little technical experience is required to install, maintain, and operate them. They operate without complicated electronics, require no power source, have a long field life, and are inexpensive.

Among their liabilities is their large size, which limits the hole to three instruments, and their limited operating tension range. Their maximum depth is limited by the height of the water column within the instrument. One ft of water column is equivalent to -0.03 bar matric potential. Thus a 9-ft instrument would only be able to measure +0.27 bar (saturated) to -0.38 bar tension. It may be possible to install instruments up to 12 ft deep, but the matric potential would need to be less than -0.29 bar to obtain readings. They are difficult to operate as constant recording instruments without the addition of complicated electronics, and they require an operator present to take readings. Soil freezing around them will affect readings, and maintenance during winter months is difficult due to the use of fluid (water and antifreeze) in the instrument.

Despite their drawbacks, tensiometers are the simplest and most effective instrument to use in many circumstances. Their small effective matric potential range and depth limitations restrict more widespread use at the RWMC. Because of their relative accuracy, tensiometers should be used whenever possible.

5.4.3.2 Gypsum Blocks. Gypsum (or resistance) blocks measure the matric potential of the soil. The gypsum blocks achieve a water tension equilibrium with the surrounding matrix, and this matric potential is measured by the resistance between two electrodes embedded in the gypsum block matrix.

A total of 50 gypsum blocks were installed in surficial sediments in seven auger holes at the depths listed in Table 14. Generally, the gypsum blocks were installed in clusters of three at each depth, and surrounded with native backfill. All gypsum blocks (except those in TH4) were calibrated from 0 to 10.0 bars of tension prior to installation. Further details of the calibration and instrumentation methods are described in FY-1985 annual report (Hubbell et al., 1985).

Each of the three gypsum blocks at a given depth yielded a set of matric potential measurements versus time. Figure 38 shows the measurements recorded by instruments in auger hole PA01 at 9.5 ft below land surface. Measurements shown in this figure are typical of the range of matric potential values produced by different gypsum blocks at the same depth. To reconcile this range in matric potentials at each depth, an arithmetic mean was calculated for each depth from the three gypsum blocks. A standard deviation, a maximum value, and a minimum value were also calculated for each depth to provide an indication of confidence and variation from the mean. Figure 39 shows the mean, maximum values, and minimum values calculated from the matric potentials shown in Figure 38. Mean values are used to analyze data trends, and the maximum and minimum values show the actual data range. Additional plots of data derived from gypsum blocks are presented in Appendix F.

Seasonal trends in matric potentials are similar for each hole. Figure 40 summarizes the mean matric potentials for the 3.0, 5.0, 10.0 and 15.0 ft instrumented depths (BLS) in auger hole T23. Matric potentials decrease in the winter months of December and January and show peak maximums in the late-spring and early summer months. The observed seasonal trends can be attributed partially to resistance measurements within the gypsum blocks, which are affected by changes in temperature. The seasonal trends in matric potential may also reflect actual changes in the moisture content of the surficial deposits. The low matric potentials recorded during the mid-winter months may be related to frozen conditions near the surface, which can inhibit infiltration of water. In late spring and early summer, infiltration can occur through snow melt and additional precipitation, increasing the matric potential readings.

TABLE 14. GYSUM BLOCK INSTALLATIONS

Hole	Date	Instrument	Depth (m)	Depth (ft)
PA1	07/11/85	G21	1.07	3.51
PA1	07/11/85	G19	1.07	3.51
PA1	07/11/85	G20	1.07	3.51
PA1	07/11/85	G17	2.89	9.48
PA1	07/11/85	G16	2.89	9.48
PA1	07/11/85	G18	2.89	9.48
T12	06/20/85	G39	1.22	4.00
T12	06/20/85	G38	1.22	4.00
T12	06/20/85	G37	1.22	4.00
T23	07/02/85	G43	0.91	2.98
T23	07/02/85	G45	0.91	2.98
T23	07/02/85	G44	0.91	2.98
T23	07/02/85	G48	1.50	4.92
T23	07/02/85	G46	1.50	4.92
T23	07/02/85	G47	1.50	4.92
T23	07/02/85	G51	3.02	9.08
T23	07/02/85	G49	3.02	9.08
T23	07/02/85	G50	3.02	9.08
T23	07/02/85	G13	4.55	14.92
T23	07/02/85	G15	4.55	14.92
T23	07/02/85	G14	4.55	14.92
TH4	04/23/85	G52	1.82	5.97
TH4	04/23/85	G53	1.82	5.97
W10	06/12/85	G26	0.91	2.98
W10	06/12/85	G27	0.91	2.98
W10	06/12/85	G25	0.91	2.98
W10	06/12/85	G28	1.52	4.98
W10	06/12/85	G30	1.52	4.98
W10	06/12/85	G29	1.52	4.98
W10	06/12/85	G33	2.29	7.51
W10	06/12/85	G32	2.29	7.51
W10	06/12/85	G31	2.29	7.51
W10	06/12/85	G02	3.05	10.00
W10	06/12/85	G03	3.05	10.00
W10	06/12/85	G01	3.05	10.00
W12	06/19/85	G36	1.22	4.00
W12	06/19/85	G35	1.22	4.00
W12	06/19/85	G34	1.22	4.00

TABLE 14. (continued)

Hole	Date	Instrument	Depth (m)	Depth (ft)
W19	06/21/85	G40	0.91	2.98
W19	06/21/85	G41	0.91	2.98
W19	06/21/85	G42	0.91	2.98
W19	06/21/85	G05	1.52	4.98
W19	06/21/85	G04	1.52	4.98
W19	06/21/85	G06	1.52	4.98
W19	06/21/85	G09	3.05	10.00
W19	06/21/85	G08	3.05	10.00
W19	06/21/85	G07	3.05	10.00
W19	06/21/85	G10	4.57	14.99
W19	06/21/85	G12	4.57	14.99
W19	06/21/85	G12	4.57	14.99

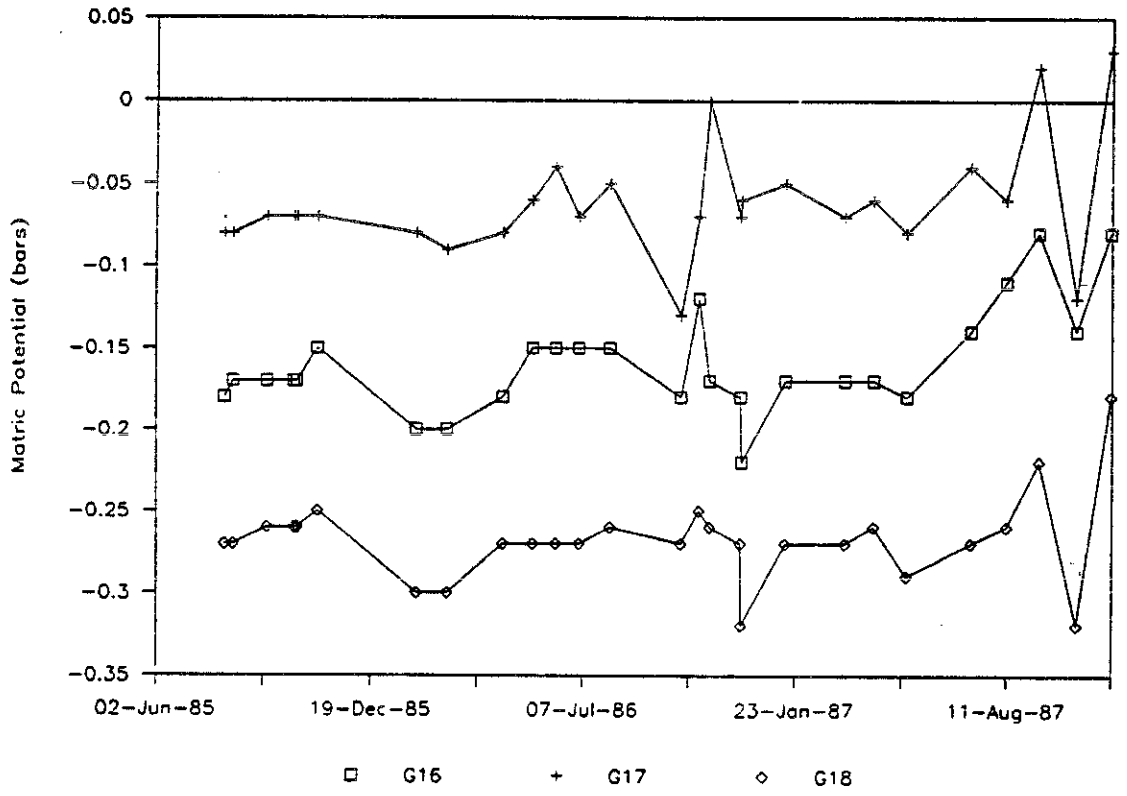

Figure 38. Matric potential values measured from auger hole PA01 at 9.5 ft below land surface.

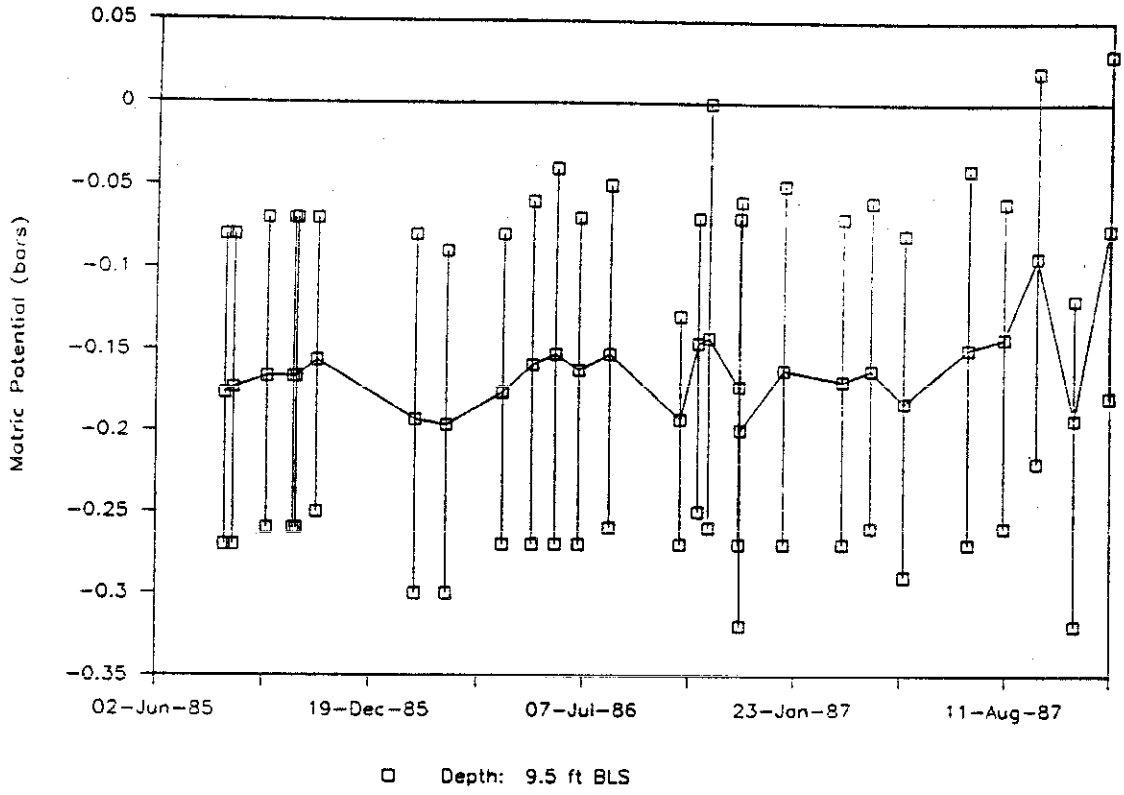

Figure 39. Mean, maximum, and minimum values calculated from the matric potential data shown in Figure 38.

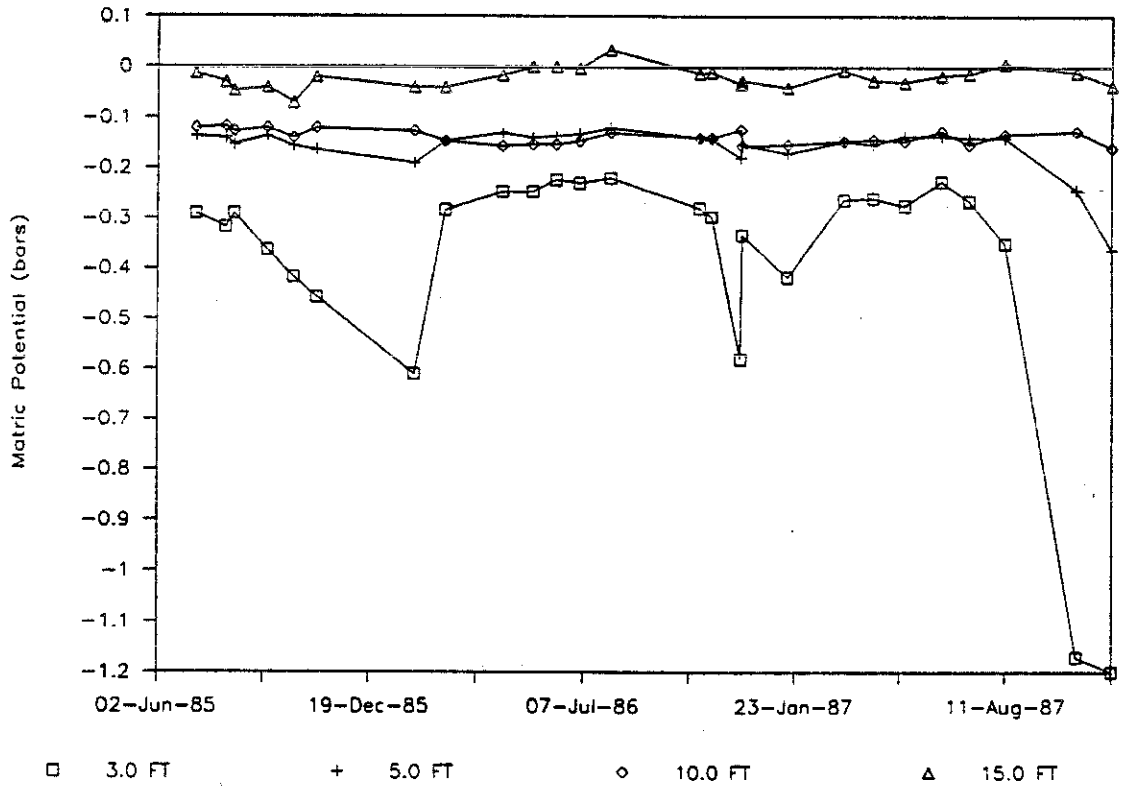

Figure 40. Mean matric potentials for instrumented depths in auger hole T23.

The mean matric potentials at different depths within each hole were compared. In general, the shallowest depth exhibited the largest variations in matric potentials over time, whereas the variations in matric potentials for the deeper gypsum blocks were generally damped or muted. Figure 40 shows this trend for auger hole T23. The shallowest depth would be expected to show the largest changes in matric potential, in response to precipitation, drying, or freezing events near the surface.

A trend of greater matric potential (less negative) was exhibited with increasing depth. If a medium was homogeneous, this would indicate increasingly wetter conditions as depth increases and the basalt-soil interface is approached. However, geologic logs do not indicate a homogeneous profile within the surficial sediments. Moisture contents will vary for a heterogeneous soil profile which is under a uniform matric potential. Thus, relative wet or dry conditions cannot be described solely on the basis of comparing matric potentials. Further information is needed, such as the relationship between moisture content and matric potential in the soil layers. This information can be obtained from laboratory experiments, using the soil samples from those holes. Neutron logging, using logs calibrated to the soil profile, would also be beneficial.

The movement of water in the surficial sediments at the RWMC is an issue of concern. Hydraulic gradients were calculated for each instrumented depth in each hole. These gradients were then compared, over time, to analyze the direction of water movement.

Figures 41, 42, 43, and 44 show the hydraulic gradients at the indicated depths for holes T23, PA01, W19, and W10, respectively. Gradients for auger holes PA01 and T23 both exhibit downward flow, but T23 also shows upward flow from 5 ft to 3 ft. Hydraulic gradients for holes W19 and W10 indicate predominantly upward flow, and this upward movement is seen both at depth and within shallower intervals. Based on the results of the hydraulic gradients, downward movement of water is evident in the surficial sediments, but does not occur consistently across the SDA.

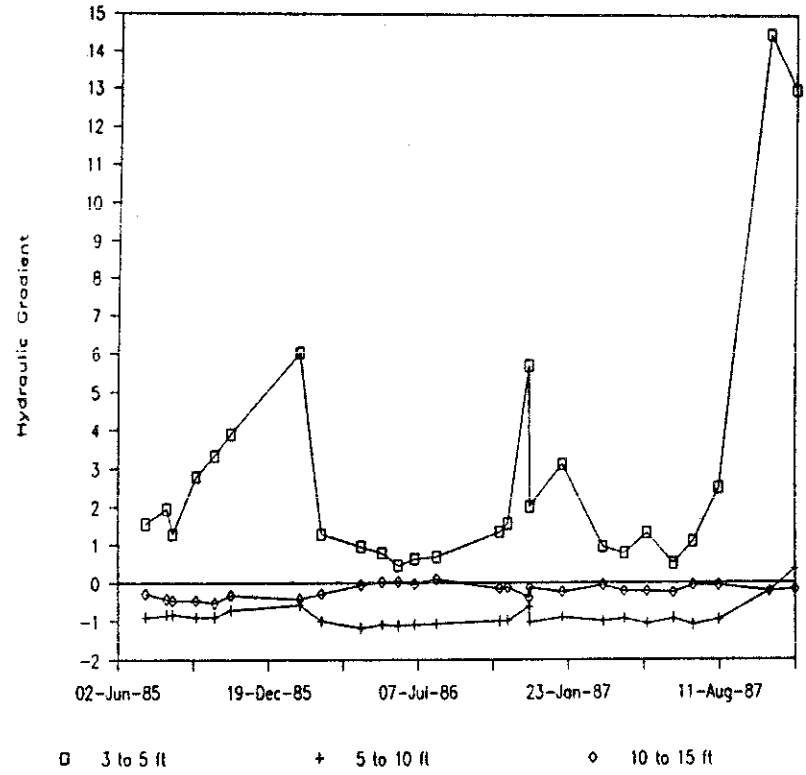

Figure 41. Hydraulic gradients calculated for auger hole T23.

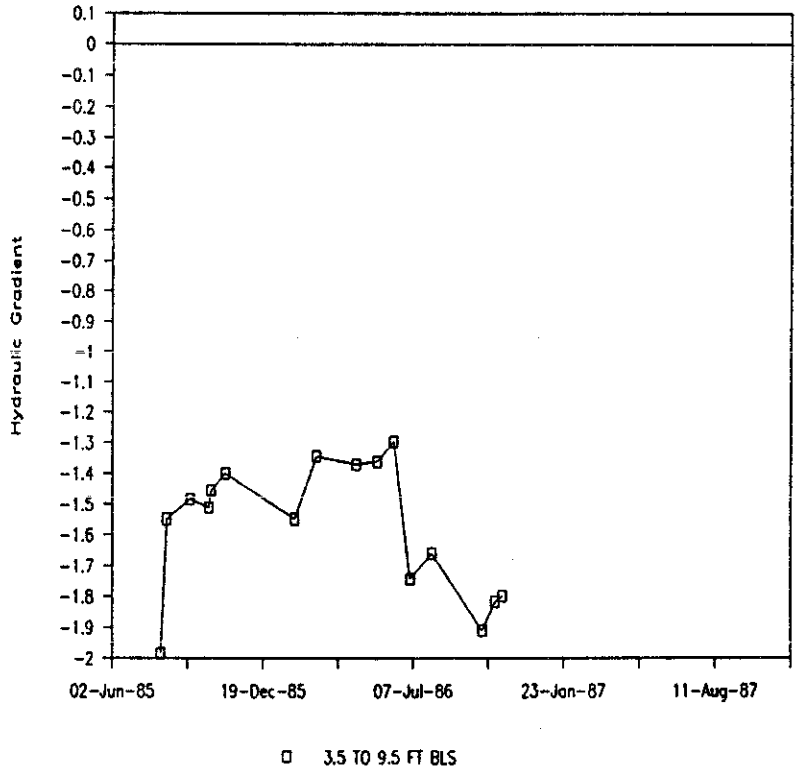

Figure 42. Hydraulic gradients calculated for auger hole PA01.

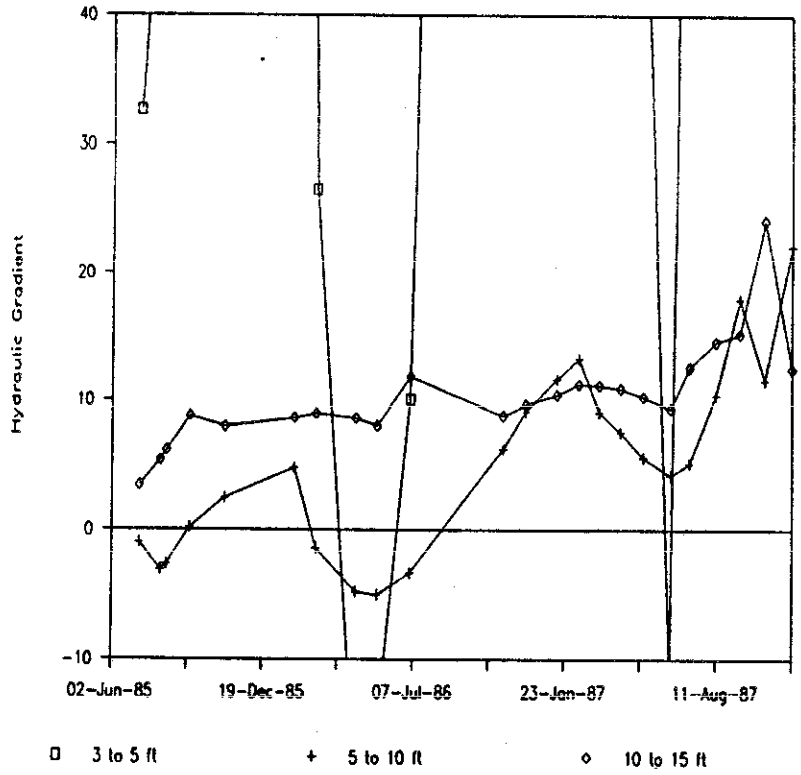

Figure 43. Hydraulic gradients calculated for auger hole W19.

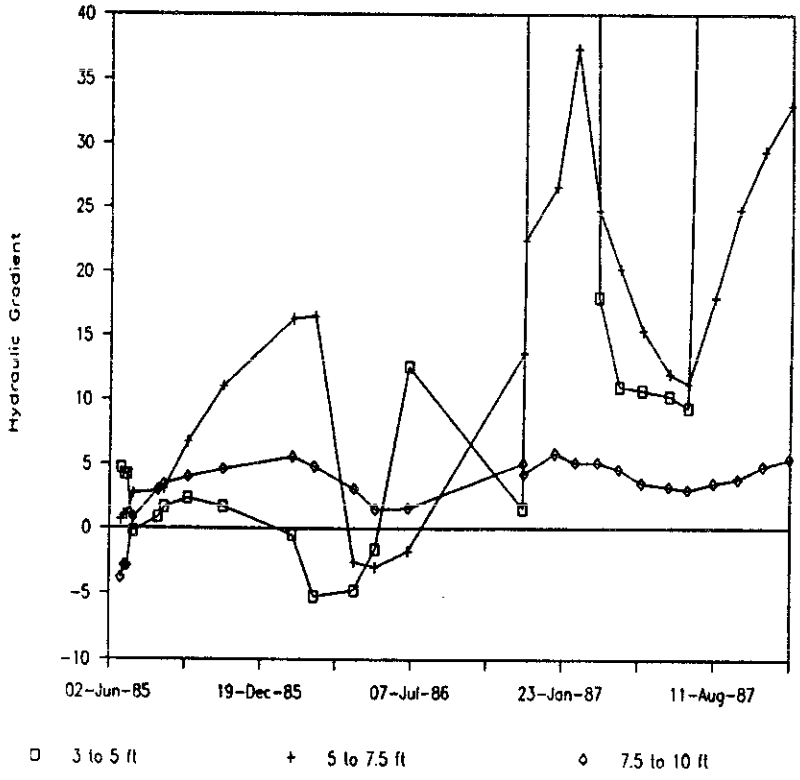

Figure 44. Hydraulic gradients calculated for auger hole W10.

For holes T23 and PA01, tensiometer data were available for comparison with gypsum block data at or very close to the same depths. The two instruments compared favorably, in terms of matric potential readings and general trends. This is seen in Figure 45, which shows the gypsum block and tensiometer data from hole T23 at 3.0 ft BLS.

The gypsum blocks generally maintained good performance over the present monitoring period and yielded reliable data. Dissolution of gypsum blocks may occur over time; gypsum blocks located in wet areas are especially susceptible to dissolution. However, only 6% of the total number of gypsum blocks installed at the RWMC have failed to date.

5.4.3.3. Heat Dissipation Sensors. Heat dissipation sensors (HDS) are electronic instruments used to measure the matric potential within a porous medium. These sensors rely on differences in heat conduction caused by changes in moisture content. They are calibrated to matric potential using a pressure plate extractor so placement in different texture sediments will not affect the readings. Further details on the sensors are included in the FY-1986 annual report (Hubbell et al., 1987).

Seventy-one heat dissipation sensors were installed in 9 shallow auger holes and twenty-seven sensors installed in three deep boreholes since 1986. Table 15 presents information on the sensors, including depth, location, and date installed. Most of the sensors were installed with three sensors at a depth (clusters) to check reproducibility of measurements. Sensors in deep boreholes are placed in sedimentary interbeds or in a sediment-filled fracture zone within the basalt. Instruments in shallow auger holes were installed at depths of 3 ft, 6 ft, and 10 ft, and at subsequent intervals of 5 ft to the sediment/basalt interface. Instruments were also installed immediately above the basalt.

The sensors are calibrated by their manufacturer, Agwatronics, of Merced, California, in the range of 0.0 to 1.0 bar tension. Approximately 40% of the sensors installed in the field show readings within the calibrated range. The other sensors show readings that, based on

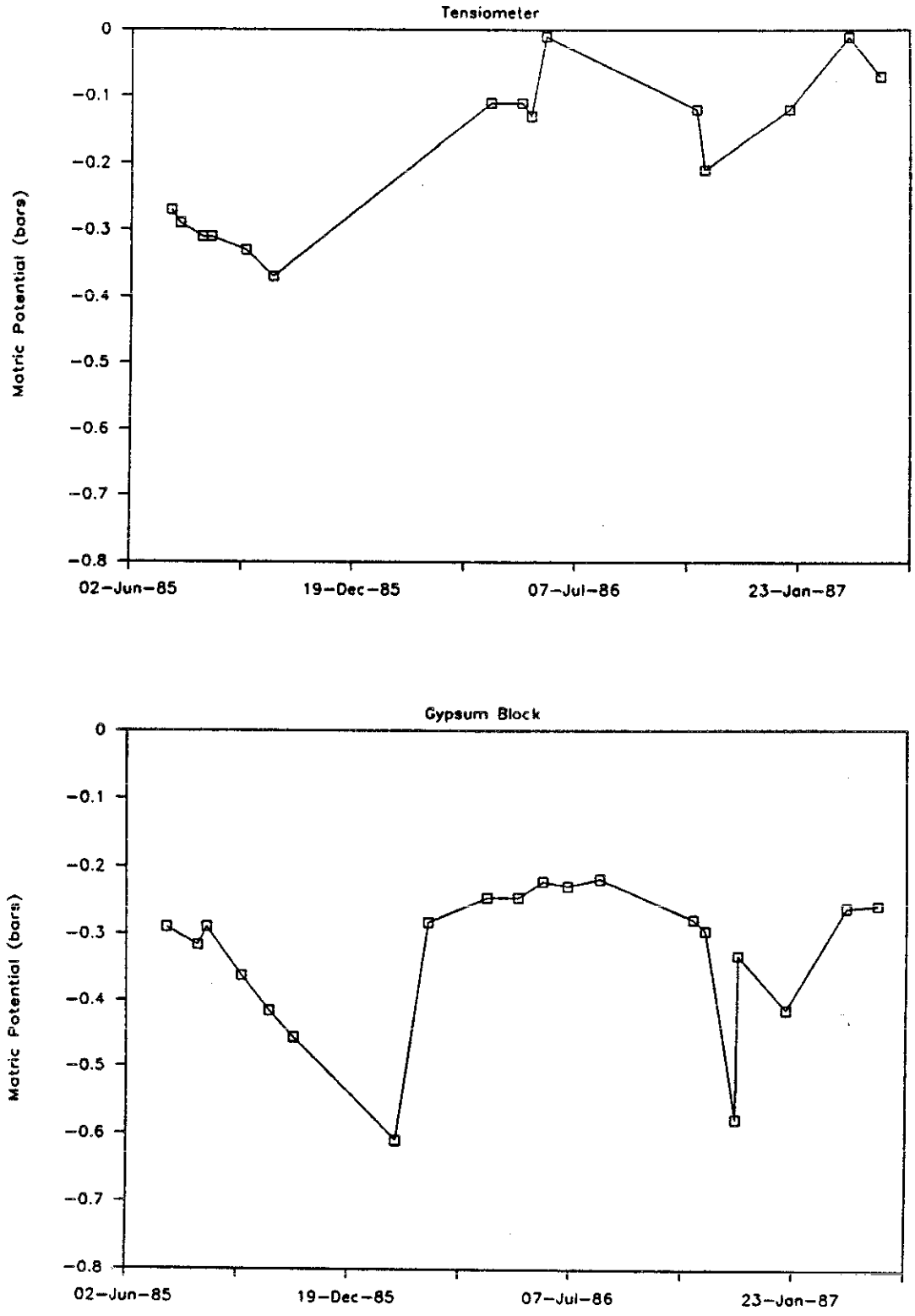

Figure 45. Matric potential readings from gypsum blocks and tensiometers in auger hole T23 at 3-ft depth.

TABLE 15. HEAT DISSIPATION SENSOR INSTALLATIONS

Hole	Date	Instrument	Depth (m)	Depth (ft)
D06	09/12/86	0654	13.11	43.01
D06	09/12/86	0501	13.19	43.27
D06	09/12/86	0661	13.26	43.50
D06	09/12/86	0660	26.63	87.37
D06	09/12/86	0525	26.65	87.43
D06	09/12/86	0655	26.68	87.53
D15	11/04/87	1183	9.60	31.49
D15	11/04/87	1050	9.68	31.76
D15	11/04/87	1164	9.68	31.76
D15	09/15/87	0656	29.64	97.24
D15	09/15/87	1019	29.73	97.54
D15	09/15/87	0657	29.73	97.54
D15	09/15/87	1029	33.60	110.24
D15	09/15/87	1045	33.69	110.53
D15	09/15/87	1046	67.77	222.35
D15	09/15/87	1048	67.84	222.58
D15	09/15/87	0647	67.84	222.58
TW1	06/25/87	0718	30.95	101.54
TW1	06/25/87	0503	30.95	101.54
TW1	06/25/87	0708	30.95	101.54
TW1	06/25/87	0607	69.05	226.55
TW1	06/25/87	1005	69.21	227.07
TW1	06/25/87	1006	69.36	227.57
TW1	06/25/87	1049	70.73	232.06
TW1	06/25/87	1016	70.73	232.06
TW1	06/25/87	0527	79.73	261.59
W05	09/22/86	0741	1.88	6.16
W05	09/22/86	0679	4.70	15.42
W06	09/23/86	0502	3.44	11.28
W09	09/17/86	0719	0.89	2.92
W09	09/17/86	0729	0.89	2.92
W09	09/17/86	0704	0.89	2.92
W09	09/17/86	0732	1.83	6.00
W09	09/17/86	0725	1.83	6.00
W09	09/17/86	0710	1.83	6.00
W09	09/17/86	0560	3.05	6.00
W09	09/17/86	0659	3.05	10.00
W09	09/17/86	0683	3.05	10.00
W09	09/17/86	0674	4.37	14.33

TABLE 15. (continued)

Hole	Date	Instrument	Depth (m)	Depth (ft)
W09	09/17/86	0676	4.37	14.33
W09	09/17/86	0677	4.37	14.33
W11	09/24/86	0760	0.91	2.98
W11	09/24/86	0735	0.91	2.98
W11	09/24/86	0762	0.91	2.98
W11	09/24/86	0734	1.83	6.00
W11	09/24/86	0743	1.83	6.00
W11	09/24/86	0751	1.83	6.00
W11	09/24/86	0758	3.05	10.00
W11	09/24/86	0755	3.05	10.00
W11	09/24/86	0757	3.05	10.00
W11	09/24/86	0497	4.95	16.24
W11	09/24/86	0663	4.95	16.24
W11	09/24/86	0740	4.95	16.24
W13	09/29/86	0761	0.91	2.98
W13	09/29/86	0753	0.91	2.98
W13	09/29/86	0658	0.91	2.98
W13	09/29/86	0707	2.03	6.66
W13	09/29/86	0035	2.03	6.66
W13	09/29/86	0696	2.03	6.66
W13	09/29/86	0759	3.05	10.00
W13	09/29/86	0744	3.05	10.00
W13	09/29/86	0752	3.05	10.00
W13	09/28/86	0694	3.91	12.82
W13	09/28/86	0684	3.91	12.82
W13	09/28/86	0745	3.91	12.82
W13	09/28/86	0763	5.49	18.01
W13	09/28/86	0749	5.49	18.01
W13	09/28/86	0750	5.49	18.01
W17	09/29/86	0517	0.91	2.98
W17	09/29/86	0748	0.91	2.98
W17	09/29/86	0695	0.91	2.98
W17	09/29/86	0731	1.83	6.00
W17	09/29/86	0644	1.83	6.00
W17	09/29/86	0688	2.74	8.98
W17	09/29/86	0664	2.74	8.98
W17	09/29/86	0738	2.74	8.98
W17	09/29/86	0649	4.57	14.99
W17	09/29/86	0713	4.57	14.99

TABLE 15. (continued)

Hole	Date	Instrument	Depth (m)	Depth (ft)
W17	09/29/86	0697	4.97	16.30
W17	09/29/86	0756	5.88	19.29
W17	09/29/86	0754	5.88	19.29
W17	09/29/86	0747	5.88	19.29
W18	09/22/86	0742	1.22	4.00
W18	09/22/86	0703	1.22	4.00
W18	09/22/86	0739	1.22	4.00
W18	09/22/86	0730	3.05	10.00
W18	09/29/86	0706	3.05	10.00
W18	09/22/86	0681	3.05	10.00
W18	09/22/86	0557	5.11	16.76
W18	09/22/86	0673	5.11	16.76
W18	09/22/86	0686	5.11	16.76
W24	09/18/86	0712	1.83	6.00
W24	09/18/86	0699	1.83	6.00
W24	09/18/86	0541	1.83	6.00
W25	09/24/86	0797	1.22	4.00
W25	09/24/86	0705	2.13	6.98
W25	09/24/86	0724	4.50	14.76

extrapolation of the calibration curve, are in the range of 1.0 to 3.0 bars tension. These data are much less accurate than the measurements read within the calibrated range. The variations in readings between sensors in the range of 0.0 to 1.0 bar tension are approximately 0.2 to 0.3 bar, while readings exceeding 1 bar vary from 0.2 to 2.0 bars between sensors.

Readings from heat dissipation sensors vary for instruments at the same depth. Figures 46, 47, 48, and 49 plot matric potential versus time at the 3.0-, 6.0-, 10.0-, and 14.0-ft depths below land surface. The readings were recorded from instruments installed in auger hole W09. Plots of the other heat dissipation sensor data are presented in Appendix G. The variation in matric potentials at some of the depths is larger than the variation between the depths. This makes it difficult to compare readings from different depths.

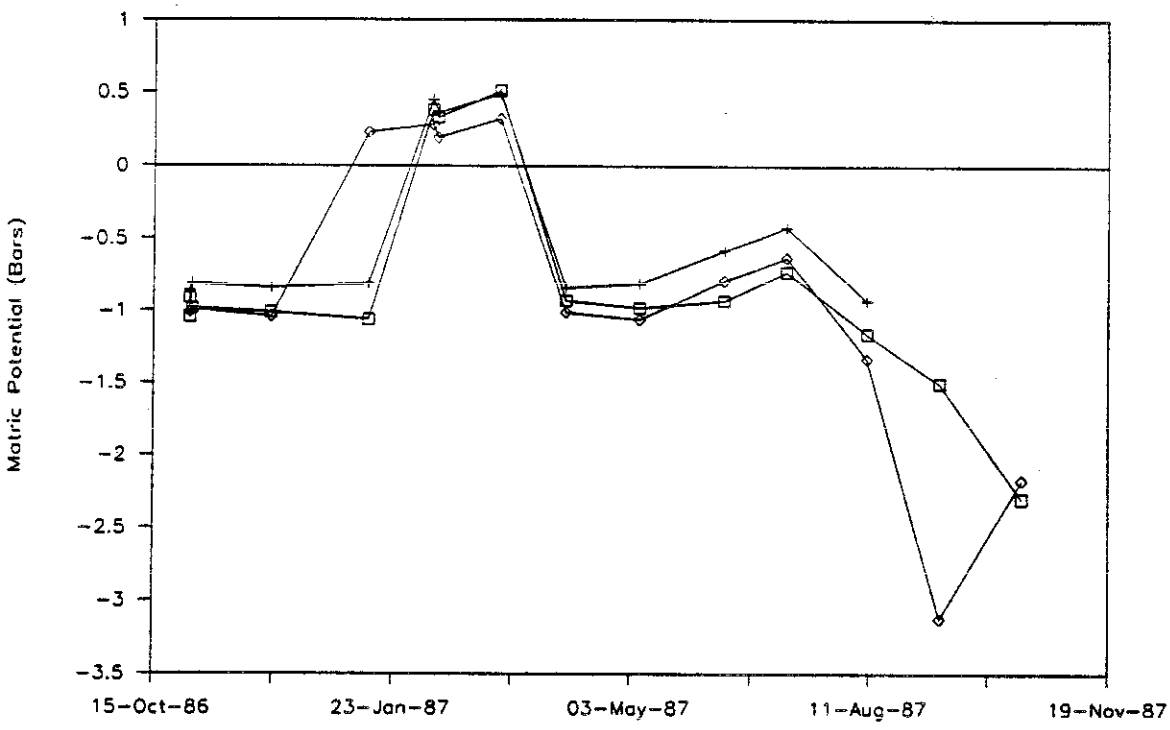

Figure 46. Readings from sensors installed 3 ft below land surface in auger hole W09.

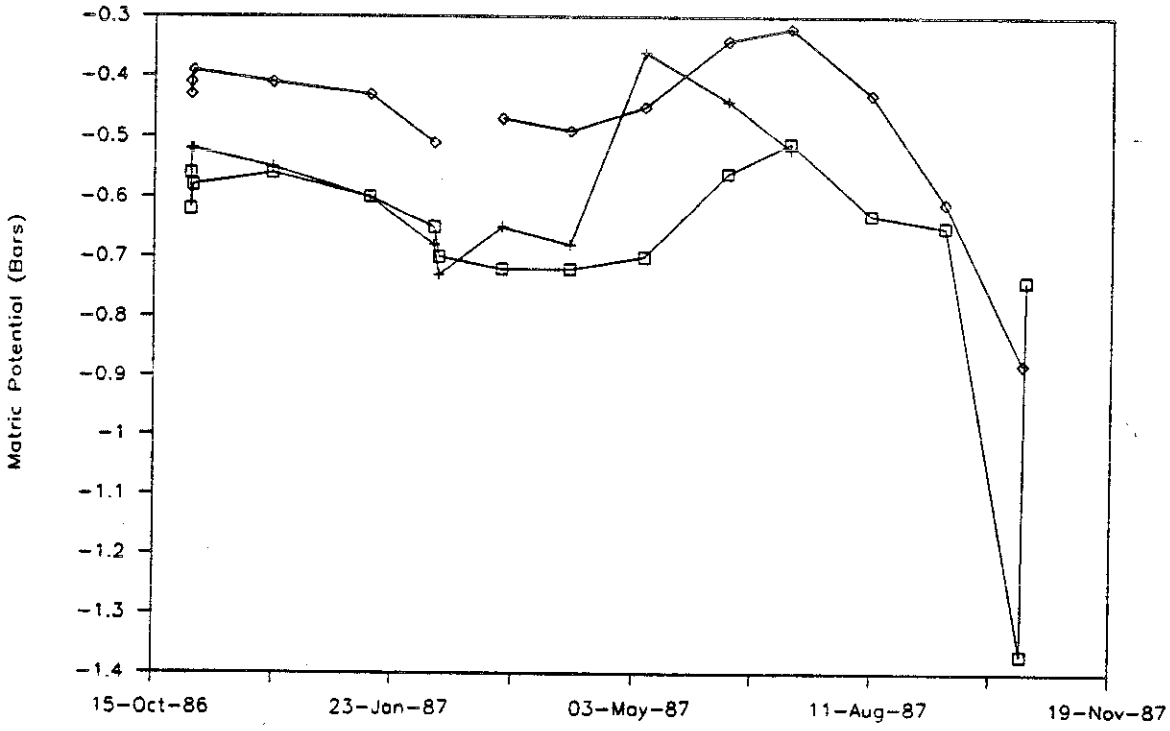

Figure 47. Readings from sensors installed 6 ft below land surface in auger hole W09.

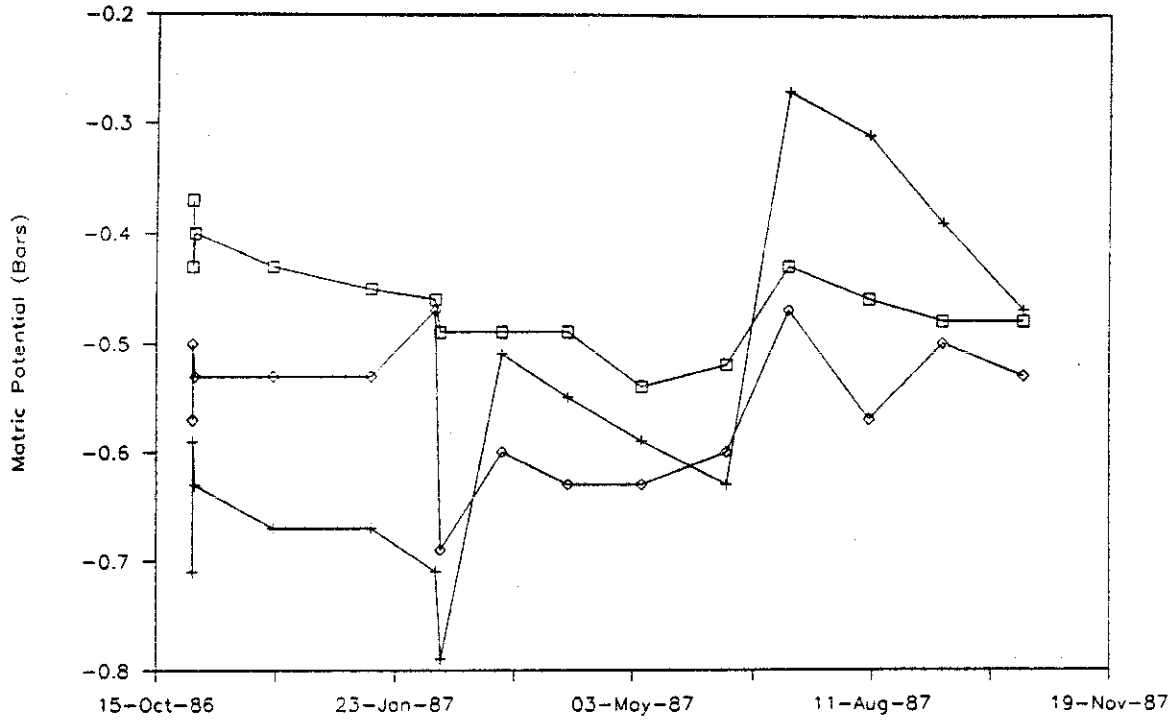

Figure 48. Readings from sensors installed 10 ft below land surface in auger hole W09.

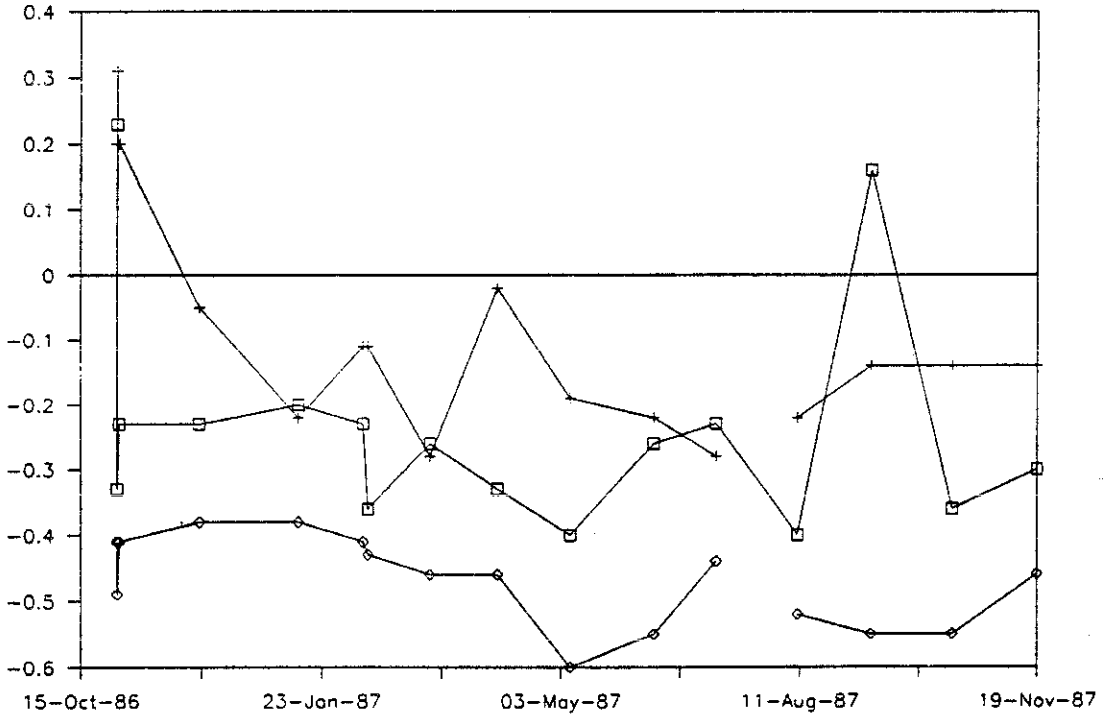

Figure 49. Readings from sensors installed 14 ft below land surface in auger hole W09.

Instruments were installed in the deep boreholes in the fall of 1986 and 1987. Data for borehole D06 are presented in Figure 50. Two of the three sensors at 44 ft give similar readings, but in July one of them starts to drift. They all show a horizontal trend in matric potential, with most readings ranging from -0.7 to -1.7 and with slight increases in March and September 1987. A suction lysimeter located in this interbed has collected water, indicating the actual matric potential must be between -0.0 and -0.65 bar. Sensors in a sediment-laden fracture zone at 88 ft below land surface (Figure 51) show matric potentials in the range of -1.5 to -2.7 bars. The variations in the readings yielded by sensors at the same depth indicate that the use of linear calibration curves is not adequate in this range of readings. These sensors all show a similar trend, but the readings vary over a bar tension.

Readings from borehole TW1 indicate matric potentials between -0.0 to -1.2 bar in the 110-ft interbed and -0.7 to -1.1 bar in the 240-ft interbed.

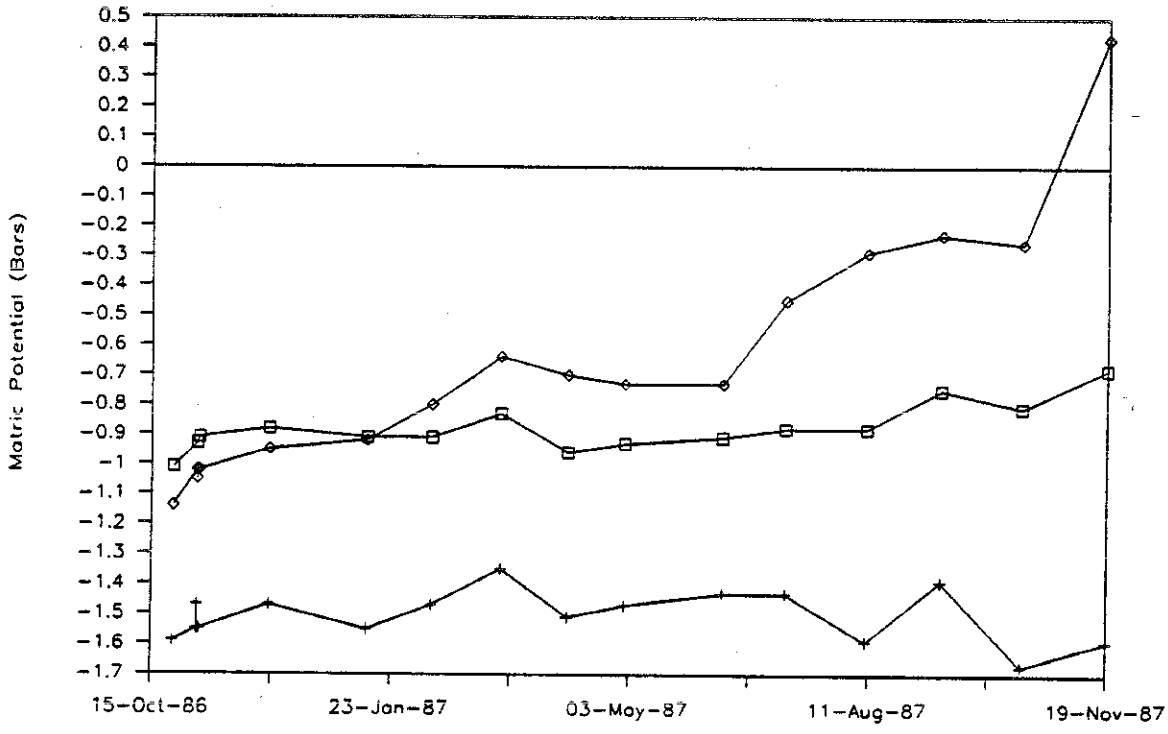

Figure 50. Readings from sensors installed 44 ft below land surface in borehole D06.

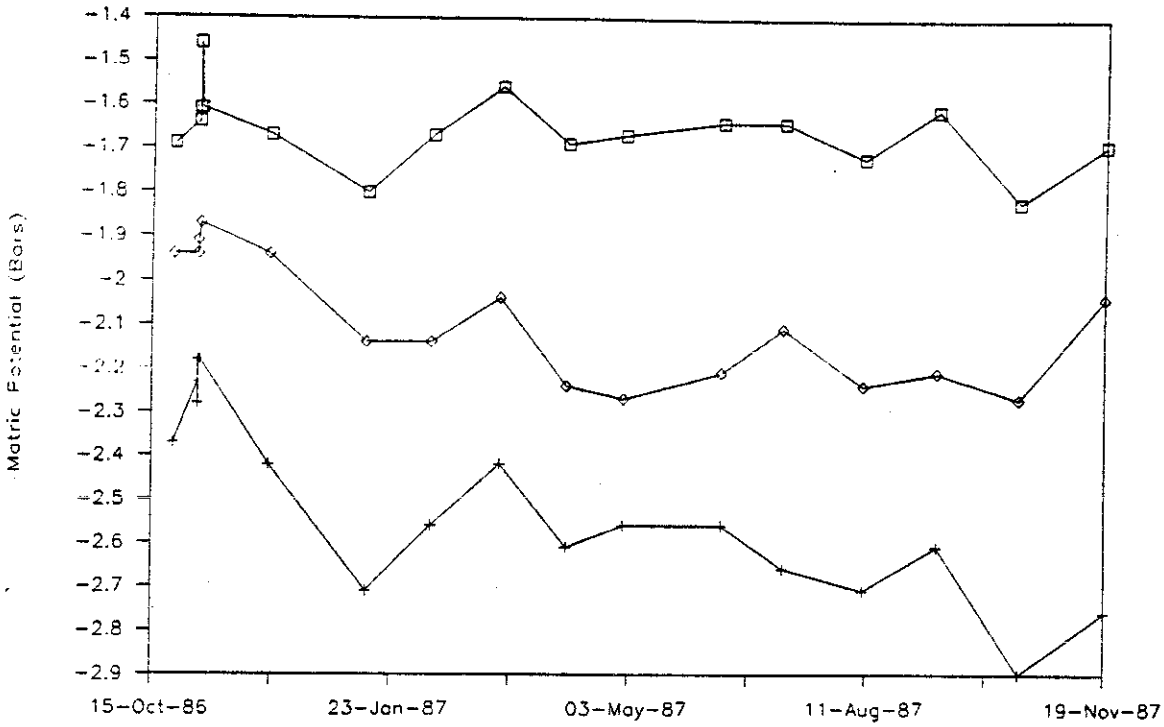

Figure 51. Readings from sensors installed 88 ft below land surface in borehole D06.

Sensors in the shallow auger holes indicate trends similar to those seen from tensiometers. The sediments have lower tensions (wetter) with depth. The matric potential fluctuations over time are greatest in the shallowest instruments and relatively constant with greater depths. Sensors in auger holes W05, W06, W24, and W25 show tensions from 0 to 1 bar, while those in W11, W13, W17, and W18 generally have tensions from 1 to 3 bars.

Some problems have been encountered in the use of heat dissipation sensors. The calibration range is limited. Currently, the heat dissipation sensors are calibrated for readings in the 0.0 to 1.0 bar range. This calibration can be extended to 3.0 or more bars tension by calibration within a pressure plate extractor, but this is a time-consuming process.

The sensors have a reported accuracy of ±0.02 bar in the calibrated range, but readings to date tentatively indicate that the actual accuracy

is closer to ±0.10 bar. The sensor's accuracy is limited by the meter used to read the sensor. A more accurate meter would obtain more accurate readings.

The sensors can only be read once per hour because the heat generated during the reading must dissipate before additional readings can be taken. In addition, the current system requires an operator to be present to take a reading.

Heat dissipation sensor failure rate at the RWMC is 8%.

Heat dissipation sensors have several advantages for use in measuring matric potential. The sensors are small in size, and the wire connection allows the instrument to be located at any depth, limited only the resistance within the wire. This is an advantage over tensiometers, which operate in the same matric potential range, but are limited by instrumentation depth. The sensors can be hard-wired to a programmable data acquisition system for taking repeated measurements without requiring a person to take the readings. Such a system would also record temperature within the sensor.

Data collected from heat dissipation sensors needs further analysis to optimize their future use. Additional sensors installed at the RWMC should be calibrated to at least 3.0 bars tension. A programmable data acquisition system should be purchased to increase the accuracy of the readings and allow detailed monitoring at selected sites. Heat dissipation sensors should be installed in future boreholes where the range of matric potential and the depth of the installation preclude the use of tensiometers.

5.4.3.4 Psychrometers. A thermocouple psychrometer is an electronic instrument used to measure the relative humidity in soil air, and from which potentials can be calculated. Because thermocouple psychrometers can measure tensions from from 1.0 to 70.0 bars, they are especially valuable

in semi-arid to arid climates. The measurement range for the thermocouple psychrometers extends beyond the range of tensiometers (0 to 1.0 bars) or gypsum blocks (0.3 to 15.0 bars).

A total of 59 psychrometers have been installed in 7 holes at the RWMC, since June of 1985. The instrumented holes, depths, and dates of psychrometer installations are listed in Table 16. The psychrometers in hole TH04 never functioned properly, so data from this hole are not included. Prior to installation, the psychrometers were factory calibrated with a one-point calibration reading at approximately 25.0 bars of tension. The matric potential readings were calculated using a single calibration curve for all psychrometers. For each hole (except W18, which has one psychrometer at each depth), a cluster of three psychrometers were placed at a specific depth in a hole. The interval was back-filled with the augered cuttings, and each instrumented interval was isolated by a layer of bentonite. A more detailed description of psychrometer calibration and installation methods is presented in the FY-1985 annual report (Hubbell et al., 1985).

A very large volume of data is produced by the psychrometers. The matric potential data alone totals over 7000 measurements. Using an electronic data collector (Wescor HP-115 Data Acquisition System) psychrometers can be scanned for readings at regular intervals over a period of time. The data yielded by psychrometers includes temperature, offset and millivolts (calibrated to matric potential). The offset attempts to compensate for temperature gradients which may exist within the psychrometer circuitry itself.

As a quality control measure, the psychrometer data was reviewed for each instrument. Matric potentials were discarded if associated with offsets of greater than 9.9 temperatures greater than 29.4°C or greater. In addition, extremely anomalous matric potentials were discarded. For some instruments (P17, P38, P50, and P51) this required discarding a major portion of the acquired matric potential data.

TABLE 16. PSYCHROMETER INSTALLATIONS

Hole	Date	Instrument	Depth (m)	Depth (ft)
T12	06/20/85	P10	1.22	4.00
T12	06/20/85	P11	1.22	4.00
T12	06/20/85	P12	1.22	4.00
TH4	04/23/85	P34	1.82	5.97
TH4	04/23/85	P35	1.82	5.97
W01	06/13/85	P02	0.91	2.98
W01	06/13/85	P03	0.91	2.98
W01	06/13/85	P01	0.91	2.98
W01	06/13/85	P06	0.91	4.98
W01	06/13/85	P04	1.52	4.98
W01	06/13/85	P05	1.52	4.98
W01	06/13/85	P09	2.13	6.98
W01	06/13/85	P08	2.13	6.98
W01	06/13/85	P07	2.13	6.98
W16	07/11/85	P16	0.91	2.98
W16	07/11/85	P17	0.91	2.98
W16	07/11/85	P18	0.91	2.98
W16	07/11/85	P13	1.42	4.65
W16	07/11/85	P15	1.42	4.65
W16	07/11/85	P14	1.42	4.65
W18	09/22/86	P50	0.61	2.00
W18	09/22/86	P51	0.91	2.98
W18	09/22/86	P52	1.22	4.00
W18	09/22/86	P54	1.52	4.98
W18	09/22/86	P55	1.83	6.00
W18	09/22/86	P56	2.13	6.98
W18	09/22/86	P57	2.34	7.67
W18	09/22/86	P59	2.74	8.98
W18	09/22/86	P61	3.05	10.00
W18	09/22/86	P65	3.35	10.99
W18	09/22/86	P66	3.66	12.00
W18	09/22/86	P67	3.96	12.99
W18	09/22/86	P68	4.23	13.87
W18	09/22/86	P69	4.57	14.99
W18	09/22/86	P70	5.02	16.47
W19	06/21/85	P20	0.91	2.98
W19	06/21/85	P19	0.91	2.98
W19	06/21/85	P21	0.91	2.98
W19	06/21/85	P23	1.52	4.98

TABLE 16. (continued)

Hole	Date	Instrument	Depth (m)	Depth (ft)
W19	06/21/85	P22	1.52	4.98
W19	06/21/85	P24	1.52	4.98
W19	06/21/85	P27	3.05	10.00
W19	06/21/85	P26	3.05	10.00
W19	06/21/85	P25	3.05	10.00
W19	06/21/85	P29	4.57	14.99
W19	06/21/85	P28	4.57	14.99
W19	06/21/85	P30	4.57	14.99
W19	06/21/85	P31	4.88	16.01
W19	06/21/85	P32	4.88	16.01
W19	06/21/85	P33	4.88	16.01
W22	06/27/85	P37	0.91	2.98
W22	06/27/85	P39	0.91	2.98
W22	06/27/85	P38	0.91	2.98
W22	06/27/85	P42	1.52	4.98
W22	06/27/85	P41	1.52	4.98
W22	06/27/85	P40	1.52	4.98
W22	06/27/85	P45	2.74	8.98
W22	06/27/85	P43	2.74	8.98
W22	06/27/85	P44	2.74	8.98

A large variability in the matric potential data is exhibited between psychrometers at the same depth. This variability is shown in Figures 52, 53, and 54, which plot matric potential versus time at the 3.0 ft, 5.0 ft and 9.0 ft depths below land surface (BLS) in hole W22. Plots of the rest of the psychrometer data are presented in Appendix H. Instrument readings plotted in Figure 53 show a range of over 9.0 bars of tension between instruments at the same depth. With so much variation being shown between instruments, it is difficult to determine hydraulic gradients. Therefore, the sources of the variation between instruments must be evaluated so that reasonable estimates of matric potential at a given depth can be determined. Statistical techniques such as analysis of variance will be used to evaluate the sources of the variation.

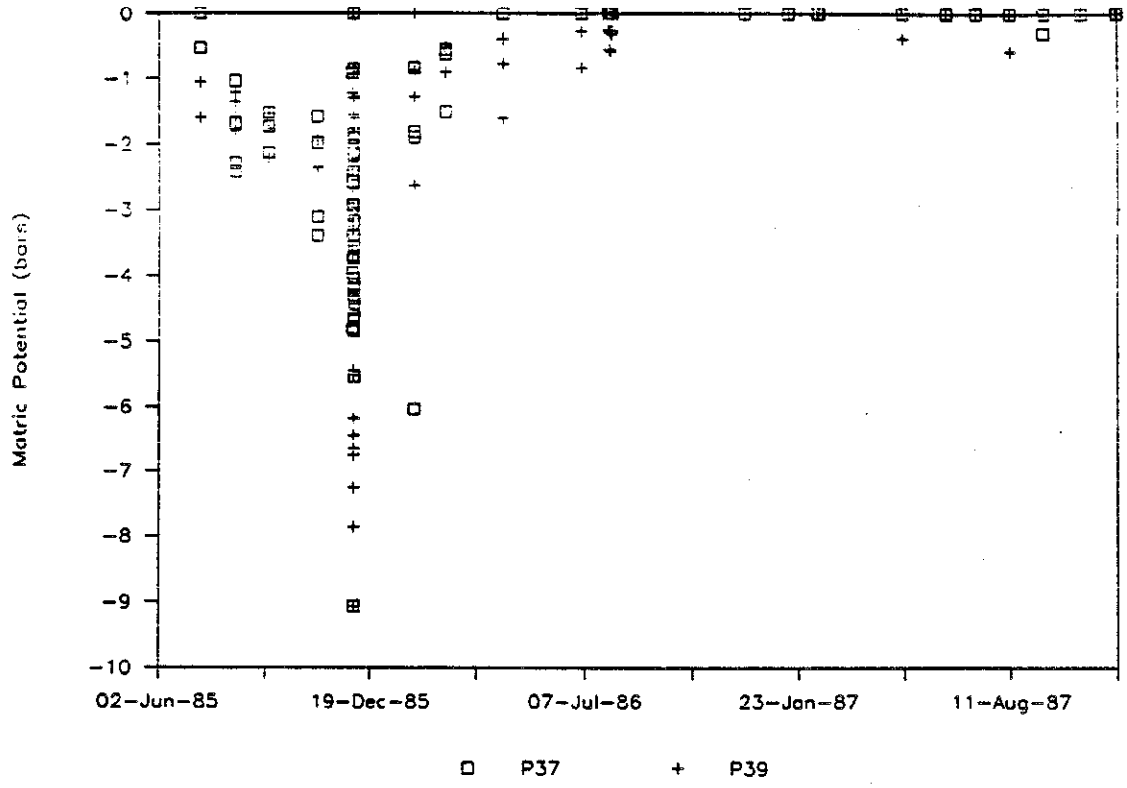

Figure 52. Matric potential versus time measured by psychrometers at 3 ft below load surface in auger hole W22.

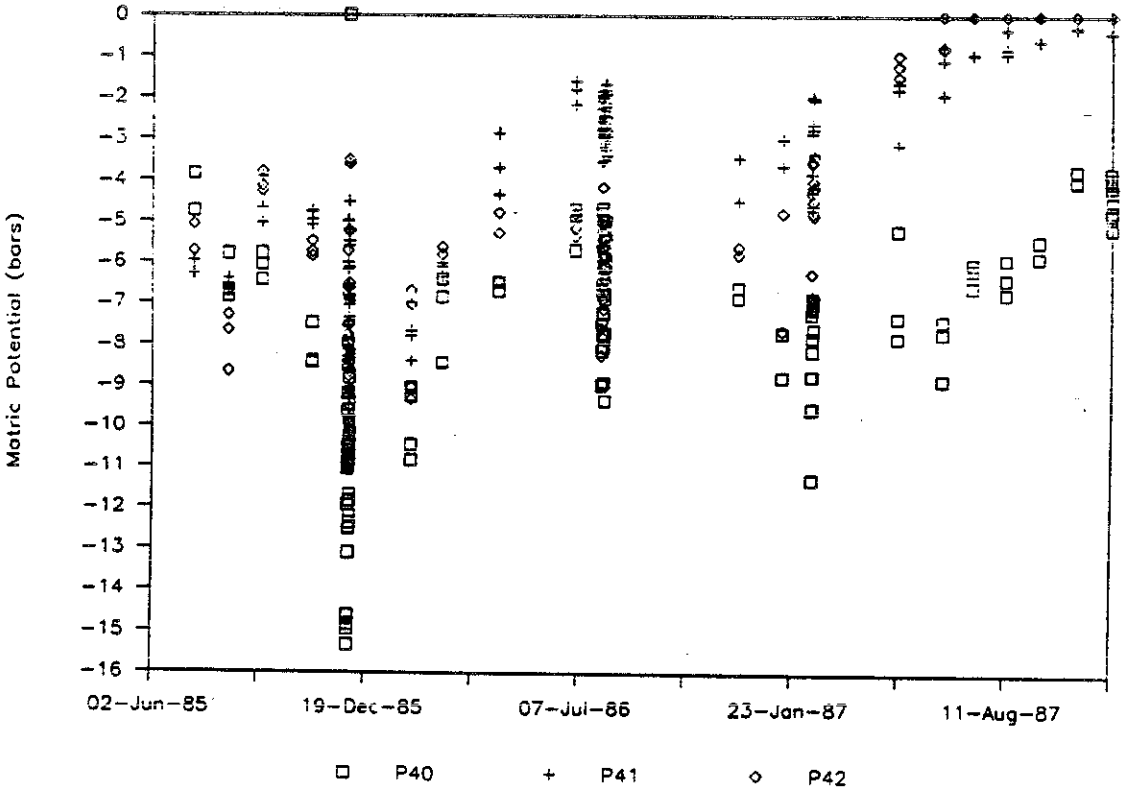

Figure 53. Matric potential versus time measured by psychrometers at 5 ft below land surface in auger hole W22.

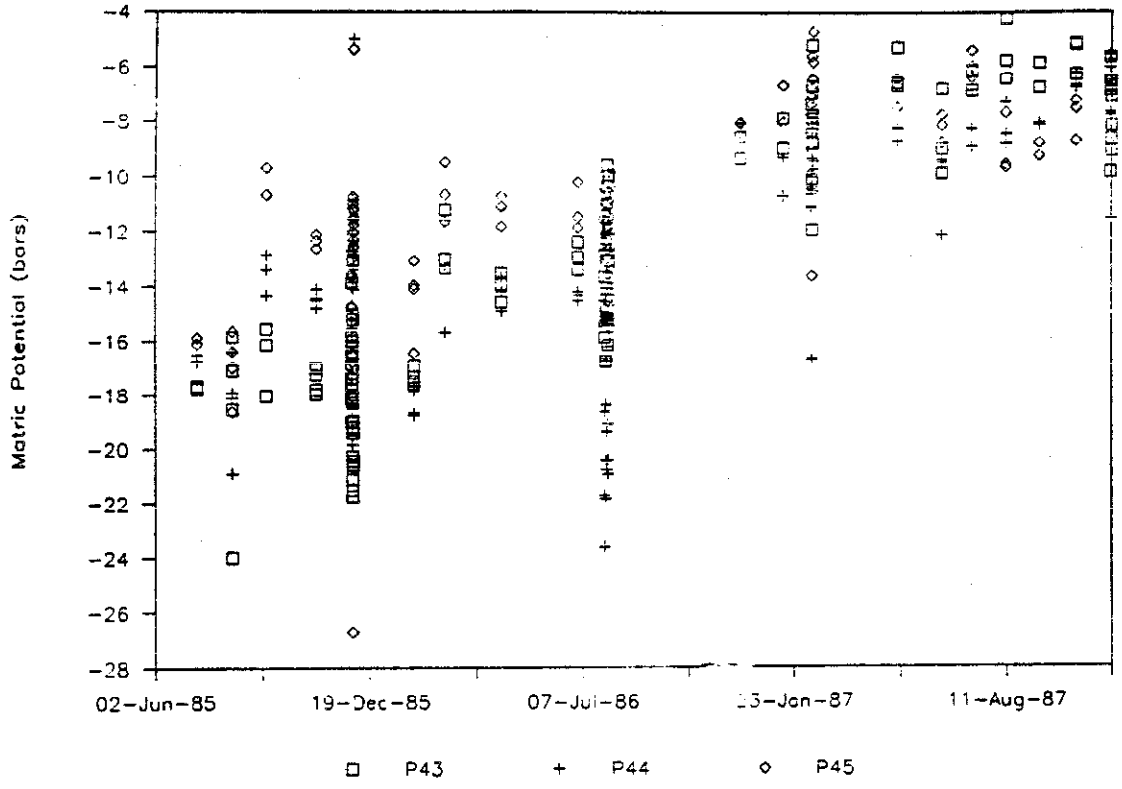

Figure 54. Matric potential versus time measured by psychrometers at 9 ft below land surface in auger hole W22.

Seasonal and diurnal fluctuations are evident in both temperature and matric potential measurements. During early August 1986, the psychrometer data was collected at 2 hour intervals over a 4 day period. Hull (1986) analyzed this data for auger hole W01 and applied a least squares regression technique to study the diurnal and seasonal cycles of both temperature and matric potential. Significant seasonal and diurnal temperature cycles were observed for all psychrometers. However, the diurnal temperature changes were not realistic for heat conduction within such a short time frame. The diurnal fluctuations were suggested to be an effect of air temperature on the measurements, resulting from temperature changes within the electronic data collection unit at the surface. Seasonal temperature cycles showed high summer temperature and lower winter temperatures (Figure 55). Statistically significant diurnal matric potential fluctuations were exhibited by 4 of the 9 psychrometers in hole W01. Seasonal matric potential cycles were not as clearly defined as for temperature, but were exhibited for all psychrometers in W01 except one (P06).

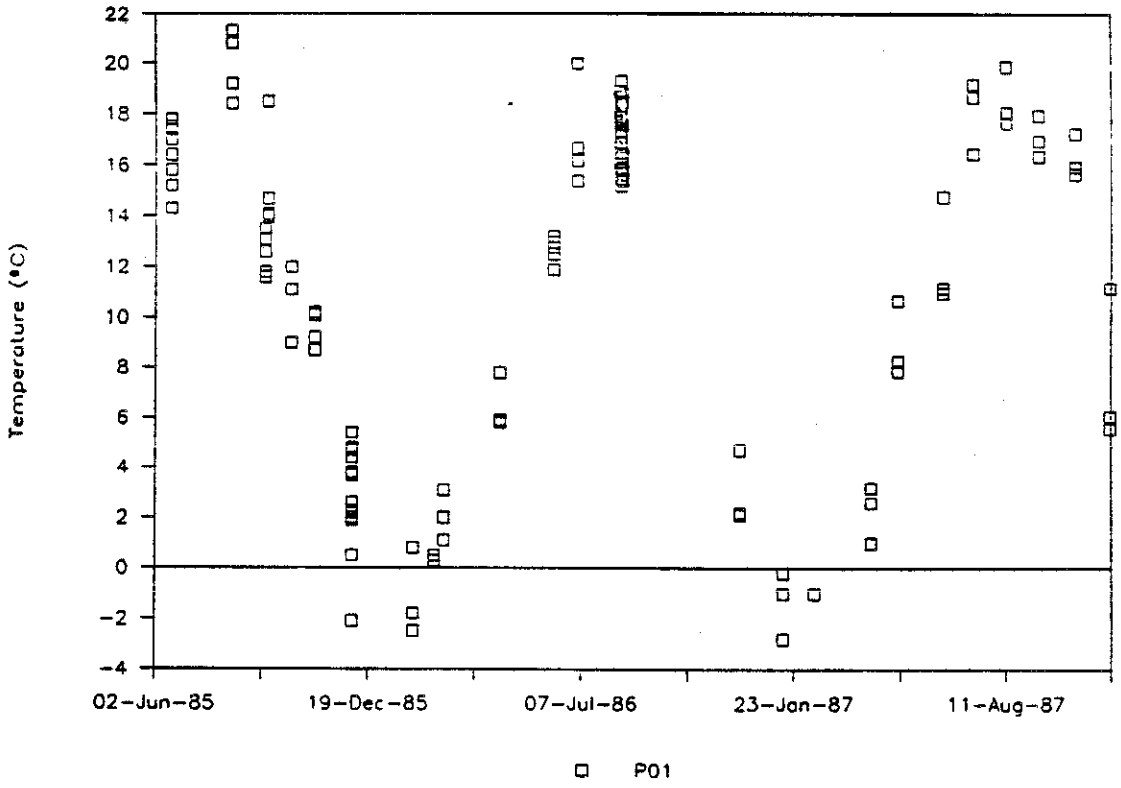

Figure 55. Seasonal fluctuations in temperature in auger hole W01 at the 3-ft depth.

For holes W18, T12 and W19, gypsum block and heat dissipation sensor data were available for comparison with psychrometer data at the same depths. Generally, the psychrometers yielded data with higher matric potentials (closer to saturation) than the other instruments and with little correlation to data yielded by gypsum blocks (see Figure 56, for example) or heat dissipation sensors. As an exception, psychrometers at the 3.0-ft depth in auger hole W19 exhibited seasonal trends in matric potentials that were very similar to those of gypsum blocks at the same depth. This is shown in Figure 57. The lowest matric potentials occur in the winter months, and the highest occur in the summer months.

Whenever possible, other types of instruments should be used instead of psychrometers. The psychrometers could be very useful instruments, because they are applicable to a range of matric potential (10 to 70 bars) in which other instruments are ineffective. However, the large variability exhibited by the data indicates the unreliability of psychrometer results. The use of psychrometers in future holes will be evaluated.

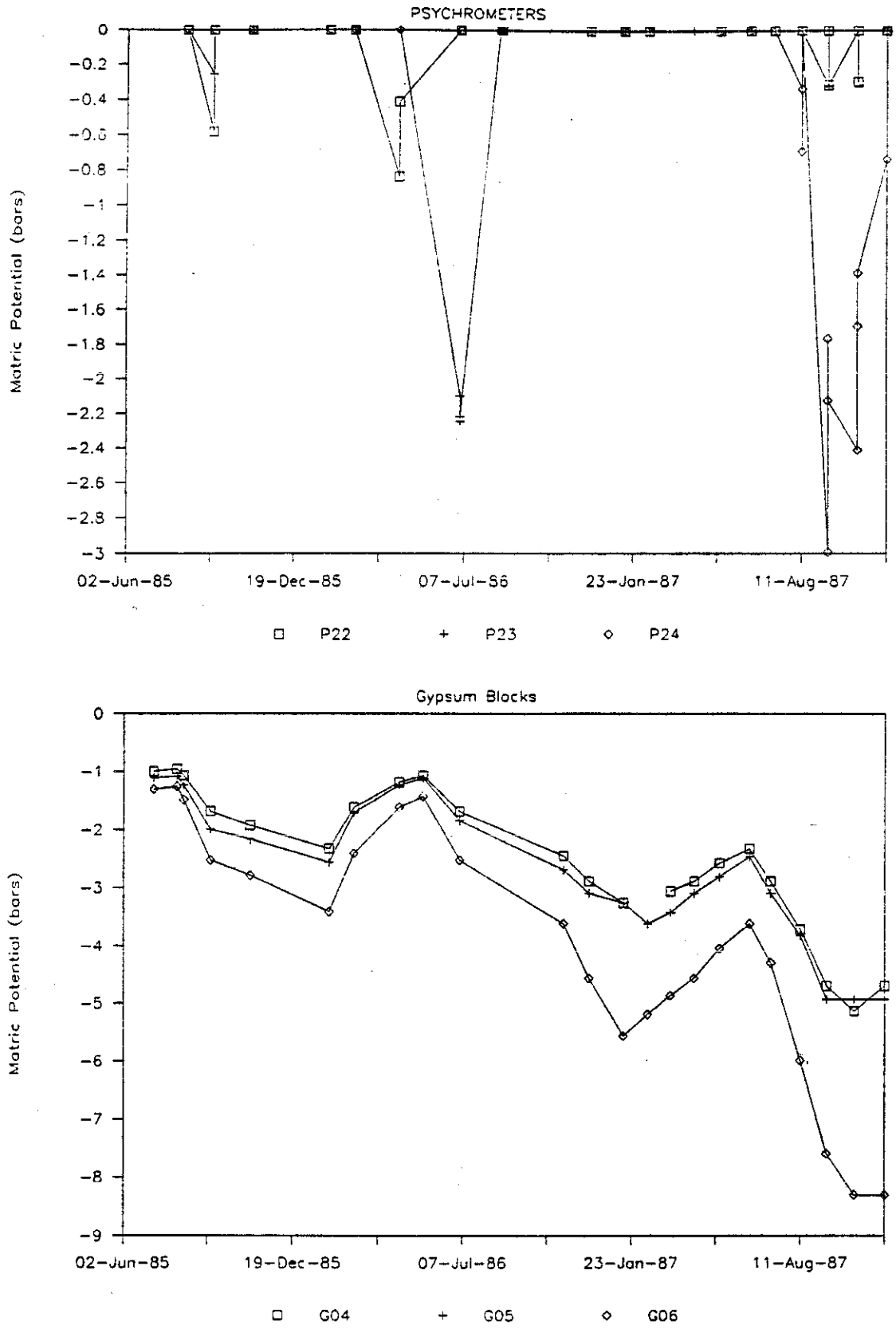

Figure 56. Matric potentials measured by psychrometers and gypsum blocks at 5 ft below land surface in auger hole W19.

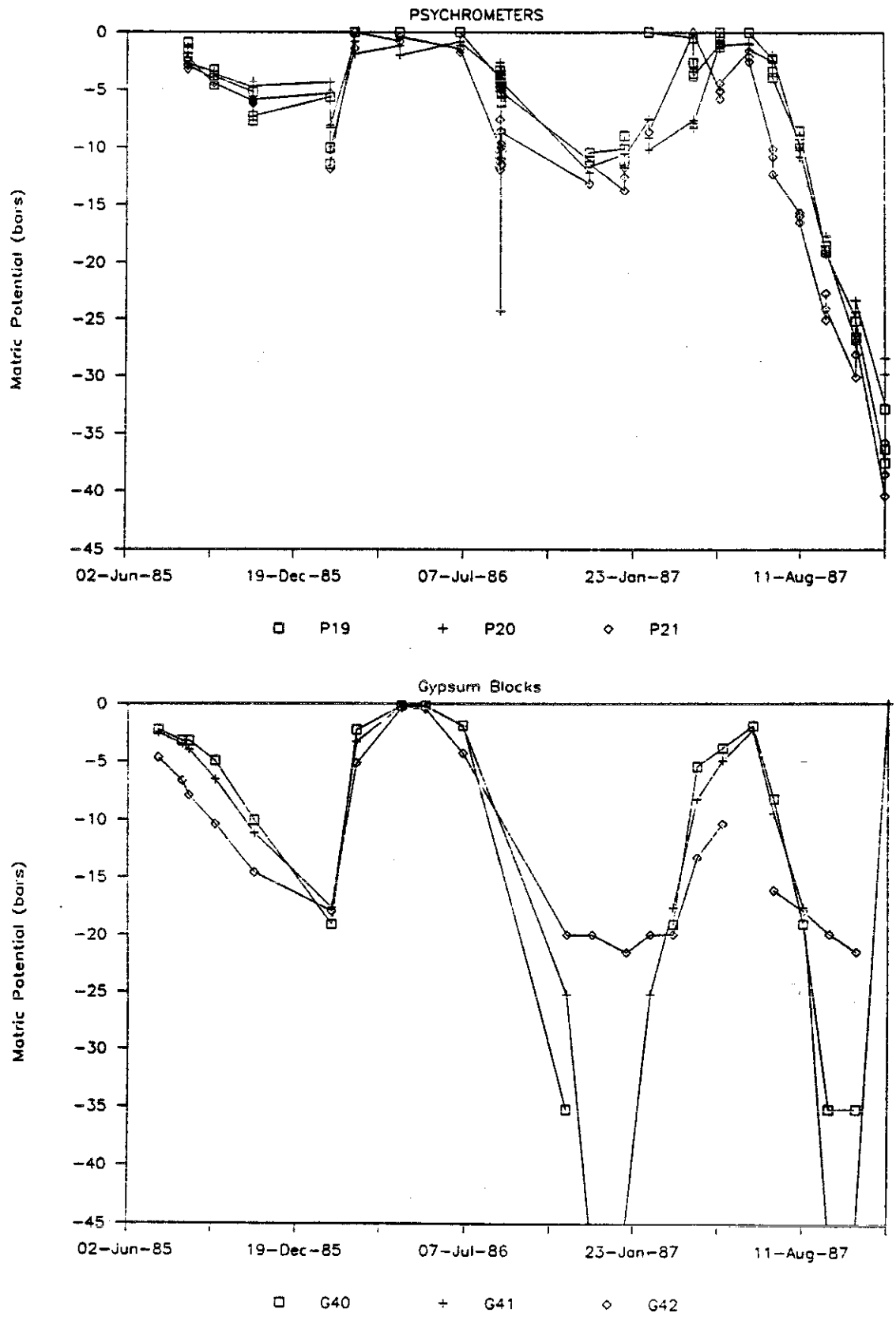

Figure 57. Matric potentials measured by psychrometers and gypsum blocks at 3 ft below land surface in auger hole W19.

5.4.3.5 Neutron Access Holes. Two neutron access tubes were installed within the SDA in November 1986. Access holes were hand augered a few feet west of shallow auger holes W02 and W06. Readings were taken at 6-in. intervals from land surface to basalt on a monthly basis. The instrument utilized is a CPN 503 DR Hydroprobe with a 50 mCi Americium-241/Be neutron source and a 1.5-in.-diameter probe.

The neutron moisture gage measures the moisture content in the soil by supplying a source of fast neutrons which are slowed by the presence of hydrogen in water. The slow neutrons are detected and counted. This count can be correlated to moisture content. Calibration curves for the soils at the SDA have not been calculated. The data is presented as the count rate to examine relative changes in moisture content. Higher count rates correspond with higher moisture contents.

The access tubes are standard 1.5 in. Schedule 40 pipe. They are installed by hand augering a hole, taking moisture samples at various depths, then pushing the tubes into the ground. The moisture samples can be utilized to calibrate the instrument with the soils. Readings can be taken at any depth or time interval. The readings are taken by lowering the source down the access tubing and activating the counter on the gauge.

Figure 58 is an example of a plot of data derived from neutron probes. This figure shows the count rate for hole W02 for June. July, August, and November, 1987. The count rate versus depth for all the months is included in Appendix I. The overall shape reflects changes in the texture of the material with sands described in the drill logs from 3.5 to 5.0 ft and 6.5 to 8.5 ft below land surface. The rest of the material is predominately silt. The sands retain less water than the silt for a given matric potential and therefore give lower count rates.

There is a noticeable attenuation of moisture movement with depth. The variation in count rate from 0.5 to 6.5 ft depth indicates the zone

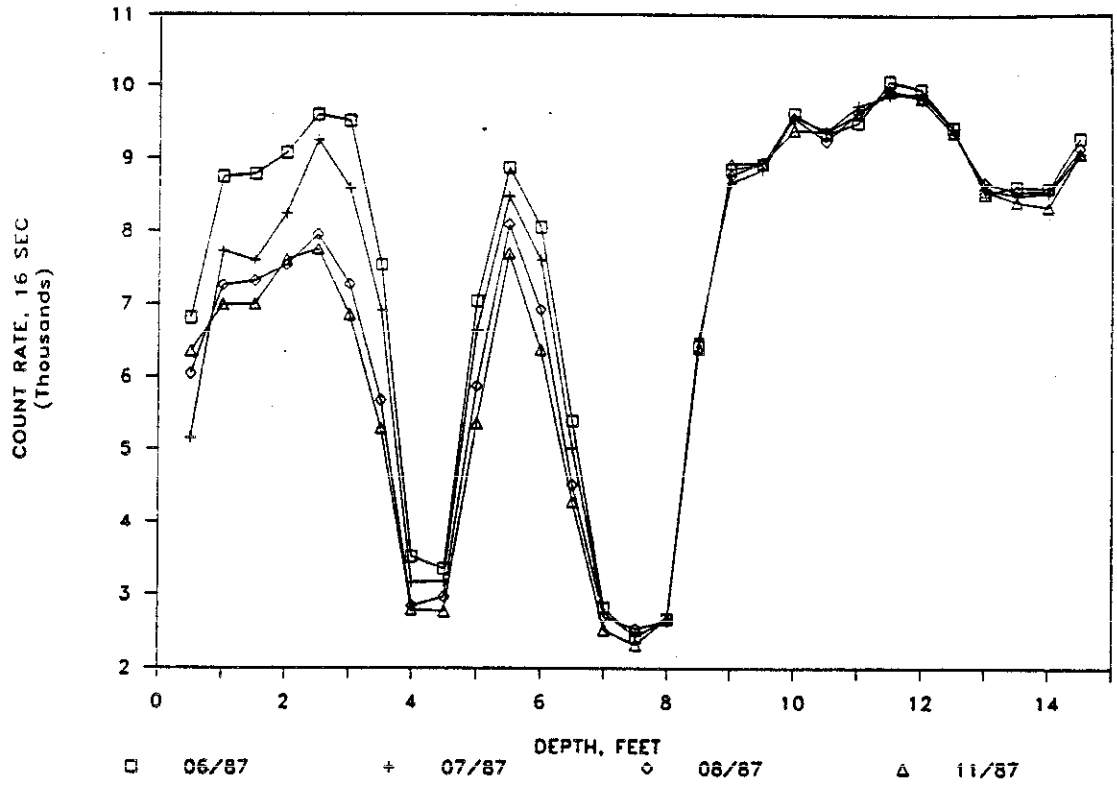

Figure 58. Neutron count rate versus depth in auger hole W02.

affected by precipitation and evapotranspiration. Beneath this depth, water in the material is less affected by these forces and moves by the force of gravity.

Overall, the sediments from 0.5 to 4.0 ft below land surface were dryest in November and December of 1986, then got progressively wetter until March, then (as shown in Figure 58) dried again to November of 1987. The sand layer at 3.5 to 5.0 ft may act as an impediment to downward flow, causing the moisture to accumulate above this layer. In the May to June period there was an increase in count rate from 3.0 ft to 7 ft followed in the subsequent 5 months by a drying trend. The wetting trend at this depth in the May to June time frame may be attributed to redistribution of water from the sediments above. The drying trend from June to November indicates the influence of evapotranspiration during the summer and fall months. The sediments below 7 ft have less variation in count rate than the material above. However, there is a small overall drying trend beneath 12.5 ft for

the entire years record. This may be occurring because this area was covered with several feet of cover material in the summer of 1986 to prevent flooding in this area.

Figure 59 presents the count rate versus depth for hole W06 for June, July, August, and November, 1987. Appendix I contains all the monthly readings for neutron access tube W02. The drill log indicated the sediment is sandy silt with minor amounts of caliche at 3 and 6 to 7 ft depth. The top 6 ft of sediment is most affected by precipitation and evaporation as indicated by large variations in count rate.

Overall, there is a general increase in count rate with increasing depth. Moisture samples taken while drilling W06 and the neutron access hole showed increasing moisture content with depth. The overall trend for the year's data indicates dry conditions in November 1986, wetting in May

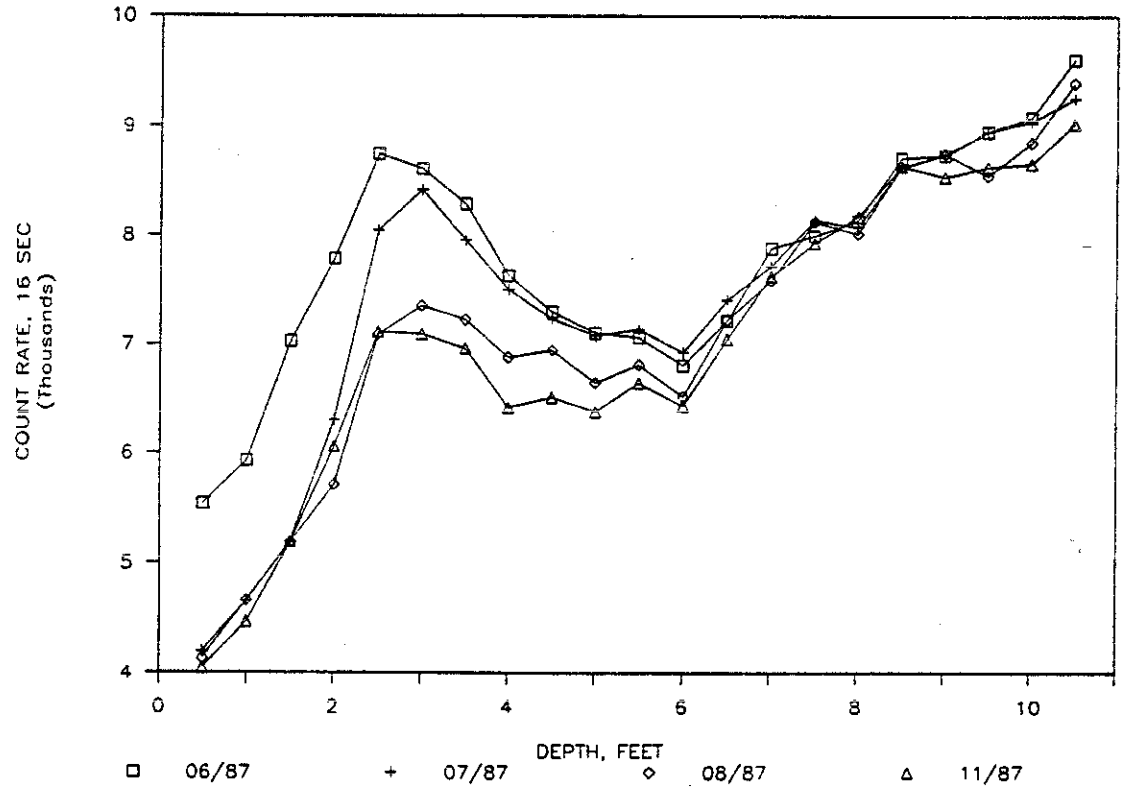

Figure 59. Neutron count rate versus depth in auger hole W06.

and then drying to November 1987. This trend is evident in Figures 58 and 59. The count rate below 6 ft depth does not show large variations, but close examination of monthly logs indicates there is wetting and drying of the sediments occurring at this depth.

The count rate on the neutron probe appears to be quite accurate and reproducible for replicate readings. The 0.5-ft intervals used in these holes gives good definition of textural boundaries and water movement in the system. Monthly readings appear to be frequent enough to give seasonal trends but the monitoring should performed on a weekly or biweekly basis during periods of recharge to obtain data on individual recharge events. Comparing tensiometer data from adjoining holes to the neutron counts indicates a good match for wetting and drying trends between these two instruments. The neutron count rate data define the most active zone in the sediments where water moves up and down depending on the seasonal forces acting on the site. The neutron probe needs to be calibrated to the different soils for quantification of water flux. More neutron access tubes should be installed throughout the SDA to characterize moisture movement. It would be useful at some installations to install the access tubes 12 in. into the basalt to obtain readings from the surficial sediment/basalt interface. Neutron probes should be installed across and within a pit to characterize moisture movement within the sediments between the pits and within the materials in the pit. Access tubes should be positioned around potential water sources (drainage ditches, depressions, flood control berms, etc.) to determine their effect on water movement within the site. Calibration curves for the neutron logging should be obtained, if possible.

5.4.3.6 Porous Cup Lysimeters. Matric potentials in sediments can be estimated using suction lysimeters. When samples are collected from a suction lysimeter a vacuum is applied and water moves from the sediment into the lysimeter. Water stops moving into the lysimeter when the tensions are equal in the sediment and the lysimeter. An approximate matric potential can be calculated by measuring the tension in the lysimeter following equilibration and accounting for the column of water in

the suction lysimeter. Lysimeters that do not hold pressure cannot be used to calculate matric potentials. Tensions were measured prior to collecting water samples for most of the lysimeters. This data has not been compiled or analyzed to date. See Section 5.2, Solution Chemistry, for additional information on the location and status of porous cup lysimeters. Lysimeters can also be utilized to estimate a range of matric potentials. If the lysimeter yields water the tension in the surrounding sediment is in the range of 0.0 to 0.65 bars. Lysimeters that do not yield water but hold the vacuum have a tension between 0.65 bar and the air entry value for the porous ceramic cup (2.4 bars). Lysimeters which will not hold pressure are either in areas where the tension exceeds 2.4 bars or have air leaks within the lysimeter. Examination of pressure drop over time, using a recording vacuum gauge, can be utilized to differentiate between the two possibilities.

5.4.3.7 Analysis of Overall Data. Matric potentials for selected depths are presented in Figures 60, 61, 62, and 63. The data are presented as tension to avoid negative signs. The tensions were recorded in May 1987. The tensions recorded from heat dissipation sensors, gypsum blocks, and psychrometers are mean values for that depth. Multiple readings at a depth represent several types of instruments for comparative purposes. Lysimeter data (wet or dry) are included when available.

The areas with the lowest tensions are in locations where water is present during portions of the year. These areas include drainage and flood control ditches, small depressions where runoff or snow melt accumulates, and areas flooded in the past. Data collected outside the SDA indicates higher tensions (relatively dryer) than data collected within the SDA. The placement of holes tended to bias the lower tension measurements because of the ease of drilling near roads (and drainage ditches).

Matric potentials decrease (approach saturation) with the depth of the hole as a general trend throughout the RWMC. Several of the holes exceed field capacity (values less than 0.1 - 0.2 bars tension), indicating the

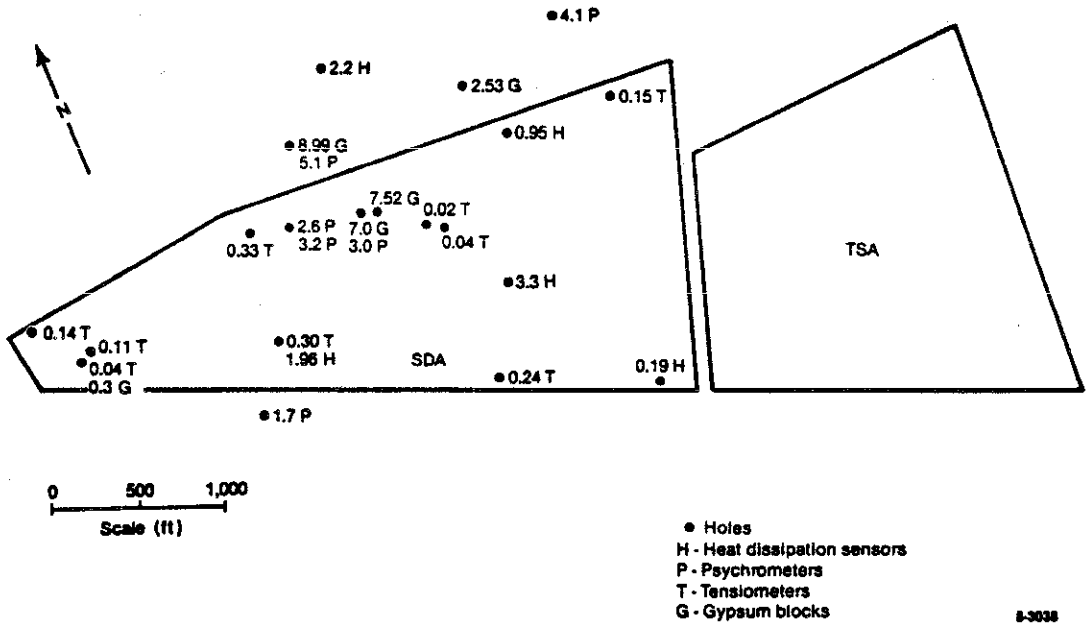

Figure 60. Tensions (bars) in surficial sediment of the RWMC from 3 to 4 ft below land surface (May 1987).

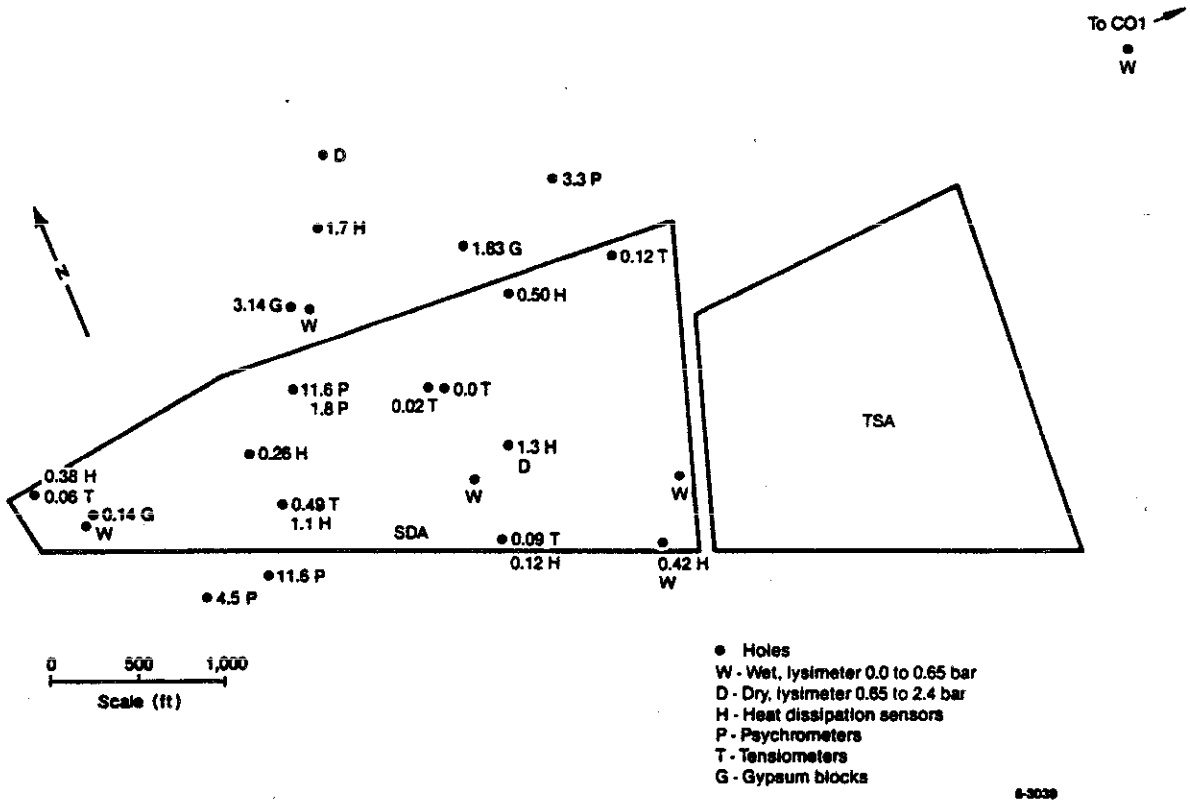

Figure 61. Tensions (bars) in surficial sediment of the RWMC from 5 to 6 ft below land surface (May 1987).

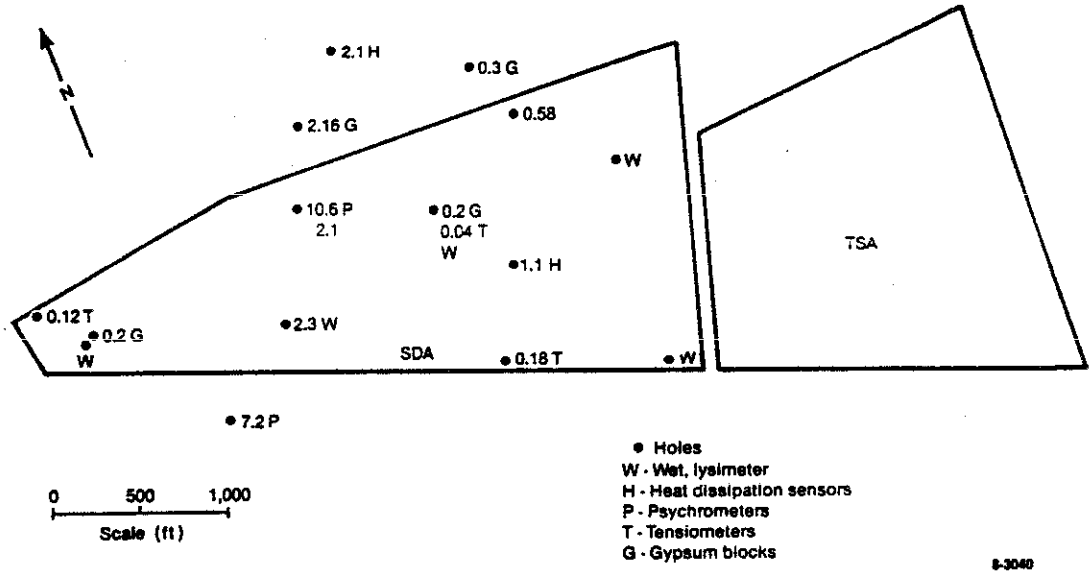

Figure 62. Tensions (bars) in surficial sediment of the RWMC from 9 to 10 ft below land surface (May 1987).

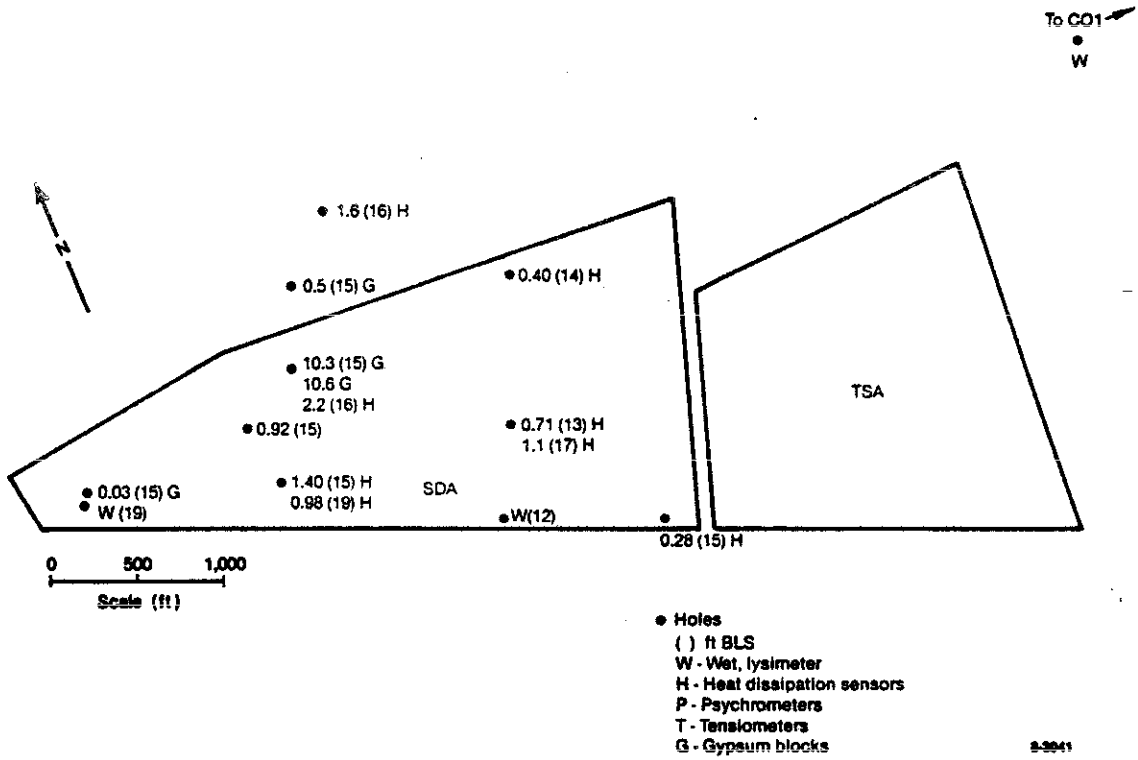

Figure 63. Tensions (bars) in surficial sediment of the RWMC from 12 to 19 ft below land surface (May 1987).

potential for gravity drainage. Hydraulic gradients calculated from instruments at various depths indicates downward moisture movement for large portions of the year for several of the holes.

Neutron data indicates the active zone of the sediments extends to a depth of 6 to 7 ft below land surface. Moisture above this depth is affected by seasonal cycles of precipitation and evaporation, whereas moisture beneath this depth moves downward predominately by the force of gravity.

Four different types of instruments are utilized to measure moisture contents or matric potentials within sediments at the RWMC. Figure 64 gives the effective range for these instruments. No one instrument can cover the entire range for all conditions present at the RWMC with the necessary accuracy. Tensiometers probably produce the most reliable matric potentials for their effective range. They are limited by their installation depth. They should be installed whenever conditions are favorable at multiple depths. Heat dissipation sensors have the potential

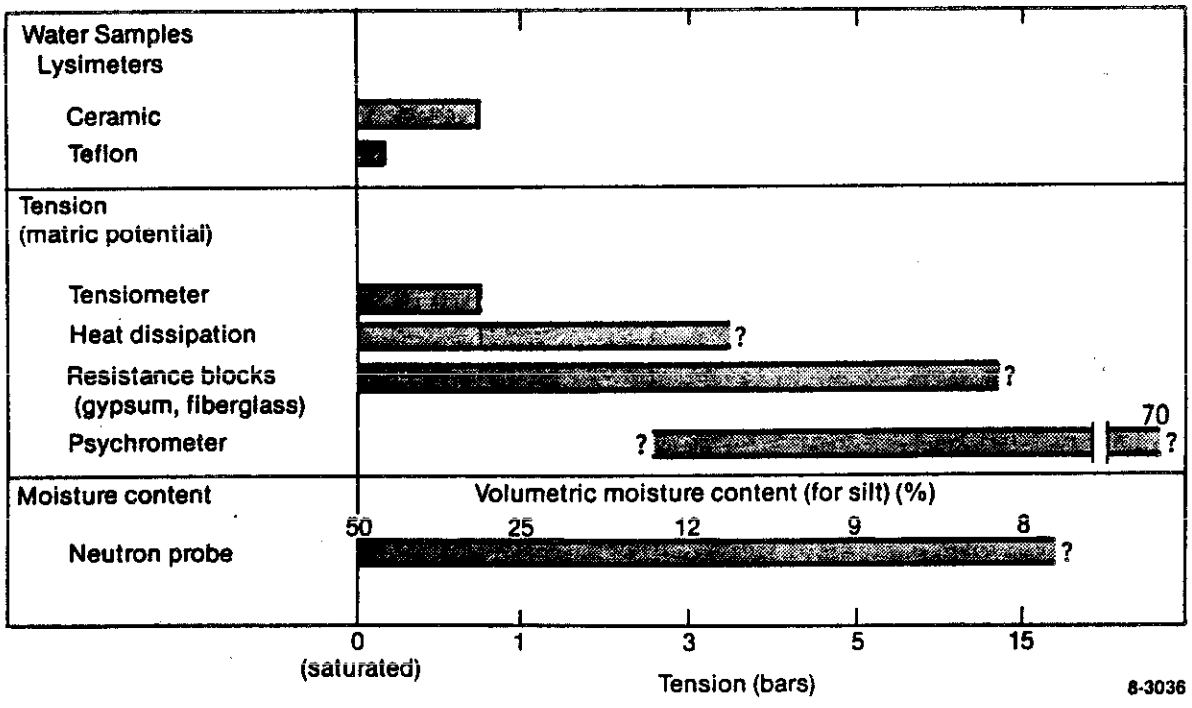

Figure 64. Effective ranges of instruments installed at the RWMC.

to cover a larger matric potential range and can be installed at nearly any depth, but their accuracy and reproducibility of reading is not as good as the tensiometers. Gypsum blocks have worked well at this site. The calibration curves need to be more sophisticated to better fit the data generated in the laboratory. This will increase their accuracy. Gypsum blocks have a short field life (due to dissolution) in wet conditions, and this should be considered in their placement. Neutron probe readings have produced a detailed image of moisture redistribution within the sediments. The probe needs to be calibrated to the RWMC soils to estimate the rate of moisture movement adjacent to the holes.

The analysis of data collected from the Subsurface Investigation Program is not complete. Data from multiple instrument clusters needs to be examined to determine which are the most useful instruments. Readings from various depths within holes need to be statistically analyzed to derive matric potentials for calculation of hydraulic heads and gradients. This data can be utilized with soil moisture characteristic curves and unsaturated hydraulic conductivity curves to quantify moisture flux adjacent to the holes.

5.5 Computer Model Development

5.5.1 Introduction

Radioactive and chemical contaminants buried at the RWMC are potential hazards if their confinement to the unsaturated zone is not maintained. Of particular concern is the potential vertical migration of contaminants to the underlying Snake River Plain aquifer. Irrespective of the final remedial action, there will be a need to make long-term predictions of potential movement of contaminants that have already migrated beyond the boundaries of the burial sites. Computer models are effective tools for making such predictions and have been widely used for this purpose at other DOE waste facilities such as Hanford, Savannah River, and Oak Ridge National Laboratory.

In addition to their use in making predictions, computer models are excellent tools for developing a full understanding of the processes that may influence the movement of the buried radioactive and chemical contaminants. Some of these processes are illustrated in Figure 65. Percolation of soil-water through the vadose zone is a primary driving force for contaminant migration. Sources of soil-water are precipitation, surface water ponding (resulting from rapid snowmelt), and seepage from adjacent ditches. In the past, flooding at the RWMC may have also been a factor in contaminant migration. Transport of dissolved contaminants through the subsurface pathway occurs by advection (i.e., by water flow), diffusion, and dispersion and is influenced by various chemical processes such as sorption, complexation, and decay. Contaminants in a colloidal form are transported by the same physical process but are also affected by filtration. Certain radionuclides (e.g., radon and tritium) and volatile organic contaminants (e.g., carbon tetrachloride and trichloroethylene) are transported primarily in the vapor phase.

Several computer models are being developed that will be used to formulate an understanding of the important transport processes at the RWMC. In addition, the models will be used to assist in answering a number of basic scientific and engineering questions relevant to the isolation performance of the disposal site, such as:

- What is the range of percolation rates and how do the rates vary over an annual period?
- When water ponds on the land surface, how does the water move through the sequence of sediments and basalt?
- What is the moisture content distribution in the vicinity of the waste?
- To what extent have previous flooding events affected contaminant movement through the vadose zone?

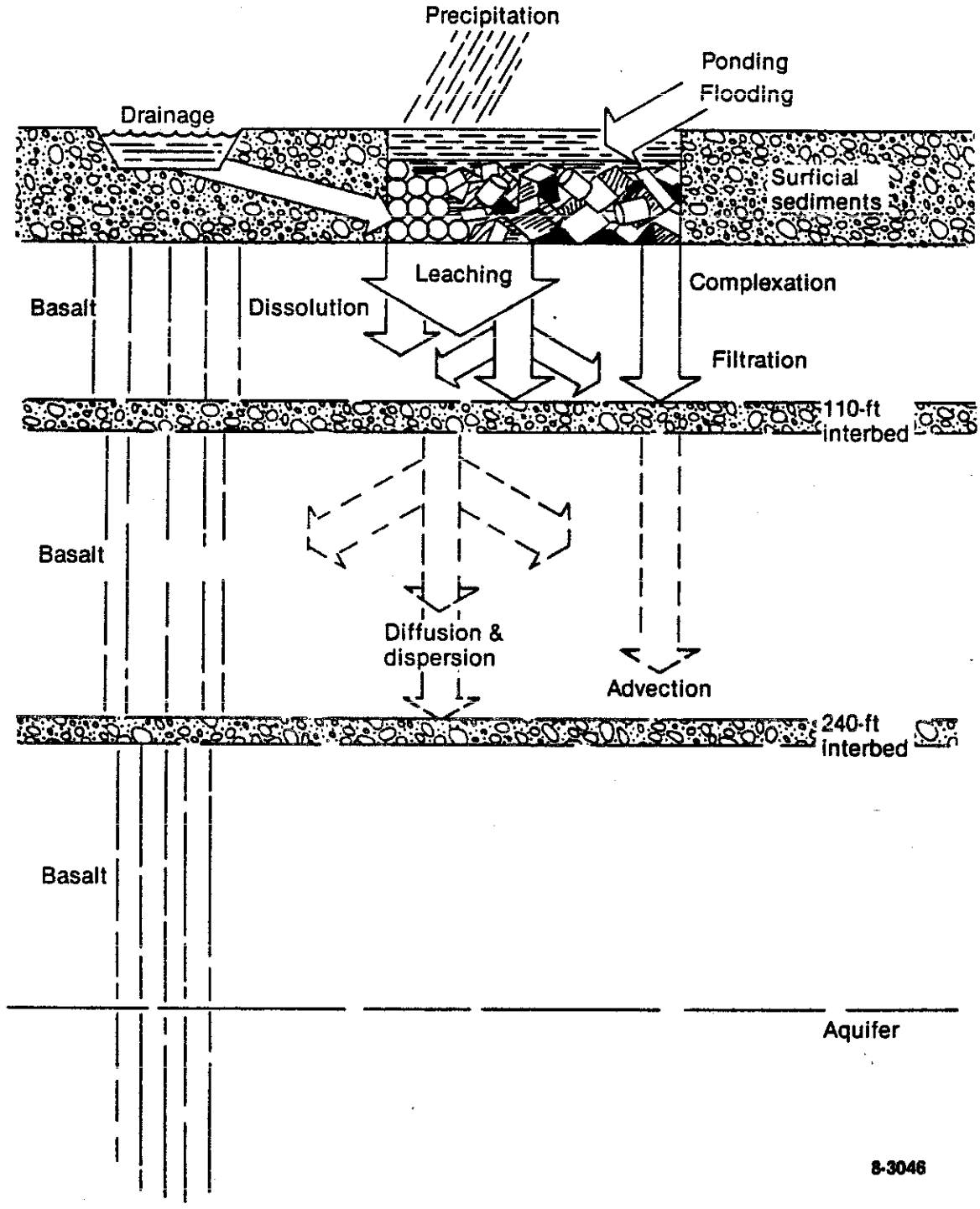

Figure 65. Conceptual model of processes involved in contaminant transport in the vadose zone.

- What are the water and contaminant travel times to the aquifer?

- Are there any potential synergistic effects between chemical and radioactive wastes that might influence contaminant transport?

- Are moisture barriers needed to minimize water percolation through the waste disposal pits?

5.5.2 Summary of Accomplishments

In this reporting period, work on the Computer Model Development task has focused on three specific areas: (1) a detailed review of previous vadose zone modeling studies at INEL, (2) acquisition and installation of several computer models for modeling unsaturated flow and contaminant transport, and (3) preliminary applications of computer models using site-specific data. Accomplishment in these three areas is summarized below.

5.5.2.1 Review of Previous Modeling Studies. In the early 1980s, two modeling studies were conducted that focused on subsurface radionuclide migration. These two studies were performed in support of studies of long-term management alternatives (DOE, 1982). The two previous studies were reviewed. Brief summaries of these reviews are presented here.

The first attempt to model unsaturated flow and transport in the RWMC vadose zone was made by Pope and Reno (1982). Their draft report was later updated and published in the paper by Humphrey et al. (1982); this work is also presented in DOE (1982). The objective of their study was to evaluate the potential upward and downward migration of radionuclides at the RWMC. A computer model was used to simulate the migration of various radionuclides through the soil for two conditions: (1) the annual cycle of precipitation/evaporation and (2) site flooding.

Simulations of moisture and radionuclide transport were performed using the one-dimensional computer code UNSAT, originally developed by Hanks and King (1973). Moisture transport was simulated for one year for

the cyclic precipitation/evaporation scenario and for 300 years for the flooding scenario. Unfortunately, these authors did not document the results of the moisture transport simulations. Radionuclide transport simulations were performed for each scenario; results from their simulations are plotted and presented in Humphrey et al., (1982).

The basic conclusion drawn by Pope and Reno was that it should take many thousands of years for radionuclides to migrate any appreciable distance. For example, these authors predicted that about 10,000 years would be required for trace levels (i.e., 10^{-9} μCi/g) of plutonium-239 to reach the sedimentary interbed at 110 ft.

In the second study, Mizell and Hull (1983) performed a similar analysis of flow and transport in the vadose zone. The main distinction of their study was that the hydraulic properties were chosen (i.e., assumed) on a different basis. These authors then repeated the analysis of Pope and Reno. Mizell and Hull performed simulations of moisture and radionuclide transport using the UNSAT computer code (Hanks and King, 1973).

The principal conclusion drawn by Mizell and Hull was that radionuclide migration should be less than that predicted in Humphrey et al., (1982). For example, Mizell and Hull predicted that it would take about 10,000 years for trace levels (i.e., 10^{-9} μCi/g) of plutonium-239 to move 20 ft, as compared to 100 ft predicted in the Pope and Reno study.

Recent field measurements, however, have indicated trace levels of plutonium-239 at the 110-ft interbed. These measurements indicate that radioactive contaminants have traveled through the vadose zone at rate significantly higher than those predicted by the two modeling studies. In view of the fact that these studies were conducted without the benefit of site-specific data, it is not surprising that the predictions are grossly inaccurate. Other factors that contributed to errors in the computer predictions are:

1. The computer model used in the two studies was not specifically applicable to an arid site vadose zone.

2. The computer model was applied without calibration against field measurements.

3. The computer model assumed that the hydraulic properties of fractured basalt were similar to those of the sediments, which is a questionable assumption.

4. Nonconservative assumptions were used regarding sorption properties of the radionuclides in the sediments and basalt.

Although the two previous studies did not produce much insight into the basic processes affecting contaminant movement, they clearly highlight the fact that reliable predictions cannot be obtained without an adequate data base and field calibrated models.

5.5.2.2 Acquisition and Development of Computer Codes. Several computer models have been acquired and installed on the INEL CRAY XMP/24 computer. These computer models are being further developed and will provide the capability to analyze the important processes and interactions that influence the migration of aqueous, nonaqueous, and vapor phase contaminants in the subsurface environment. In particular, the computer models will allow the analysis of such processes as:

- Natural moisture movement in the multilayer, heterogeneous, anisotropic medium

- Environmental heat transfer and its effects on the net water influx and vapor phase transport

- Air flow induced by barometric pressure changes and its effects on dispersion of vapor phase contaminants

- Transport of immiscible chemical contaminants

- Transport of dissolved radioactive and chemical contaminants as a function of percolation rates.

The suite of computer codes is currently being tested and documented and is also being used in preliminary modeling efforts. At present, five major computer models have been installed on the INEL CRAY computer for modeling transport through the subsurface. These models are:

1. SEMTRA This 1-dimensional model is being used to predict water percolation rates in the vadose zone as a function of precipitation, evapotranspiration, solar heating, and cooling.

2. FEMTRA This 2-dimensional model is being used to predict moisture movement in layered, heterogeneous, fractured porous media in multiple dimensions.

3. TRACR3D This 3-dimensional model is being used to predict contaminant transport through the vadose zone as a result of discrete events, e.g. flooding.

4. MAGNUM This model, capable of either 2- or 3-dimensional modeling, is being used to predict groundwater or soil-air flow paths, velocities, and travel times to the receptor boundaries.

5. CHAINT This 2-dimensional model is being used to predict transport of liquid or vapor phase contaminants, contaminant concentrations, and fluxes in the aquifer.

In addition to the major computer models, eight other codes, referred to as support codes and models, have been acquired and implemented. These support codes and models are summarized in the Table 17.

TABLE 17. PRINCIPAL USES OF SUPPORT CODES AND MODELS

Codes and Models	Principal Use
SOIL	This program performs nonlinear least squares fits to laboratory data on soil moisture data and generates analytic functions for the moisture release curve and hydraulic conductivity curve. These functions are input to the SEMTRA, FEMTRA, and TRACR3D codes.
PATH	This code computes the groundwater flow paths and travel times from the point of input to the aquifer to designated receptor boundaries. The output of this code is a computer plot showing the contaminant pathways through the aquifer and travel times along those pathlines.
VELPLT	This computer program computes the liquid and vapor phase velocities. These velocities are computed using the predictions generated with the MAGNUM or CHAINT models. The output of the code is a plot of the velocity vectors superimposed on the geologic cross-section.
CHTFLX	This computer code calculates the contaminant release rates and cumulative release at designated boundaries. The code uses the results from the CHAINT model and produces graphical output.
PORFLO	This computer model is used to cross-check the flow and transport predictions of the MAGNUM and CHAINT models.
PARAM	This code is used for interactive plotting of the predictions generated by the SEMTRA, FEMTRA, MAGNUM, CHAINT, and PORFLO models. The code output consists of time history plots and/or profile plots.
CONTOUR	This code is used for interactive plotting of the predictions generated by the FEMTRA, MAGNUM, CHAINT, and PORFLO models. The code output consists of contour plots showing the vertical and/or horizontal distribution of hydraulic driving forces and/or contaminant concentrations.
FE Software	A suite of support software used to generate, check, optimize, and plot the input data for the finite element models, (i.e., SEMTRA, FEMTRA, MAGNUM, and CHAINT computer models).

5.5.2.3 Preliminary Applications of Computer Models. Model applications were initiated in the following four areas: (1) analysis and curve fitting of soil hydraulic properties, (2) simulation of environmental heat transfer and calculation of soil temperature profiles, (3) simulation of moisture transport for surface water ponding conditions, and (4) analysis of organic vapor transport from the waste disposal pits. Highlights and example results from these model applications are presented here.

The computer code SOIL was used to analyze laboratory data on the moisture release curve (i.e., relation between capillary pressure and volumetric moisture content). The SOIL code fits a closed-form equation to the measured data using nonlinear least squares and then computes the hydraulic conductivity curve using an empirical theory. The specific mathematical approach used in the code is described by Van Genuchten (1978 and 1980). An example of outputs from the SOIL computer code is presented in Figure 66, which was derived from data obtained from laboratory analysis of a soil sample from borehole D10. These curves will vary depending on the properties of the soil sample (particle size, clay content, etc.). These curves are specifically used for:

- Estimating the moisture content levels of the interbeds directly from the field measured values of matric potential
- Estimating the hydraulic conductivity of the sediments as a function of moisture content or matric potential
- As input data to computer models that predict percolation rates through the vadose zone.

These curves represent the most fundamental characterization of the moisture properties of the vadose zone and are essential to a quantitative understanding of the processes controlling moisture movement.

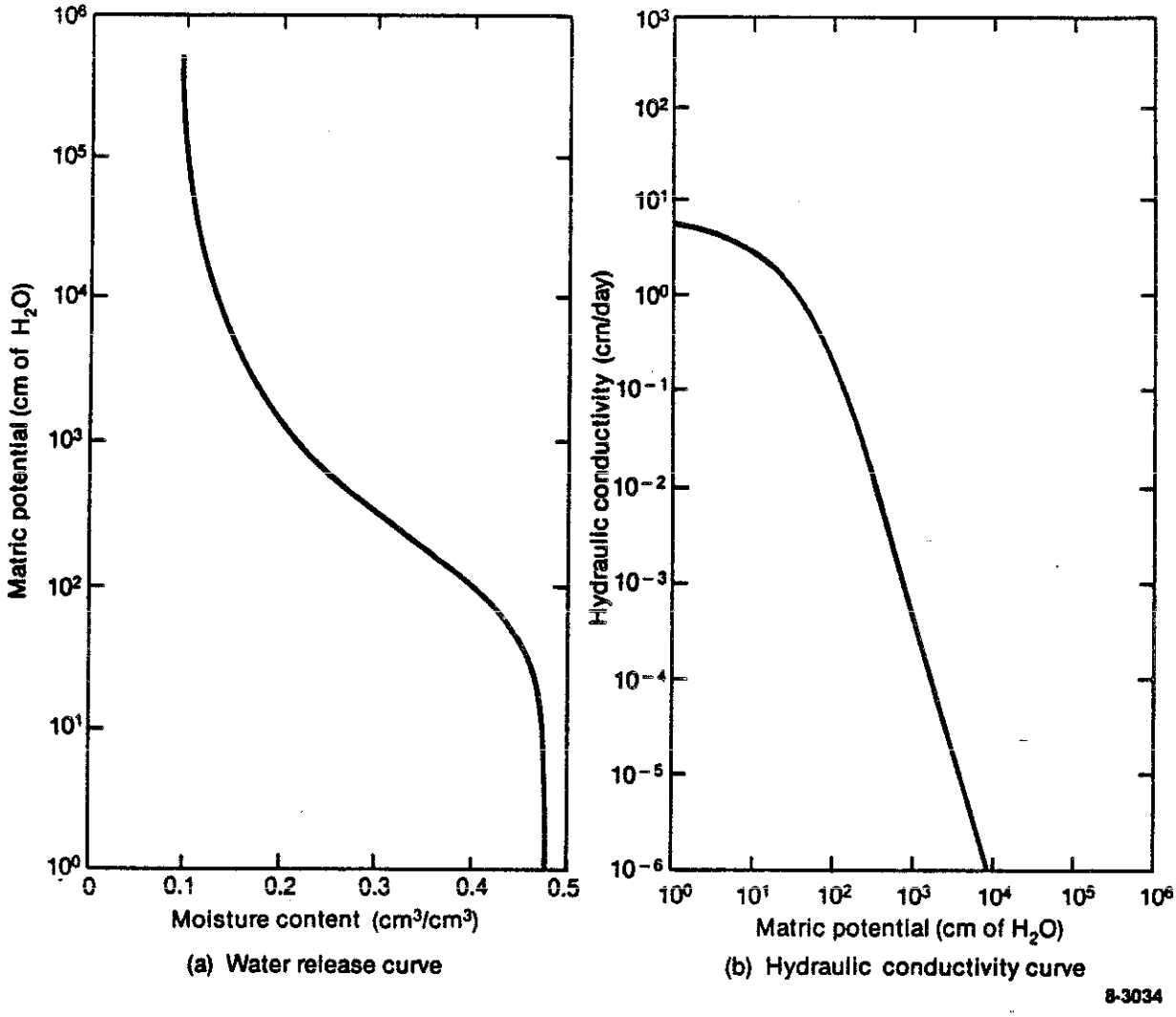

Figure 66. Soil-moisture relations generated by the SOIL computer code (sample taken from deep borehole D10).

Soil temperatures in the upper portion of the vadose zone were simulated using the SEMTRA computer code (Baca et al., 1978), which was developed at Hanford. The purpose of this application was to estimate the temperature ranges and variations that occur in the vicinity of the waste disposal pits. Soil temperature measurements (Yanskey et al., 1966) collected near Test Area North (TAN) were used to calibrate the model. The SEMTRA code was run to simulate daily average temperatures in the subsurface. Calculated soil temperatures for various months are presented in Figure 67. In subsequent effort, the SEMTRA code will be calibrated using soil temperatures measured at the Test Trench facility located at the RWMC.

Soil temperature is an important hydrologic parameter because it plays a key role in a number of processes, such as:

- Evapotranspiration and its contribution to the net water flux at the air-soil interface
- Release of the vapor phases from volatile liquid contaminants that have leaked into the sediments
- Variation of soil hydraulic conductivity resulting from changes in fluid density and viscosity
- Vapor phase transport of soil-moisture.

Because of its strong effect on flow and transport processes, soil temperature and its variation is a basic factor that must be included in the vadose zone models.

The TRACR3D computer code (Travis, 1984), developed at Los Alamos National Laboratory, was applied to model the process of soil moisture movement in the upper portion of the vadose zone. The soil moisture profiles computed for this simulation with the TRACR3D code are shown in Figure 68. The purpose of this simulation was to study the patterns of

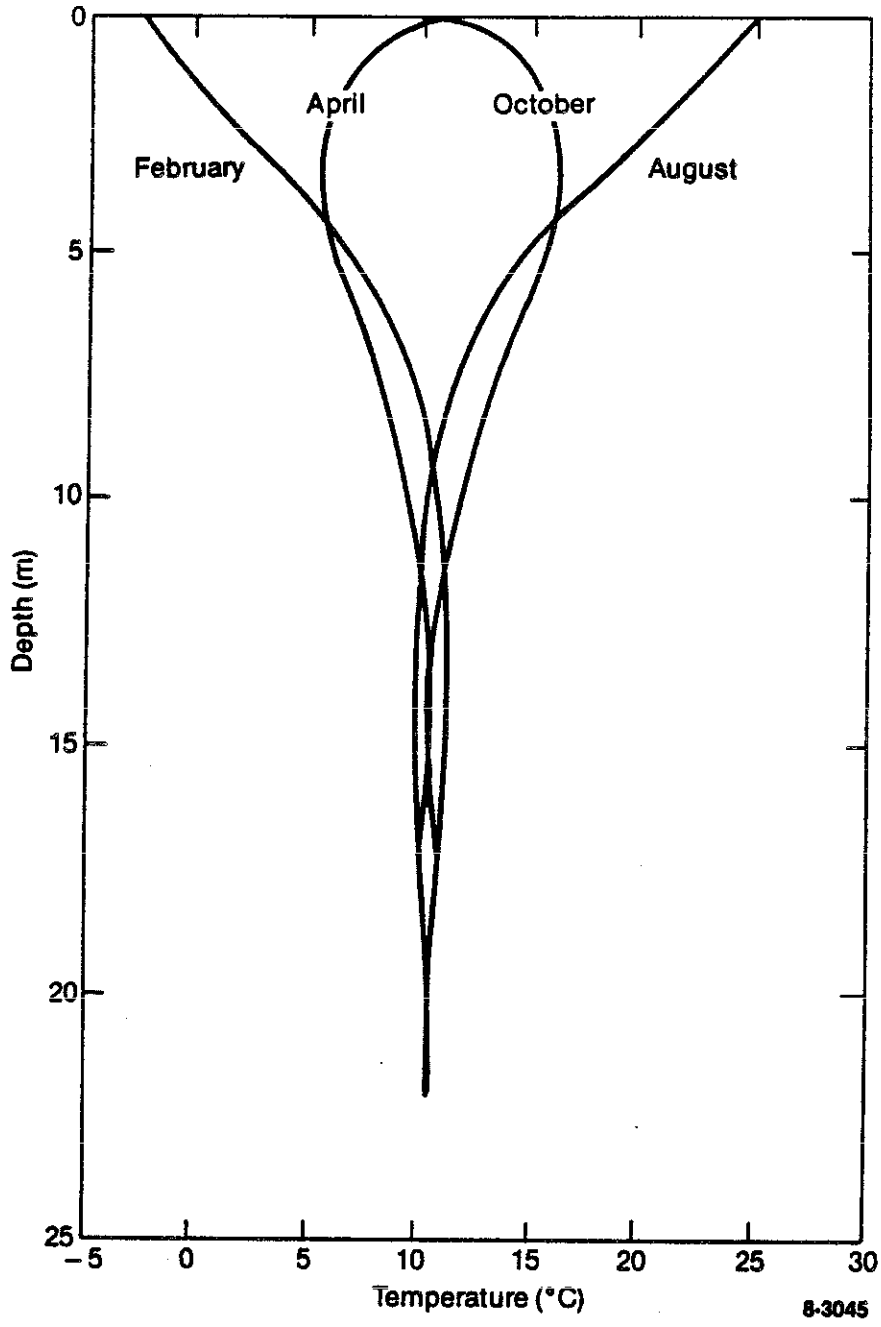

Figure 67. Soil temperature profiles computed using the SEMTRA computer code.

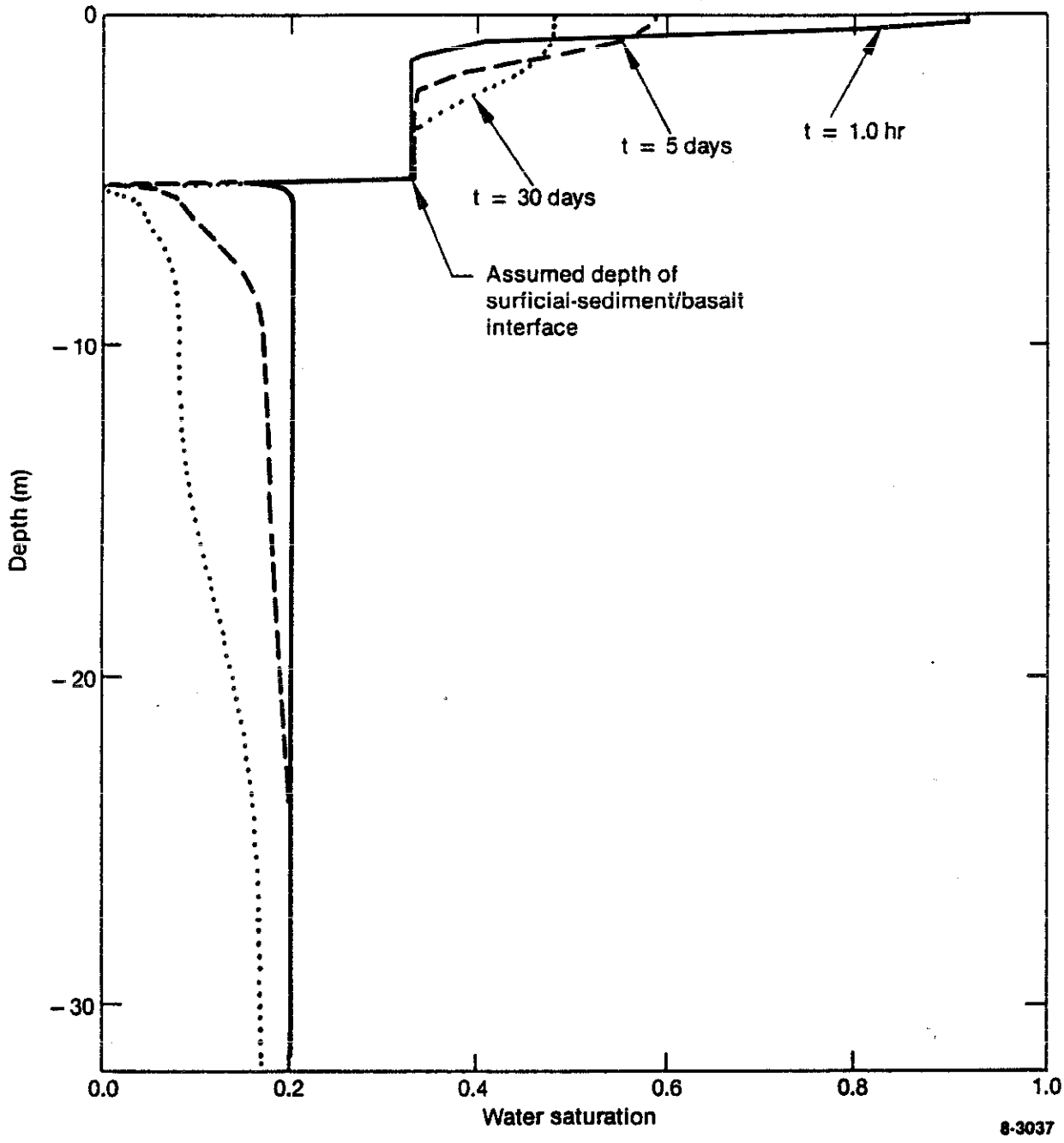

Figure 68. Soil moisture profiles computed using the TRACR3D computer code.

soil moisture movement resulting from water ponding at the soil surface. The simulation was also intended specifically to test the numerical capabilities of the code. The simulation assumed initial saturations of 0.35 in the surficial sediments and 0.20 in the underlying basalt, and a release to the soil surface (by ponding) of 10 cm of water. In addition, it was assumed that the basalt had a permeability of approximately four orders of magnitude greater than that of the sediments. The simulations indicate that a steep moisture front moves slowly through the surficial sediments. Upon reaching the sediment-basalt interface, the moisture drains quickly into the basalt.

The CHAINT computer code (Baca et al., 1984; Kline et al., 1985), developed at Hanford, was used to simulate the organic vapor transport from the disposal pits at the RWMC. The computer simulation represents a practical application of the CHAINT code to a site-specific contaminant transport problem. The basic objective of the computer simulation was to evaluate the nature and scope of the VOC problem. A number of technical issues were also evaluated, including:

- What factors are controlling the vapor release rate?
- Which volatile organic compound is of most concern?
- What is the possible extent of the vapor plume?
- How long will the vapor problems persist?
- What potential remedial measures should be evaluated?

Using the estimated inventories of organic compounds (disposed in pits 4, 5, 6, 9, and 10) and a vapor release submodel, the CHAINT computer code generated a simulation of the vapor plume history from 1966 to 1987. The code calculated vapor diffusion through the subsurface and the concentrations of the organic vapors at various points in space and time. The VOCs of the output in the pits consisted of carbon tetrachloride,

chloroform, trichloroethylene, tetrachloroethylene, and trichloroethane. A sample from the computer simulation of the carbon tetrachloride plume is shown in Figure 69.

The computer study of the organic vapor problem at the RWMC indicated that:

- Soil temperature is a key factor controlling vapor release rate
- Carbon tetrachloride appears to be the volatile organic compound of primary concern
- The carbon tetrachloride plume appears to have spread a significant distance in the lateral direction and vertically to the water table
- The carbon tetrachloride plume may persist in the subsurface for tens of years, if no remedial measures are used
- Air stripping may be a very effective and inexpensive remedial measure.

5.5.3 Discussion

In this reporting period, significant progress has been made in assembling the computer modeling capability needed to address the issues of waste disposal at the RWMC. This progress was made primarily by acquiring existing computer models have been developed and applied at other DOE sites. There remains, however, a need to demonstrate the adequacy of the various computer codes to handle the unique hydrogeology beneath the RWMC. In addition, there is a need for some basic research into flow in unsaturated fractured basalt because no definitive theory currently exists that explains the physics of flow under these conditions. In this section, we outline the current view regarding the adequacy of the computer models, specific research areas that need to be addressed, and discussion of data needs.

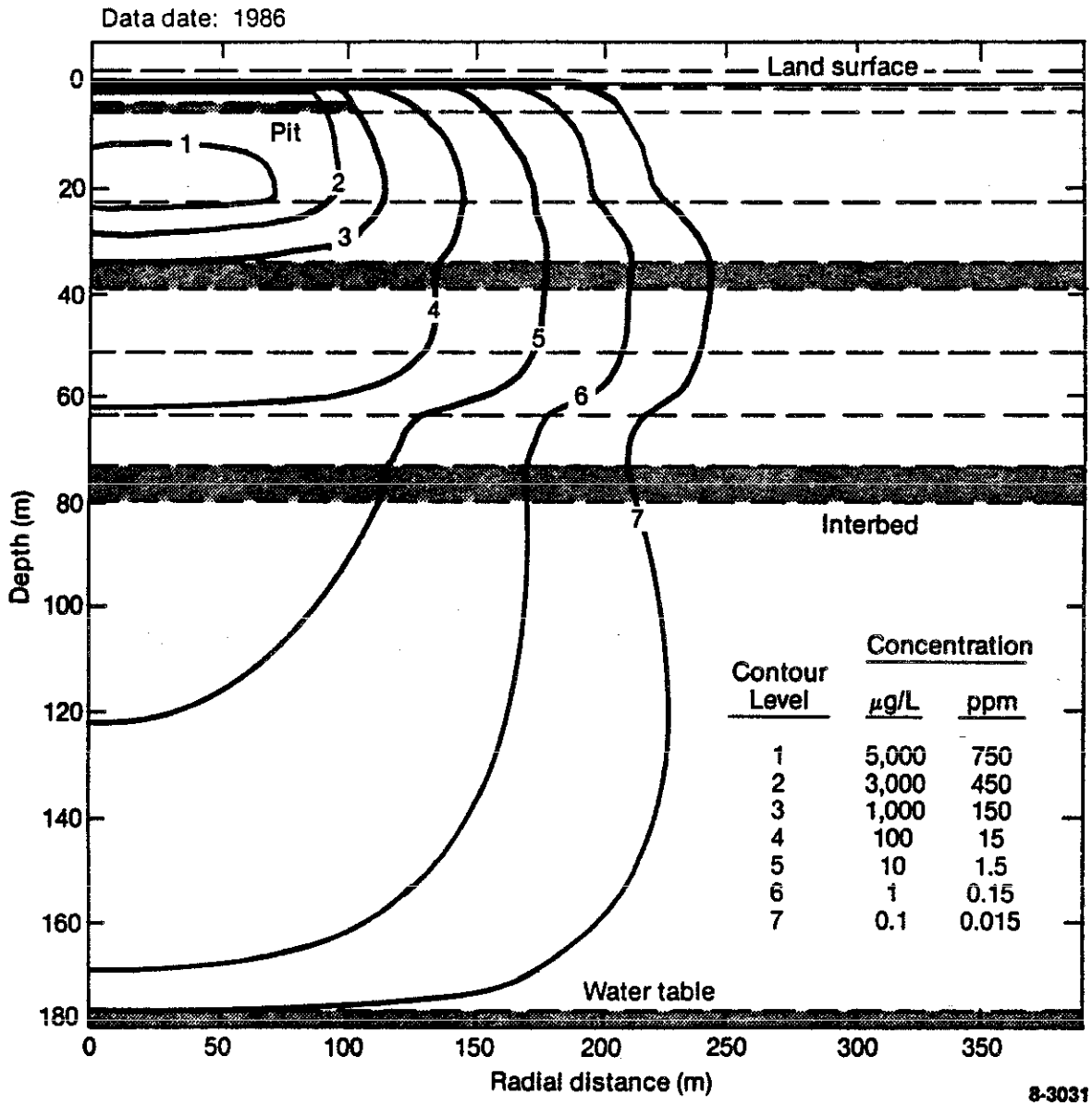

Figure 69. Organic vapor plume simulation generated using the CHAINT computer code.

5.5.3.1 Adequacy of Computer Models. The full suite of computer models (discussed in Section 5.5.2.2) that has been acquired has been tested using available site data. The results of this initial testing indicate that the computer models will be able to simulate a wide range of hydrogeologic conditions and scenarios of interest. There are two areas, however, that will require some additional code refinement.

In the first area, the SEMTRA code will need to be refined to improve its capability to: (1) realistically describe evapotranspiration effects, (2) explicitly compute the solar heating and cooling at the air-soil interface from meteorologic data, and (3) better handle the large permeability contrasts that exist between the sedimentary and basalt layers. These model refinements will involve a relatively small man-effort but will substantially improve the model's predictive capability.

In the second area, the TRACR3D code will need to be streamlined and, to some extent, debugged. Preliminary testing of the TRACR3D code indicates that it is a very powerful simulation tool with exceptionally robust numerical algorithms. The version of the code provided to INEL by Los Alamos National Laboratory, however, is an experimental version. The TRACR3D code is still very much in a development stage, and the final version of code is not expected be available until late FY-1988 or early FY-1989. Another limitation of the code is that the existing documentation (Travis, 1984) is out of date with the current version. An interim user's guide was prepared during this reporting period for use by the INEL staff.

5.5.3.2 Research Needs. At present, the computer models represent a strong and defensible basis for assessing the isolation performance of the burial sites at the RWMC. One area that it theoretically tenuous, however, is the representation of the soil moisture characteristics of the basalts in the unsaturated zone. Currently, the computer models utilize empirical relations for the water release and hydraulic conductivity curves of basalt. Examples of these curves are shown in Figure 70. These curves represent, at best, educated guesses of the soil moisture characteristics of the fractured basalt, because unlike the curves shown in Figure 66 for

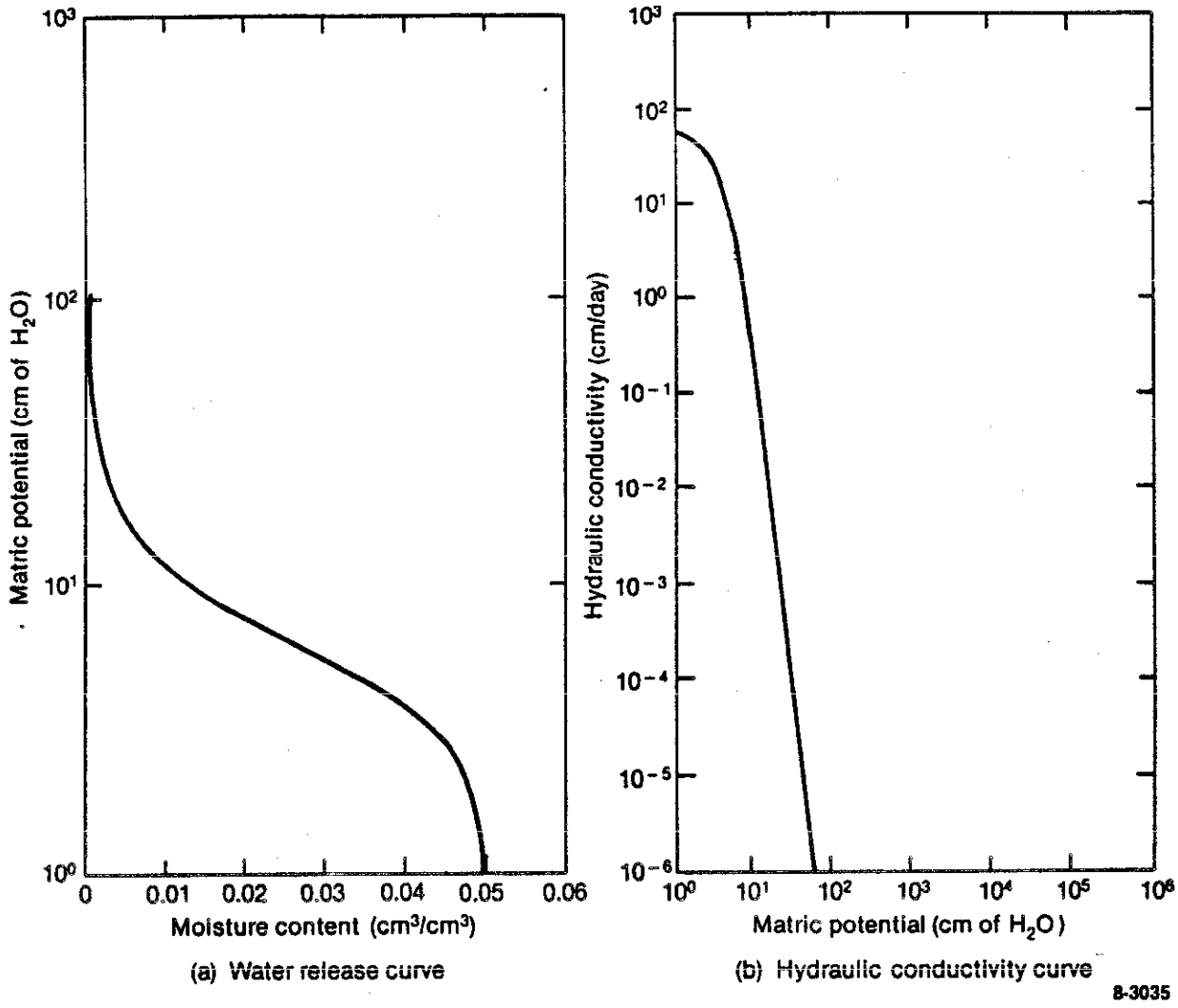

Figure 70. Soil moisture characteristics of the basalt as derived from empirical relations.

sediments, they are derived from empirical relations instead of actual data obtained from laboratory analysis of samples. There is a definite need to conduct laboratory experiments and to develop a methodology for estimating these curves from the fracture characteristics determined from cores.

The properties of unsaturated fractured rocks is a new area of research, and only recently have theories been proposed in the literature (Wang and Narasimhan, 1985). Laboratory studies are needed to provide a

basis for developing a sound mathematical theory of unsaturated flow in fractured rocks. To address this need, a joint effort between the INEL and the University of Utah is planned.

Another area of needed research is waste leachability and the development of a source term submodel. There is a need to initiate an effort to develop a source term submodel that will process laboratory data from leach tests and generate input data for the computer models. This submodel should consider the properties of the waste, properties of surficial sediments, and percolation rates. The output of the source term submodel would be the mass release rate as a function of time.

5.5.3.3 Data Needs and Emphasis. The current characterization program is designed to provide the data needed for calibration of the models and for the ultimate assessment of the isolation performance of the RWMC. From the initial modeling studies that were conducted in this reporting period, it is apparent that greater emphasis needs to be placed on the collection of data for soil moisture characterization of the sedimentary zones. In particular, significantly more data are needed for the following three parameters:

- Saturated hydraulic conductivity
- Water release curve (matric potential versus moisture content)
- Effective porosity.

These data can be determined from laboratory testing of available soil samples.

Future analysis and interpretation of the existing field data will provide key input to the computer modeling effort. Interpretations of matric potential data, for example, will be especially important to the development of a conceptual model of how water moves through the unsaturated zone. Without this conceptual model, no meaningful computer

modeling would be possible. These data can be used to begin calibration of the unsaturated flow models SEMTRA and TRACR3D. A closely coordinated effort is planned between the modeling and the data collection activity at the Test Trench.

Greater emphasis needs to be placed on collection of laboratory data (applicable to the RWMC subsurface environment) pertaining to chemical properties (e.g., sorption and solubility) of the key radionuclides. Laboratory studies should be undertaken to address the issue of possible colloidal transport of selected radionuclides.

Additional geologic characterization of the RWMC is needed with particular emphasis on identifying zones in the basalt that might act as preferential pathways. Basalt core samples should be examined and tested in the laboratory to characterize the nature of basalt porosity. Fracture logging should be performed to provide data on the fracture frequency, aperture, and orientation. Geologic evaluations are needed to address the question of potential large-scale discontinuities through the basalts. This type of information is crucial to the analysis of contaminant transport through the vadose zone.

5.6 Radionuclide Concentrations

5.6.1 Introduction

Interbed sediment samples obtained during drilling activities at the RWMC were subjected to several analytical procedures to determine the presence of 29 radionuclides. These radionuclides are listed as follows:

^{46}Sc	^{103}Ru	^{152}Eu
^{51}Sc	^{106}Rh	^{154}Eu
^{54}Mn	^{110m}Ag	^{155}Eu
^{58}Co	^{124}Sb	^{181}Hf
^{60}Co	^{125}Sb	^{182}Ta

^{59}Fe	^{134}Cs	^{203}Hg
^{65}Zn	^{137}Cs	^{238}Pu
^{90}Sr	^{141}Ce	$^{239.240}Pu$
^{95}Zr	^{144}Ce	^{241}Am
^{96}Nb	^{144}Pr	

From this listing of 29 radionuclides, seven radionuclides were positively detected at measurable levels (measured value was greater than three times the standard deviation): ^{238}Pu, $^{239,240}Pu$, ^{241}Am, ^{90}Sr, ^{137}Cs, ^{60}Co, and ^{154}Eu. The radiochemistry laboratory analyzed samples for ^{238}Pu, $^{239,240}Pu$ and ^{241}Am using alpha spectrometry. (The presence of ^{241}Am was determined by both alpha spectrometry and gamma counting, but because the alpha calculation is more sensitive and accurate, only the alpha spectrometric value is listed.) Beta counting was used for ^{90}Sr analysis. These alpha and beta values were determined by using 1000 minute and 200 minute counts, respectively (unless otherwise indicated in the tables). ^{137}Cs, ^{60}Co, and ^{154}Eu were measured by gamma counting. Sediment-water samples collected from porous cup lysimeters were analyzed for the same 29 radionuclides. Analyses of sediment-water samples will aid in determining the extent of radionuclide contamination and the degree of contaminant mobility.

5.6.2 Summary of Accomplishments

A total of 112 sediment samples from the FY-1985 shallow drilling program and 30 sediment samples from FY-1986 shallow drilling program were submitted for radiochemical analyses using gamma spectroscopy, alpha spectroscopy, and beta counting. A total of 14 sediment samples from the FY-1986 deep drilling program were submitted for these same radiochemical analyses. In addition, twelve sediment-water samples collected from porous cup lysimeters were subjected to alpha, beta, and gamma radionuclide determinations.

5.6.3 Discussion

5.6.3.1 Sediment Sample Analyses. Results of the radiochemical analyses of samples obtained during the FY-1985 and FY-1986 shallow drilling programs are given in Tables 18 and 19, respectively. Results of the radiochemical analyses of samples obtained from FY-1986 deep drilling, along with some of the FY-1987 deep drilling sample analysis results, are given in Table 20. Of the 29 radionuclides listed in Section 5.6.1, only those that showed positive results in the samples are listed in the tables. Because ^{60}Co and ^{154}Eu were not detected in any of the 1986 shallow drilling samples or in any of the deep drilling samples analyzed to date, these radionuclides are not listed in Tables 19 and 20.

Entries in these tables consist of the reported concentration of each radionuclide followed by a measure of the analytical uncertainty estimated at the one standard deviation level. This uncertainty incorporates all random uncertainties incurred anywhere in the entire measurements process.

A significant number of entries in Tables 18, 19, and 20 have negative signs. Obviously, negative concentrations cannot be real. They arise because both gross (sample plus background) and background radioactivity counts are subject to the same random variation. When gross radioactivity is about the same as background radioactivity, the difference (the calculated level of radioactivity in the sample) is sometimes negative.

Radionuclide determinations are considered to be positive when the reported concentration is greater than three times the analytical uncertainty. All analytical uncertainties shown in the tables have been properly propagated (Sill, 1982). A positive determination is equivalent to saying there is approximately 99% confidence that the radionuclide is actually present in the sample.

The majority of positive sample detections listed in Tables 18 and 19 are associated with auger samples collected close to land surface (within 20 inches of the surface). Of the 44 positive values for radionuclides in

TABLE 18. RWMC SEDIMENT SAMPLE RADIOCHEMICAL ANALYSIS RESULTS: SAMPLE FROM THE FY-1985 SHALLOW DRILLING PROGRAM

Sample	Depth (in.)	^{238}Pu (μCi/g)	$^{239,240}Pu$ (μCi/g)	^{241}Am (μCi/g)	^{90}Sr (μCi/g)	^{60}Co (μCi/g)	^{137}Cs (μCi/g)	^{154}Eu (μCi/g)
Auger Hole WO1								
C-11M	20	2.0 ± 1.4 E-09	-6 ± 8 E-10	-8 ± 8 E-10	3.1 ± 1.5 E-08	-14 ± 8 E-09	9 ± 9 E-09	-2.2 ± 1.0 E-08
C-12M	41	1.7 ± 1.3 E-09	1.0 ± 1.3 E-09	-2 ± 10 E-10	5.8 ± 1.9 E-08*	20 ± 8 E-09	5 ± 9 E-09	-17 ± 7 E-09
C-13M	62	2.1 ± 1.4 E-09	-6 ± 8 E-10	6 ± 10 E-10	0.8 ± 1.6 E-08	-4 ± 9 E-09	0 ± 1.0 E-08	-1.1 ± 1.8 E-08
C-14M	83	1.1 ± 0.9 E-09	2.2 ± 1.3 E-09	1.3 ± 1.6 E-09	9 ± 3 E-08	0 ± 9 E-07	23 ± 8 E-09	3.1 ± 1.9 E-08
Auger Hole WO2								
C-24M	20	4.5 ± 0.4 E-08*	2.56 ± 0.14 E-06*	2.46 ± 0.11 E-06*	5.2 ± 0.3 E-07*	2.0 ± 1.0 E-08	180 ± 7 E-08*	1 ± 9 E-09
C-25M	41	4 ± 2 E-09	-7 ± 10 E-10	9 ± 12 E-10	1.1 ± 1.6 E-08	11 ± 7 E-09	4 ± 8 E-09	0.5 ± 1.7 E-08
C-26M	62	2.9 ± 1.5 E-09	7 ± 13 E-10	-7 ± 10 E-10	4.7 ± 1.8 E-08	1.4 ± 1.5 E-08	-4 ± 8 E-09	-5 ± 2 E-08
C-27M	83	4.1 ± 0.4 E-08*	1.44 ± 0.04 E-06*	2.5 ± 1.1 E-09	2.9 ± 1.6 E-08	10 ± 7 E-09	8 ± 8 E-09	-1 ± 7 E-09
C-28M	104	2.5 ± 1.6 E-09	-6 ± 9 E-10	-3 ± 9 E-10	4 ± 2 E-08	9 ± 8 E-09	-2 ± 3 E-08	-6 ± 2 E-08
C-29M	125	2 ± 2 E-09	1.8 ± 1.4 E-09	8 ± 10 E-10	-0.3 ± 1.7 E-08	-9 ± 9 E-09	3 ± 9 E-09	-1.9 ± 1.5 E-08
C-30M	146	2.4 ± 1.5 E-09	3 ± 9 E-10	-1.5 ± 0.8 E-09	0.3 ± 1.7 E-08	2 ± 9 E-09	-4 ± 9 E-09	-1 ± 3 E-08
C-31M	166	4 ± 2 E-09	4 ± 13 E-10	1 ± 9 E-10	3.2 ± 1.8 E-08	6 ± 2 E-08*	3.0 ± 1.7 E-08	-0.8 ± 1.6 E-08
Auger Hole WO3								
C-32M	20	1.3 ± 0.2 E-08*	5.5 ± 0.2 E-07*	1.63 ± 0.06 E-06*	2.0 ± 0.2 E-07*	2 ± 8 E-09	10.0 ± 1.1 E-08*	7 ± 3 E-09
C-33M	41	2.6 ± 1.4 E-09	3 ± 9 E-10	-6 ± 12 E-10	2.7 ± 0.2 E-07*	-0.4 ± 1.8 E-08	-14 ± 7 E-09	-4 ± 3 E-09
C-34M	60	1 ± 3 E-09	3 ± 3 E-09	6 ± 11 E-10	5 ± 2 E-08	0.7 ± 1.9 E-08	2.6 ± 1.2 E-08	1.4 ± 1.4 E-08
C-35M	79	2.3 ± 1.6 E-09	-1.2 ± 1.0 E-09	-1 ± 9 E-10	0.9 ± 1.6 E-08	-6 ± 8 E-09	1 ± 8 E-09	-1.1 ± 1.4 E-08
C-36M	100	2.2 ± 1.5 E-09	-3 ± 10 E-10	1.3 ± 0.3 E-08*	6.6 ± 1.8 E-08	-22 ± 7 E-09	-3 ± 8 E-09	-7 ± 2 E-08
C-37M	121	1.3 ± 1.9 E-09	1.3 ± 1.3 E-09	7 ± 10 E-10	3.8 ± 1.7 E-08	-3 ± 9 E-09	-9 ± 9 E-09	-6 ± 4 E-08
Auger Hole WO4								
C-38M	20	8.8 ± 1.8 E-09*	8.2 ± 0.5 E-08*	7.4 ± 0.5 E-08*	1.0 ± 1.6 E-08	24 ± 8 E-09*	4.2 ± 1.0 E-08*	-3 ± 3 E-09
C-39M	41	5.2 ± 1.7 E-09*	2.8 ± 0.3 E-08*	9.2 ± 0.5 E-08*	1 ± 2 E-08	-2 ± 6 E-09	15 ± 7 E-09	-1.0 ± 1.2 E-08
C-40M	62	1.7 ± 1.6 E-09	1.0 ± 1.1 E-09	-1 ± 8 E-10	1.9 ± 0.3 E-07	-0.9 ± 1.3 E-08	-5 ± 8 E-09	-9 ± 3 E-09
C-41M	83	0.8 ± 1.1 E-09	1.1 ± 1.1 E-09	1.2 ± 1.7 E-09	0 ± 4 E-08	-7 ± 8 E-09	5 ± 9 E-09	-0 ± 2 E-08
C-42M	104	0.9 ± 1.5 E-09	0.4 ± 1.2 E-09	-0.6 ± 1.3 E-09	2 ± 3 E-08	-2 ± 9 E-09	13 ± 7 E-09	9 ± 9 E-09
C-43M	125	0.5 ± 1.3 E-09	0.5 ± 1.1 E-09	-0.1 ± 1.2 E-09	2 ± 3 E-08	5 ± 9 E-09	16 ± 9 E-09	-0 ± 1.6 E-08
C-44M	148	2.0 ± 1.1 E-09	6 ± 7 E-10	-2.0 ± 1.0 E-09	1.1 ± 0.4 E-07	-1 ± 8 E-09	5 ± 8 E-09	0.6 ± 1.4 E-08
C-45M	171	1.7 ± 1.5 E-09	0.8 ± 1.3 E-09	-0.3 ± 1.1 E-09	9 ± 3 E-08	-0.7 ± 1.5 E-08	-2.2 ± 1.9 E-08	1 ± 3 E-08
C-46M	193	1.4 ± 1.4 E-09	1.0 ± 1.4 E-09	-0.2 ± 1.0 E-09	2 ± 3 E-08	16 ± 3 E-08*	6 ± 3 E-08	-4 ± 4 E-08
C-47M	214	0.5 ± 1.1 E-09	8 ± 9 E-10	0.0 ± 1.2 E-09	6 ± 3 E-08	-6 ± 7 E-09	11 ± 7 E-09	-0.8 ± 1.6 E-08
C-48M	236	0.8 ± 1.2 E-09	8 ± 9 E-10	-0.2 ± 1.1 E-09	4 ± 4 E-08	-1 ± 8 E-09	16 ± 8 E-09	0.4 ± 1.6 E-08
C-49M	258	0.7 ± 1.0 E-09	1.9 ± 1.5 E-09	-0.1 ± 1.2 E-09	7.4 ± 1.9 E-08*	-23 ± 9 E-09	3 ± 7 E-09	1.1 ± 1.1 E-08
C-50M	279	3.1 ± 1.7 E-09	0.8 ± 1.0 E-09	-0.1 ± 1.2 E-09	4 ± 4 E-08	4 ± 9 E-09	7 ± 8 E-09	0 ± 1.7 E-08

TABLE 18. (continued)

Sample	Depth (in.)	^{238}Pu (μCi/g)	$^{239,240}Pu$ (μCi/g)	^{241}Am (μCi/g)	^{90}Sr (μCi/g)	^{60}Co (μCi/g)	^{137}Cs (μCi/g)	^{154}Eu (μCi/g)
Auger Hole W08								
C-109M	18	1.3 ± 1.1 E-09	0 ± 9 E-09	0 ± 9 E-09	5.4 ± 1.9 E-08	-16 ± 9 E-09	6.4 ± 1.2 E-08*	1 ± 5 E-08
C-110M	39	3.0 ± 1.4 E-09	1.3 ± 0.2 E-08*	5.3 ± 0.4 E-08*	3 ± 3 E-08	-1.0 ± 1.0 E-08	4.7 ± 1.1 E-08*	-2 ± 3 E-08
C-111M	60	5 ± 2 E-09	2.35 ± 0.10 E-07*	1.16 ± 0.03 E-06*	7.9 ± 0.4 E-07*	36 ± 1.7 E-8*	55 ± 3 E-08*	0.2 ± 1.0 E-08
C-112M	81	1.3 ± 1.7 E-09	5 ± 9 E-10	-0.2 ± 1.1 E-09	5 ± 3 E-08	0.2 ± 1.1 E-08	-5 ± 8 E-09	-4 ± 2 E-08
C-113M	102	4.4 ± 1.7 E-09	1.2 ± 1.4 E-09	-3 ± 9 E-10	2 ± 2 E-08	-7 ± 8 E-09	5 ± 8 E-09	0.8 ± 1.2 E-08
C-114M	122	1.8 ± 1.3 E-09	8 ± 9 E-10	0 ± 9 E-10	0 ± 3 E-09	-1 ± 7 E-09	8 ± 8 E-09	-1 ± 3 E-08
C-115M	142	0.7 ± 1.3 E-09	9 ± 9 E-10	-0.2 ± 1.0 E-09	-3 ± 3 E-08	0.9 ± 1.0 E-08	0 ± 1.0 E-08	-2 ± 3 E-08
C-116M	163	0.5 ± 1.0 E-09	7 ± 8 E-10	0.4 ± 1.2 E-09	-2 ± 4 E-08	0.9 ± 1.2 E-08	1.0 ± 1.1 E-08	0.6 ± 1.8 E-08
C-117M	184	1.2 ± 1.1 E-09	0.5 ± 1.0 E-09	-0.4 ± 1.1 E-09	0 ± 4 E-08	-24 ± 9 E-09	-17 ± 7 E-09	0.8 ± 1.6 E-08
C-118M	207	0.7 ± 1.2 E-09	0.7 ± 1.0 E-09	1.0 ± 1.2 E-09	0 ± 3 E-08	0.6 ± 1.0 E-08	0.2 ± 1.0 E-08	5 ± 9 E-09
C-119M	231	1.0 ± 1.3 E-09	0.6 ± 1.3 E-09	-5 ± 9 E-10	1 ± 3 E-08	-4 ± 7 E-09	-4 ± 8 E-08	-6 ± 7 E-09
C-120M	252	1.0 ± 0.9 E-09	4 ± 7 E-10	-0.2 ± 1.2 E-09	-3 ± 3 E-08	1.2 ± 1.5 E-08	13 ± 9 E-09	-6 ± 9 E-09
C-121B	265	0 ± 9 E-09	1.6 ± 1.4 E-09	0 ± 9 E-09	2 ± 2 E-08	--	--	--
C-121M	--	--	--	--	--	-0.2 ± 1.2 E-08	13 ± 9 E-09	-2 ± 8 E-09
Auger Hole W10								
C-15M	19	2.0 ± 1.8 E-09	8 ± 10 E-10	-2 ± 10 E-10	2.4 ± 1.6 E-08	0 ± 8 E-09	15 ± 8 E-09	0.1 ± 1.3 E-08
C-16M	40	1.5 ± 1.5 E-09	-1.5 ± 1.4 E-09	0.0 ± 1.3 E-09	5 ± 2 E-08	0.1 ± 1.8 E-08	3.4 ± 1.2 E-08	-0.6 ± 1.2 E-08
C-17M	61	1.9 ± 1.2 E-09	-8 ± 7 E-10	-1 ± 10 E-10	1.9 ± 1.6 E-08	-2 ± 9 E-09	4 ± 9 E-09	0.5 ± 1.4 E-08
C-18M	82	1 ± 2 E-09	0.5 ± 1.1 E-09	-0.3 ± 1.1 E-09	2 ± 3 E-08	-0 ± 2 E-08	3.5 ± 1.3 E-08	-2.3 ± 1.6 E-08
C-19M	103	2.3 ± 1.2 E-09	-3 ± 7 E-10	-1.1 ± 0.9 E-08	4.1 ± 1.6 E-08	1 ± 8 E-09	-1 ± 8 E-09	-10 ± 7 E-09
Auger Hole W12								
C-53M	19	7 ± 10 E-10	9 ± 9 E-10	1.6 ± 1.6 E-09	5 ± 2 E-08	0.6 ± 1.7 E-08	1.8 ± 1.1 E-08	-2 ± 5 E-08
C-54M	40	1.3 ± 0.7 E-09	4.7 ± 1.0 E-09*	-1.3 ± 1.1 E-09	3 ± 2 E-08	-0.7 ± 1.3 E-08	8.6 ± 1.2 E-08*	0.2 ± 1.2 E-08
Auger Hole T12								
C-55M	20	0 ± 9 E-09	0 ± 9 E-09	8 ± 2 E-09*	2 ± 2 E-08	-0.3 ± 1.8 E-08	9.6 ± 1.3 E-08*	-0 ± 1.3 E-08
C-56M	41	2 ± 2 E-09	1 ± 2 E-09	-2 ± 11 E-10	1.1 ± 0.2 E-07*	--	--	--
C-57M	56	2.3 ± 1.6 E-09	5.5 ± 1.6 E-09*	3 ± 14 E-10	2 ± 2 E-08	-1.6 ± 1.9 E-08	-8 ± 8 E-09	-4 ± 7 E-09
Auger Hole W16								
C-106M	18	0 ± 9 E-09	2 ± 6 E-10	-4 ± 9 E-10	1.0 ± 1.7 E-08	-0.4 ± 1.2 E-08	1.5 ± 1.0 E-08	-0.4 ± 1.0 E-08
C-107M	39	1.5 ± 1.2 E-09	8 ± 9 E-10	10 ± 12 E-11	2 ± 14 E-09	-14 ± 8 E-09	15 ± 9 E-09	-3 ± 8 E-09
C-108M	55	5 ± 2 E-09	1.63 ± 0.09 E-07*	0 ± 9 E-09	4 ± 2 E-08	-70 ± 6 E-09	-29 ± 4 E-09	13 ± 5 E-09

TABLE 18. (continued)

Sample	Depth (in.)	^{238}Pu (μCi/g)	$^{239,240}Pu$ (μCi/g)	^{241}Am (μCi/g)	^{90}Sr (μCi/g)	^{60}Co (μCi/g)	^{137}Cs (μCi/g)	^{154}Eu (μCi/g)
Auger Hole W19								
C-60M	18	9 ± 10 E-10	-6 ± 8 E-10	5 ± 11 E-10	1.9 ± 0.4 E-07*	1.1 ± 1.3 E-08	5 ± 9 E-09	-13 ± 8 E-09
C-61M	39	0.6 ± 1.1 E-09	0.4 ± 1.2 E-09	-0.2 ± 1.5 E-09	2 ± 4 E-08	22 ± 5 E-08*	4 ± 3 E-08	-0 ± 3 E-08
C-62M	60	1.1 ± 1.2 E-09	1.1 ± 1.3 E-09	0.0 ± 1.0 E-09	-4 ± 3 E-08	-5 ± 7 E-09	-5 ± 7 E-09	-13 ± 7 E-09
C-63M	81	1.6 ± 1.4 E-09	8 ± 9 E-10	-0.4 ± 1.0 E-09	1 ± 3 E-08	2 ± 9 E-09	-14 ± 9 E-09	-4 ± 8 E-09
C-64M	102	8 ± 7 E-10	5 ± 6 E-10	-1.7 ± 0.8 E-09	2 ± 2 E-08	5 ± 9 E-09	13 ± 9 E-09	-0 ± 8 E-09
C-65M	123	1.3 ± 1.5 E-09	1.0 ± 1.1 E-09	-0.2 ± 1.2 E-09	4 ± 4 E-08	1 ± 2 E-08	1.5 ± 1.2 E-08	-1 ± 2 E-08
C-66M	144	0.8 ± 1.5 E-09	0.5 ± 1.0 E-09	-3 ± 9 E-10	-1 ± 3 E-08	1.4 ± 1.8 E-08	1.8 ± 1.1 E-08	0 ± 4 E-08
C-67M	165	1.6 ± 1.6 E-09	1.8 ± 1.7 E-09	-0.1 ± 1.1 E-09	1 ± 2 E-08	0.9 ± 1.8 E-08	2.1 ± 1.1 E-08	0 ± 8 E-09
C-68M	186	1.8 ± 1.2 E-09	1.3 ± 1.1 E-09	0.5 ± 1.1 E-09	-7 ± 4 E-08	-0.3 ± 1.9 E-08	2.3 ± 1.2 E-08	17 ± 9 E-09
C-69M	199	1.4 ± 1.6 E-09	5 ± 9 E-10	-2 ± 11 E-10	2 ± 2 E-08	-0.8 ± 1.7 E-08	2.1 ± 1.1 E-08	29 ± 9 E-09*
Auger Hole W20								
C-76M	19	1.8 ± 0.2 E-08*	1.47 ± 0.07 E-07*	7.2 ± 0.4 E-08*	1.9 ± 0.3 E-07*	15 ± 9 E-09	15.2 ± 1.3 E-08*	0.8 ± 1.0 E-08
C-77M	40	1.1 ± 1.4 E-09	4 ± 7 E-10	-0.5 ± 1.0 E-09	2 ± 3 E-08	-6 ± 9 E-09	-7 ± 9 E-09	-4 ± 3 E-09
C-78M	61	0.6 ± 1.1 E-09	0.4 ± 1.0 E-09	-0.3 ± 1.1 E-09	-2 ± 3 E-08	-1 ± 9 E-09	-4 ± 9 E-09	12 ± 8 E-09
C-79M	82	1.1 ± 1.5 E-09	-6 ± 9 E-10	-0 ± 9 E-09	3 ± 3 E-08	-0.8 ± 1.9 E-08	-19 ± 9 E-09	-8 ± 8 E-09
Auger Hole W22								
C-71M	19	9 ± 8 E-10	4 ± 8 E-10	-4 ± 11 E-10	3 ± 3 E-08	2 ± 2 E-08	1.4 ± 1.1 E-08	-0 ± 9 E-09
C-72M	40	0.5 ± 1.0 E-09	5 ± 7 E-10	-0.1 ± 1.0 E-09	3 ± 3 E-08	1.6 ± 1.9 E-08	2.7 ± 1.1 E-08	-1.3 ± 1.3 E-08
C-73M	61	1.0 ± 1.1 E-09	6 ± 9 E-10	0.0 ± 1.1 E-09	-1 ± 4 E-08	-1 ± 2 E-08	0.5 ± 1.2 E-08	-0.2 ± 1.6 E-08
C-74M	82	2.5 ± 1.3 E-09	5 ± 9 E-10	-0.2 ± 1.1 E-09	2 ± 4 E-08	2 ± 2 E-08	3.3 ± 1.4 E-08	-0.6 ± 1.9 E-08
C-75M	100	9 ± 9 E-10	-2 ± 8 E-10	9 ± 15 E-10	3 ± 2 E-08	0.7 ± 1.9 E-08	2.1 ± 1.2 E-08	8 ± 9 E-09
Auger Hole W23								
C-80B	18	4.2 ± 1.0 E-08*	1.10 ± 0.05 E-06*	8.0 ± 0.4 E-07*	2 ± 2 E-08	4.9 ± 1.0 E-08*	43 ± 2 E-08*	8 ± 8 E-09
C-81M	39	0.8 ± 1.2 E-09	0.5 ± 1.1 E-09	-0.3 ± 1.1 E-09	-1 ± 4 E-08	-42 ± 8 E-09	-31 ± 8 E-09	4 ± 8 E-09
C-82M	60	3.0 ± 1.6 E-09	8 ± 2 E-09*	-0.3 ± 1.2 E-09	-1 ± 3 E-08	-0.4 ± 1.0 E-08	-2 ± 9 E-09	-2 ± 8 E-09
C-83M	81	0.7 ± 1.0 E-09	-5 ± 7 E-10	-6 ± 9 E-10	-2 ± 4 E-08	-0.3 ± 1.1 E-08	-9 ± 7 E-09	-4 ± 6 E-09
C-84M	102	8 ± 9 E-10	4 ± 6 E-10	-0.1 ± 1.4 E-09	-1 ± 3 E-08	-0.2 ± 1.2 E-08	-9 ± 7 E-09	-3 ± 7 E-09
C-85M	123	3 ± 2 E-09	4 ± 14 E-10	6 ± 11 E-10	1 ± 2 E-08	-9 ± 7 E-09	1 ± 7 E-09	-3 ± 6 E-09
C-86M	144	2.0 ± 1.6 E-09	2.9 ± 1.7 E-09	-0.5 ± 1.0 E-09	1 ± 3 E-08	-11 ± 7 E-09	0.6 ± 1.0 E-08	-1.5 ± 1.0 E-08
C-87M	165	0.5 ± 1.0 E-09	5 ± 9 E-10	0.0 ± 1.2 E-09	4 ± 3 E-08	-1.8 ± 1.0 E-08	-0 ± 1.0 E-08	1 ± 9 E-09
C-88M	186	0.7 ± 1.2 E-09	0.5 ± 1.0 E-09	-6 ± 9 E-10	4 ± 4 E-08	-20 ± 9 E-09	-1.3 ± 1.0 E-08	-1 ± 8 E-09
C-89M	207	0.7 ± 1.2 E-09	9 ± 9 E-10	1.3 ± 0.2 E-08	2 ± 3 E-08	-04 ± 1.4 E-08	-12 ± 9 E-09	-5.4 ± 1.8 E-08
C-90M	228	1.7 ± 1.1 E-09	2 ± 8 E-10	-4 ± 9 E-10	1 ± 2 E-08	5 ± 8 E-09	-12 ± 8 E-09	8 ± 7 E-09

TABLE 18. (continued)

Sample	Depth (in.)	^{238}Pu (μCi/g)	$^{239,240}Pu$ (μCi/g)	^{241}Am (μCi/g)	^{90}Sr (μCi/g)	^{60}Co (μCi/g)	^{137}Cs (μCi/g)	^{154}Eu (μCi/g)
Auger Hole T23								
C-91M	19	6.6 ± 1.3 E-08*	4.53 ± 0.15 E-06*	7.5 ± 0.2 E-06*	2.0 ± 0.3 E-07*	-1 ± 9 E-09	31.2 ± 1.8 E-08*	11 ± 8 E-09
C-92M	40	2.6 ± 1.4 E-09	2.4 ± 0.3 E-08*	6.5 ± 0.4 E-08*	0 ± 3 E-08	0.7 ± 1.5 E-08	3.0 ± 1.2 E-08	0.1 ± 1.4 E-08
C-93M	61	1.2 ± 1.5 E-09	0.8 ± 1.4 E-09	0.0 ± 1.9 E-09	3 ± 3 E-08	-3 ± 6 E-08	8 ± 9 E-09	-0.7 ± 1.2 E-08
C-94M	82	7 ± 8 E-10	5 ± 8 E-10	2 ± 4 E-09	2 ± 3 E-08	-3 ± 4 E-08	2 ± 7 E-09	12 ± 9 E-09
C-96M	114	2.34 ± 0.12 E-07*	1.6 ± 1.8 E-09	4 ± 10 E-10	4 ± 2 E-08	-3 ± 3 E-08	-1 ± 7 E-09	-3 ± 6 E-09
C-97M	135	0.7 ± 1.6 E-09	0.9 ± 1.4 E-09	0.3 ± 1.4 E-09	3 ± 3 E-08	-2 ± 4 E-08	2 ± 7 E-09	-2 ± 8 E-09
C-98M	156	0.6 ± 1.0 E-09	4 ± 7 E-10	-0.4 ± 1.1 E-09	1 ± 4 E-08	-3 ± 7 E-08	-0.2 ± 1.0 E-08	-0.7 ± 1.3 E-08
C-99M	177	0.7 ± 1.0 E-09	5 ± 8 E-10	-0.3 ± 1.3 E-09	-4 ± 3 E-08	-6 ± 6 E-08	-5 ± 9 E-09	-11 ± 9 E-09
C-100M	198	0.7 ± 1.0 E-09	0.7 ± 1.2 E-09	0.6 ± 1.2 E-09	3 ± 3 E-08	-3 ± 6 E-08	-6 ± 8 E-09	10 ± 8 E-09
C-101M	219	0.5 ± 1.4 E-09	0.7 ± 1.3 E-09	5 ± 9 E-10	0 ± 4 E-08	-4 ± 5 E-08	9 ± 8 E-09	3 ± 8 E-09
C-102M	234	3 ± 10 E-10	6 ± 10 E-10	-1.7 ± 1.0 E-09	1 ± 3 E-08	-6 ± 3 E-08	-5 ± 8 E-09	-6 ± 8 E-09
Auger Hole C02								
C-103M	17	6 ± 14 E-10	3 ± 11 E-10	3 ± 15 E-10	2.0 ± 1.8 E-08	-4 ± 5 E-08	-7 ± 9 E-09	1 ± 8 E-09
C-104M	38	1.1 ± 1.7 E-09	0 ± 9 E-09	0 ± 9 E-09	1 ± 2 E-08	-0.2 ± 1.6 E-08	1.5 ± 1.0 E-08	-3 ± 9 E-09
C-105M	57	0 ± 9 E-09	1.4 ± 1.5 E-09	0 ± 9 E-09	6 ± 2 E-08	-4 ± 4 E-08	-12 ± 9 E-09	-8 ± 8 E-09
Auger Hole PA01								
C-122M	19	3.8 ± 0.4 E-07*	8.4 ± 0.2 E-06*	1.62 ± 0.05 E-05*	1.9 ± 0.3 E-07*	1.0 ± 1.3 E-08	23 ± 1.7 E-08*	-7 ± 9 E-09
C-123M	39	1.1 ± 1.2 E-09	0.6 ± 1.0 E-09	-0.3 ± 1.1 E-09	4 ± 3 E-08	0.3 ± 1.0 E-08	11 ± 9 E-09	4 ± 9 E-09
C-124M	60	1.6 ± 1.2 E-09	1.3 ± 1.0 E-09	0.2 ± 1.1 E-09	1 ± 3 E-08	-3 ± 3 E-08	-8 ± 7 E-09	3 ± 3 E-08
C-125M	81	1.0 ± 1.5 E-09	2.1 ± 1.7 E-09	0 ± 9 E-09	-1 ± 2 E-08	0 ± 2 E-08	-1 ± 6 E-09	1.7 ± 1.8 E-08
C-126M	102	0.6 ± 1.0 E-09	4 ± 9 E-10	-0.1 ± 1.1 E-09	-1 ± 3 E-08	-3.6 ± 1.1 E-08	-1 ± 5 E-09	-13 ± 6 E-09
C-127M	123	4 ± 7 E-10	4 ± 5 E-10	-0.3 ± 1.0 E-09	0 ± 3 E-08	0 ± 2 E-08	1.0 ± 1.1 E-08	-0.4 ± 1.0 E-08
C-128M	144	0.8 ± 1.2 E-09	0.4 ± 1.0 E-09	-0.4 ± 1.0 E-09	4 ± 3 E-08	-0.7 ± 1.0 E-08	1.1 ± 1.1 E-08	-0.4 ± 1.0 E-08
C-129M	168	1.3 ± 1.0 E-09	1.1 ± 0.8 E-09	0 ± 9 E-09	3 ± 3 E-08	0.6 ± 1.3 E-08	0.2 ± 1.0 E-08	-12 ± 9 E-09
Auger Hole PA02								
C-130M	20	7.0 ± 2.0 E-09*	1.03 ± 0.06 E-07*	2.94 ± 0.12 E-07*	5 ± 3 E-08	0.6 ± 1.8 E-08	6.1 ± 1.1 E-08*	0.8 ± 1.1 E-08
C-131M	54	6.4 ± 0.2 E-06*	3.34 ± 0.06 E-05*	1.54 ± 0.03 E-04*	1.28 ± 0.04 E-06*	1.3 ± 1.4 E-08	18.7 ± 1.5 E-08*	0 ± 2 E-08
C-132M	75	1.3 ± 0.3 E-07*	8.2 ± 0.7 E-07*	4.37 ± 0.19 E-06*	6.7 ± 0.3 E-07*	--	--	--

*Sample result positive (i.e., greater than three sigma).

TABLE 19. RWMC SEDIMENT SAMPLE RADIOCHEMICAL ANALYSIS RESULTS: SAMPLES FROM THE FY-1986 SHALLOW DRILLING PROGRAM

Sample	Depth (in.)	^{238}Pu (μCi/g)	$^{239,240}Pu$ (μCi/g)	^{241}Am (μCi/g)	^{90}Sr (μCi/g)	^{137}Cs μCi/g)
Auger Hole WO5						
C224M	10	2.1 ± 1.2 E-09	2.2 ± 0.3 E-08*	6.0 ± 0.5 E-08*	8 ± 5 E-08	1.88 ± 0.13 E-07*
C226M	50	0.8 ± 1.5 E-09	0.8 ± 1.2 E-09	1 ± 2 E-09	4.6 ± 1.9 E-08	9 ± 7 E-09
C227M	82	0.7 ± 1.1 E-09	5 ± 9 E-10	-0.1 ± 1.4 E-09	4 ± 4 E-08	-1 ± 7 E-09
C228M	102	1 ± 4 E-10	-2 ± 3 E-10	0.2 ± 1.0 E-09	7 ± 3 E-08	1.3 ± 0.9 E-08
C230M	139	4 ± 4 E-09	2 ± 4 E-09	5 ± 6 E-09	1 ± 3 E-08	-2 ± 8 E-09
C232M	182	0.7 ± 1.1 E-09	4 ± 8 E-10	4 ± 4 E-09	5 ± 7 E-08	4 ± 8 E-09
Auger Hole WO6						
C233M	10	0.8 ± 1.2 E-09	0.6 ± 1.0 E-09	1.3 ± 0.2 E-08*	5 ± 3 E-08	1.13 ± 0.12 E-07*
C235M	62	0.6 ± 1.0 E-09	6 ± 9 E-10	0.0 ± 1.2 E-09	3 ± 4 E-08	-4 ± 7 E-09
C238M	122	0.8 ± 1.8 E-09	0.8 ± 1.7 E-09	0.0 ± 1.2 E-09	6 ± 4 E-08	3 ± 7 E-09
Auger Hole WO9						
C284M	10	1.1 ± 0.2 E-08*	7.3 ± 0.2 E-07*	2.28 ± 0.06 E-06*	9 ± 4 E-08	2.9 ± 0.9 E-08*
C287M	94	0.7 ± 1.3 E-09	1.1 ± 1.0 E-09	0 ± 1 E-10	5 ± 2 E-08	8 ± 7 E-09
C291M	171	4 ± 9 E-10	4 ± 6 E-10	0.0 ± 1.2 E-09	0 ± 2 E-08	-0 ± 8 E-09
Auger Hole W13						
C258M	10	0.5 ± 1.5 E-09	0.8 ± 1.4 E-09	1 ± 2 E-09	5 ± 3 E-08	1.09 ± 0.12 E-07*
C260M	50	1.0 ± 1.3 E-09	1.0 ± 1.0 E-09	2.8 ± 0.3 E-08*	2.0 ± 0.4 E-07*	1.0 ± 0.9 E-08
C261M	82	1.9 ± 1.1 E-09	2.3 ± 0.3 E-08*	5.5 ± 0.4 E-08*	5 ± 2 E-08	5.8 ± 1.1 E-08*
C265M	162	0.8 ± 1.2 E-09	5 ± 8 E-10	0.5 ± 1.3 E-09	2 ± 3 E-08	0 ± 8 E-09
C267M	202	0.8 ± 1.4 E-09	8 ± 9 E-10	0.0 ± 1.5 E-09	2 ± 3 E-08	1.2 ± 1.0 E-08
Auger Hole W17						
C272M	10	4 ± 7 E-10	4 ± 6 E-10	-0.2 ± 1.2 E-09	5 ± 4 E-08	1.4 ± 0.8 E-08
C277M	122	6 ± 8 E-10	4 ± 6 E-10	0.6 ± 1.2 E-09	6 ± 7 E-08	1.6 ± 0.8 E-09
C283M	239	6 ± 8 E-10	4 ± 7 E-10	0.0 ± 1.1 E-09	6 ± 4 E-08	-1 ± 8 E-09
Auger Hole W18						
C248M	10	0.6 ± 1.2 E-09	0.6 ± 1.1 E-09	-0.2 ± 1.4 E-09	5 ± 3 E-08	6 ± 7 E-09
C252M	102	8 ± 9 E-10	3 ± 9 E-10	1.5 ± 1.8 E-09	2 ± 4 E-08	1.6 ± 0.8 E-09
C257M	194	0.5 ± 1.3 E-09	0.8 ± 1.0 E-09	0.7 ± 1.2 E-09	1 ± 3 E-08	1 ± 8 E-09

TABLE 19. (continued)

Sample	Depth (in.)	^{238}Pu (μCi/g)	$^{239,240}Pu$ (μCi/g)	^{241}Am (μCi/g)	^{90}Sr (μCi/g)	^{137}Cs μCi/g)
Auger Hole W24						
C209M	19	5 ± 9 E-10	5 ± 7 E-10	-0.4 ± 1.1 E-09	5 ± 4 E-08	2.7 ± 0.8 E-08*
C211M	59	1.0 ± 1.1 E-09	5 ± 8 E-10	0 ± 2 E-09	-1 ± 4 E-08	3.3 ± 1.2 E-08
C213M	113	1.0 ± 1.3 E-09	2 ± 8 E-10	0.1 ± 1.1 E-09	0 ± 2 E-08	0.9 ± 1.0 E-08
Auger Hole W25						
C243M	90	7 ± 8 E-10	-5 ± 7 E-10	-0.3 ± 1.2 E-09	1 ± 4 E-08	1.5 ± 0.7 E-08
C246M	162	0.4 ± 1.2 E-09	0.4 ± 1.1 E-09	0.6 ± 1.2 E-09	6 ± 6 E-08	7 ± 9 E-09
C247M	179	0.7 ± 1.2 E-09	0.7 ± 1.0 E-09	0 ± 2 E-09	3 ± 2 E-08	1 ± 8 E-09

*Sample result positive (i.e., greater than three sigma).

TABLE 20. RWMC SEDIMENT SAMPLE RADIOCHEMICAL ANALYSIS RESULTS: SAMPLES FROM THE DEEP DRILLING PROGRAM

Sample	Depth (ft-in.)	^{238}Pu (μCi/g)	$^{239,240}Pu$ (μCi/g)	^{241}Am (μCi/g)	^{90}Sr (μCi/g)	^{137}Cs (μCi/g)
Deep Hole D02						
D-13	1-2 to 1-8	2.6 ± 0.2 E-07*	1.13 ± 0.05 E-06*	1.52 ± 0.06 E-06*	1.9 ± 0.3 E-07*	7.2 ± 1.0 E-08*
D-17	9-2 to 9-8	6 ± 9 E-10	0.6 ± 1.1 E-09	0.3 ± 1.2 E-09	-2 ± 3 E-08	1 ± 8 E-09
D-20	15-6 to 16-0	1.49 ± 0.18 E-08*	2.55 ± 0.09 E-07*	5.0 ± 0.5 E-08*	1.3 ± 0.3 E-07*	10 ± 7 E-09
D-30	233-10 to 224-4	1.3 ± 1.3 E-09	8 ± 9 E-10	-0.1 ± 1.0 E-09	-2 ± 4 E-08	-2 ± 8 E-09
D-31	224-4 to 226-4	2.6 ± 1.1 E-09	7 ± 8 E-10	0.0 ± 1.2 E-09	2 ± 3 E-08	4 ± 7 E-09
D-34 (field split)	230-0 to 230-4	6.5 ± 1.9 E-09*	0.8 ± 1.0 E-09	0.3 ± 1.3 E-09	4 ± 3.0	-0 ± 7 E-09
D-34 (lab split)	230-0 to 230-4	3.22 ± 0.17 E-08*	5.8 ± 0.2 E-08*	--	--	--
D-34 (lab split, 4000-min count)	230-0 to 230-4	1.5 ± 0.4 E-09*	2 ± 3 E-10	--	--	--
D-34 (lab split, 4000-min count)	230-0 to 230-4	3.3 ± 0.6 E-09*	3 ± 4 E-10	--	--	--
D-34A (field split, 4000-min count)	229-8 to 230-0	2.4 ± 0.7 E-09*	3 ± 6 E-10	--	--	--
D-34A (lab split)	229-8 to 230-0	1.3 ± 1.1 E-09	-3 ± 7 E-10	--	--	--
D-34A (lab split)	229-8 to 230-0	1.4 ± 1.1 E-09	4 ± 6 E-10	--	--	--
D-35	232-3 to 232-7	1.6 ± 1.7 E-09	1.1 ± 1.0 E-09	-0.2 ± 1.2 E-09	2 ± 3 E-08	7 ± 7 E-09
D-36	233-9 to 234-2	1.8 ± 1.5 E-09	1.1 ± 1.4 E-09	-0.3 ± 1.2 E-09	2 ± 4 E-08	0 ± 6 E-09
D-37	234-9 to 235-2	1.4 ± 1.1 E-09	1.0 ± 0.9 E-09	0.2 ± 1.4 E-09	-3 ± 4 E-08	1.3 ± 0.7 E-08
Deep Hole D06A						
D-29	47-0 to 49-0	1.5 ± 1.2 E-09	7 ± 7 E-10	-2 ± 9 E-10	4 ± 3 E-08	5 ± 2 E-08
Deep Hole TW1						
D-42 (field split)	101-0 to 101-2	1.7 ± 0.2 E-08*	7.4 ± 0.4 E-07*	4.4 ± 0.2 E-07*	5 ± 4 E-08	--
D-42 (lab subsplit)	101-0 to 101-2	1.18 ± 0.17 E-08*	6.1 ± 0.3 E-07*	4.7 ± 0.2 E-07*	--	--
D-43A (field split)	101-2 to 101-7	4.6 ± 1.4 E-09*	1.97 ± 0.13 E-07*	1.03 ± 0.08 E-07*	4 ± 3 E-08	--
D-43 (field subsplit)	101-2 to 101-7	6.3 ± 1.7 E-09*	1.90 ± 0.13 E-07*	1.06 ± 0.09 E-07*	--	--
D-43A (lab subsplit)	101-2 to 101-7	6.5 ± 1.6 E-09*	2.00 ± 0.13 E-07*	1.37 ± 0.11 E-07*	--	--
D-47	225-9 to 225-11	-4 ± 6 E-10	8 ± 7 E-10	2 ± 9 E-10	6 ± 3 E-08	--
D-47 (lab subsplit)	225-9 to 225-11	7 ± 7 E-10	2 ± 6 E-10	0.5 ± 1.0 E-09	--	--
D-48	226-10 to 227-7	0.8 ± 1.1 E-09	3 ± 6 E-10	1.2 ± 1.4 E-09	3 ± 3 E-08	3 ± 1.6 E-08
D-48 (lab subsplit)	226-10 to 227-7	5 ± 9 E-10	2 ± 7 E-10	0.7 ± 1.1 E-09	--	--
D-48 (lab subsplit)	226-10 to 227-7	6 ± 7 E-10	7 ± 7 E-10	0.6 ± 1.2 E-09	--	--

*Sample result positive (i.e., greater than three sigma).

FY-1985 and FY-1986 shallow drilling samples, 24 positive results are associated with the uppermost sample collected. The surficial soil of the RWMC has been analyzed for radionuclide concentrations (Arthur, 1982), and their background values are much higher (approximately two orders of magnitude) than the detection limits used for radionuclide analyses in the Subsurface Investigations Program. Slight downward movement of radionuclide ions from the surficial soil into the subsurface would be expected from the natural weathering process. This would explain the presence of somewhat higher concentrations of radionuclides a few feet deep beneath the surface.

However, positive radionuclide values were detected also in samples taken from much deeper in the surficial sediments. These deeper (up to 21 ft deep) positive values reflect migration of radionuclides from waste buried at the RWMC.

As shown in Table 20, positive radionuclide values were detected in samples from the Deep Drilling program. Borehole D02 was drilled during the FY-1986 season and TW1 during FY-1987. Positive values for ^{238}Pu and $^{239,240}Pu$ were detected in samples obtained from the 240-ft interbed in borehole D02. The Radiological and Environmental Sciences Laboratory (RESL) analyzed sediment from the same interval and did not detect positive values. To reconfirm these results, hole TW1 was drilled within 15 ft of the location of D02. Positive detections for ^{238}Pu, $^{239,240}Pu$, and ^{241}Am were made in sediments of the 110-ft interbed of hole TW1; however, no positive results were detected in the 240-ft interbed of TW1. A confirmation of the positive results from the 110-ft interbed of hole TW1 was made by RESL (Table 21).

5.6.3.2 Lysimeter Water Sample Analyses. Twelve sediment-water samples were collected from porous cup lysimeters installed in holes drilled during the FY-1985 and FY-1986 seasons. These water samples were analyzed for the same radionuclide parameters as were the sediment samples (see Section 5.6.3.1). One of the suction lysimeter samples, from L08 in hole W23, had positive ^{241}Am and/or ^{238}Pu concentrations at the three

TABLE 21. RESULTS OF ANALYSES CONDUCTED BY EG&G AND BY RESL: SEDIMENT SAMPLES FROM THE 110-ft INTERBED IN BOREHOLE TW1

		EGG			RESL		
Sample	Depth (ft-in.)	^{238}Pu (μCi/g)	$^{239,240}Pu$ (μCi/g)	^{241}Am (μCi/g)	^{238}Pu (μCi/g)	$^{239,240}Pu$ (μCi/g)	^{241}Am (μCi/g)
D-43B	101-0	1.7 ± 0.2 E-08*	7.4 ± 0.4 E-07*	4.4 ± 0.2 E-07*		No split available	
D-43B (lab subsplit)	101-0	1.18 ± 0.17 E-07*	6.1 ± 0.3 E-07*	4.7 ± 0.2 E-07*		No split available	
D-43A	101-2	4.6 ± 1.4 E-09*	1.97 ± 0.13 E-07*	1.3 ± 0.08 E-08*	10 ± 3 E-09*	1.78 ± 0.13 E-07*	8.47 ± 0.95 E-08*
D-43A (lab subsplit)	101-2	6.3 ± 1.7 E-09*	1.90 ± 0.13 E-07*	1.06 ± 0.09 E-07*	N.D.	1.68 ± 0.09 E-07*	9.08 ± .075 E-07*
D-43A (lab subsplit)	101-2	6.5 ± 1.6 E-09*	2.00 ± 0.13 E-07*	1.37 ± 0.11 E-07*	3.9 ± 1.3 E-09	1.7 ± 0.09 E-07*	1.07 ± 0.09 E-07*

* Sample result positive (i.e., greater than three sigma).

sigma level (99% certainty). This lysimeter is located approximately 12 ft below land surface. Refer to Table 22 for a listing of radionuclide concentrations.

5.6.3.3 Conclusion. The migration of radionuclides has occurred at the RWMC. Mobilization of radionuclide ions has taken place in the shallow subsurface of the surficial cover. Most of the positive detections are presumably associated with the downward movement of radionuclides from the surface soil. The deep migration of radionuclides has followed a downward path from the buried waste through the highly fractured basalt into the 110-ft interbed and possibly the 240-ft interbed. Results of analyses of samples from the 240-ft interbed were inconclusive.

TABLE 22. RWMC LYSIMETER WATER SAMPLE ANALYSIS RESULTS

Borehole	Lysimeter Number	Date	Depth (ft-in.)	$^{239,240}Pu$ µCi/ml	^{238}Pu and/or ^{241}Am µCi/ml
PA01	L15	06/13/86	14-4	7 ± 5 E-11	6 ± 5 E-11
W04	L05	06/13/86	6-2	2 ± 3 E-11	2 ± 3 E-11
W25	L28	05/01/87	15-6	1 ± 4 E-11	2 ± 3 E-11
W06	L27	05/01/85	11-9	1 ± 3 E-11	1 ± 3 E-11
PA02	L16	06/13/86	8-8	2 ± 3 E-11	1.3 ± 0.6 E-10
PA01	L15	04/30/87	14-4	8 ± 7 E-11	5 ± 7 E-11
W23	L09	06/13/86	7-8	2 ± 4 E-11	5 ± 7 E-11
W04	L04	08/26/86 + 09/04/86**	15-5	5 ± 4 E-11	7 ± 6 E-11
TH4	L18	06/13/86	4-0	4 ± 7 E-11	1.3 ± 1.3 E-10
W23	L08	05/01/87	11-1	6 ± 6 E-11	5.3 ± 1.3 E-10*
W05	L25	04/30/87	10-0	4 ± 7 E-11	1.6 ± 1.2 E-10
W02	L01	04/30/87	14-0	2 ± 3 E-11	7 ± 5 E-11

*Positive sample result (greater than 3 times sigma).

**L04, W04 is a composite sample from two days sampling.

6. CONCLUSIONS

The Subsurface Investigations Program at the RWMC made progress in FY-1987 toward obtaining its two program objectives: a field calibration of a model to predict long-term radionuclide migration and measurement of the actual migration to date.

Three deep boreholes were drilled at the RWMC to collect sample material for evaluation of radionuclide content in the interbeds, to determine geologic and hydrologic characteristics of the sediments, and to provide as monitoring sites for moisture movement in these sediments. Strict contamination controls were followed during drilling and sampling to ensure core samples were not cross-contaminated.

A health physics survey was conducted daily to guard against cross-contamination between surficial background radioactivity and sedimentary samples from the interbeds. Positive smear values were detected from the drilling of boreholes TW1 and D15. However, there is no association between these smears and sampling of the interbeds; the positive detections were presumably a result of contact with dust from surficial sediment.

Two deep boreholes were instrumented with heat dissipation sensors and suction lysimeters. Instrument readings were taken from 23 shallow auger holes, two neutron access tubes, and three deep boreholes on a monthly basis. A database was set up to store the large volume of data collected since June 1985 for this program. Data were input and stored on an IBM-AT using the DBASE III software package.

Core samples from the weighing lysimeters were analyzed for particle size distribution and with x-ray diffraction. Reading from the sensors in the weighing lysimeters were discontinued. Weight data will be recorded.

The meteorological station at the Test Trench was modified to provide additional data to determine evapotranspiration rates at the RWMC. Thermocouple psychrometers were calibrated for sensor rotation and

calibration verification. Preparations were instigated for the installation of a simulated waste trench. Soil cores from test trench auger holes were analyzed for particle size distribution, mineralogy and soil moisture characteristic curve.

Twenty-four soil water samples were collected from suction lysimeters and analyzed for major ion chemistry.

Organic chemicals were detected in water samples collected from USGS aquifer monitoring wells surrounding the RWMC and from air samples collected from boreholes drilled within the SDA. Concentrations of carbon tetrachloride, chloroform, 1,1,1-trichloroethane, and trichloroethylene were found above detection limits in several RWMC water wells. One sample exceeded proposed EPA maximum concentration levels of 5 µg/L for drinking water. Carbon tetrachloride in the air of one of the boreholes exceeded the EPA recommended time weighted average (TWA) value of 30 mg/m^3. Drilling and instrumenting of boreholes for this program was discontinued so that procedures could be revised to deal with these organic substances.

Sampling of ambient air, air in boreholes, and soil gases was conducted at the RWMC to determine the identity, location, and relative concentration of selected chlorinated and aromatic VOCs. These sampling efforts indicated that carbon tetrachloride, 1,1,1-trichloroethane, trichloroethylene, and tetrachloroethylene are migrating from a number of the pits. The major sources of organics are Pits 4, 5, 6, 9, and 10. Measurable concentrations of VOCs occur in soil gases at distances from 2000 to 3400 ft from the SDA boundary. Analyses of gases collected at various depths from holes north and east of the SDA indicate maximum gas concentrations around 100 ft, and measurable concentrations to 570 ft.

Data collected for the Net Downward Flux portion of the study were graphed and examined for trends. The lowest matric potentials generally occur in areas where water collects at land surface during portions of the year. These areas include drainage and flood control ditches, small

depressions where runoff or snow melt accumulates, and areas flooded in the past. Data collected outside the SDA indicates larger matric potentials (relatively dryer) than within the SDA.

Matric potentials decrease (approach saturation) with increasing depth of the shallow augerholes. Several of the holes exceed field capacity (values less than 0.1 - 0.2 bars tension), indicating the potential for gravity drainage.

Neutron data indicates the active zone of moisture in the sediments extends to a depth of 6 to 7 ft below land surface. Moisture above this depth is affected by seasonal cycles of precipitation and evaporation, whereas moisture beneath this depth moves downward, predominately by the force of gravity. Hydraulic gradients calculated from instrumentation indicate downward moisture movement during much of the year for several of the instrumented holes.

The Computer Model Development focused on a detailed review of previous vadose zone modeling studies at INEL, acquisition and installation of a suite of computer models for unsaturated flow and contaminant transport, and preliminary applications of computer models using site specific data.

Examination of past modeling efforts indicates the need for an adequate data base and field calibrated models to obtain reliable predictions. Thirteen models and codes were installed on the CRAY computer; the models are being refined and will be used to evaluate radionuclide and chemical transport in the RWMC subsurface environment.

A vapor release model was used to simulate the vapor plume history from 1966 to 1987. The preliminary computer simulation indicated that about 80 percent of the original inventory of organics was released to the sediment from the pit in the vapor phase, of which about 90 percent has escaped to the atmosphere, and that this organic vapor plume extends to the water table of the Snake River Plain Aquifer.

A total of 142 soil samples from shallow auger holes drilled during FY-1985 and FY-1986 were subjected to radiochemical analyses. These samples were augered from the surficial cover of the RWMC. Results of these analyses indicate that most migration is occurring near land surface and may be related to downward migration of radionuclides from weathering of the sediment at land surface. Positive values detected from sediments deeper in the surficial cover (to 21 ft) indicate migration of radionuclides from buried waste.

Twelve sediment-water samples were collected from suction lysimeters installed in auger holes drilled during shallow drilling in FY-1986 and FY-1986. A positive value was detected in one of these lysimeter water samples.

Deep drilling during FY-1986 and FY-1987 produced 27 samples for radiochemical analysis. Positive plutonium concentrations at three times the standard deviation (99% certainty) were detected at the 110-ft interbed. Positive plutonium values at the 240-ft interbed could not be confirmed.

The body of subsurface data available to date provides good evidence that radionuclides have migrated from the buried waste downward to the 110-ft sedimentary interbed and some evidence that migration has occurred to the 240-ft sedimentary interbed. The amount of water available as the transporting agent has been reduced by improvements made to the surface drainage system at the RWMC. Volatile organic compounds from the buried waste have migrated through the unsaturated zone primarily as vapors but also as liquids. These compounds have been detected at low concentration in water from the Snake River Plain Aquifer.

REFERENCES

Arthur, W. J., 1982, "Radionuclide Concentrations in Vegetation at a Solid Waste Disposal Area in Southeastern Idaho," Journal of Environmental Quality, Vol. 11, pp. 394-399.

Baca, R. G., I. P. King, and W. R. Norton, 1978, "Finite Element Models for Simultaneous Heat and Moisture Transport in Unsaturated Soils," Proceedings of the Second International Conference on Finite Elements in Water Resources, Imperial College, Pentech Press, London.

Baca, R. G., R. C. Arnett, and D. W. Langford, 1984, "Modeling Fluid Flow in Fractured-Porous Rock Masses by Finite Element Techniques," International Journal for Numerical Methods in Fluids, Vol. 4, pp. 337-348.

Barraclough, J. T., J. B. Robertson, and V. H. Janzer, 1976, Hydrology of the Solid Waste Burial Ground as Related to the Potential Migration of Radionuclides, Idaho National Engineering Laboratory, IDO-22056.

Brown, R. W., 1970, "Measurement of Water Potential with Thermocouple Psychrometers: Construction and Applications," USDA Forest Service Res. Pap. INT-80.

Burgus, W. H. and S. E. Maestas, 1976, The 1975 RWMC Core Drilling Program, IDO-10065.

DOE (U.S. Department of Energy), 1982, Environmental and Other Evaluations of Alternatives for Management of Defense Transuranic Waste at the Idaho National Engineering Laboratory, DOE/IDO-10103, Vol. 1 & 2.

DOE (U.S. Department of Energy), 1983, A Plan for Studies of Subsurface Radionuclide Migration at the Radioactive Waste Management Complex of the Idaho National Engineering Laboratory, DOE/ID-10116.

Groenewold, G. S. and P. N. Pink, "Sampling and Analysis of RWMC SDA Air, Soil Gas, and Well Gas," EG&G Interoffice Correspondence, GSG-63-87, December 1987.

Hubbell, J. M., L. C. Hull, T. G. Humphrey, B. F. Russell, J. R. Pittman, and R. M. Cannon, 1985, Annual Progress Report: FY-1985--Subsurface Investigations Program at the Radioactive Waste Management Complex of the Idaho National Engineering Laboratory, DOE-ID 10136.

Hubbell, J. M., L. C. Hull, T. G. Humphrey, B. F. Russell, J. R. Pittman, and P. R. Fischer, 1987, Annual Progress Report: FY-1986--Subsurface Investigations Program at the Radioactive Waste Management Complex of the Idaho National Engineering Laboratory, DOE-ID 10153.

Hanks, R. J. and L. G. King, 1973, Irrigation Management for Control of Quality of Irrigation Return Flow, EPA R2-73-265, U.S. Environmental Protection Agency, Washington, D.C.

Hull, L. C., 1986, Letter to J. M. Hubbell, LCH-17-86, "Psychrometer Data," September 30.

Humphrey, T. G., 1980, Subsurface Migration of Radionuclides at the Radioactive Waste Management Complex--1978, EGG-2026.

Humphrey, T. G., T. H. Smith, and M. C. Pope, 1982, "Projected Subsurface Migration of Radionuclides from Buried Idaho National Engineering Laboratory Transuranic Waste," Nuclear Technology, Vol. 58, pp. 136-149.

Humphrey, T. G. and F. H. Tingey, 1978, The Subsurface Migration of Radionuclides at the Radioactive Waste Management Complex 1976-1977, TREE-1171.

Kline, N. W., R. L. England, and R. G. Baca, 1985, CHAINT Computer Code: Users Guide, RHO-BW-CR-144P, Rockwell Hanford Operations, Richland, Washington.

Meyn, R. L. and R. S. White, 1972, "Calibration of Thermocouple Psychrometers: A Suggested Procedure for Development of a Reliable Predictive Model," in Psychrometry in Water Relations Research, pp. 56-64, R. W. Brown and B. P. Van Haveren, eds., Utah Agricultural Experiment Station, Utah State University, Logan, Utah.

Mizell, S. A. and L. C. Hull, 1983, Preliminary Modeling of Radionuclide Migration through the Subsurface at the INEL Radioactive Waste Management Complex Using the Unsaturated Flow and Transport Model UNSAT, RE-PB-83-038, EG&G Idaho, Inc., Idaho Falls, Idaho.

Pope, M. C. and H. W. Reno, 1982, Modeling Radionuclide Transport in the Unsaturated Zone Beneath the Radioactive Waste Management Complex, (Draft Report), EG&G Idaho, Inc., Idaho Falls, Idaho.

Schmalz, B. L., 1972, Radionuclide Distribution in Soil Mantle of the Lithosphere as a Consequence of Waste Disposal at the National Reactor Testing Station, IDO-10049.

Sill, C. W., 1982, "Some Deficiencies in Analyzing Leachates and Reporting Results," Nuclear and Chemical Waste Management, Vol. 3, pp. 144-147.

Travis, B. J., 1984, TRACR3D: A Model of Flow and Transport in Porous-Fractured Media, LA-9667-MS, Los Alamos National Laboratory, Los Alamos, New Mexico.

Van Genuchten, M. T., 1978, Calculating the Unsaturated Hydraulic Conductivity with a New Closed-Form Analytical Model, Water Resources Program, Princeton University.

Van Genuchten, M. T., 1980, "A Closed-Form Equation for Predicting the Hydraulic conductivity of Unsaturated Soils," Soil Science Society of America Journal, Vol. 44, pp. 892-898.

Wang, J. S. Y., and T. N. Narasimhan, 1985, "Hydrologic Mechanisms Governing Fluid Flow in a Partially Saturated, Fractured, Porous Medium," Water Resources Research, Vol. 21, No. 12, pp. 1861-1874.

Yanskey, G. R., E. H. Markee, Jr., and A. P. Richter, 1966, Climatography of the National Reactor Testing Station, IDO-12048, Institute for Atmospheric Sciences, Environmental Sciences Services Administration, Idaho Falls, ID.

APPENDIX A
GEOLOGIC DESCRIPTION OF DEEP DRILLING SAMPLES

APPENDIX A

GEOLOGIC DESCRIPTION OF DEEP DRILLING SAMPLES

The deep drill holes were drilled using several different sampling methodologies to optimize sample recovery in the various geologic materials. Basalt was drilled with either a tricone bit or a wire line coring tool. Sample descriptions are more complete from the cored intervals than those drilled with a tricone bit because the intervals drilled with a tricone bit have very small samples obtained from a cyclone separator.

The interbeds were sampled using a HXB wire line drilling system or Shelby tube samplers. The descriptions are for the sediment samples contained in the shoe of the sampler for the specified depths. The depth relative to land surface, texture, sorting, color, and roots were determined in the field with some textural classifications supplemented by LaMotte test results. Texture refers to the relative proportions of sand, silt, and clay in the sample. In a sample with a name such as sandy silt, the sample is predominantly silt with a lesser amount of sand. If the LaMotte test was used, a parenthesis will follow the textural name with the percentage of sand, silt, and clay in that order. Munsell soil color charts were used to determine color.

TABLE A-1. DRILL HOLE TW-1

Depth (ft-in.)	Sample Number	Sample Recovery (%)	Tool	Sample Description
0-0 to 16-6	--	NA	Auger	--
16-9 to 21-9	D-38	100%	HXB wireline core	Dense, basalt, gray (2.5Y 6/0) fractured, fractures filled w/sediment, few vesicles
21-9 to 26-0	--	--	Tricone bit	Basalt, hard
26-0 to 30-0	--	--	Tricone bit	Rubble zone, sandy silt, light yellowish brown (10YR 5/3) and reddish basalt
30-0 to 45-0	--	--	Tricone bit	Basalt, gray
45-0 to 50-0	--	NA	Tricone bit	Basalt, purple, possible rubble zone lost circulation
50-0 to 55-0	--	NA	Tricone bit	No sample, presumably basalt
55-0 to 60-0	--	NA	Tricone bit	No sample, presumably basalt
60-0 to 65-0	--	NA	Tricone bit	No sample, presumably basalt
65-0 to 70-0	--	NA	Tricone bit	Basalt, gray
70-0 to 71-0	--	NA	Tricone bit	No sample, presumably basalt
71-0 to 73-0	--	NA	Tricone bit	No sample, penetration rate increased, softer material
73-0 to 76-0	--	NA	Tricone bit	No sample, presumably basalt
76-0 to 87-9	--	NA	Tricone bit	No sample, poor circulation, void 76-0 to 76-6
87-9 to 91-9	D-39	81	HXB wireline core	Basalt, dense, small vesicles, fractured, fractures filled w/silt, gray (10YR 5/1)
91-9 to 95-8	D-40	100	HXB wireline core	Basalt, dense, fractured, fractures filled w/silt, gray (10YR 5/1). Bottom 1 inch of core is rubble with silt and sand.
95-8 to 98-2	D-41	100	HXB wireline core	Basalt, dense, gray (10YR 5/1)
98-2 to 101-2	D-42	100	HXB wireline core	Basalt, dark gray (2.5YR 3/0) Bottom 2 inches clay, brown (10YR 5/4), wet
101-2 to 101-7	D-43	100	Shelby tube	Sandy silt, poorly sorted, red (2.5YR 5/8), dry
101-7 to 101-9	D-44	100	Shelby tube	Sandy silt, well sorted, weak red (10R 4/4), slightly moist, no reaction with HCl

TABLE A-1. (continued)

Depth (ft-in.)	Sample Number	Sample Recovery (%)	Tool	Sample Description
101-9 to 103-5	D-45	25	HXB wireline core	Silty sand, very fine to coarse grained, poorly sorted, well rounded to angular. Quartz grains are mostly frosted, no reaction with HCl
103-5 to 108-0	--	--	Tricone bit (7-5/8 in.)	No sample
108-0 to 112-0	--	--	Tricone bit (5-7/8 in.)	Basalt, gray
112-0 to 123-0	--	--	Tricone bit (5-7/8 in.)	Basalt, gray
123-0 to 128-0	--	--	Tricone bit (5-7/8 in.)	Basalt, gray (2.5YR 5/0)
128-0 to 133-0	--	--	Tricone bit (5-7/8 in.)	Basalt, gray to weak red (2.5YR 5/2)
133-0 to 138-0	--	--	Tricone bit (5-7/8 in.)	Basalt, gray to reddish gray (10R 5/1)
138-0 to 143-0	--	--	Tricone bit (5-7/8 in.)	Basalt, gray-reddish gray (10R 5/1)
143-0 to 168-0	--	--	Tricone bit (5-7/8 in.)	Basalt, gray-reddish gray (10R 5/1)
168-0 to 170-0	--	--	Tricone bit (5-7/8 in.)	Basalt, gray (7.5YR 4/0)
170-0 to 173-0	--	--	Tricone bit (5-7/8 in.)	Basalt, gray (10R 5/1) penetration rate increased
173-0 to 178-0	--	--	Tricone bit (5-7/8 in.)	No Sample
178-0 to 183-0	--	--	Tricone bit (5-7/8 in.)	Basalt, gray (10YR 5/1)
183-0 to 194-0	--	--	Tricone bit (5-7/8 in.)	Basalt, gray (2.5Y 5/0)
194-0 to 218-11	--	--	Tricone bit (5-7/8 in.)	No sample, poor circulation
218-11 to 223-11	D-46	100	HXB wireline core	Basalt, dense, some vesicles 1 mm, fractured near top, no sediment fill in fractures, gray (2.5Y 5/0)
223-11 to 225-11	D-47	46	HXB wireline core	Basalt, gray, to 225°-9°, 225-9 to 225-9 1/2 is clay, well sorted, light gray (10YR 7/2) moist, 225-9 1/2 to 225-11 is clayey silt, well sorted red (10YR 5/8) no reaction with HCl, clay at top of interbed appears to be transported from above interbed
225-11 to 227-7	D-48	100	HXB wireline core	Clayey silt, well sorted, red (10R 5/8), strong HCl reaction

TABLE A-1. (continued)

Depth (ft-in.)	Sample Number	Sample Recovery (%)	Tool	Sample Description
227-7 to 228-5	--	0	HXB wireline core	No sample received
228-5 to 229-6	D-49	100	Shelby tube	Silt, well sorted, reddish yellow (5YR 7/6) slightly moist, strong HCl reaction
229-6 to 229-10	--	0	Shelby tube	Lost, shelby tube, no sample
229-10 to 230-0	D-50	100	Shelby tube	Silt, well sorted, yellowish red (5YR 5/6) strong HCl reaction, moist
230-0 to 231-1	D-51	92	Shelby tube	Silt, well sorted, yellowish red (5YR 5/6) moist, strong HCl reaction
231-1 to 231-3	--	--	Tricone bit (5-7/8 in.)	Silty clay, (00, 38, 62) well sorted, some sand, (5YR 4/6) strong HCl reaction
231-3 to 232-0	--	--	Tricone bit (5-7/8 in.)	Sandy silt, yellowish brown (5YR 4/6) slightly moist, strong HCl reaction
232-0 to 233-3	--	--	Tricone bit (5-7/8 in.)	Sand, (82, 11, 07), reddish brown (5YR 4/4), poorly sorted, medium to coarse grained, subangular, quartz feldspar and basalt fragments. Mild HCl reaction.
233-0 to 233-7	D-52 & D-53	100	Shelby tube	Sandy silt, (30, 35, 35), poorly sorted, red (2.5YR 4/6)moist, strong HCl reaction
233-7 to 234-6	--	--	Tricone bit (5-7/8 in.)	Silty sand, (81, 08, 11), poorly sorted, very fine to coarse grained, yellowish red (5YR 4/6) strong HCl reaction, slightly moist, quartz, feldspar and basalt fragments.
234-6 to 235-6	--	--	Tricone bit (5-7/8 in.)	Silty sand, (81, 08, 11), poorly sorted, very fine to coarse grained, dark reddish brown (5YR 3/4), slightly moist, strong HCl reaction, quartz, feldspar and basalt fragments
235-6 to 236-6	--	--	Tricone bit (5-7/8 in.)	Sand, (80, 07, 13), poorly sorted, very fine to coarse grained. Dark reddish brown (5YR 3/4), Mild HCl reaction, quartz, feldspar and basalt fragments (70% basalt) slightly moist.
236-6 to 237-6	--	--	Tricone bit (5-7/8 in.)	Sand, (67, 03, 30), poorly sorted, very fine to coarse grained. Dark reddish brown (5YR 3/4), mild HCl reaction, quartz, feldspar and basalt fragments, slightly moist.

TABLE A-2. DRILL HOLE D15

Depth (ft-in.)	Sample Number	Sample Recovery (%)	Tool	Sample Description
0-0 to 1-6	--	--	Auger	Silt, (08, 64, 28), well sorted, pale brown (10YR 6/3) slight HCl reaction
1-6 to 1-9	--	100	HXB wireline core	Vesicular basalt, fractured, gray (7.5YR 5/0), fractures have sediment in filling. Vesicles are 2-5 mm in diameter
1-9 to 6-9	--	50	HXB wireline core	Vesicular basalt, gray (7.5YR 6/0) vesicles are 2-10 mm in diameter w/white mineralization in same
6-9 to 8-0	--	--	Tricone bit (7-7/8 in.)	Basalt
8-0 to 17-8	--	--	Tricone bit (7-7/8 in.)	Basalt
17-8 to 20-0	--	--	Tricone bit (7-7/8 in.)	Basalt, gray (10YR 6/11)
20-0 to 25-0	--	--	Tricone bit (7-7/8 in.)	Basalt, gray (10YR 5/1), some sediment
25-0 to 28-0	--	--	Tricone bit (7-7/8 in.)	Basalt
28-0 to 30-0	--	--	Tricone bit (7-7/8 in.)	Basalt, gray (10YR 6/1)
30-0 to 31-11	--	--	Tricone bit (7-7/8 in.)	Basalt, increase drilling rate from 30 ft 10 in. to 31 ft 4 in.. Possible interbed
31-11 to 34-9	D-54	18	HXB wireline core	Sandy silt, (47, 53, 00), dark red (2.5YR 4/8), no HCl reaction
34-9 to 39-9	D-55	100	HXB wireline core	Sandy silt, dark red (2.5YR 4/8) no HCl Reaction. Basalt, dark gray (10YR 5/1) dense with small vesicles begins at 35 ft 3 in. Interbed 30-10 to 35-3
39-9 to 41-0	--	--	Tricone bit 7-5/8 in.	Basalt
41-0 to 44-0	--	--	Tricone bit 7-5/8 in.	Basalt
44-0 to 44-9	--	--	Tricone bit 7-5/8 in.	Sandy silt, poorly sorted, some roots, red (2.5YR 5/6) no HCl reaction, dry
44-9 to 46-9	D-56	75	HXB wireline core	Basalt, vesicular, fractured, top 3 inches ash-like, gray (10YR 5/1), fractures filled with silt, pale brown (10YR 7/3) strong HCl reaction

TABLE A-2. (continued)

Depth (ft-in.)	Sample Number	Sample Recovery (%)	Tool	Sample Description
46-9 to 50-0	--	--	Tricone bit (7-5/8 in.)	Basalt, gray to reddish brown.
50-0 to 55-0	--	--	Tricone bit (7-5/8 in.)	Basalt, gray (2.5YR 5/0)
55-0 to 60-0	--	--	Tricone bit (7-5/8 in.)	Basalt, gray (2.5YR 5/0)
60-0 to 68-0	--	--	Tricone bit (7-5/8 in.)	Basalt, fractured, gray (2.5YR 5/0)
68-0 to 75-0	--	--	Tricone bit (7-5/8 in.)	Basalt, fractured, red-gray, fractures filled with caliche
75-0 to 80-0	--	--	Tricone bit (7-5/8 in.)	Basalt, gray (2.5Y 5/0), slightly fractured, fracture filling material is light brownish gray (10YR 6/2), no HCl reaction
80-0 to 88-0	--	--	Tricone bit (7-5/8 in.)	Basalt, fractured, gray (2.5Y 5/0) fractures filled with sediment/caliche, very pale brown (10YR 7/3)
88-0 to 89-10	D-57	100	HXB wireline core	Basalt, dense, horizontal fractures, fractures filled with caliche
89-10 to 90-0	--	100	HXB wireline core	Basalt, very dense
90-0 to 94-4	D-58	96	HXB wireline core	Basalt, vesicular, fractured, gray, large 16 inches long vertical fracture with some sediment infilling
94-4 to 96-9	D-59	31	HXB wireline core	Basalt, very vesicular, fractured, dark gray, fractures filled with wet yellow-brown sediment. Bottom 4 inches was interbed, silty, clayey sand, (57, 23, 20) brown (7.5YR 5/6) slight HCl reaction, very wet
96-9 to 97-10	--	0	HXB wireline core	No sample
97-10 to 98-8	D-60	69	Shelby tube	Gravel, poorly sorted, brown (10YR 5/3), gravel pieces up to 2.5 cm x 1.5 cm. Moist
98-8 to 99-3	D-61	71	Shelby tube	Gravel, poorly sorted, reddish brown, moist
99-3 to 99-5	D-62	100	Shelby tube	Sandy gravel, light red, moist

TABLE A-2. (continued)

Depth (ft-in.)	Sample Number	Sample Recovery (%)	Tool	Sample Description
99-5 to 106-0	--	--	Tricone bit (7-7/8 in.)	Sandy gravel, coarse, brown (10YR 5/3)
106-0 to 106-6	--	--	Tricone bit (7-7/8 in.)	Clayey silt, poorly sorted, brown (10YR 5/3), moist, no HCl reaction
106-6 to 107-6	D-65	83	HXB wireline core	Gravel and clay. 3 inch gravel followed by clay. Clay is brown (10YR 5/2), moist
107-6 to 108-7	D-66	23	HXB wireline core	Clay, well sorted, dark grayish brown (10YR 4/2), moist, no HCl reaction
108-7 to 111-0	D-67	62	HXB wireline core	Clay, well sorted, brown (10YR 5/3), moist, strong HCl reaction
110-0 to 112-2	D-68	71	HXB wireline core	Clay, brown (10YR 4/3) moist, strong HCl reaction. Bottom 3 inches basalt
112-2 to 112-6	D-69	100	HXB wireline core	Silty clay, well sorted grayish brown (10YR 5/2), moist, strong HCl reaction bottom 2 inches basalt, vesicular, gray (10YR 5/1)
112-6 to 113-4	D-70	100	HXB wireline core	Basalt, vesicular, gray (2.5YR 5/2), vesicles are approximately 3 mm with sediment infilling
113-4 to 117-4	D-71	100	HXB wireline core	Basalt, vesicular, fractured, gray (2.5Y 5/0), some sediment in fractures
117-4 to 123-9	--	--	Tricone bit (7-7/8 in.)	Basalt
123-9 to 129-6	--	--	Tricone bit (7-7/8 in.)	Basalt
129-6 to 133-0	--	--	Tricone bit (7-7/8 in.)	Cinders, red
133-0 to 139-10	--	--	Tricone bit (7-7/8 in.)	Basalt, red (10R 4/2), some obsidian
139-10 to 145-0	--	--	Tricone bit (7-7/8 in.)	Basalt, some olivine
145-0 to 170-0	--	--	Tricone bit (7-7/8 in.)	Basalt with cinder zones
170-0 to 190-0	--	--	Tricone bit (7-7/8 in.)	Basalt, gray
190-0 to 200-0	--	--	Tricone bit (7-7/8 in.)	No sample return
200-0 to 210-0	--	--	Tricone bit (7-7/8 in.)	No sample return, void 204-205
210-0 to 215-0	--	--	Tricone bit (7-7/8 in.)	Basalt, dense

TABLE A-2. (continued)

Depth (ft-in.)	Sample Number	Sample Recovery (%)	Tool	Sample Description
215-0 to 217-2	--	--	Tricone bit (7-7/8 in.)	Basalt, dense, drilling rate increased near bottom
217-2 to 220-0	D-72	100	HXB wireline core	Basalt, fractured, vesicular, dark gray (10YR 4/1), vesicles 1-2 mm in diameter. Fractures filled with gray-green brown sediment.
220-2 to 222-5	D-73	28	HXB wireline core	Basalt, dense, vesicular (top 1-3) basalt, fractured, fractures filled with sand and clay that is brown (10YR 5/3) and poorly sorted. This zone is 7 inches thick. Bottom 2 inches is fine silty sand, poorly sorted, reddish yellow (5YR 6/8), moist. Interbed at 221°-10°
222-5 to 224-5	D-74	71	HXB wireline core	Clay and silt, well sorted, red (2.5YR 4/6) No HCl reaction, slightly moist
224-5 to 226-8	D-75	59	HXB wireline core	Clay, silty clay, well sorted red (2.5YR 4/4) to brown. No HCl reaction, moist
226-8 to 279-5	D-76	3	HXB wireline core	Clay, well sorted, red (2.5YR 4/6) strong HCl reaction, dry
229-5 to 233-5	D-77	67	HXB wireline core	Clay grading to silt, well sorted dark yellowish brown (10YR 4/4) strong HCl reaction, moist
233-5 to 237-4	D-78	100	HXB wireline core	Clay grading to silt, well sorted, Brown (10YR 5/3), strong HCl reaction, moist
237-4 to 239-4	D-79	100	HXB wireline core	Clay grading to silt. Clay, brown (10YR 4/3) grading to silt, thinly laminated with very fine sand. Yellowish brown (10YR 5/4) reacts with HCl, slightly moist
239-4 to 243-6	D-80	100	HXB wireline core	Basalt, vesicular with a fine white (10YR 8/2) lining in vesicles, grading to vesicular basalt, followed by a 2 inch sand layer, gray-brown (10YR 4/2) with basalt pebbles. Bottom 3 ft 10 in. is vesicular basalt with horizontal fractures up to 1 mm wide. Fractures are sediment filled. Vesicles are 2-3 cm in diameter. Basalt is dark gray (7.5YR 4/2)

TABLE A-3. DRILL HOLE D10

Depth (ft-in.)	Sample Number	Sample Recovery (%)	Tool	Sample Description
0 to 8-6	--	--	Auger	No sample
8-6 to 11-4	D-81	65	HXB wireline core	Dark gray basalt, small to moderate size vesicles, fractured, soil in fractures
11-4 to 12-0	D-82	50	HXB wireline core	Dark gray basalt, small to moderate size vesicles, fractures
12-0 to 13-6	D-83	89	HXB wireline core	Dark gray basalt, moderate to large size vesicles, dense
13-6 to 17-5	D-84	100	HXB wireline core	Dark gray basalt, small to moderate size vesicles, fractures
17-5 to 22-4	D-85	100	HXB wireline core	Dark gray basalt, dense, few fractures, very small to small vesicles
22-4 to 24-8	D-86	100	HXB wireline core	Dark gray basalt, very dense, very few fractures very small vesicles
24-8 to 29-8	D-87	98	HXB wireline core	Dark gray basalt, very dense, very few fractures, very small vesicles
29-8 to 31-6 1/2	D-88	100	HXB wireline core	Light to medium gray basalt, very dense, very few fractures, very small vesicles
31-6 1/2 to 34-8	D-89	62	HXB wireline core	Medium to fine sand, bright reddish orange, Munsell color is red, no reaction to HCl, from 34-0 to 34-8 is a reddish brown clayey silt and clayey very fine sand, dry, no reaction with HCl
34-8 to 36-0	D-90	88	HXB wireline core	Clayey silt and clayey very fine sand reddish brown color, very moist to wet, no reaction with HCl
36-0 to 38-10 3/4	--	--	HXB wireline core	No sample recovery. Some of this interbed sediment was sticking to outside of wire line core: clayey silt and very fine clayey sand, reddish brown, dry, no reaction with HCl

TABLE A-3. (continued)

Depth (ft-in.)	Sample Number	Sample Recovery (%)	Tool	Sample Description
38-10 3/4 to 41-7 1/2	D-91	94	HXB wireline core	Dark gray basalt, dense, small to moderate size vesicles, fractured. Toward bottom of core interval is cinder zone and brecciated basalt
41-7 1/2 to 42-3/4	D-92	76	HXB wireline core	Dark gray brecciated basalt and cinders, medium size vesicles
42-3/4 to 44-4/5	D-93	100	HXB wireline core	Dark gray basalt, fractures, orange brown sediment in fractures, moderate to large vesicles
44-4/5 to 49-4/5	D-94	92	HXB wireline core	Dark gray basalt, medium to large vesicles, large fractures with brown sediment filling fractures
49-4/5 to 54-3 4/5	D-95	100	HXB wireline core	49 ft 4/5 in. to 51 ft 6 4/5 in.: dark gray basalt, moderate to large vesicles, large fractures 51 ft 6 4/5 in. to 54 ft 3 4/5 in.: dark gray basalt, very dense, small to very small vesicles, no fractures
54-3 4/5 to 59-3 4/5	D-96	98	HXB wireline core	54 ft 3/45 in. to 56 ft 6 3/10 in.: dark gray basalt, small vesicles, no fractures, dense 56 ft 6 3/10 in. to 58 ft 4/5 in.: moderate to dark gray basalt, medium to large vesicles, fractures 58 ft 4/5 in. to 59 ft 3 4/5 in.: black cinders
59-3 4/5 to 62-11	D-97	97	HXB wireline core	Moderate to dark gray basalt, moderately dense to dense, medium to large vesicles, fractured
62-11 to 66-2	D-98	95	HXB wireline core	62 ft 11 in. to 65 ft 0 in.: moderate to dark gray basalt, medium to large size vesicles, fractures 65 ft 0 in. to 66 ft 2 in.: cinders, dark gray to black
66-2 to 69-8	D-99	74	HXB wireline core	Dark gray basalt, medium to large size vesicles, dense, fractures, orange brown sediment in fractures

TABLE A-3. (continued)

Depth (ft-in.)	Sample Number	Sample Recovery (%)	Tool	Sample Description
69-8 to 74-8	D-100	100	HXB wireline core	69 ft 8 in. to 73 ft 11 1/2 in.: dark gray basalt, medium to large size vesicles, dense fractures, orange brown sediment in fractures 73 ft 11 1/2 in. to 74 ft 8 in.: cinders, black
74-8 to 79-0	D-101	100	HXB wireline core	74 ft 8 in. to 75 ft 6 in.: conders, red brown 75 ft 6 in. to 79 ft 0 in. dark gray basalt, medium to large size vesicles, dense, fractures, sediment in fractures
79-0 to 79-11	D-102	23	HXB wireline core	Medium gray basalt, moderate to large size vesicles
79-11 to 84-11	D-103	100	HXB wireline core	Dark gray basalt, large to very large size vesicles, dense, fractures, sediment in fractures
84-11 to 90-2	D-104	100	HXB wireline core	Dark gray basalt, very small size vesicles to no vesicles, very dense, few fractures, fractures filled with clay
90-2 to 95-2	D-105	88	HXB wireline core	90 ft 2 in. to 92 ft 6 in.: moderate gray basalt, very small vesicles, very dense, few fractures 92 ft 6 in. to 95 ft 2 in.: dark gray basalt, moderate to large size vesicles, fractured The "110-ft" interbed was reached with this core. Sediment was not recovered; however, the bottom of the basalt core was covered with reddish orange sediment

APPENDIX B

GEOLOGIC DESCRIPTION OF WEIGHING LYSIMETER AND TEST TRENCH SAMPLES

TABLE B-1. PARTICLE SIZE ANALYSIS, EAST LYSIMETER SAMPLE
Depth--8.75-10.75 in

SIZE CLASS (mm)	METHOD OF ANALYSIS	WEIGHT IN CLASS *	WEIGHT % IN CLASS	CUMULATIVE WEIGHT %
>4.75	DRY SIEVE	0.80	1.19	1.19
4.75-0.425	DRY SIEVE	1.33	1.99	3.18
0.425-0.074	DRY SIEVE	14.90	22.24	25.42
0.074-0.062	PIPET		7.75	33.17
0.062-0.031	PIPET		24.60	57.77
0.031-0.016	PIPET		17.90	75.67
0.016-0.008	PIPET	FOR	7.46	83.13
0.008-0.004	PIPET	<0.074 mm	3.72	86.85
0.004-0.002	PIPET	TOTAL WT.=	4.47	91.32
0.002-0.001	PIPET	49.96	1.49	92.81
0.001-0.0005	PIPET		3.73	96.54
<0.0005	PIPET		3.35	99.89
TOTALS		66.99	99.89	99.89

* ALL WEIGHTS IN GRAMS

TABLE B-2. PARTICLE SIZE ANALYSIS, NEUTRON ACCESS HOLE-1
Depth--1.0 ft

SIZE CLASS (mm)	METHOD OF ANALYSIS	WEIGHT IN CLASS *	WEIGHT % IN CLASS	CUMULATIVE WEIGHT %
>4.00	DRY SIEVE	0.00	0.00	0.00
2.00-4.00	DRY SIEVE	0.00	0.00	0.00
1.00-2.00	DRY SIEVE	0.00	0.00	0.00
0.50-1.00	DRY SIEVE	0.04	0.18	0.18
0.25-0.50	DRY SIEVE	0.66	2.97	3.15
0.125-0.25	DRY SIEVE	1.44	6.47	9.62
0.062-0.125	DRY SIEVE	2.04	9.17	18.79
0.031-0.062	PIPET		28.15	46.94
0.016-0.031	PIPET		12.99	59.93
0.008-0.016	PIPET	FOR	6.50	66.43
0.004-0.008	PIPET	<0.062 mm	10.83	77.26
0.002-0.004	PIPET	TOTAL WEIGHT=	2.17	79.43
0.001-0.002	PIPET	18.07	4.33	83.76
0.0005-0.001	PIPET		2.17	85.92
<0.0005	PIPET		14.08	100.00
TOTALS		22.25	100.00	100.00

TABLE B-3. PARTICLE SIZE ANALYSIS, NEUTRON ACCESS HOLE-1
Depth--2.0 ft

SIZE CLASS (mm)	METHOD OF ANALYSIS	WEIGHT IN CLASS *	WEIGHT % IN CLASS	CUMULATIVE WEIGHT %
>4.00	DRY SIEVE	0.00	0.00	0.00
2.00-4.00	DRY SIEVE	0.00	0.00	0.00
1.00-2.00	DRY SIEVE	0.03	0.13	0.13
0.50-1.00	DRY SIEVE	0.04	0.17	0.30
0.25-0.50	DRY SIEVE	1.10	4.69	4.99
0.125-0.25	DRY SIEVE	2.71	11.56	16.55
0.062-0.125	DRY SIEVE	3.23	13.78	30.33
0.031-0.062	PIPET		17.91	48.25
0.016-0.031	PIPET		11.94	60.19
0.008-0.016	PIPET	FOR	11.94	72.13
0.004-0.008	PIPET	<0.062 mm	3.98	76.11
0.002-0.004	PIPET	TOTAL WEIGHT=	5.97	82.09
0.001-0.002	PIPET	16.33	1.99	84.08
0.0005-0.001	PIPET		1.99	86.07
<0.0005	PIPET		13.93	100.00
TOTALS		23.44	100.00	100.00

* ALL WEIGHTS IN GRAMS

TABLE B-4. PARTICLE SIZE ANALYSIS, NEUTRON ACCESS HOLE-1
Depth--3.0 ft

SIZE CLASS (mm)	METHOD OF ANALYSIS	WEIGHT IN CLASS *	WEIGHT % IN CLASS	CUMULATIVE WEIGHT %
>4.00	DRY SIEVE	0.00	0.00	0.00
2.00-4.00	DRY SIEVE	0.00	0.00	0.00
1.00-2.00	DRY SIEVE	0.01	0.03	0.03
0.50-1.00	DRY SIEVE	0.01	0.03	0.07
0.25-0.50	DRY SIEVE	1.42	4.93	5.00
0.125-0.25	DRY SIEVE	2.90	10.08	15.08
0.062-0.125	DRY SIEVE	3.46	12.02	27.10
0.031-0.062	PIPET		23.33	50.43
0.016-0.031	PIPET		15.55	65.98
0.008-0.016	PIPET	FOR	7.78	73.76
0.004-0.008	PIPET	<0.062 mm	5.83	79.59
0.002-0.004	PIPET	TOTAL WEIGHT=	5.83	85.42
0.001-0.002	PIPET	20.98	1.94	87.36
0.0005-0.001	PIPET		0.00	87.36
<0.0005	PIPET		12.64	100.00
TOTALS		28.78	100.00	100.00

TABLE B-5. PARTICLE SIZE ANALYSIS, NEUTRON ACCESS HOLE-1
Depth--4.0 ft

SIZE CLASS (mm)	METHOD OF ANALYSIS	WEIGHT IN CLASS *	WEIGHT % IN CLASS	CUMULATIVE WEIGHT %
>4.00	DRY SIEVE	0.00	0.00	0.00
2.00-4.00	DRY SIEVE	0.00	0.00	0.00
1.00-2.00	DRY SIEVE	0.00	0.00	0.00
0.50-1.00	DRY SIEVE	0.01	0.04	0.04
0.25-0.50	DRY SIEVE	0.32	1.13	1.16
0.125-0.25	DRY SIEVE	1.83	6.45	7.61
0.062-0.125	DRY SIEVE	3.71	13.08	20.69
0.031-0.062	PIPET		29.61	50.30
0.016-0.031	PIPET		10.57	60.87
0.008-0.016	PIPET	FOR	6.34	67.22
0.004-0.008	PIPET	<0.062 mm	4.23	71.45
0.002-0.004	PIPET	TOTAL WEIGHT=	4.23	75.68
0.001-0.002	PIPET	22.50	4.23	79.91
0.0005-0.001	PIPET		2.11	82.02
<0.0005	PIPET		17.98	100.00
TOTALS		28.37	100.00	100.00

* ALL WEIGHTS IN GRAMS

TABLE B-6. PARTICLE SIZE ANALYSIS, NEUTRON ACCESS HOLE-1
Depth--5.0 ft

SIZE CLASS (mm)	METHOD OF ANALYSIS	WEIGHT IN CLASS *	WEIGHT % IN CLASS	CUMULATIVE WEIGHT %
>4.00	DRY SIEVE	0.00	0.00	0.00
2.00-4.00	DRY SIEVE	0.00	0.00	0.00
1.00-2.00	DRY SIEVE	0.08	0.29	0.29
0.50-1.00	DRY SIEVE	0.07	0.26	0.55
0.25-0.50	DRY SIEVE	2.23	8.17	8.72
0.125-0.25	DRY SIEVE	3.83	14.04	22.76
0.062-0.125	DRY SIEVE	2.48	9.09	31.85
0.031-0.062	PIPET		7.27	39.12
0.016-0.031	PIPET		9.09	48.21
0.008-0.016	PIPET	FOR	9.09	57.30
0.004-0.008	PIPET	<0.062 mm	9.09	66.38
0.002-0.004	PIPET	TOTAL WEIGHT=	5.45	71.83
0.001-0.002	PIPET	18.59	5.45	77.28
0.0005-0.001	PIPET		-3.63	73.65
<0.0005	PIPET		26.35	100.00
TOTALS		27.28	100.00	100.00

TABLE B-7. PARTICLE SIZE ANALYSIS, NEUTRON ACCESS HOLE-1
Depth--6.0 ft

SIZE CLASS (mm)	METHOD OF ANALYSIS	WEIGHT IN CLASS *	WEIGHT % IN CLASS	CUMULATIVE WEIGHT %
>4.00	DRY SIEVE	0.00	0.00	0.00
2.00-4.00	DRY SIEVE	0.00	0.00	0.00
1.00-2.00	DRY SIEVE	0.00	0.00	0.00
0.50-1.00	DRY SIEVE	0.02	0.08	0.08
0.25-0.50	DRY SIEVE	2.93	12.15	12.23
0.125-0.25	DRY SIEVE	4.42	18.33	30.56
0.062-0.125	DRY SIEVE	2.30	9.54	40.09
0.031-0.062	PIPET		15.25	55.34
0.016-0.031	PIPET		2.18	57.52
0.008-0.016	PIPET	FOR	10.89	68.41
0.004-0.008	PIPET	<0.062 mm	6.54	74.95
0.002-0.004	PIPET	TOTAL WEIGHT=	4.36	79.30
0.001-0.002	PIPET	14.45	4.36	83.66
0.0005-0.001	PIPET		0.00	83.66
<0.0005	PIPET		16.34	100.00
TOTALS		24.12	100.00	100.00

* ALL WEIGHTS IN GRAMS

TABLE B-8. PARTICLE SIZE ANALYSIS, NEUTRON ACCESS HOLE-1
Depth--8.0 ft

SIZE CLASS (mm)	METHOD OF ANALYSIS	WEIGHT IN CLASS *	WEIGHT % IN CLASS	CUMULATIVE WEIGHT %
>4.00	DRY SIEVE	0.00	0.00	0.00
2.00-4.00	DRY SIEVE	0.00	0.00	0.00
1.00-2.00	DRY SIEVE	0.00	0.00	0.00
0.50-1.00	DRY SIEVE	0.00	0.00	0.00
0.25-0.50	DRY SIEVE	0.82	3.61	3.61
0.125-0.25	DRY SIEVE	2.40	10.57	14.18
0.062-0.125	DRY SIEVE	2.23	9.82	24.00
0.031-0.062	PIPET		24.32	48.32
0.016-0.031	PIPET		8.11	56.43
0.008-0.016	PIPET	FOR	8.11	64.53
0.004-0.008	PIPET	<0.062 mm	2.03	66.56
0.002-0.004	PIPET	TOTAL WEIGHT=	6.08	72.64
0.001-0.002	PIPET	17.26	2.03	74.67
0.0005-0.001	PIPET		6.08	80.75
<0.0005	PIPET		19.25	100.00
TOTALS		22.71	100.00	100.00

TABLE B-9. PARTICLE SIZE ANALYSIS, NEUTRON ACCESS HOLE-1
Depth--9.0 ft

SIZE CLASS (mm)	METHOD OF ANALYSIS	WEIGHT IN CLASS *	WEIGHT % IN CLASS	CUMULATIVE WEIGHT %
>4.00	DRY SIEVE	0.00	0.00	0.00
2.00-4.00	DRY SIEVE	0.00	0.00	0.00
1.00-2.00	DRY SIEVE	0.00	0.00	0.00
0.50-1.00	DRY SIEVE	0.04	0.17	0.17
0.25-0.50	DRY SIEVE	0.40	1.70	1.87
0.125-0.25	DRY SIEVE	1.58	6.70	8.56
0.062-0.125	DRY SIEVE	2.11	8.94	17.51
0.031-0.062	PIPET		22.00	39.51
0.016-0.031	PIPET		17.60	57.10
0.008-0.016	PIPET	FOR	4.40	61.50
0.004-0.008	PIPET	<0.062 mm	6.60	68.10
0.002-0.004	PIPET	TOTAL WEIGHT=	8.80	76.90
0.001-0.002	PIPET	19.46	2.20	79.10
0.0005-0.001	PIPET		6.60	85.70
<0.0005	PIPET		14.30	100.00
TOTALS		23.59	100.00	100.00

* ALL WEIGHTS IN GRAMS

TABLE B-10. PARTICLE SIZE ANALYSIS, NEUTRON ACCESS HOLE-1
Depth--10.0 ft

SIZE CLASS (mm)	METHOD OF ANALYSIS	WEIGHT IN CLASS *	WEIGHT % IN CLASS	CUMULATIVE WEIGHT %
>4.00	DRY SIEVE	0.00	0.00	0.00
2.00-4.00	DRY SIEVE	0.00	0.00	0.00
1.00-2.00	DRY SIEVE	0.00	0.00	0.00
0.50-1.00	DRY SIEVE	0.00	0.00	0.00
0.25-0.50	DRY SIEVE	0.85	2.68	2.68
0.125-0.25	DRY SIEVE	2.90	9.15	11.83
0.062-0.125	DRY SIEVE	3.00	9.46	21.29
0.031-0.062	PIPET		20.99	42.28
0.016-0.031	PIPET		8.40	50.68
0.008-0.016	PIPET	FOR	12.59	63.27
0.004-0.008	PIPET	<0.062 mm	2.10	65.37
0.002-0.004	PIPET	TOTAL WEIGHT=	8.40	73.76
0.001-0.002	PIPET	24.95	2.10	75.86
0.0005-0.001	PIPET		6.30	82.16
<0.0005	PIPET		17.84	100.00
TOTALS		31.70	100.00	100.00

* ALL WEIGHTS IN GRAMS

TABLE B-11. SEDIMENT SAMPLE CHARACTERISTICS, NEUTRON ACCESS HOLE-1, 1.0 FT DEPTH

SIZE CLASS (MM)	REACTION TO 10% HCl	COLOR *	ROUNDNESS **	SPHERICITY **	MINERALOGY ***
BULK SAMPLE	moderate	10YR 5/2, med. yellow-brown	0.3, sub-angular	0.7	quartz 50% plagioclase 25% basalt fragments 20% calcite 3% chert ? 2%
>4.00 2.00-4.00 1.00-2.00		***** NO FRACTIONS OF THESE SIZES *****			
0.50-1.00	moderate	10YR 7/2, pale orange-yellow brown	0.3, sub-angular	0.9	quartz plagioclase basalt fragments minor calcite
0.25-0.50	moderate	10YR 5/2, med. yellow brown	0.3, sub-angular	0.7	quartz plagioclase basalt fragments
0.125-0.25	strong	10YR 6/2, pale yellow brown	0.3, sub-angular	0.7	quartz plagioclase basalt fragments minor calcite
0.062-0.125	strong	10YR 7/2, pale orange-yellow brown	0.3, sub-angular	0.5	quartz plagioclase basalt fragments minor calcite
<0.062	strong	10YR 7/2, pale orange-yellow brown	0.3, sub-angular	0.5	quartz plagioclase ? basalt fragments ?

* FROM GEOLOGICAL SOCIETY OF AMERICA ROCK COLOR CHART
** FROM KRUMBEIN & SLOSS, 1963, STRATIGRAPHY AND SEDIMENTATION, W.H. FREEMAN & CO., 660 PP.
*** APPROXIMATE 2 GIVEN FOR BULK SAMPLE, MINERALOGY FOR INDIVIDUAL FRACTIONS LISTED IN DECREASING ABUNDANCE.

TABLE B-12. SEDIMENT SAMPLE CHARACTERISTICS, NEUTRON ACCESS HOLE-1, 2.0 FT DEPTH

SIZE CLASS (MM)	REACTION TO 10% HCl	COLOR *	ROUNDNESS **	SPHERICITY **	MINERALOGY ***
BULK SAMPLE	moderate	10YR 5/2, med. yellow-brown	0.5, sub-rounded	0.7	quartz 60% plagioclase 15% basalt fragments 20% calcite 3% chert 2%
>4.00 2.00-4.00		***** NO FRACTIONS OF THESE SIZES *****			
1.00-2.00	slight	10YR 3/2, dark greyish brown	0.5, sub-rounded	0.7	basalt fragments
0.50-1.00	moderate	10YR 6/2, pale yellow brown	0.5, sub-rounded	0.7	quartz plagioclase basalt fragments minor calcite
0.25-0.50	moderate	10YR 5/2, med. yellow brown	0.5, sub-rounded	0.5	basalt fragments quartz plagioclase calcite
0.125-0.25	moderate	10YR 5/2, med. yellow brown	0.5, sub-rounded	0.5	quartz basalt fragments plagioclase minor calcite
0.062-0.125	strong	10YR 5/2, med. yellow brown	0.3, sub-angular	0.5	quartz plagioclase basalt fragments minor calcite
<0.062	strong	10YR 6/2, pale yellow brown	0.3, sub-angular	0.5	quartz plagioclase ? basalt fragments ?

* FROM GEOLOGICAL SOCIETY OF AMERICA ROCK COLOR CHART
** FROM KRUMBEIN & SLOSS, 1963, STRATIGRAPHY AND SEDIMENTATION, W.H. FREEMAN & CO., 660 PP.
*** APPROXIMATE % GIVEN FOR BULK SAMPLE, MINERALOGY FOR INDIVIDUAL FRACTIONS LISTED IN DECREASING ABUNDANCE.

TABLE B-13. SEDIMENT SAMPLE CHARACTERISTICS, NEUTRON ACCESS HOLE-1, 3.0 FT DEPTH

SIZE CLASS (mm)	REACTION TO 10% HCl	COLOR *	ROUNDNESS **	SPHERICITY **	MINERALOGY ***
BULK SAMPLE	moderate	10YR 5/2, med. yellow-brown	0.5, sub-rounded	0.7	quartz 50% basalt fragments 25% plagioclase 20% quartzite pebbles 4% calcite 1%
>4.00 2.00-4.00		***** NO FRACTIONS OF THESE SIZES *****			
1.00-2.00	slight	10YR 2/2, dusky yellow brown	0.7, rounded	0.9	quartzite pebbles
0.50-1.00	slight	10YR 2/2, dusky yellow brown	0.3, sub-angular	0.5	quartzite pebbles basalt fragments
0.25-0.50	slight	10YR 5/2, med. yellow brown	0.3, sub-angular	0.5	quartz basalt fragments plagioclase
0.125-0.25	moderate	10YR 5/2, med. yellow brown	0.7, sub-rounded	0.7	quartz plagioclase basalt fragments calcite
0.062-0.125	moderate	10YR 6/2, pale yellow brown	0.7, sub-rounded	0.7	quartz plagioclase basalt fragments
<0.062	strong	10YR 7/2, pale orange-yellow brown	0.3, sub-angular	0.5	quartz minor basalt fragments

* FROM GEOLOGICAL SOCIETY OF AMERICA ROCK COLOR CHART
** FROM KRUMBEIN & SLOSS, 1963, STRATIGRAPHY AND SEDIMENTATION, W.H. FREEMAN & CO., 660 PP.
*** APPROXIMATE % GIVEN FOR BULK SAMPLE, MINERALOGY FOR INDIVIDUAL FRACTIONS LISTED IN DECREASING ABUNDANCE.

TABLE B-14. SEDIMENT SAMPLE CHARACTERISTICS, NEUTRON ACCESS HOLE-1, 4.0 FT DEPTH

SIZE CLASS (mm)	REACTION TO 10% HCl	COLOR *	ROUNDNESS **	SPHERICITY **	MINERALOGY ***
BULK SAMPLE	moderate	10YR 6/2, pale yellow-brown	0.3, sub-angular	0.5	quartz 60% plagioclase 25% basalt fragments 14% calcite 1%
>4.00 2.00-4.00 1.00-2.00		***** NO FRACTIONS OF THESE SIZES *****			
0.50-1.00	slight	10YR 6/2, pale yellow-brown	0.5, sub-rounded	0.7	basalt fragments quartz plagioclase
0.25-0.50	moderate	5YR 7/1, light yellow olive grey	0.3, sub-angular	0.5	quartz plagioclase basalt fragments minor calcite
0.125-0.25	moderate	10YR 5/2, med. yellow brown	0.3, sub-angular	0.7	quartz plagioclase basalt fragments calcite
0.062-0.125	moderate	10YR 6/2, pale yellow brown	0.3, sub-angular	0.5	quartz plagioclase basalt fragments
<0.062	moderate	10YR 7/2, pale orange-yellow brown	0.3, sub-angular	0.5	quartz plagioclase basalt fragments

* FROM GEOLOGICAL SOCIETY OF AMERICA ROCK COLOR CHART
** FROM KRUMBEIN & SLOSS, 1963, STRATIGRAPHY AND SEDIMENTATION, W.H. FREEMAN & CO., 660 PP.
*** APPROXIMATE % GIVEN FOR BULK SAMPLE, MINERALOGY FOR INDIVIDUAL FRACTIONS LISTED IN DECREASING ABUNDANCE.

TABLE B-15. SEDIMENT SAMPLE CHARACTERISTICS, NEUTRON ACCESS HOLE-1, 5.0 FT DEPTH

SIZE CLASS (MM)	REACTION TO 10% HCl	COLOR *	ROUNDNESS **	SPHERICITY **	MINERALOGY ***
BULK SAMPLE	slight	10YR 5/2, med. yellow-brown	0.5, sub-angular	0.7	quartz 70% basalt fragments 20% plagioclase 8% muscovite 2%
>4.00 2.00-4.00		***** NO FRACTIONS OF THESE SIZES *****			
1.00-2.00	slight	10YR 4/2, dark yellow brown	0.7, rounded	0.7	basalt fragments
0.50-1.00	slight	10YR 5/2, med. yellow-brown	0.7, rounded	0.7	basalt fragments quartzite ?
0.25-0.50	slight	10YR 5/2, med. yellow brown	0.3, sub-angular	0.5	basalt fragments quartz plagioclase
0.125-0.25	very slight	10YR 5/2, med. yellow brown	0.1, angular	0.7	quartz plagioclase basalt fragments
0.062-0.125	slight	10YR 6/2, pale yellow brown	0.3, sub-angular	0.7	quartz plagioclase basalt fragments muscovite
<0.062	slight	10YR 7/2, pale orange-yellow brown	0.1, angular	0.5	quartz plagioclase basalt fragments muscovite

* FROM GEOLOGICAL SOCIETY OF AMERICA ROCK COLOR CHART
** FROM KRUMBEIN & SLOSS, 1963, STRATIGRAPHY AND SEDIMENTATION, W.H. FREEMAN & CO., 660 PP.
*** APPROXIMATE % GIVEN FOR BULK SAMPLE, MINERALOGY FOR INDIVIDUAL FRACTIONS LISTED IN DECREASING ABUNDANCE.

TABLE B-16. SEDIMENT SAMPLE CHARACTERISTICS, NEUTRON ACCESS HOLE-1, 6.0 FT DEPTH

SIZE CLASS (mm)	REACTION TO 10% HCl	COLOR *	ROUNDNESS **	SPHERICITY **	MINERALOGY ***
BULK SAMPLE	slight	10YR 6/2, pale yellow-brown	0.3, sub-angular	0.5	quartz 65% plagioclase 30% basalt fragments 5%
>4.00 2.00-4.00 1.00-2.00		***** NO FRACTIONS OF THESE SIZES *****			
0.50-1.00	none	10YR 6/2, pale yellow-brown	0.1, angular	0.7	quartz plagioclase minor basalt fragments
0.25-0.50	slight	10YR 6/2, pale yellow-brown	0.3, sub-angular	0.5	quartz plagioclase minor basalt fragments
0.125-0.25	slight	10YR 5/2, med. yellow brown	0.3, sub-angular	0.5	quartz plagioclase basalt fragments
0.062-0.125	slight	10YR 7/2, pale orange-yellow brown	0.3, sub-angular	0.5	quartz plagioclase basalt fragments
<0.062	none	10YR 5/2, med. yellow brown	0.3, sub-angular	0.3	quartz plagioclase ? minor basalt fragments

* FROM GEOLOGICAL SOCIETY OF AMERICA ROCK COLOR CHART
** FROM KRUMBEIN & SLOSS, 1963, STRATIGRAPHY AND SEDIMENTATION, W.H. FREEMAN & CO., 660 PP.
*** APPROXIMATE % GIVEN FOR BULK SAMPLE, MINERALOGY FOR INDIVIDUAL FRACTIONS LISTED IN DECREASING ABUNDANCE.

TABLE B-17. SEDIMENT SAMPLE CHARACTERISTICS, NEUTRON ACCESS HOLE-1, 8.0 FT DEPTH

SIZE CLASS (MM)	REACTION TO 10% HCl	COLOR *	ROUNDNESS **	SPHERICITY **	MINERALOGY ***
BULK SAMPLE	none	10YR 6/2, pale yellow brown	0.3, sub-angular	0.5	quartz 70% plagioclase 15% basalt fragments 14% muscovite 1%
>4.00 2.00-4.00 1.00-2.00 0.50-1.00	***** NO FRACTIONS OF THESE SIZES *****				
0.25-0.50	none	10YR 6/2, pale yellow brown	0.5, sub-rounded	0.7	quartz plagioclase basalt fragments
0.125-0.25	none	10YR 6/2, pale yellow brown	0.3, sub-angular	0.5	quartz plagioclase basalt fragments minor muscovite
0.062-0.125	none	10YR 6/2, pale yellow brown	0.3, sub-angular	0.5	quartz plagioclase basalt fragments minor muscovite
<0.062	none	10YR 7/2, pale orange-yellow brown	0.3, sub-angular	0.5	quartz plagioclase basalt fragments

* FROM GEOLOGICAL SOCIETY OF AMERICA ROCK COLOR CHART
** FROM KRUMBEIN & SLOSS, 1963, STRATIGRAPHY AND SEDIMENTATION, W.H. FREEMAN & CO., 660 PP.
*** APPROXIMATE % GIVEN FOR BULK SAMPLE, MINERALOGY FOR INDIVIDUAL FRACTIONS LISTED IN DECREASING ABUNDANCE.

TABLE B-18. SEDIMENT SAMPLE CHARACTERISTICS, NEUTRON ACCESS HOLE Hole-1, 9.0 FT DEPTH

SIZE CLASS (mm)	REACTION TO 10% HCl	COLOR *	ROUNDNESS **	SPHERICITY **	MINERALOGY ***
BULK SAMPLE	slight	10YR 5/2, med. yellow brown	0.3, sub-angular	0.5	quartz 55% basalt fragments 45%
>4.00 2.00-4.00 1.00-2.00		***** NO FRACTIONS OF THESE SIZES *****			
0.50-1.00	none	10YR 5/2, med. yellow brown	0.3, sub-angular	0.5	basalt fragments quartz
0.25-0.50	slight	10YR 6/2, pale yellow brown	0.3, sub-angular	0.5	basalt fragments quartz
0.125-0.25	slight	10YR 5/2, med. yellow brown	0.3, sub-angular	0.5	basalt fragments quartz
0.062-0.125	slight	10YR 6/2, pale yellow brown	0.3, sub-angular	0.5	quartz basalt fragments
<0.062	none	10YR 5/2, med. yellow brown	0.1, angular	0.3	quartz minor basalt fragments

* FROM GEOLOGICAL SOCIETY OF AMERICA ROCK COLOR CHART
** FROM KRUMBEIN & SLOSS, 1963, STRATIGRAPHY AND SEDIMENTATION, W.H. FREEMAN & CO., 660 PP.
*** APPROXIMATE % GIVEN FOR BULK SAMPLE, MINERALOGY FOR INDIVIDUAL FRACTIONS LISTED IN DECREASING ABUNDANCE.

TABLE B-19. SEDIMENT SAMPLE CHARACTERISTICS, NEUTRON ACCESS HOLE-1, 10.0 FT DEPTH

SIZE CLASS (mm)	REACTION TO 10% HCl	COLOR *	ROUNDNESS **	SPHERICITY **	MINERALOGY ***
BULK SAMPLE	none	10YR 6/2, pale yellow brown	0.3, sub-angular	0.5	quartz 60% plagioclase 25% basalt fragments 14% muscovite 1%
>4.00 2.00-4.00 1.00-2.00 0.50-1.00		***** NO FRACTIONS OF THESE SIZES *****			
0.25-0.50	none	10YR 6/2, pale yellow brown	0.5, sub-rounded	0.7	basalt fragments quartz
0.125-0.25	none	10YR 6/2, pale yellow brown	0.7, rounded	0.7	quartz plagioclase basalt fragments
0.062-0.125	none	10YR 6/2, pale yellow brown	0.3, sub-angular	0.7	quartz plagioclase basalt fragments minor muscovite
<0.062	none	10YR 7/2, pale orange-yellow brown	0.3, sub-angular	0.5	quartz plagioclase minor basalt fragments

* FROM GEOLOGICAL SOCIETY OF AMERICA ROCK COLOR CHART
** FROM KRUMBEIN & SLOSS, 1963, STRATIGRAPHY AND SEDIMENTATION, W.H. FREEMAN & CO., 660 PP.
*** APPROXIMATE % GIVEN FOR BULK SAMPLE, MINERALOGY FOR INDIVIDUAL FRACTIONS LISTED IN DECREASING ABUNDANCE.

TABLE B-20. NEUTRON ACCESS HOLE-2, SOIL MOISTURE CHARACTERISTIC CURVE DATA

Sample depth (feet)	Soil bulk density (g/cc)	Volume % natural moisture	Volume percent moisture at selected tensions (bars)						
			0.3	0.5	0.7	1.0	5.0	10.0	15.0
2	1.51	28.36	26.80	26.31	24.96	23.85	15.38	12.97	11.99
4	1.20	11.70	23.61	22.87	20.87	19.60	14.24	12.73	12.11
6	1.52	16.90	26.55	26.47	25.33	24.43	19.76	18.04	17.55
8	1.63	19.60	28.15	28.40	27.91	27.54	24.51	23.00	22.50
10	1.64	22.18	29.99	30.11	29.50	29.05	26.27	24.22	23.77
12	1.46	21.81	29.38	29.38	28.76	28.15	25.25	23.77	23.24
14	1.65	23.53	29.71	29.71	29.13	28.68	26.35	25.08	24.55
16	1.61	21.85	32.20	32.41	32.08	31.46	26.19	23.85	23.12
18	1.33	11.42	27.29	26.92	23.69	21.32	14.69	13.26	12.48

TABLE B-21. NEUTRON ACCESS HOLE-2A, SOIL MOISTURE CHARACTERISTIC CURVE DATA

Sample depth (feet)	Soil bulk density (g/cc)	Volume % natural moisture	Volume percent moisture at selected tensions (bars)						
			0.3	0.5	0.7	1.0	5.0	10.0	15.0
2	1.59	25.04	29.62	28.89	26.68	25.33	16.69	14.32	13.09
4	1.31	12.44	26.35	23.81	21.07	19.97	15.26	14.24	13.05
6	1.76	18.78	32.90	32.16	31.10	29.87	24.67	23.00	21.44
10	1.71	22.71	33.76	33.35	32.65	32.20	28.56	26.92	26.06
12	1.75	24.55	34.90	34.45	33.80	33.31	30.11	28.72	27.66
14	1.70	23.81	32.16	31.71	31.10	30.56	28.11	27.54	26.55
16	1.84	25.70	37.36	37.07	37.07	36.58	32.08	30.03	28.07

TABLE B-22. NEUTRON ACCESS HOLE-3A, SOIL MOISTURE CHARACTERISTIC CURVE DATA

Sample depth (feet)	Soil bulk density (g/cc)	Volume % natural moisture	Volume percent moisture at selected tensions (bars)						
			0.3	0.5	0.7	1.0	5.0	10.0	15.0
2	1.57	31.22	32.32	31.51	30.65	29.42	20.66	16.49	14.48
4	1.37	32.00	37.56	35.54	33.61	31.92	24.04	20.23	18.36
6	1.54	27.50	31.96	30.92	30.25	29.66	26.74	23.82	21.90

TABLE B-23. NEUTRON ACCESS HOLE-6, SOIL MOISTURE CHARACTERISTIC CURVE DATA

Sample depth (feet)	Soil bulk density (g/cc)	Volume % natural moisture	Volume percent moisture at selected tensions (bars)						
			0.3	0.5	0.7	1.0	5.0	10.0	15.0
2	1.52	28.93	33.55	32.04	30.77	29.62	23.00	20.05	18.00
4	1.59	14.59	21.60	20.05	18.94	17.96	15.79	12.56	10.84
6	1.38	19.19	26.39	24.96	23.81	22.75	19.03	17.14	15.55
8	1.28	12.15	22.55	22.26	20.29	19.27	15.55	14.24	13.05
18	1.53	27.91	41.08	40.51	39.53	38.46	30.81	27.58	25.08

TABLE B-24. NEUTRON ACCESS HOLE-9, SOIL MOISTURE CHARACTERISTIC CURVE DATA

Sample depth (feet)	Soil bulk density (g/cc)	Volume % natural moisture	Volume percent moisture at selected tensions (bars)						
			0.3	0.5	0.7	1.0	5.0	10.0	15.0
1	1.25	12.79	25.68	23.49	21.97	20.27	14.63	12.75	10.80
2	1.32	12.10	28.58	24.86	22.71	20.56	16.22	13.03	11.33
3	1.61	15.17	32.53	28.38	25.92	23.79	17.27	14.91	13.42
4	1.29	19.86	28.89	25.53	23.90	22.05	18.49	17.33	15.16
5	1.64	20.60	33.16	31.40	30.30	29.34	25.96	24.73	22.79
6	1.64	19.81	31.85	30.36	29.62	28.72	26.31	24.65	22.24
7	1.56	19.24	32.90	30.79	29.62	28.64	26.80	25.49	23.47
8	1.60	21.42	34.41	33.33	32.82	31.98	30.32	29.46	27.62
9	1.55	19.42	29.32	28.58	28.21	27.86	26.62	26.13	23.67
10	1.60	15.99	31.73	30.18	29.34	28.36	24.67	23.24	20.15
11	1.52	25.09	38.24	37.50	37.05	36.52	32.86	31.30	28.48
12	1.61	23.22	35.66	35.02	34.64	34.21	32.02	30.38	28.93
13	1.63	20.55	35.00	34.27	33.65	33.02	29.58	28.27	26.74
14	1.72	15.92	32.61	31.53	30.65	29.44	24.53	23.00	21.34
15	1.79	17.60	34.10	33.47	32.98	32.34	29.87	28.76	25.55
16	1.66	16.12	34.39	33.24	32.16	30.65	25.20	24.28	21.13
17	1.59	15.08	35.84	32.75	30.30	27.80	21.60	20.32	17.92
18	1.70	14.30	38.71	33.20	33.20	29.85	22.79	21.58	18.21

APPENDIX C
RESULTS OF SOIL GAS SAMPLE ANALYSES

APPENDIX C
RESULTS OF SOIL GAS SAMPLE ANALYSES

Figure C-1 is a map of the SDA showing the grid that was defined to determine the sampling points for the soil gas survey. The locations of the sampling points are also shown on Figure C-1. Table C-1 lists the results of the anlayses of samples taken from the sampling points shown on Figure C-1.

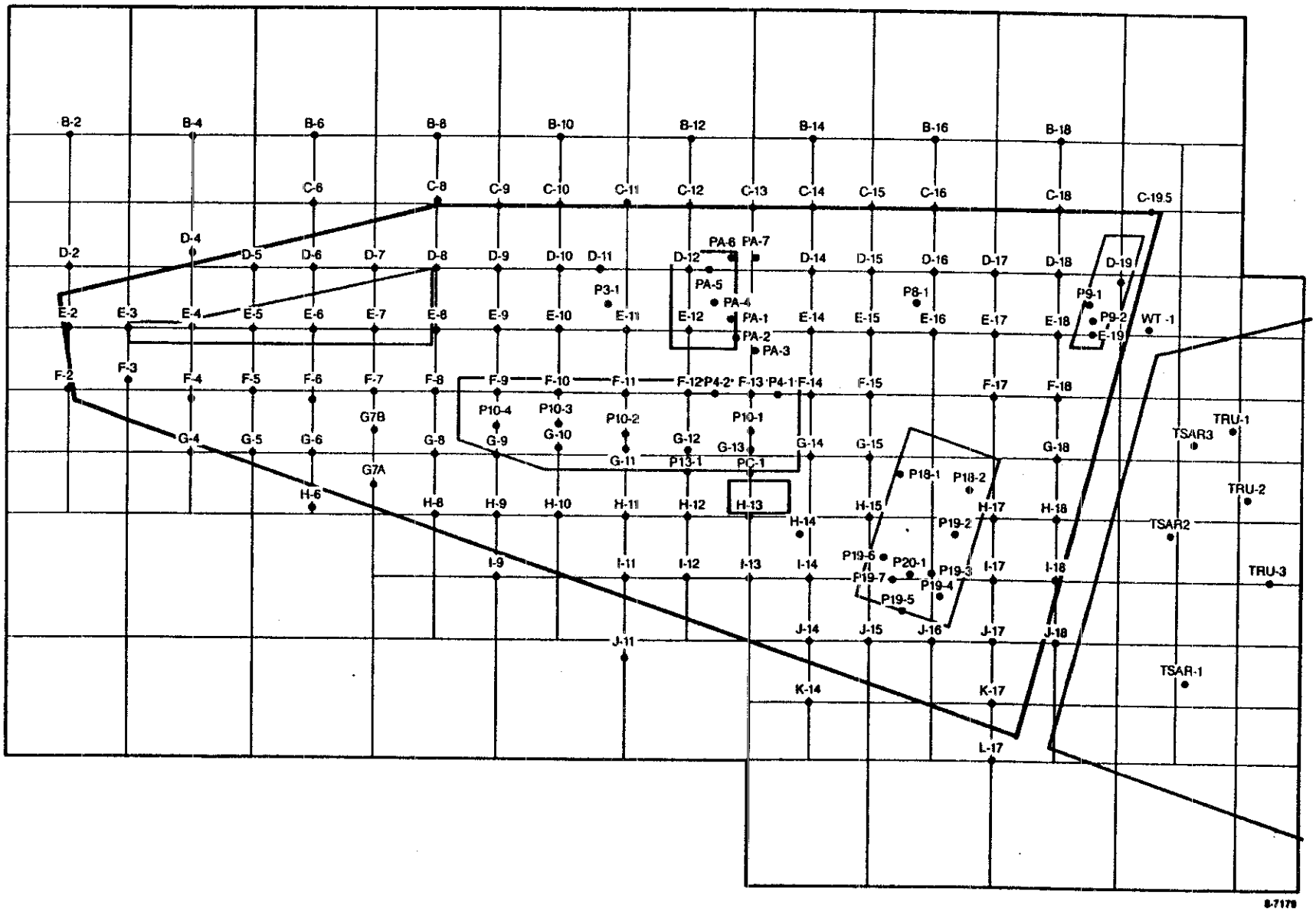

Figure C-1. Locations of sampling points for the soil gas survey.

TABLE C-1. RESULTS OF SOIL GAS ANALYSES (μg/L)

Grid	East	North	Sample Depth (in.)	1,1,1-Trichloroethane	Carbon Tetrachloride	Tri-chloroethylene	Tetra-chloroethylene
** Wells							
77-1-2	2175	2900	171 ft	P	2.3	0.04	0.1
77-1-3	2175	2900	153 ft	5.0	20.0	5	2.4
77-1-4	2175	2900	112 ft	5.0	20.0	4	1
77-1-5	2175	2900	104 ft	0.8	4.0	0.9	0.4
77-1-6	2175	2900	66 ft	7.0	4.0	8	2
78-4-1	2175	2975	335 ft	<0.01	0.6	0.04	0.04
78-4-2	2175	2975	253 ft	<0.01	2.0	0.03	0.03
78-4-3	2175	2975	227 ft	<0.01	0.1	<0.01	<0.01
78-4-4	2175	2975	118 ft	<0.01	26.0	6	2
78-4-5	2175	2975	78 ft	<0.01	36.0	9	2
** B							
B-02	200	2400	24	<0.01	0.3	0.02	0.07
B-04	600	2400	2	<0.01	0.4	0.03	0.04
B-06	1000	2400	28	<0.01	0.05	<0.01	0.01
B-08	1400	2400	30	<0.01	1.0	0.04	0.05
B-10	1800	2400	29	<0.01	0.4	<0.01	0.03
B-12	2200	2400	21	<0.01	0.7	P	P
B-14	2600	2400	30	<0.01	0.8	0.1	<0.01
B-16	3000	2400	19	<0.01	0.2	0.04	0.02
B-18	3400	2400	18	<0.01	0.2	0.05	0.03
** C							
C-06	1000	2200	17	<0.01	0.4	<0.01	0.04
C-08	1400	2225	28	<0.01	3.8	0.2	0.4
C-09	1600	2200	18	<0.01	2.0	<0.01	0.07
C-10	1800	2225	20	<0.01	5.0	1	0.8
C-11	2000	2200	28	<0.01	5.6	0.4	0.04
C-12	2200	2200	20	<0.01	3.1	0.8	0.2
C-13	2400	2200	31	<0.01	1.0	<0.01	<0.01
C-14	2600	2200	31	P	19.0	3	1
C-15	2800	2200	18	<0.01	2.0	P	0.4
C-16	3000	2200	15	P	0.9	0.05	0.05
C-18	3400	2200	30	P	1.5	0.06	0.1
C-19.5	3700	2200	30	0.1	0.5	0.02	0.1
** D							
D-02	200	2000	29	<0.01	P	<0.01	<0.01
D-04	600	2045	20	<0.01	0.2	0.01	0.04
D-05	800	2000	12	P	0.1	<0.01	0.04
D-06	1000	2000	12	P	0.1	0.04	0.2

TABLE C-1. (continued)

Grid	East	North	Sample Depth (in.)	1,1,1-Trichloroethane	Carbon Tetrachloride	Tri-chloroethylene	Tetra-chloroethylene
D-07	1200	2000	12	<0.01	0.04	<0.01	0.02
D-08	1400	2000	12	1.0	<0.01	<0.01	<0.01
D-09	1600	2000	17	P	0.1	<0.01	0.5
D-10	1800	2000	30	P	0.4	0.1	0.1
D-11	1925	2000	30	1.2	0.4	0.2	0.8
D-12	2200	2000	25	<0.01	1.0	240	0.01
D-14	2600	2000	32	P	50.0	28	6
D-15	2800	2000	30	<0.01	2	<0.01	<0.01
D-16	3000	2000	30	<0.01	0.5	<0.01	<0.01
D-17	3200	2000	30	<0.01	0.3	<0.01	<0.01
D-18	3400	2000	30	<0.01	1	<0.01	0.03
D-19	3600	1975	30	P	4.7	1.1	4.0
** E							
E-02	200	1800	12	<0.01	0.02	<0.01	<0.01
E-03	400	1800	12	1.3	<0.01	0.6	1
E-04	600	1800	12	2	<0.01	4	0.03
E-05	800	1800	12	1.2	<0.01	0.01	0.2
E-06	1000	1800	12	<0.01	4.8	0.02	1.4
E-06	1000	1800	12	15	12	12	2.4
E-07	1200	1800	8	1	1	1	1.6
E-08	1400	1800	12	0.9	1.2	4	0.6
E-09	1600	1800	30	8	3	2	2
E-10	1800	1800	30	1	2	P	P
E-11	2000	1800	30	0.4	0.3	1	2
E-12	2200	1800	12	<0.01	<0.01	<0.01	<0.01
E-14	2600	1800	30	8	P	<0.01	4.7
E-15	2800	1600	28	310	<0.01	4	7
E-15	2800	1800	28	48	5	0.8	5.2
E-15	2800	1800	28	170	P	1.6	6
E-15	2800	1800	28	120	<0.01	0.08	3
E-15	2800	1800	28	280	P	3.2	7
E-16	3000	1800	30	<0.01	0.2	<0.01	P
E-17	3200	1800	30	<0.01	2	<0.01	<0.01
E-18	3400	1800	35	10	12	9.4	2.1
E-19	3525	1800	30	<0.01	1000	150	40
E-19	3525	1800	30	P	1230	200	34
E-19	3525	1800	30	P	1400	100	25
E-19	3525	1800	30	P	900	690	30
E-19	3525	1800	30	P	640	80	20
E-19	3525	1800	30	P	1200	100	21
E-19.5	3700	1825	32	P	0.3	<0.01	<0.01

TABLE C-1. (continued)

Grid	East	North	Sample Depth (in.)	1,1,1-Trichloroethane	Carbon Tetrachloride	Tri-chloroethylene	Tetra-chloroethylene
** F							
F-02	200	1600	30	<0.01	0.1	<0.01	<0.01
F-03	400	1625	12	<0.01	0.2	<0.01	0.7
F-04	600	1575	12	<0.01	<0.01	<0.01	<0.01
F-05	800	1600	12	<0.01	0.02	<0.01	0.01
F-06	1000	1570	12	<0.01	0.07	<0.01	1
F-07	1200	1600	12	<0.01	0.1	<0.01	0.7
F-08	1400	1600	11	P	0.03	<0.01	<0.01
F-09	1600	1600	30	8	2	2	2
F-10	1800	1600	31	17	5	2	2
F-11	2000	1600	30	13	1	1	3
F-12	2200	1600	30	4	10	1	7
F-13	2400	1600	30	P	29	4	2
F-14	2600	1600	30	<0.01	0.09	0.05	0.1
F-15	2800	1600	26	P	13	3	2
F-17	3200	1600	30	0.02	P	P	P
F-18	3400	1600	20	2	<0.01	1 0.5	
** G							
G-04	600	1400	30	<0.01	0.05	<0.01	<0.01
G-05	800	1400	12	0.01	0.02	<0.01	<0.01
G-06	1000	1400	12	0.03	0.04	<0.01	<0.01
G-07A	1200	1300	12	<0.01	0.2	<0.01	<0.01
G-07B	1200	1475	12	<0.01	0.04	<0.01	<0.01
G-08	1400	1400	12	<0.01	0.4	0.2	0.04
G-09	1600	1400	26	P	0.2	P	P
G-10	1800	1425	30	<0.01	23	7	12
G-11	2000	1425	32	<0.01	50	20	27
G-12	2200	1420	30	2.5	2.4	1.5	0.4
G-13	2400	1425	30	<0.01	2	3.3	0.5
G-14	2600	1400	32	<0.01	2	0.2	0.2
G-15	2800	1400	32	<0.01	<0.01	<0.01	<0.01
G-18	3400	1400	20	0.04	0.05	0.02	0.2
** H							
H-06	1000	1225	31	<0.01	0.5	<0.01	0.02
H-08	1400	1200	12	<0.01	<0.01	<0.01	<0.01
H-09	1600	1200	30	0.2	2.4	0.2	0.08
H-10	1800	1200	25	<0.01	2	0.1	0.03
H-11	2000	1200	30	<0.01	0.3	0.01	0.02
H-12	2200	1200	30	<0.01	1	0.8	1
H-13	2400	1200	30	<0.01	0.2	<0.01	<0.01
H-14	2575	1150	30	<0.01	<0.01	<0.01	<0.01

TABLE C-1. (continued)

Grid	East	North	Sample Depth (in.)	1,1,1-Trichloroethane	Carbon Tetrachloride	Tri-chloroethylene	Tetra-chloroethylene
H-15	2800	1200	30	<0.01	0.01	<0.01	0.01
H-17	3200	1200	30	4	<0.01	0.01	0.2
H-18	3400	1200	30	4	<0.01	<0.01	<0.08
** I							
I-09	1600	1000	30	<0.01	4	0.2	0.08
I-11	2000	1000	30	<0.01	0.9	<0.01	P
I-12	2200	1000	25	0.7	0.3	<0.01	P
I-13	2400	1000	30	<0.01	0.4	<0.01	0.01
I-14	2600	1000	30	<0.01	1.1	P	P
I-14	2600	1000	30	<0.01	<0.01	<0.01	<0.01
I-17	3200	1000	31	3	<0.01	<0.01	0.08
I-18	3400	1000	30	<0.01	0.3	0.02	0.04
** J							
J-11	2000	750	20	<0.01	0.03	<0.01	<0.01
J-14	2600	800	29	3.8	<0.01	<0.01	<0.01
J-15	2800	800	27	180	P	<0.01	P
J-16	3000	800	26	0.01	0.01	0.01	<0.01
J-17	3200	800	30	0.2	0.3	0.06	0.04
J-18	3400	800	30	<0.01	<0.01	<0.01	<0.01
** K							
K-14	2600	600	21	<0.01	0.4	0.03	0.02
K-17	3200	600	32	<0.01	0.06	<0.01	0.01
** L							
L-17	3200	400	30	<0.01	0.02	<0.01	<0.01
** Neutron Access Tubes							
NAT-02	3360	770	13 ft	1	0.3	0.07	0.07
NAT-03	3470	1210	10 ft	5	4	1	0.4
NAT-04	3580	1650	10 ft	<0.01	5	1	0.4
NAT-05	3675	2120	9 ft	<0.01	4	0.4	0.3
NAT-07	3455	1675	10 ft	<0.01	22	4	1
NAT-19	1740	2090	15 ft	P	24	1	2
NAT-22	1265	1900	8 ft	P	19	0.5	<0.01
NAT-26	500	1920	11 ft	P	22	2	3
NAT-27	260	1775	12 ft	<0.01	8	<0.01	1
NAT-W02	3310	2070	10 ft	<0.01	P	<0.01	<0.01

TABLE C-1. (continued)

Grid	East	North	Sample Depth (in.)	1,1,1-Trichloroethane	Carbon Tetrachloride	Tri-chloroethylene	Tetra-chloroethylene
** Pit Samples							
P03-1	1950	1900	30	50	10	9	5
P04-1	2500	1600	31	<0.01	4	1	1
P04-2	2300	1600	31	<0.01	2300	9	10
P08-1	2950	1900	30	P	<0.01	<0.01	<0.01
P09-1	3500	1900	31	<0.01	0.3	<0.01	<0.01
P09-2	3510	1850	31	<0.01	1000	8	13
P10-1	2400	1485	26	0.4	3.8	P	1.8
P10-2	2000	1475	30	<0.01	160	21	19
P10-3	1800	1500	30	<0.01	100	30	9
P10-3	1800	1500	30	<0.01	470	4	10
P10-4	1600	1500	30	<0.01	28	22	2
P13-1	2200	1350	26	<0.01	0.08	<0.01	<0.01
P18-1	2900	1350	28	<0.01	<0.01	<0.01	<0.01
P18-2	3125	1300	25	<0.01	<0.01	<0.01	<0.01
P19-2	3075	1150	10 ft	<0.01	0.05	<0.01	0.01
P19-3	3000	1025	10 ft	<0.01	<0.01	<0.01	<0.01
P19-4	3025	950	10 ft	P	0.02	<0.01	<0.01
P19-5	2900	900	10 ft	<0.01	0.06	0.01	0.02
P19-6	2850	1075	10 ft	<0.01	0.2	0.03	0.04
P19-7	2875	1000	10 ft	P	P	<0.01	<0.01
P20-1	2925	1025	10 ft	2	1	0.6	2
PA-1	2350	1850	30	<0.01	8	3.2	9.7
PA-2	2350	1750	30	<0.01	3.8	1.3	5.7
PA-3	2425	1750	29	<0.01	3.0	1	2.2
PA-4	2300	1900	29	<0.01	1.9	0.4	2.5
PA-5	2275	2000	25	<0.01	3.5	0.6	4
PA-6	2350	2050	28	<0.01	12	4.6	13
PA-7	2425	2050	30	<0.01	5.4	4.6	7.8
PC-1	2400	1350	25	<0.01	2	<0.01	<0.01
** Transuranic Storage Area							
TRU-1	3970	1475	20 ft	20	32	36	<0.01
TRU-2	4044	1349	20 ft	0.4	3	0.6	<0.01
TRU-3	4121	980	20 ft	24	22	6	2
TSAR1	3875	692	13	<0.01	0.3	<0.01	<0.01
TSAR2	3763	1211	22	<0.01	0.1	<0.01	<0.01
TSAR3	3802	1462	27	<0.01	0.5	<0.01	<0.01
** Well							
WWW1-1	-1600	1800	15 ft	<0.01	8.8	1.6	0.4
WWW1-2	-1600	1800	48 ft	<0.01	8	1.2	0.4
WWW1-3	-1600	1800	74 ft	<0.01	30	3.8	0.9

TABLE C-1. (continued)

Grid	East	North	Sample Depth (in.)	1,1,1-Trichloroethane	Carbon Tetrachloride	Tri-chloroethylene	Tetra-chloroethylene
WWW1-4	-1600	1800	112 ft	P	6.6	1	0.4
WWW1-5	-1600	1800	135 ft	P	28	4	1
WWW1-6	-1600	1800	180 ft	P	3	2	0.4
WWW1-7	-1600	1800	240 ft	<0.01	0.9	P	P
** Field Blanks[a]							
XP-01	0	0	0	<0.01	<0.01	<0.01	<0.01
XP-02	0	0	0	<0.01	P	<0.01	<0.01
XP-03	0	0	0	<0.01	<0.01	<0.01	<0.01
XP-04	0	0	0	<0.01	P	<0.01	<0.01
XP-05	0	0	0	P	P	P	P
XP-06	0	0	0	<0.01	P	<0.01	<0.01
XP-07	0	0	0	<0.01	0.01	<0.01	<0.01
XP-08	0	0	0	P	P	<0.01	<0.01
XP-09	0	0	0	P	P	<0.01	<0.01
XP-10	0	0	0	P	P	<0.01	<0.01
XP-11	0	0	0	P	P	<0.01	<0.01
XP-12	0	0	0	P	P	<0.01	<0.01
XP-13	0	0	0	P	P	P	P
XP-14	0	0	0	P	P	<0.01	<0.01
XP-15	0	0	0	P	P	<0.01	<0.01
XP-16	0	0	0	<0.01	<0.01	<0.01	<0.01
XP-17	0	0	0	<0.01	P	<0.01	<0.01
XP-18	0	0	0	<0.01	P	<0.01	<0.01
XP-19	0	0	0	<0.01	0.01	<0.01	<0.01
XP-19	0	0	0	<0.01	<0.01	<0.01	<0.01
XP-20	0	0	0	<0.01	0.05	0.05	0.05
XP-21	0	0	0	<0.01	P	<0.01	<0.01
XP-22	0	0	0	<0.01	<0.01	<0.01	<0.01
XP-23	0	0	0	<0.01	P	<0.01	<0.01
** Outside the Grid							
Z-01	2300	2994	32	<0.01	0.06	<0.01	<0.01
Z-02	2833	3000	13	<0.01	0.2	0.01	<0.01
Z-03	3015	3558	17	<0.01	0.08	<0.01	<0.01
Z-04	3222	4138	31	<0.01	0.2	0.01	<0.01
Z-05	3170	4585	23	<0.01	<0.01	<0.01	<0.01
Z-06	4504	1889	30	<0.01	2	0.03	0.1
Z-07	5095	2359	30	<0.01	0.2	0.01	0.2
Z-08	5860	2806	27	<0.01	0.2	0.01	0.01
Z-09	6497	3246	27	<0.01	0.02	<0.01	<0.01
Z-10	-573	1627	21	P	P	<0.01	<0.01
Z-11	-1355	2013	13	P	P	<0.01	<0.01
Z-12	-1881	2329	16	<0.01	0.03	<0.01	<0.01

TABLE C-1. (continued)

Grid	East	North	Sample Depth (in.)	1,1,1-Trichloroethane	Carbon Tetrachloride	Tri-chloroethylene	Tetra-chloroethylene
Z-13	1528	412	30	<0.01	0.9	0.05	0.07
Z-14	1186	-33	30	<0.01	0.9	0.05	0.08
Z-15	842	-334	18	P	0.2	<0.01	<0.01
Z-16	-873	-2980	28	P	0.2	<0.01	<0.01

Note: P indicates that the constituent was detected in the sample at an unquantified level.

a. Field blanks collected by pulling ambient air through a probe and collecting a sample of the air in a syringe.

APPENDIX D
STRUCTURE FOR DATABASE

Structure for database: C:instrmts.dbf
Number of data records: 310
Date of last update : 01/14/88

Field	Field Name	Type	Width	Dec
1	INST	Character	5	
2	WELL	Character	3	
3	DEPTH	Numeric	7	2
4	DATE_INST	Date	8	
5	X0	Numeric	10	5
6	X1	Numeric	10	5
7	X2	Numeric	10	5
8	X3	Numeric	10	5
9	X4	Numeric	10	5
10	MATERIALS	Character	64	
11	NOTES	Character	72	
** Total **			210	

Structure for database: C:wells.dbf
Number of data records: 35
Date of last update : 11/12/87

Field	Field Name	Type	Width	Dec
1	WELL	Character	3	
2	DRILLED	Date	8	
3	TOT_DEPTH	Numeric	6	2
4	X_COORD	Numeric	10	2
5	Y_COORD	Numeric	10	2
6	ELEVATION	Numeric	8	2
7	INST_LIST	Character	180	
8	SURFCAS_L	Numeric	10	2
9	SURFCAS_D	Numeric	8	2
10	ABANDON	Date	8	
11	TREATMENT	Character	180	
** Total **			432	

Structure for database: C:psychrom.dbf
Number of data records: 9253
Date of last update : 11/24/87

Field	Field Name	Type	Width	Dec
1	WELL	Character	3	
2	INST	Character	5	
3	DATE	Date	8	
4	TIME	Character	5	
5	TEMP	Numeric	5	2
6	OFFSET	Numeric	5	2
7	MVOLTS	Numeric	5	2
8	MATPOT	Numeric	8	3
** Total **			45	

Structure for database: C:labchem.dbf
Number of data records: 51
Date of last update : 12/14/87

Field	Field Name	Type	Width	Dec
1	INST	Character	5	
2	DATE	Date	8	
3	TIME	Character	5	
4	NA	Numeric	8	2
5	K	Numeric	8	2
6	CA	Numeric	8	2
7	MG	Numeric	8	2
8	FE	Numeric	8	2
9	AL	Numeric	8	2
10	SIO2	Numeric	8	2
11	B	Numeric	8	2
12	LI	Numeric	8	2
13	SR	Numeric	8	2
14	ZN	Numeric	8	2
15	HCO3	Numeric	8	2
16	CL	Numeric	8	2
17	F	Numeric	8	2
18	SO4	Numeric	8	2
19	BR	Numeric	8	2
20	NO3	Numeric	8	2
21	PO4	Numeric	8	2
22	TDS	Numeric	8	2
23	OTHER	Character	60	
** Total **			231	

Structure for database: C:heatbloc.dbf
Number of data records: 1121
Date of last update : 12/15/87

Field	Field Name	Type	Width	Dec
1	WELL	Character	3	
2	INST	Character	5	
3	DATE	Date	8	
4	TIME	Character	5	
5	MEAS	Numeric	8	2
6	MATPOT	Numeric	8	2
** Total **			38	

Structure for database: C:tension.dbf
Number of data records: 394
Date of last update : 01/14/88

Field	Field Name	Type	Width	Dec
1	WELL	Character	3	
2	INST	Character	5	
3	DATE	Date	8	
4	TIME	Character	5	
5	MEAS	Numeric	4	
6	MATPOT	Numeric	8	2
7	VOL	Numeric	4	
** Total **			38	

Structure for database: C:probe.dbf
Number of data records: 553
Date of last update : 12/23/87

Field	Field Name	Type	Width	Dec
1	WELL	Character	3	
2	STD	Numeric	5	
3	CHISQ	Numeric	4	2
4	P	Numeric	4	
5	DEPTH	Numeric	8	2
6	DATE	Date	8	
7	TIME	Character	5	
8	MEAS	Numeric	8	2
9	MATPOT	Numeric	8	2
** Total **			54	

Structure for database: C:fldchem.dbf
Number of data records: 84
Date of last update : 11/04/87

Field	Field Name	Type	Width	Dec
1	INST	Character	5	
2	DATE	Date	8	
3	TIME	Character	5	
4	TEMP	Numeric	5	1
5	FLD_PH	Numeric	5	2
6	FLD_SPC	Numeric	6	
7	LAB_SPC	Numeric	6	
8	VOL	Numeric	5	
9	BROMIDE	Numeric	5	1
10	DIS_OX	Numeric	5	1
11	EH	Numeric	5	2
** Total **			61	

Structure for database: C:gypblock.dbf
Number of data records: 1212
Date of last update : 12/17/87

Field	Field Name	Type	Width	Dec
1	WELL	Character	3	
2	INST	Character	5	
3	DATE	Date	8	
4	TIME	Character	5	
5	MEAS	Numeric	4	
6	MATPOT	Numeric	8	2
** Total **			34	

APPENDIX E
TENSIOMETER DATA

PA01, HYDRAULIC HEAD, 6 TO 9 FT

T08 AND T07

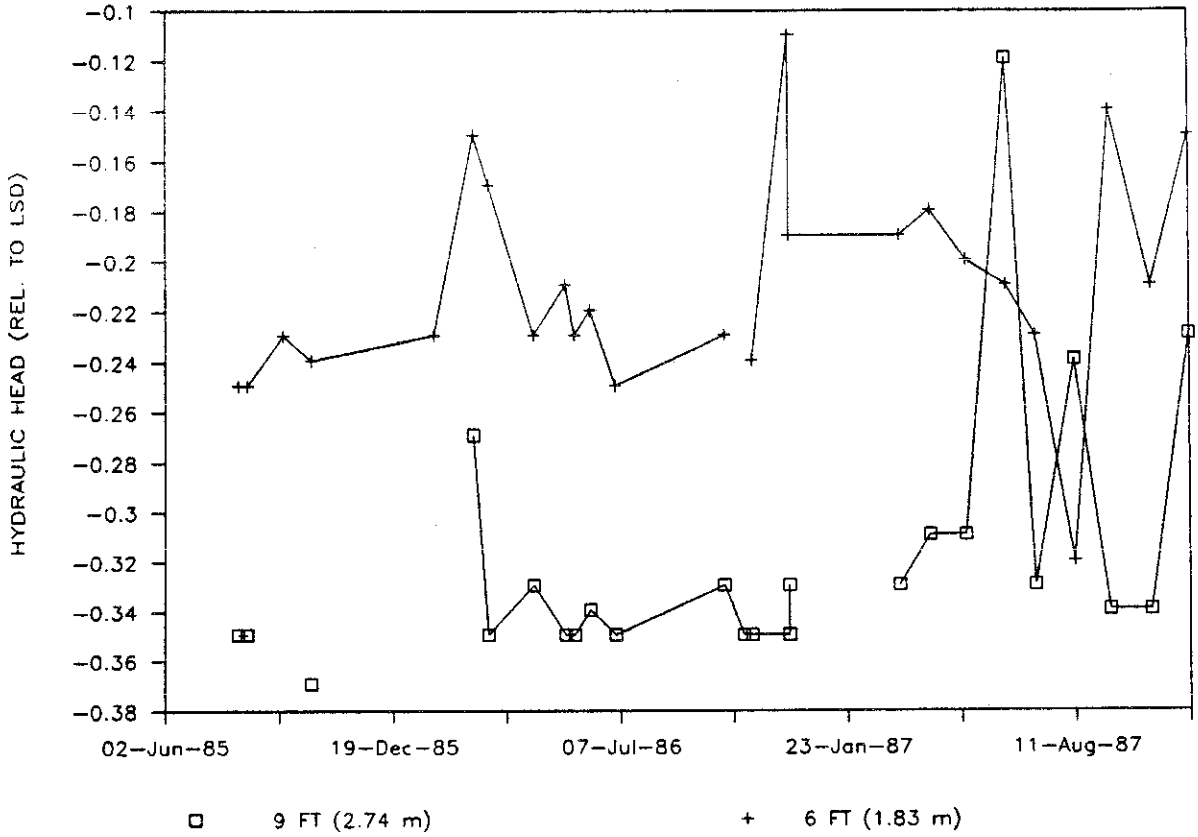

□ 9 FT (2.74 m) + 6 FT (1.83 m)

PA02, 3 AND 6 FT BLS

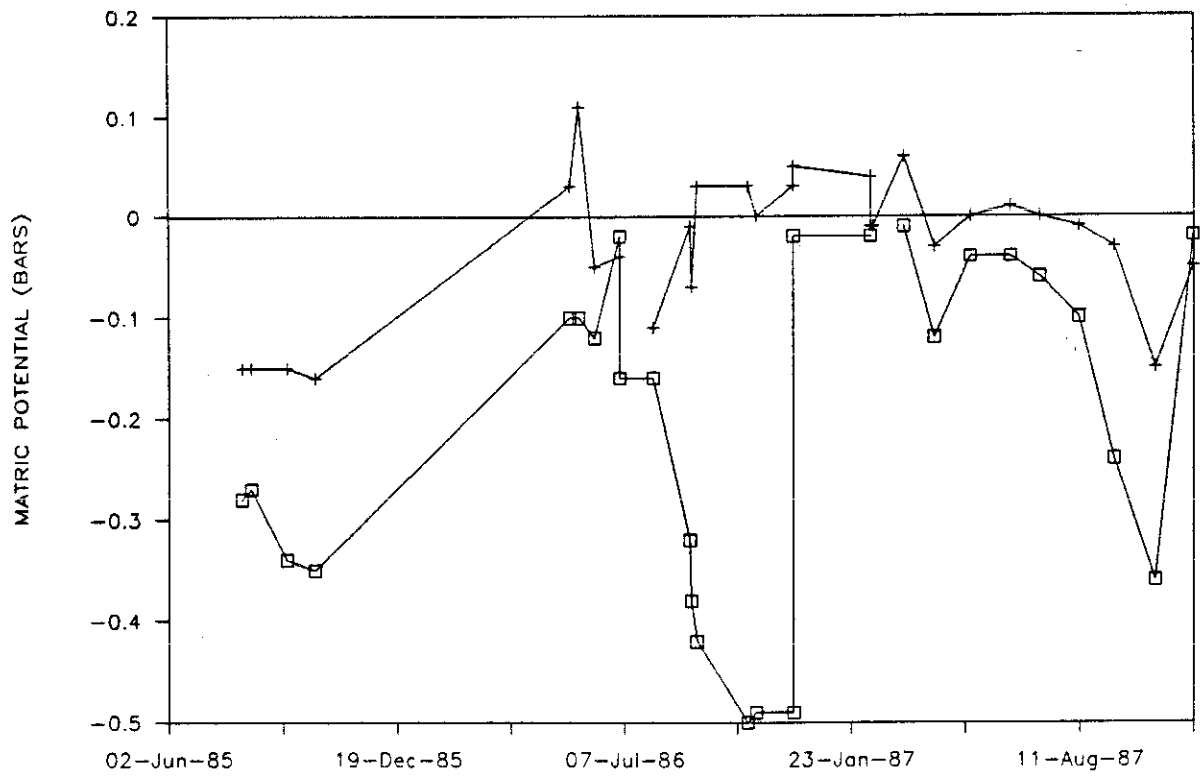

□ 3 FT (0.91 m) + 6 FT (1.83 m)

HYDRAULIC GRADIENT, PA01 3 FT TO 6 FT

T08 AND T09

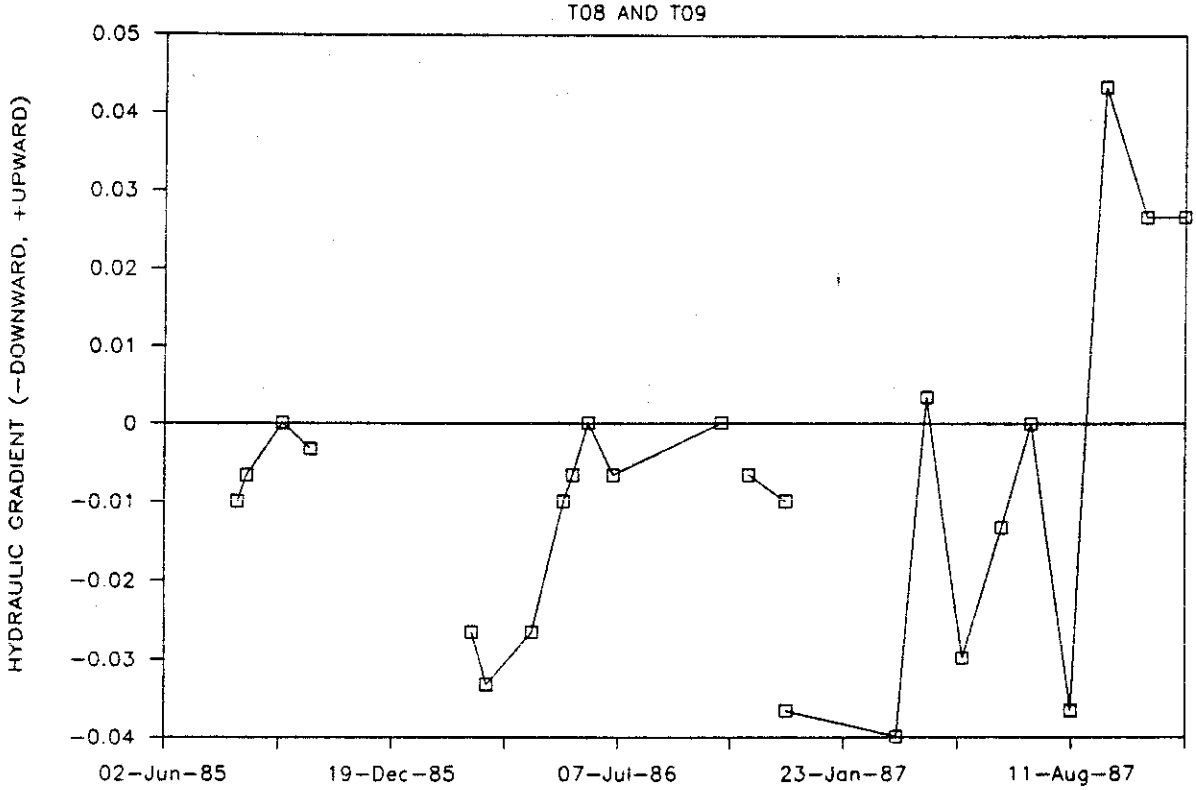

HYDRAULIC GRADIENT, PA01 6 FT TO 9FT

T07 AND T08

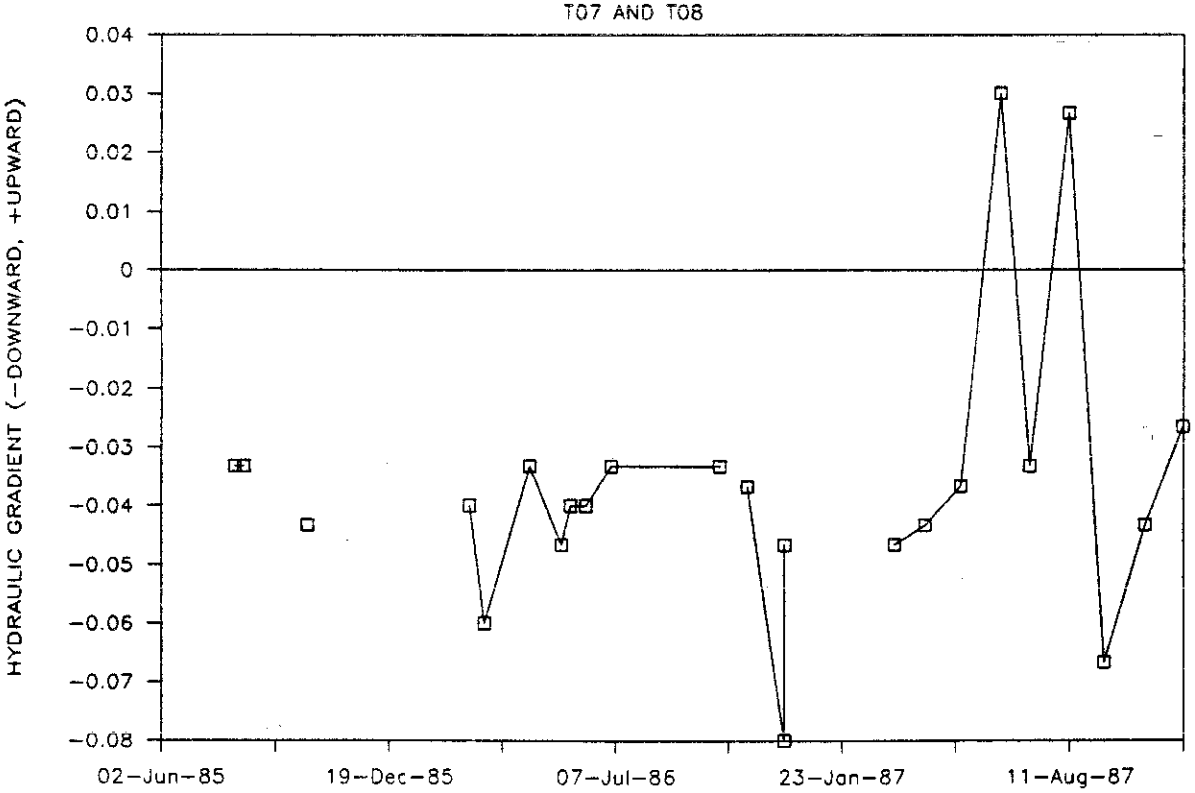

HYDRAULIC GRADIENT, PA01 3 FT TO 9 FT

T07 AND T09

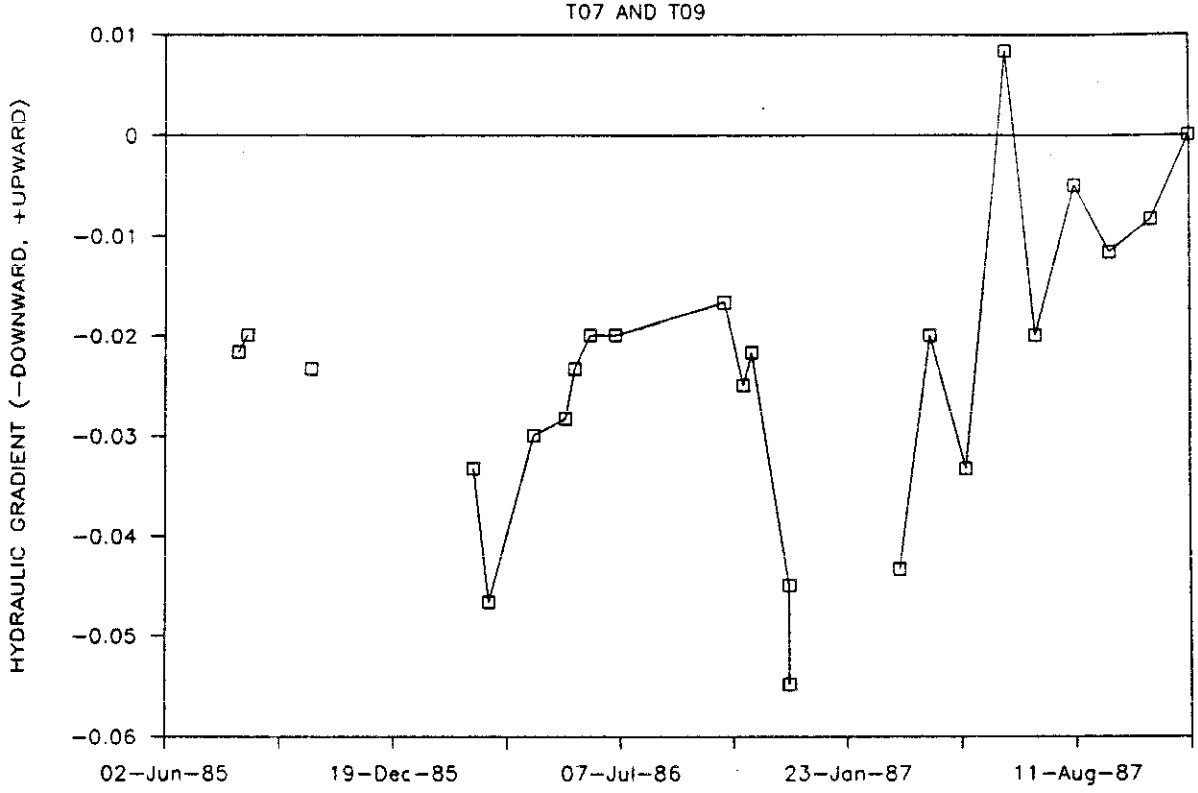

PA01, HYDRAULIC HEADS, 3 AND 6 FT

T09 AND T08

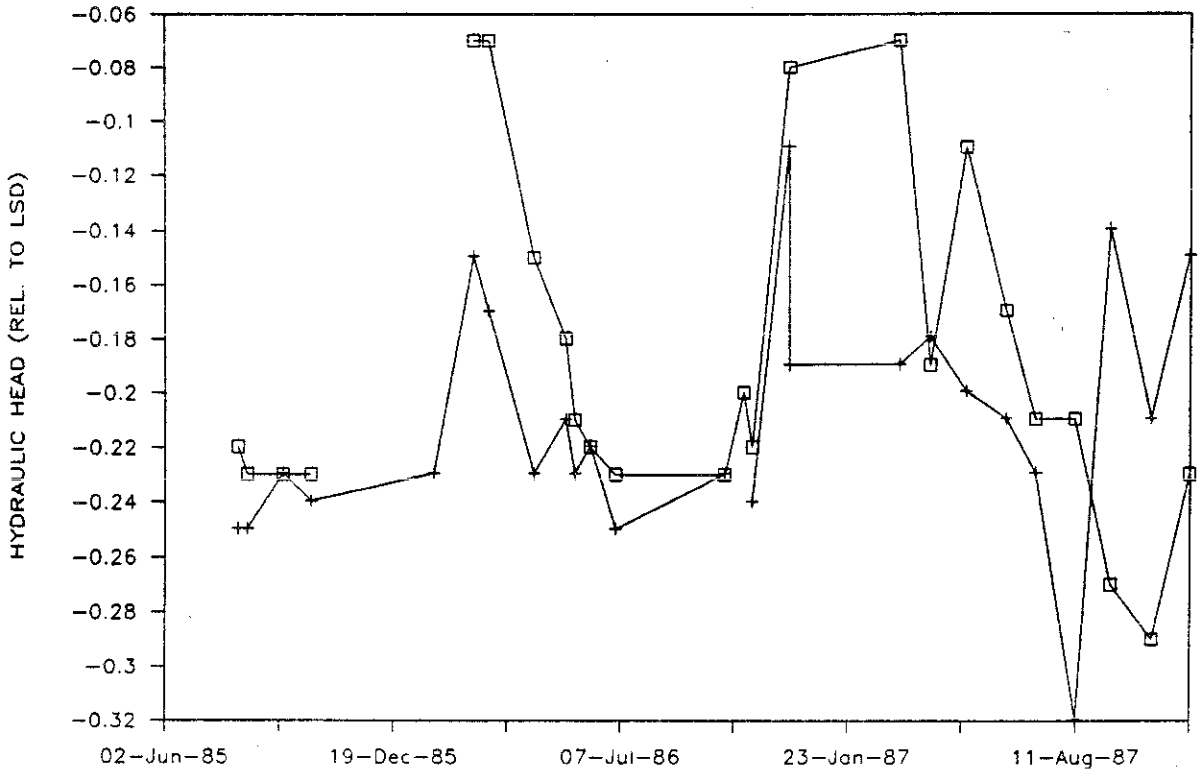

WELL PA01, 3, 6 AND 9 FT BLS

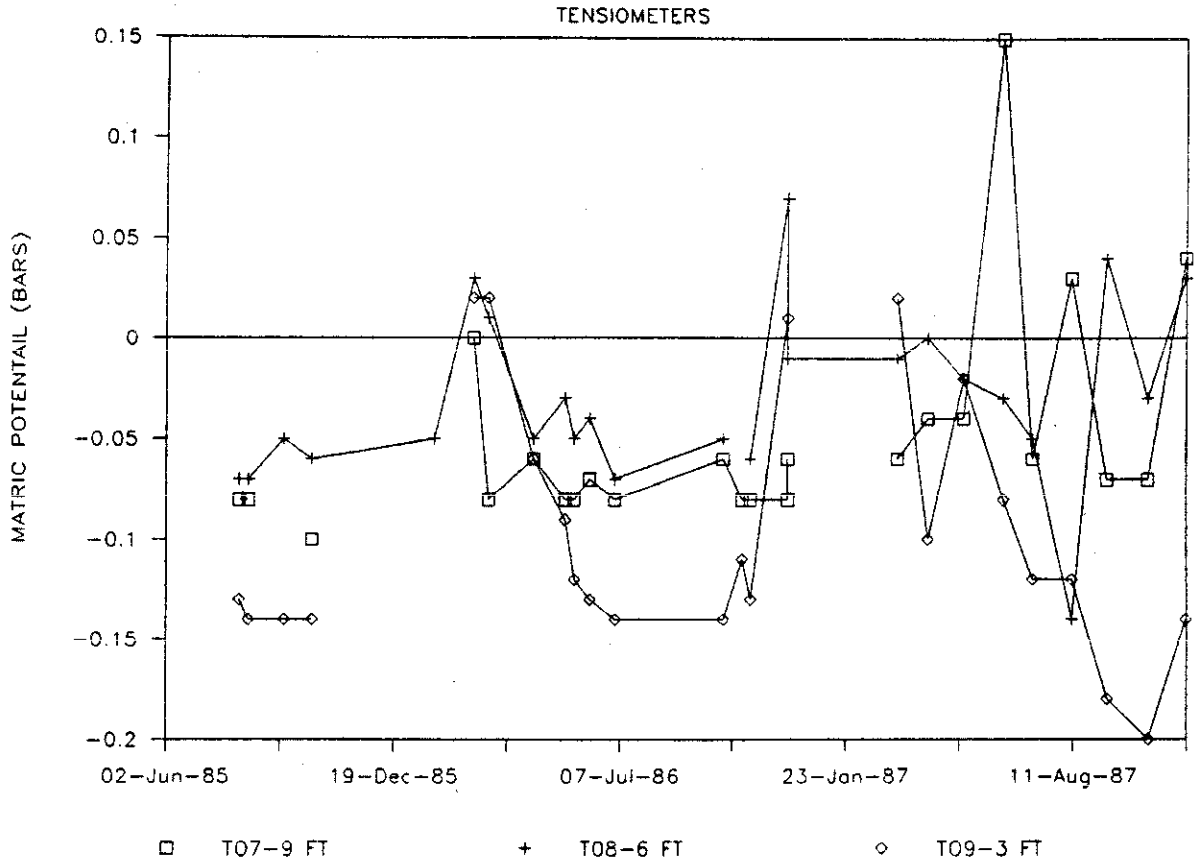

WELL T23, 3 FT BLS

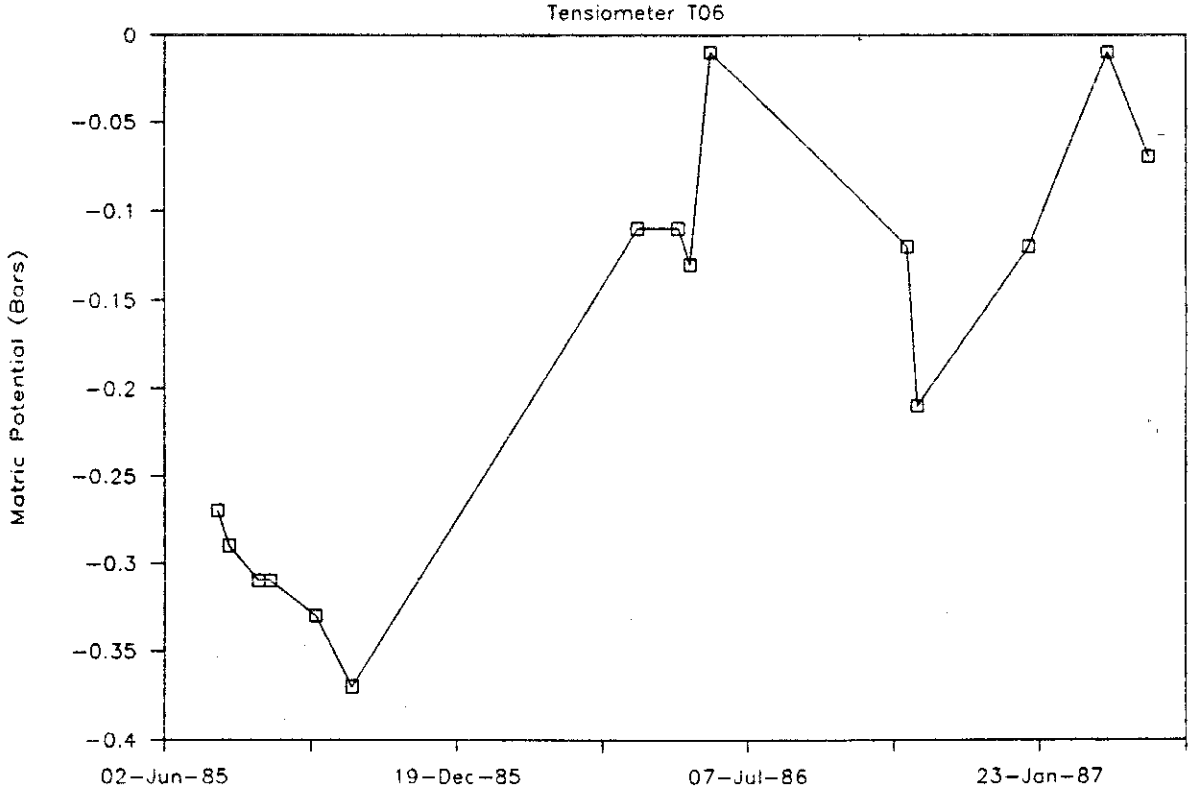

WELL W02, HYDRAULIC HEADS

TO1 AND TO2

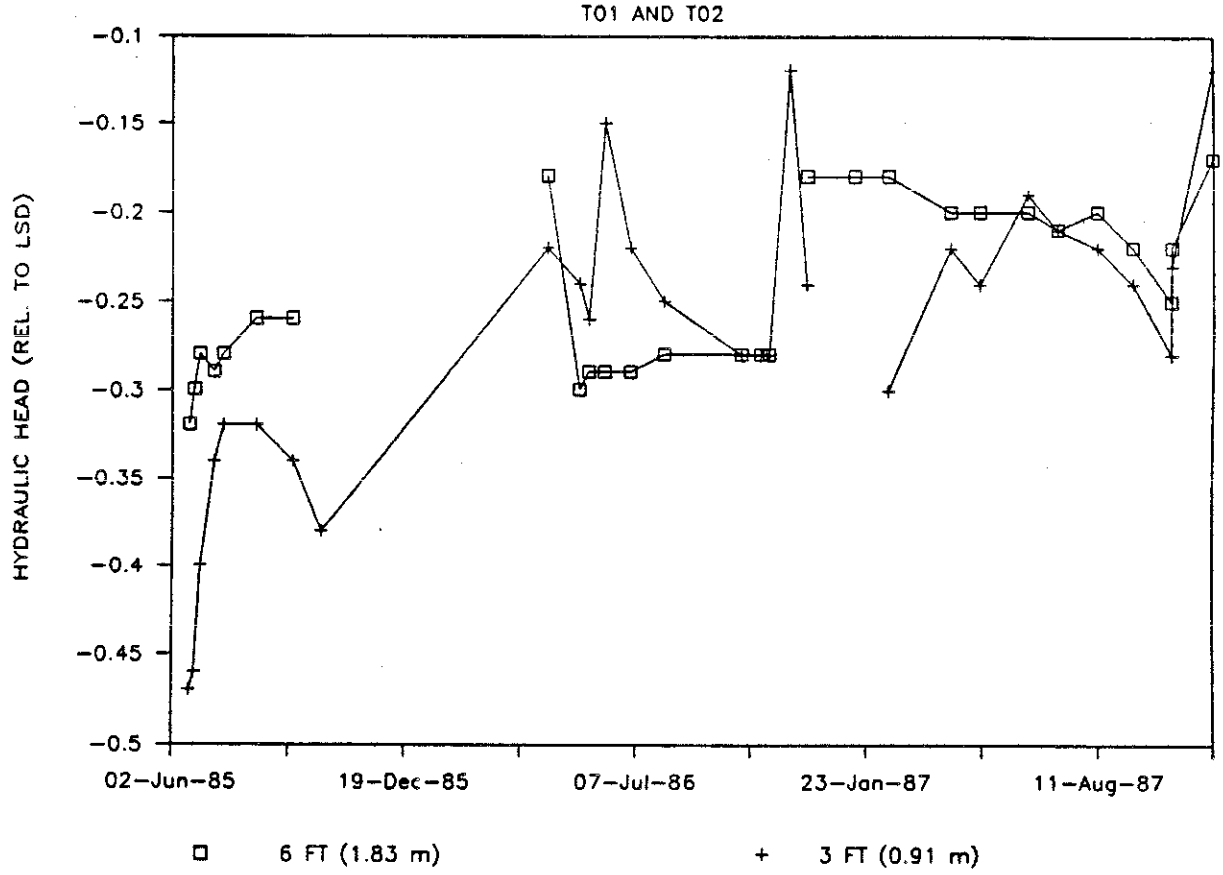

□ 6 FT (1.83 m) + 3 FT (0.91 m)

WELL W24, 3, 6 and 9 FT BLS

TENSIOMETERS T14, T13 and T12

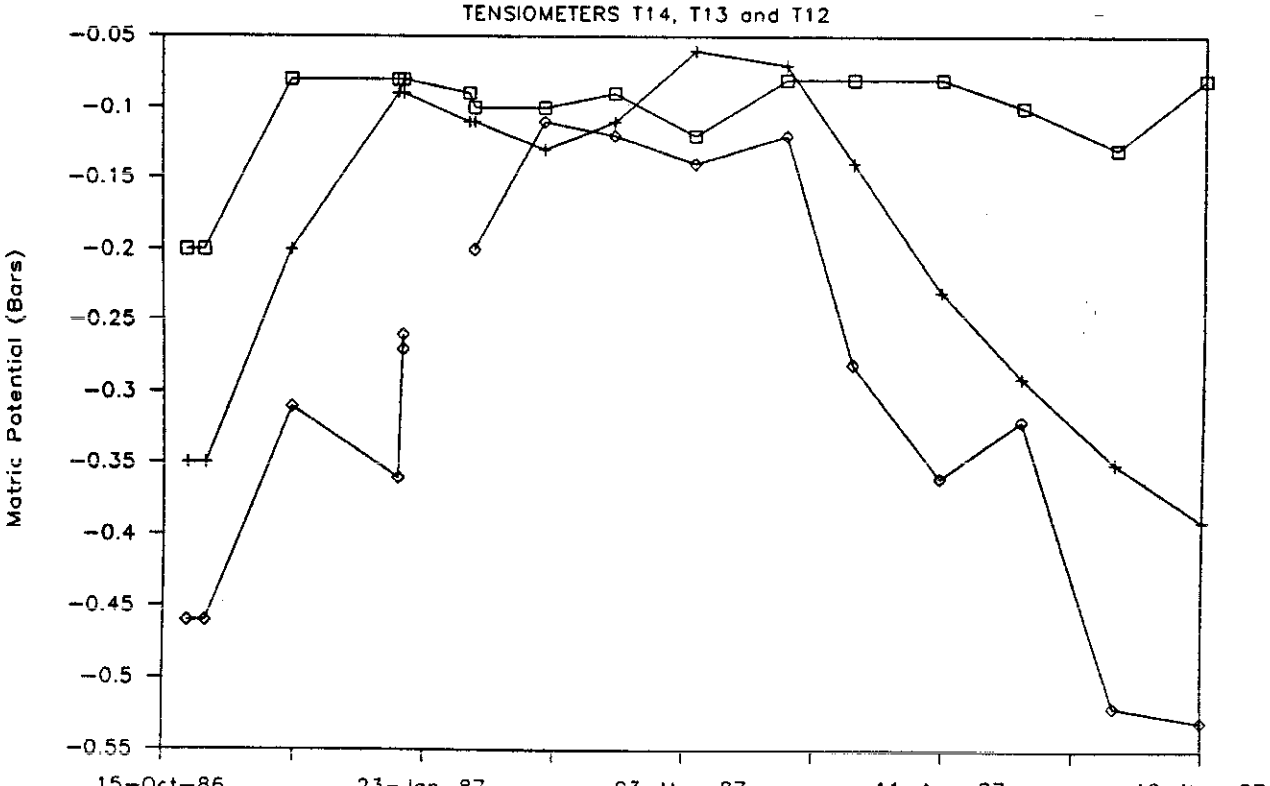

T12 (BOX-9'), T13 (+-6'), T14(DIA-3')

W24, HYDRAULIC HEAD, 6 AND 9 FT

T08 AND T09

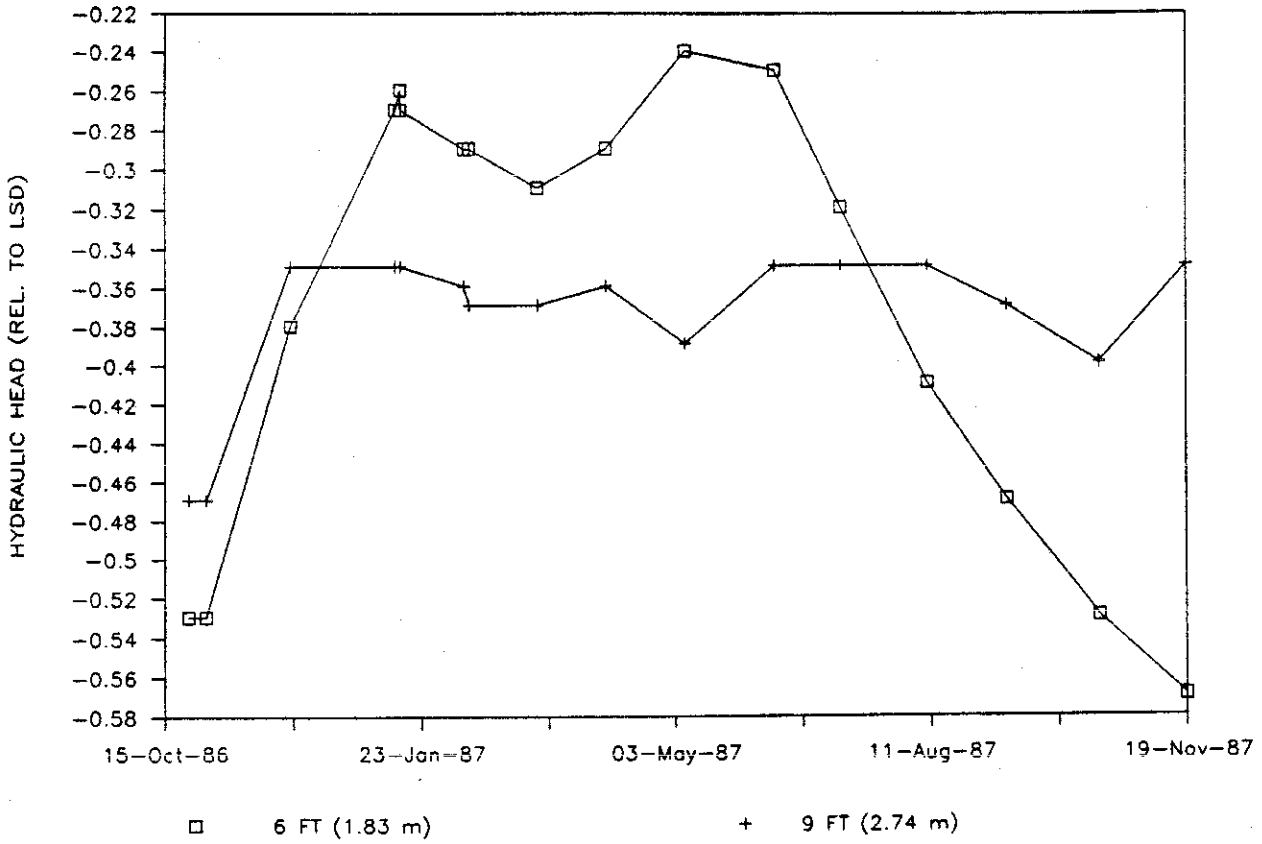

WELL W24, GRADIENT

T12, T13 AND T14

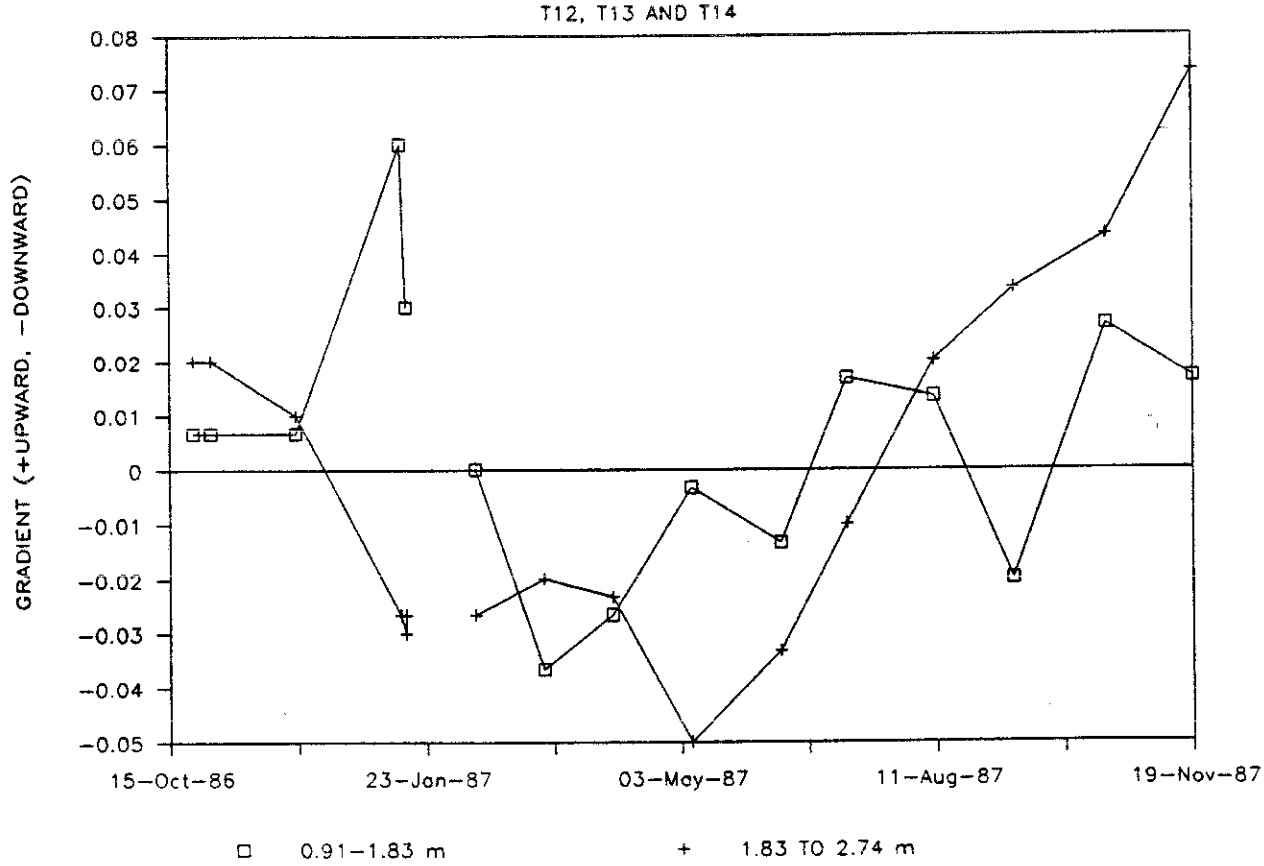

W17, HYDRAULIC HEADS, 3 AND 6 FT

T18 AND T19

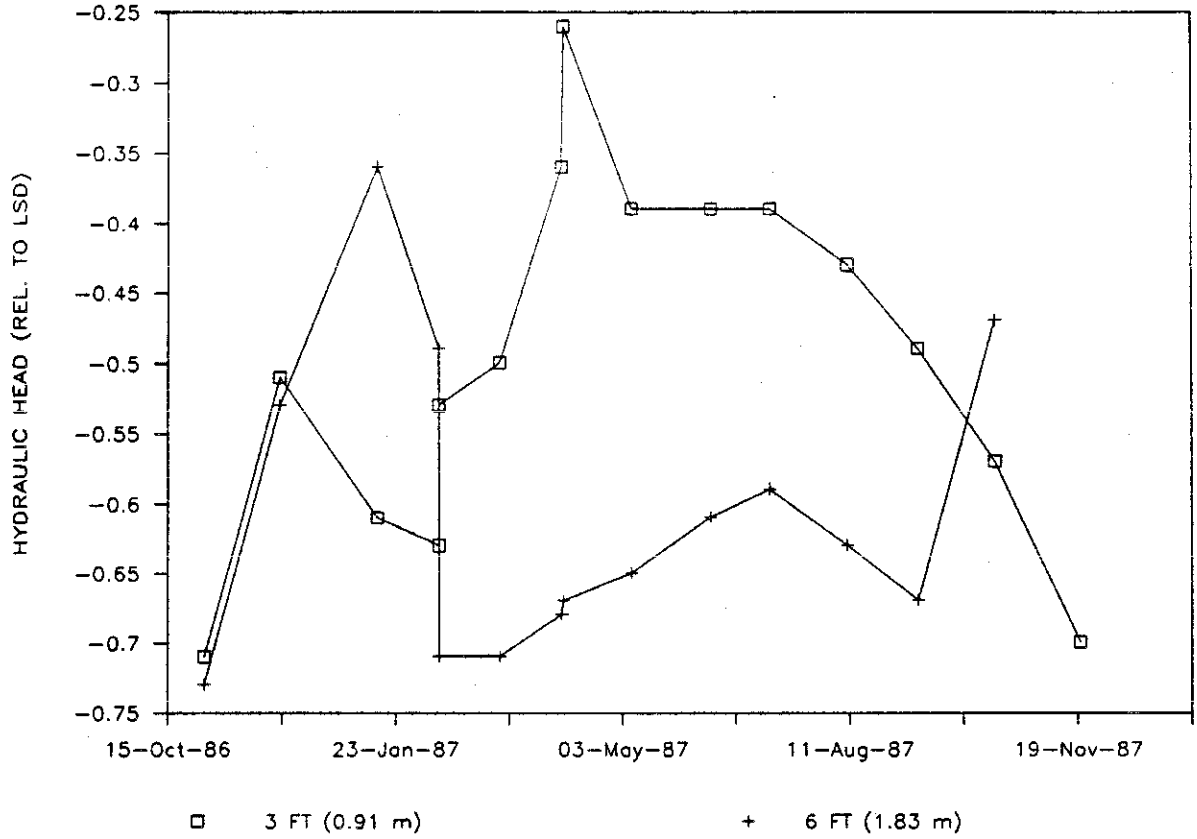

□ 3 FT (0.91 m) + 6 FT (1.83 m)

W24, HYDRAULIC HEAD, 3 AND 6 FT

T08 AND T09

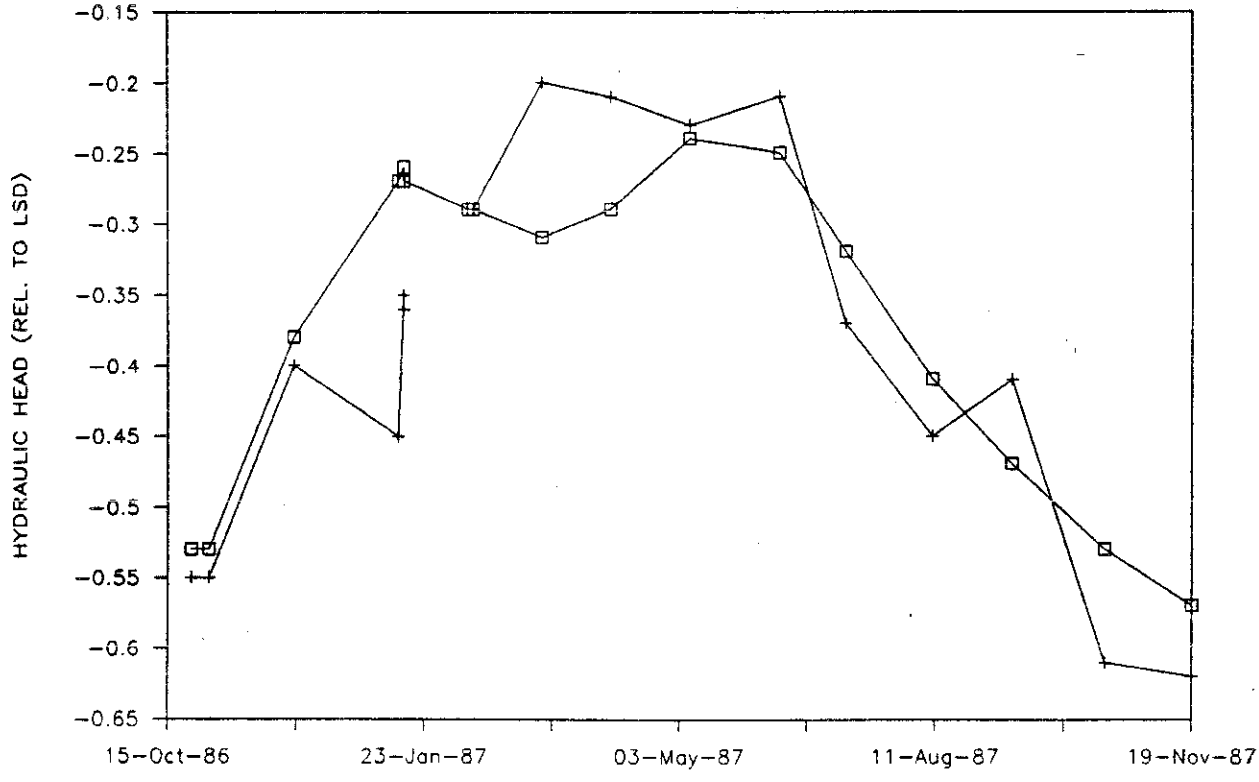

□ 6 FT (1.83 m) + 3 FT (0.91 m)

WELL W02, GRADIENT

T01 AND T02

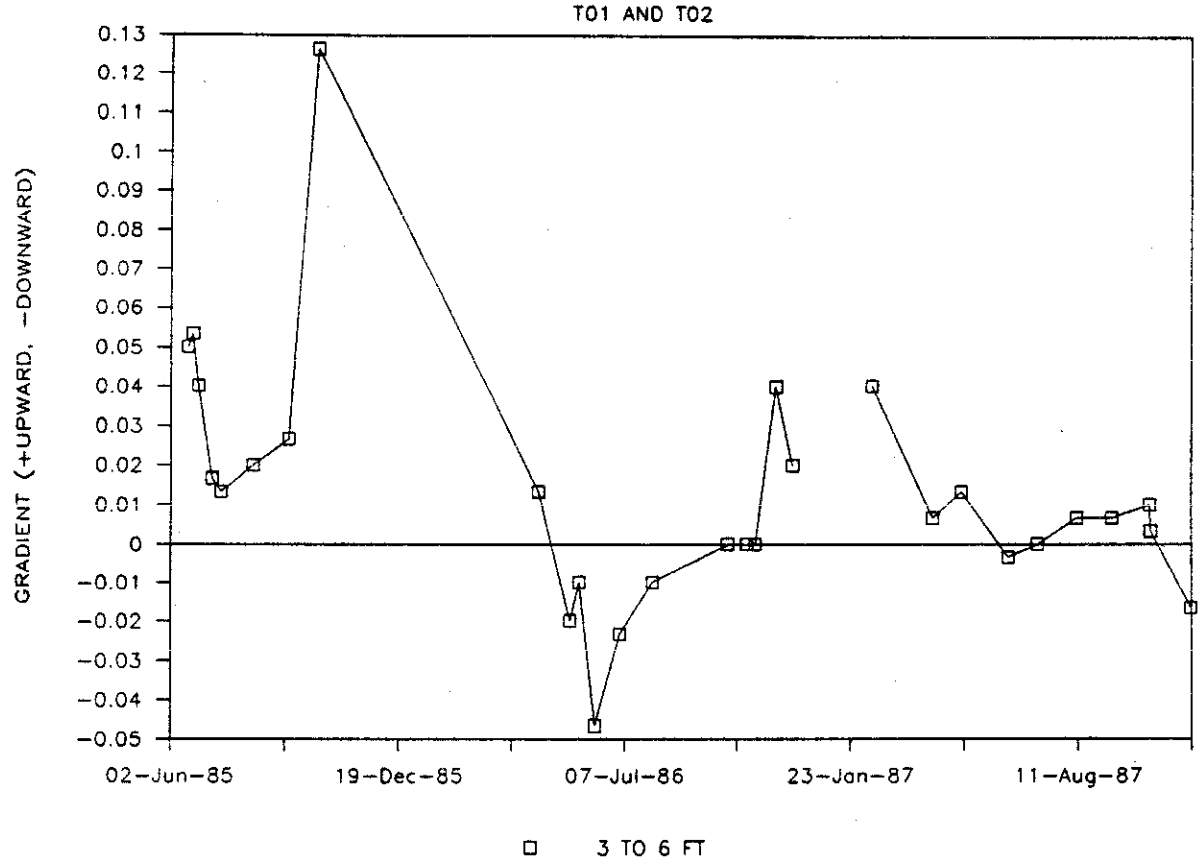

□ 3 TO 6 FT

W06, HYDRAULIC HEAD, 3 AND 6 FT

T16 AND T17

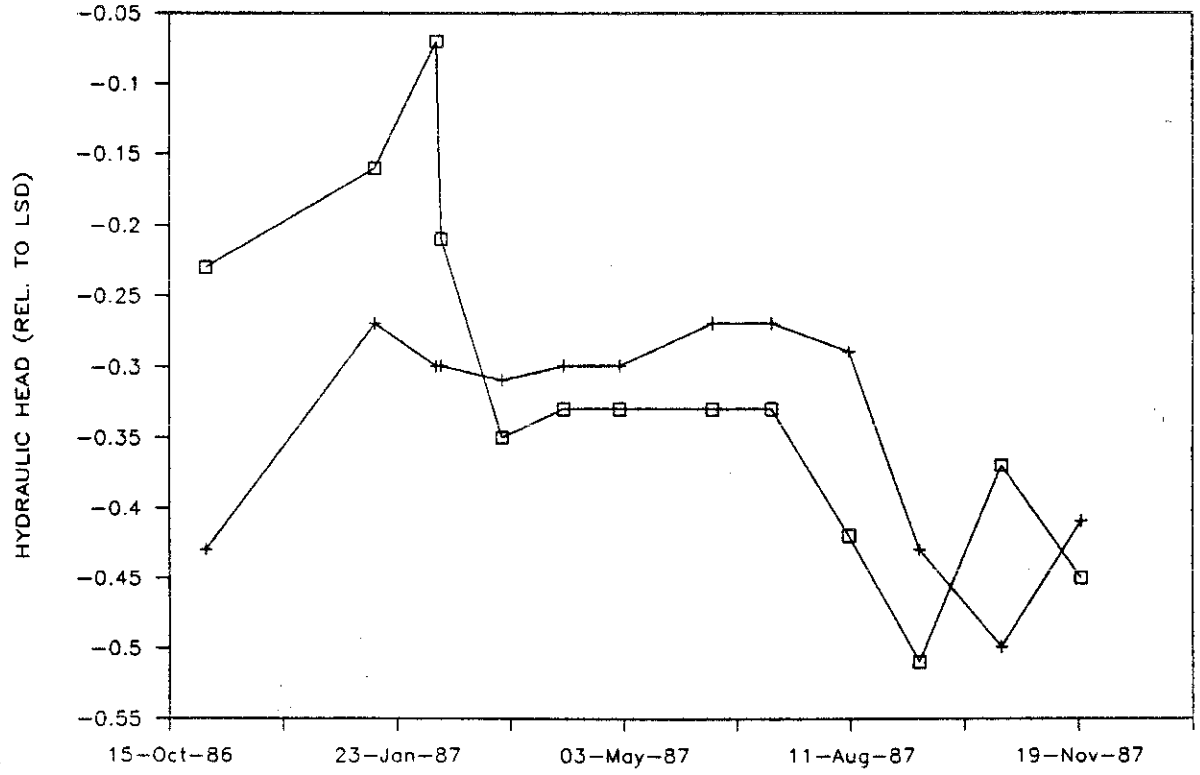

□ 3 FT (0.91 m) + 6 FT (1.83 m)

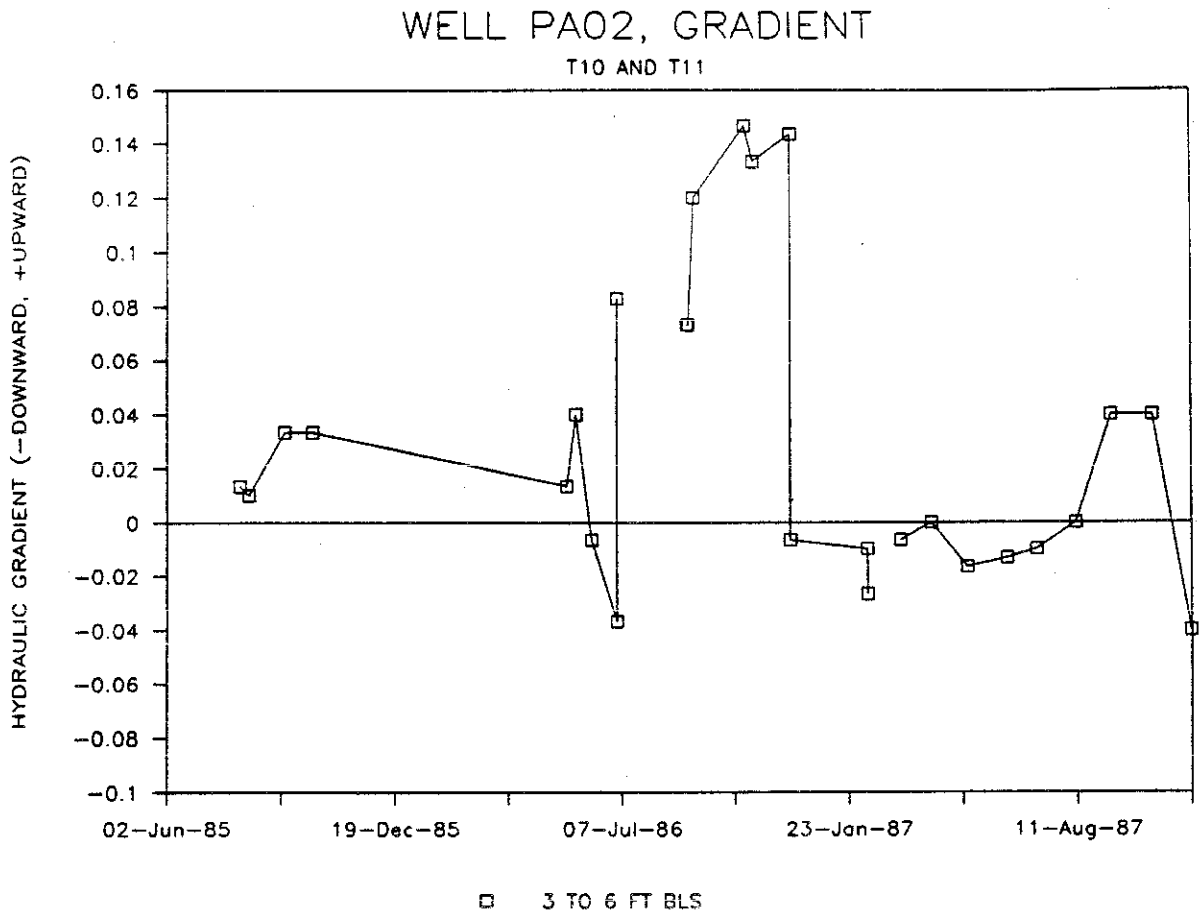
WELL PA02, GRADIENT
T10 AND T11
HYDRAULIC GRADIENT (-DOWNWARD, +UPWARD)
0.16
0.14
0.12
0.1
0.08
0.06
0.04
0.02
0
-0.02
-0.04
-0.06
-0.08
-0.1
02-Jun-85
19-Dec-85
07-Jul-86
23-Jan-87
11-Aug-87
3 TO 6 FT BLS

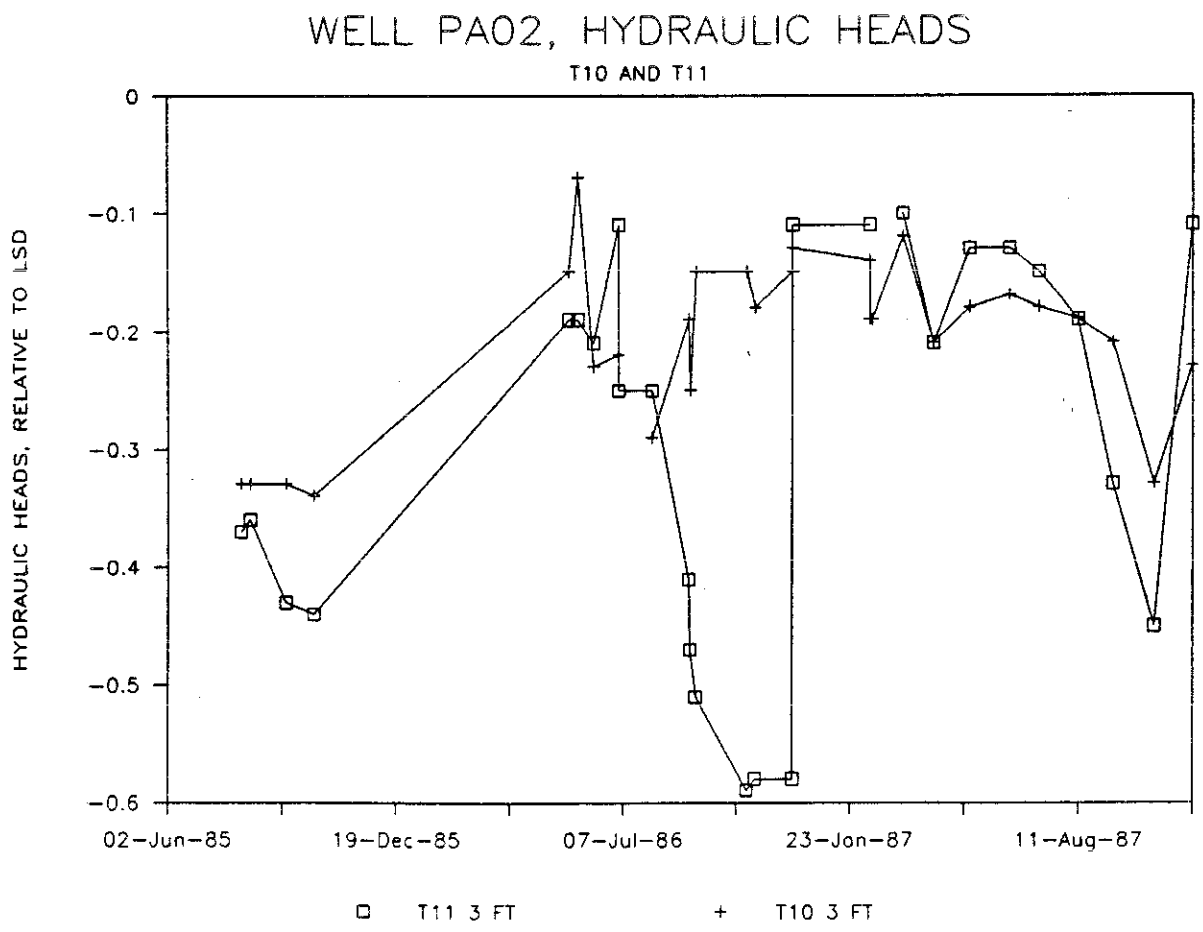
WELL PA02, HYDRAULIC HEADS
T10 AND T11
HYDRAULIC HEADS, RELATIVE TO LSD
0
-0.1
-0.2
-0.3
-0.4
-0.5
-0.6
02-Jun-85
19-Dec-85
07-Jul-86
23-Jan-87
11-Aug-87
T11 3 FT
T10 3 FT

WELL W20, 4 FT BLS

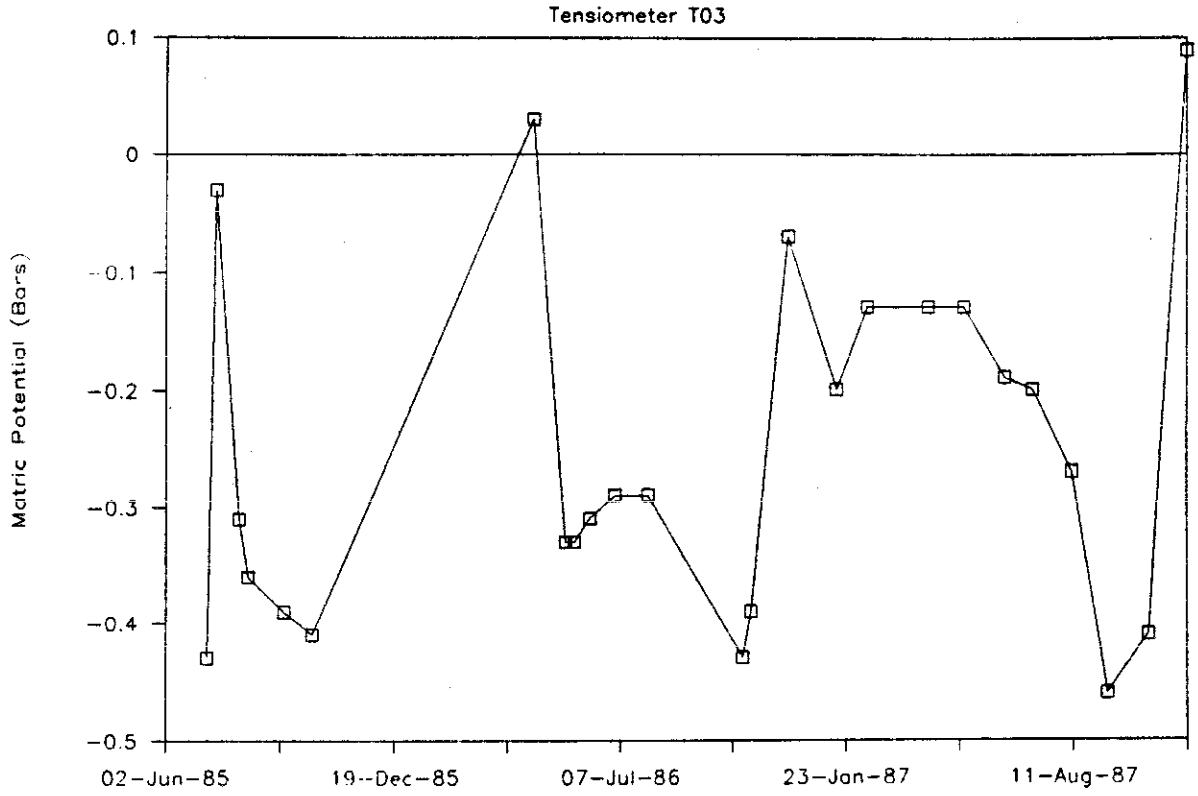

WELL W23, 3 FT BLS

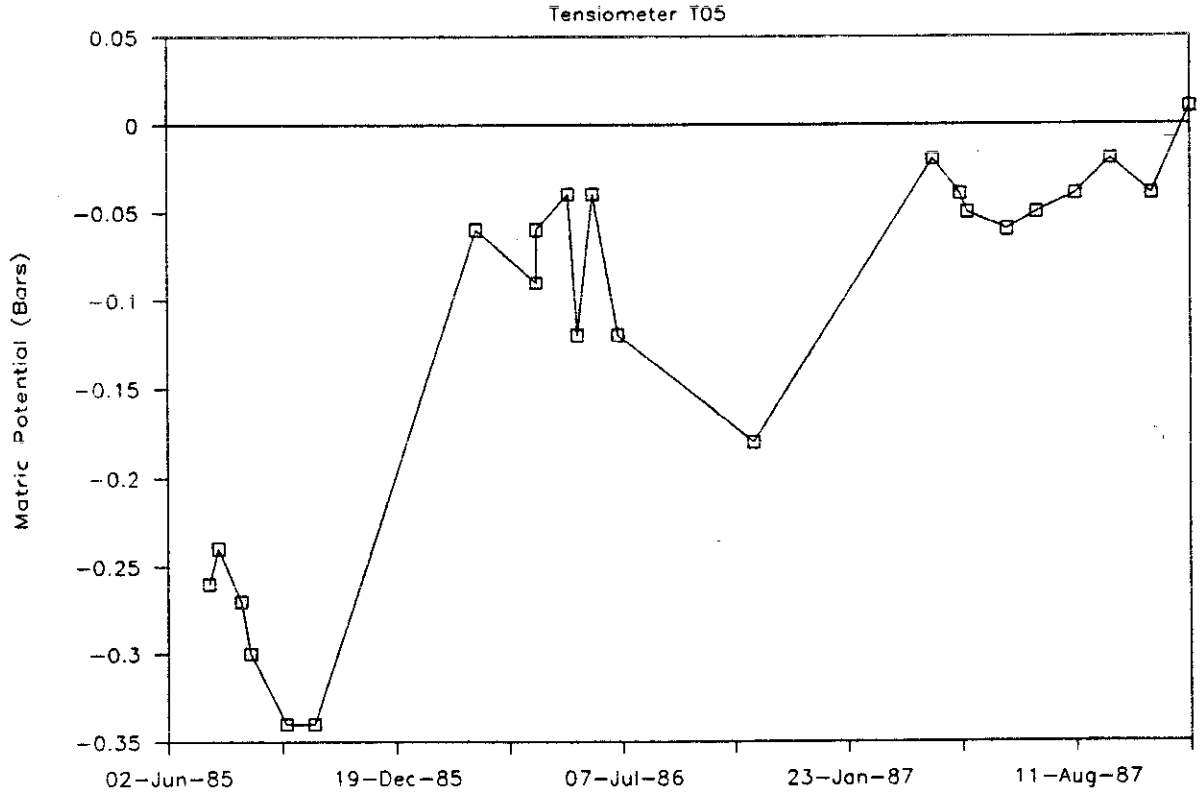

APPENDIX F
GYPSUM BLOCK DATA

WELL PA1, GYPSUM BLOCKS

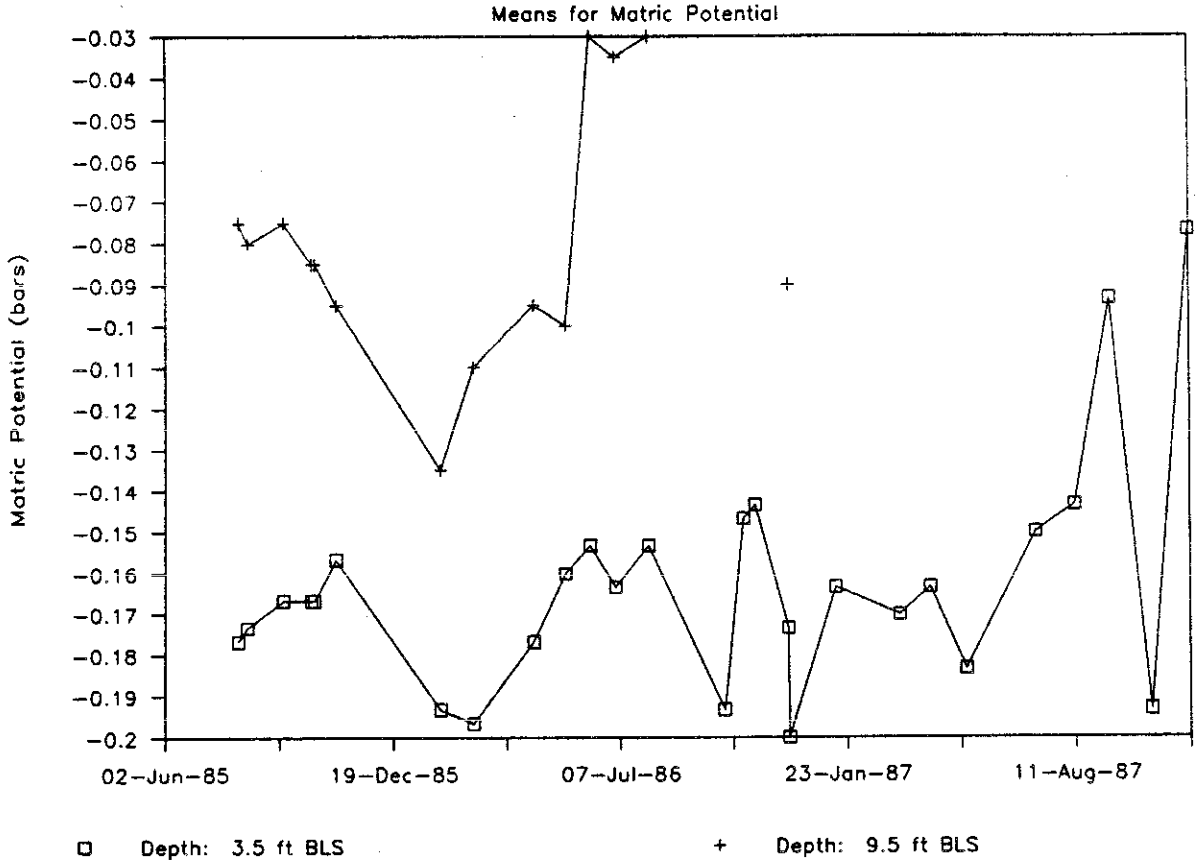

□ Depth: 3.5 ft BLS + Depth: 9.5 ft BLS

WELL 10, GYPSUM BLOCKS

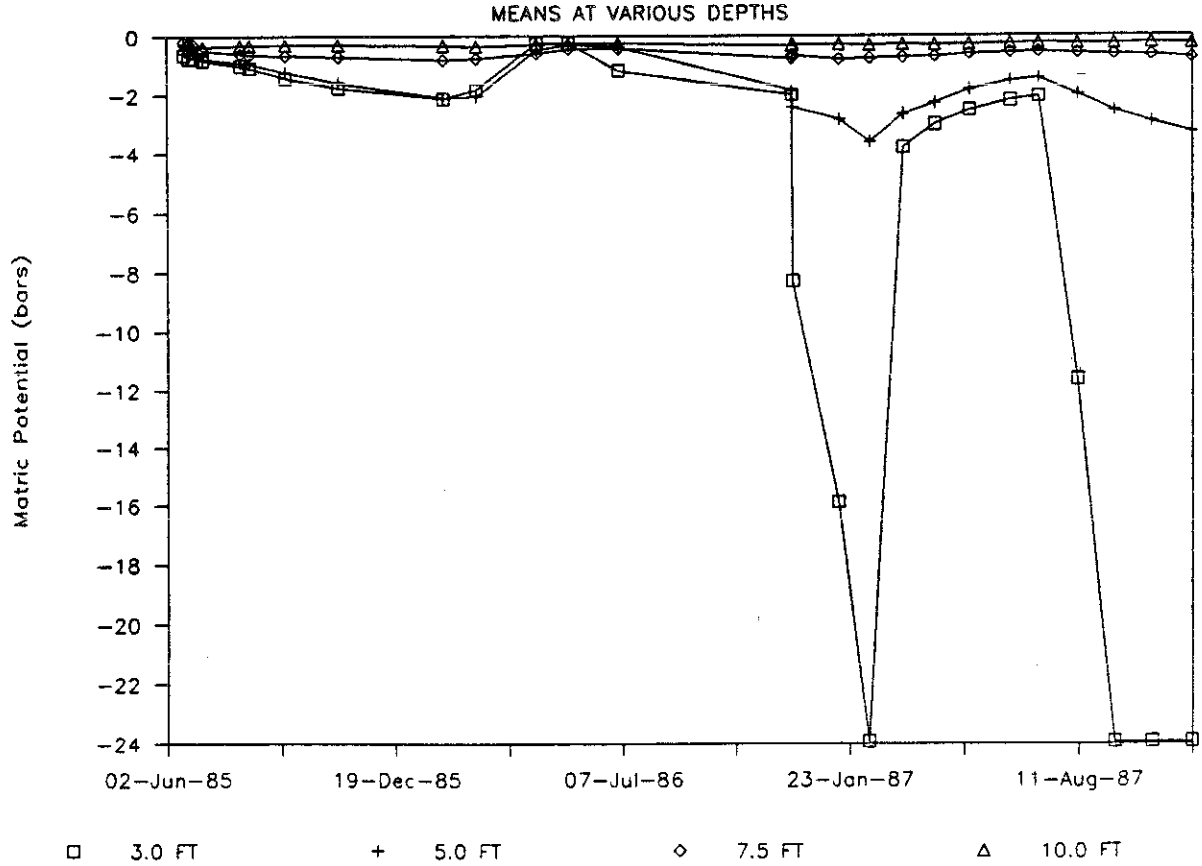

□ 3.0 FT + 5.0 FT ◇ 7.5 FT △ 10.0 FT

WELL 12, GYPSUM BLOCKS

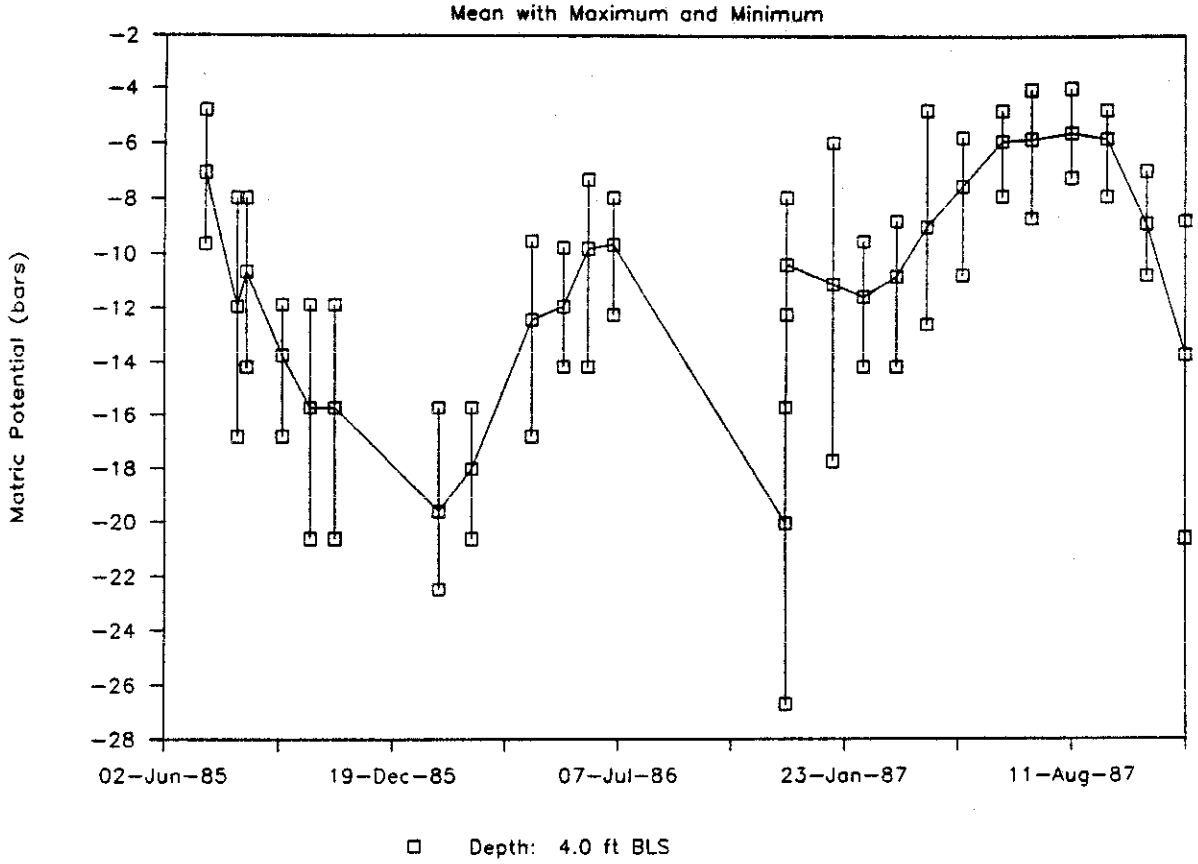

WELL 19, GYPSUM BLOCKS

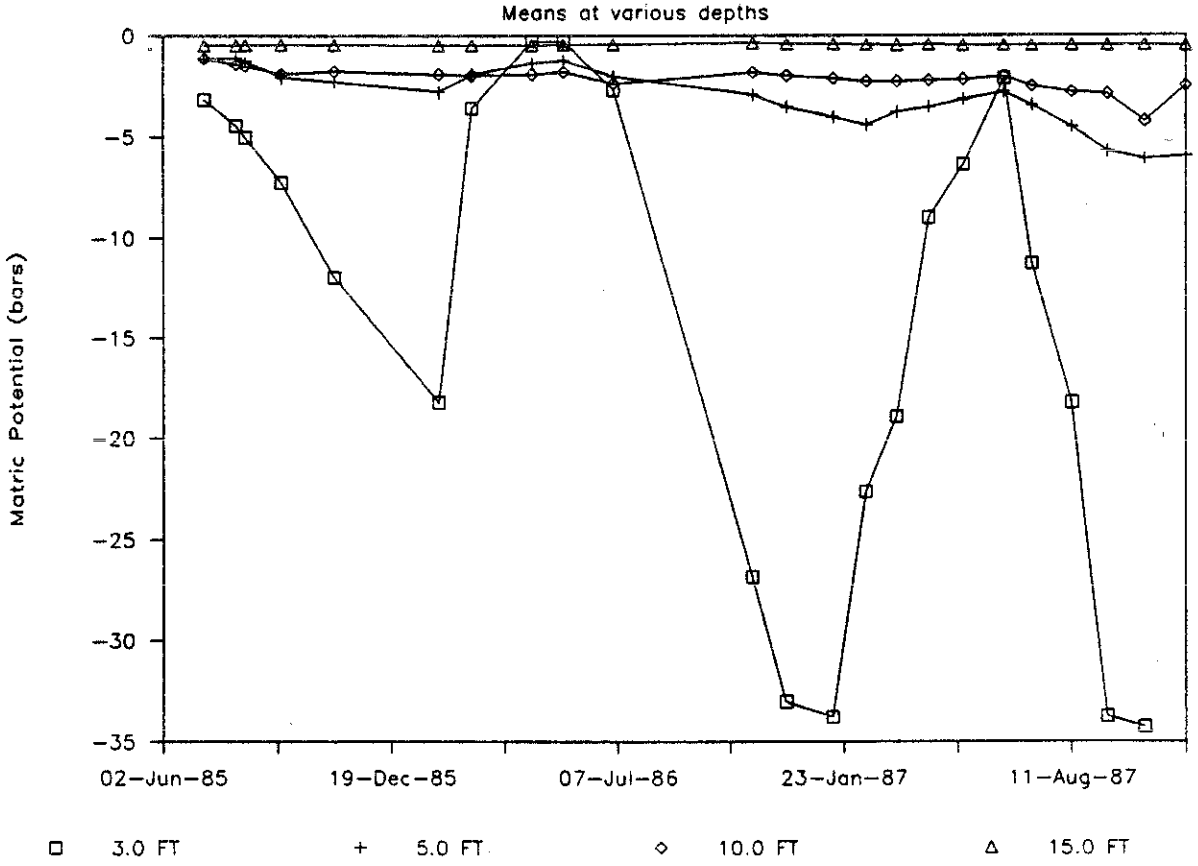

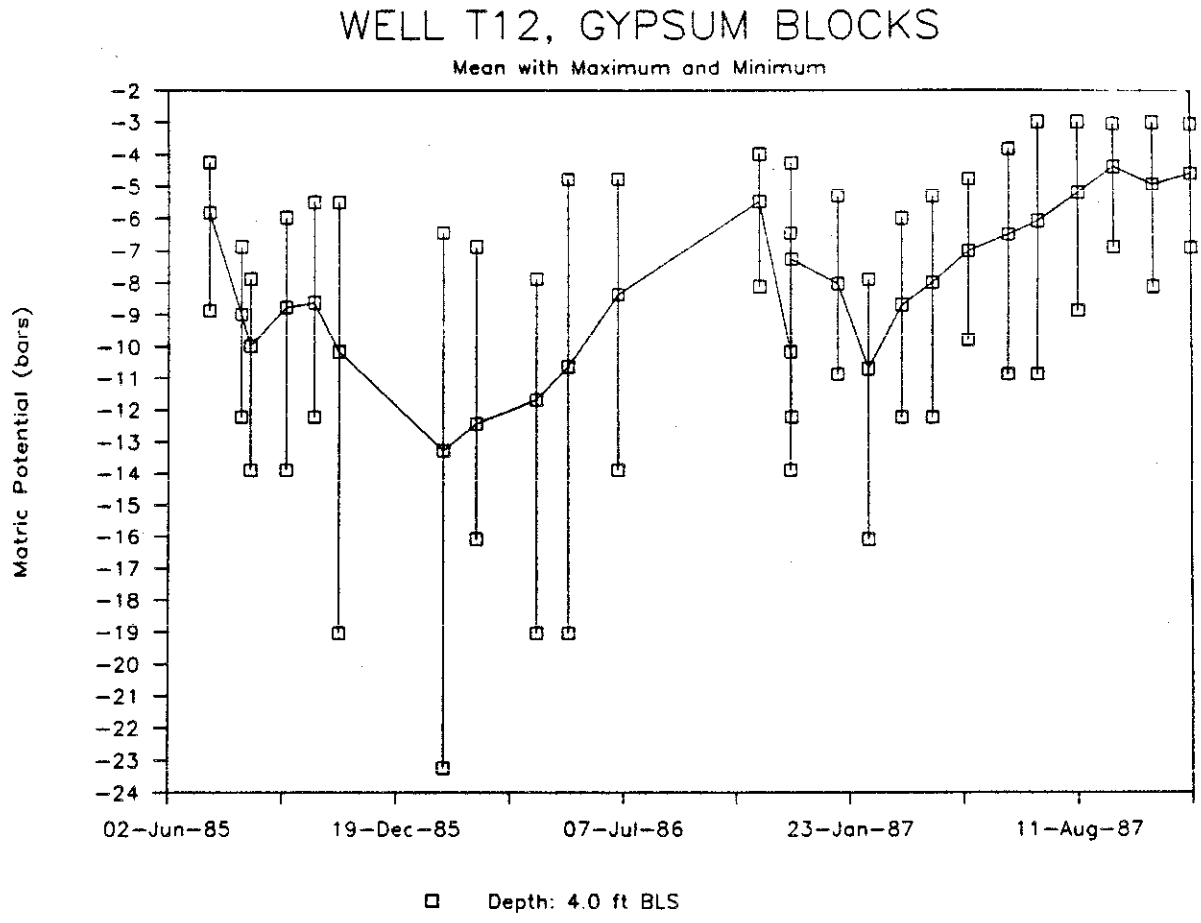
WELL T12, GYPSUM BLOCKS
Mean with Maximum and Minimum
Matric Potential (bars)
-2
-3
-4
-5
-6
-7
-8
-9
-10
-11
-12
-13
-14
-15
-16
-17
-18
-19
-20
-21
-22
-23
-24
02-Jun-85
19-Dec-85
07-Jul-86
23-Jan-87
11-Aug-87
Depth: 4.0 ft BLS

APPENDIX G
HEAT DISSIPATION SENSOR DATA

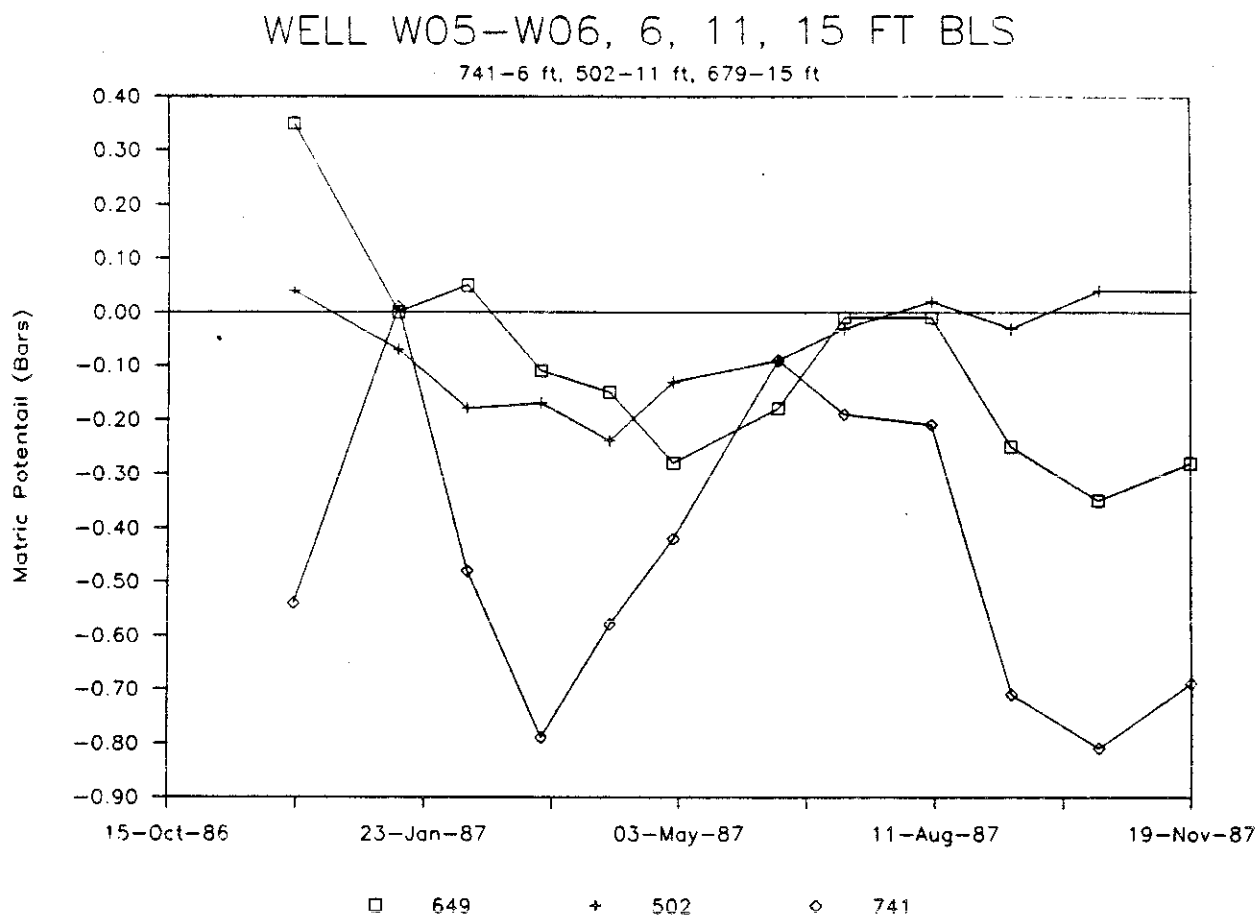
WELL W05–W06, 6, 11, 15 FT BLS
741–6 ft, 502–11 ft, 679–15 ft
Matric Potentail (Bars)
0.40
0.30
0.20
0.10
0.00
−0.10
−0.20
−0.30
−0.40
−0.50
−0.60
−0.70
−0.80
−0.90
15–Oct–86
23–Jan–87
03–May–87
11–Aug–87
19–Nov–87
649
502
741

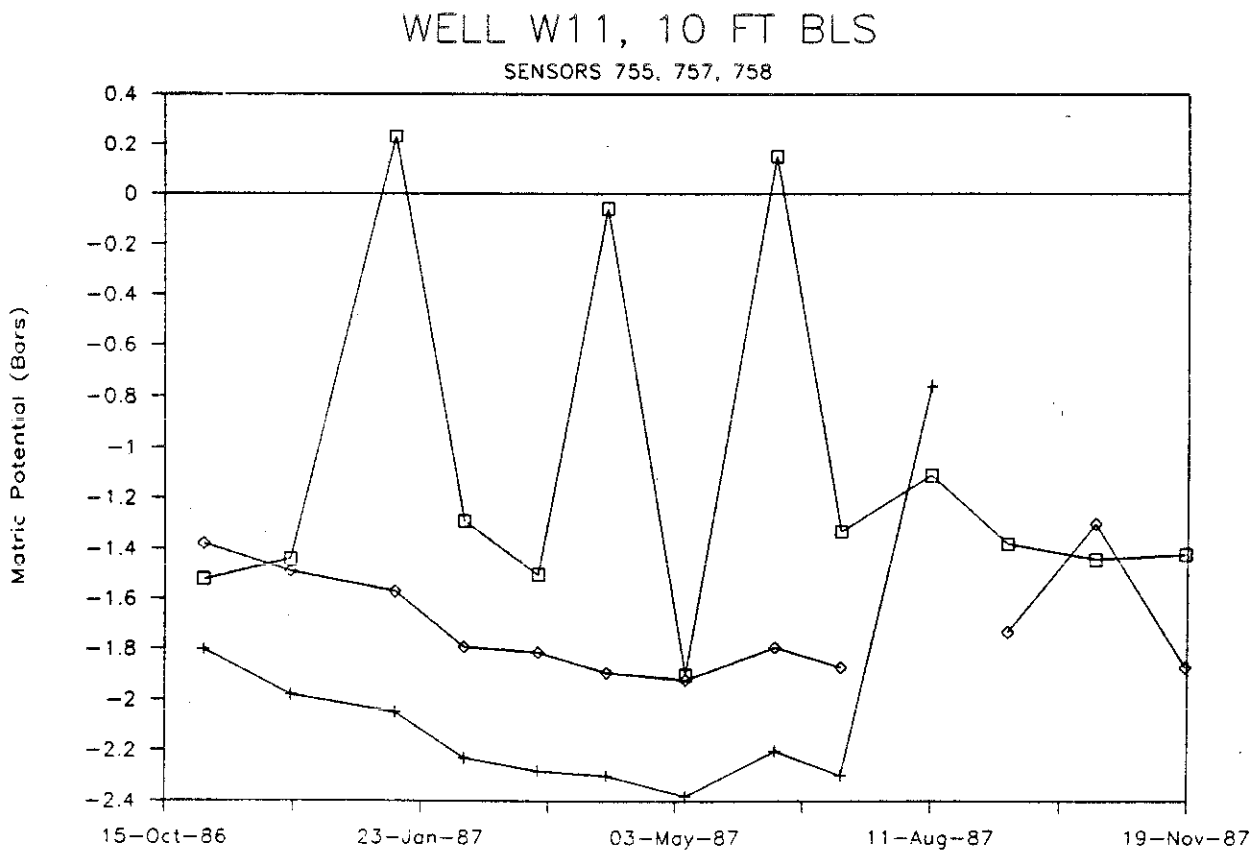
WELL W11, 10 FT BLS
SENSORS 755, 757, 758
Matric Potential (Bars)
0.4
0.2
0
−0.2
−0.4
−0.6
−0.8
−1
−1.2
−1.4
−1.6
−1.8
−2
−2.2
−2.4
15–Oct–86
23–Jan–87
03–May–87
11–Aug–87
19–Nov–87

WELL W11, 16 FT BLS

SENSORS 497, 663, 740

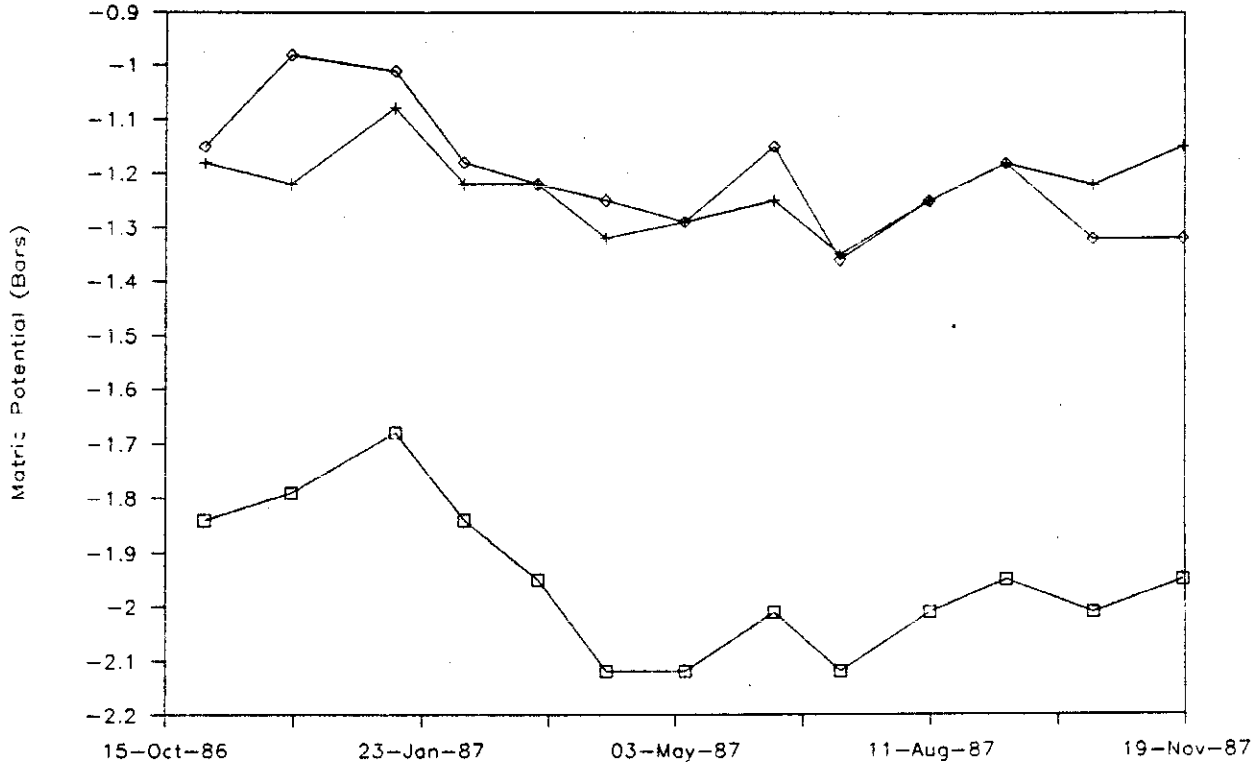

WELL W11, 3 FT BLS

SENSORS 735, 760, 762

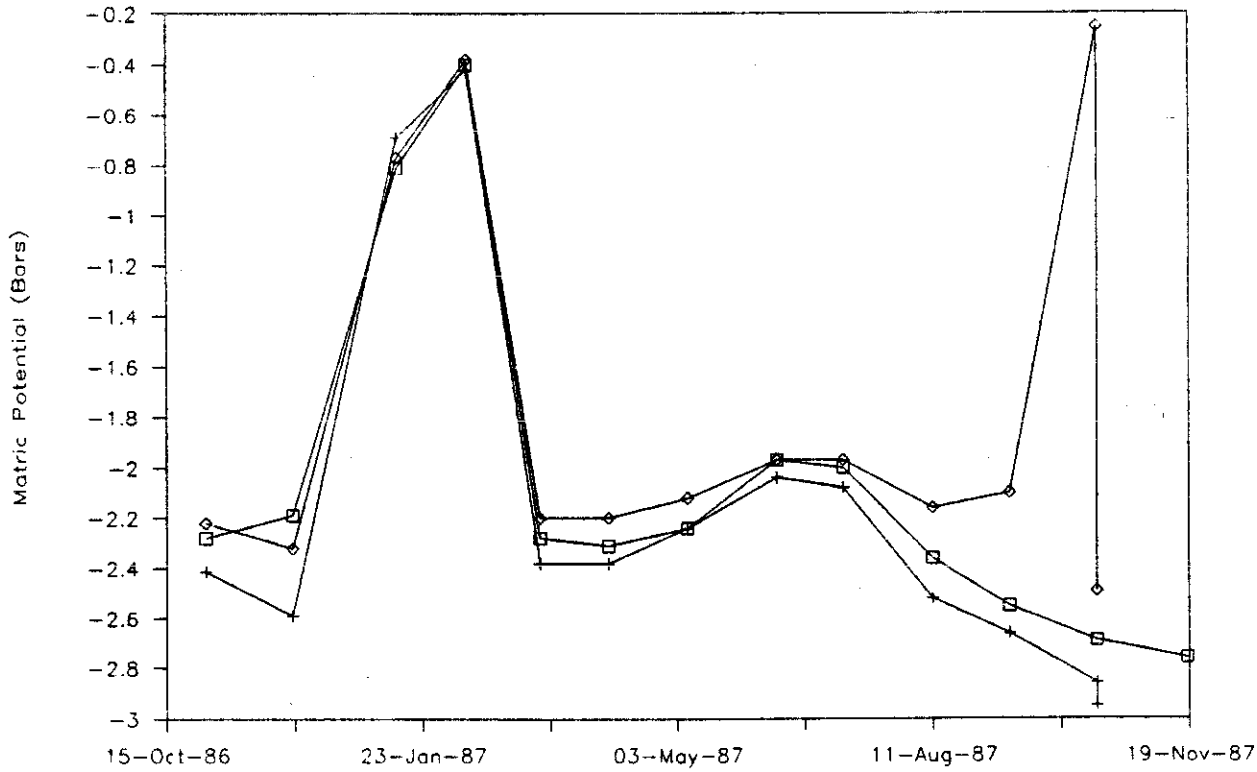

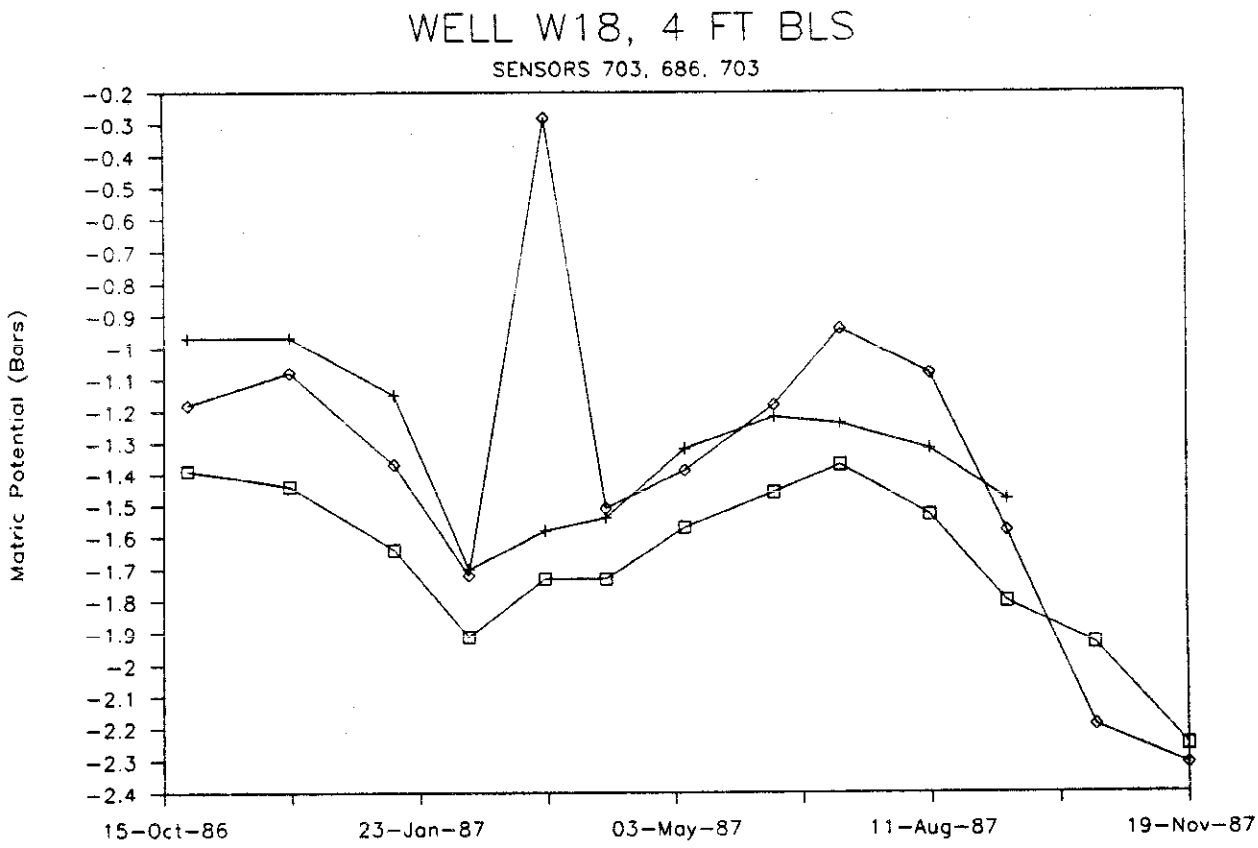
WELL W18, 4 FT BLS
SENSORS 703, 686, 703
Matric Potential (Bars)
-0.2
-0.3
-0.4
-0.5
-0.6
-0.7
-0.8
-0.9
-1
-1.1
-1.2
-1.3
-1.4
-1.5
-1.6
-1.7
-1.8
-1.9
-2
-2.1
-2.2
-2.3
-2.4
15-Oct-86
23-Jan-87
03-May-87
11-Aug-87
19-Nov-87

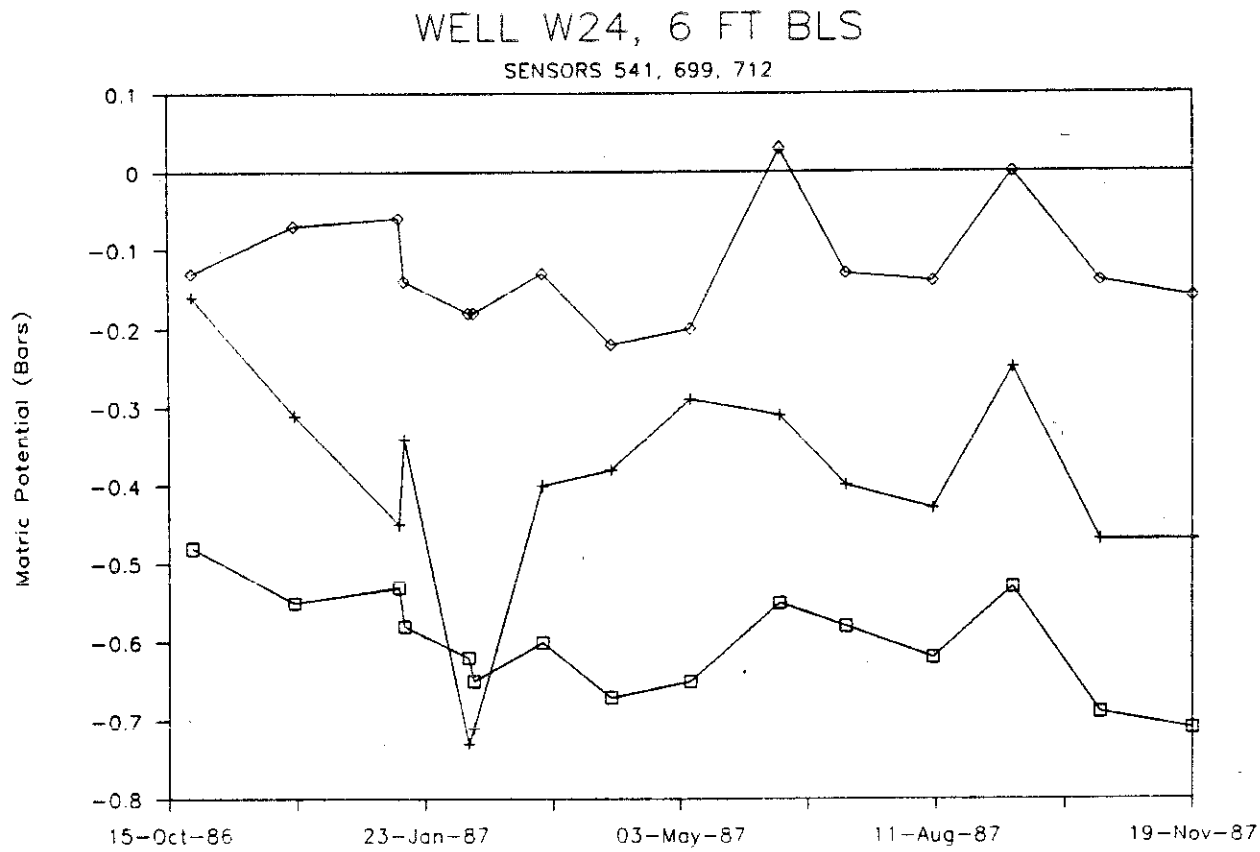
WELL W24, 6 FT BLS
SENSORS 541, 699, 712
Matric Potential (Bars)
0.1
0
-0.1
-0.2
-0.3
-0.4
-0.5
-0.6
-0.7
-0.8
15-Oct-86
23-Jan-87
03-May-87
11-Aug-87
19-Nov-87

WELL W25, 4, 7 AND 14 FT BLS

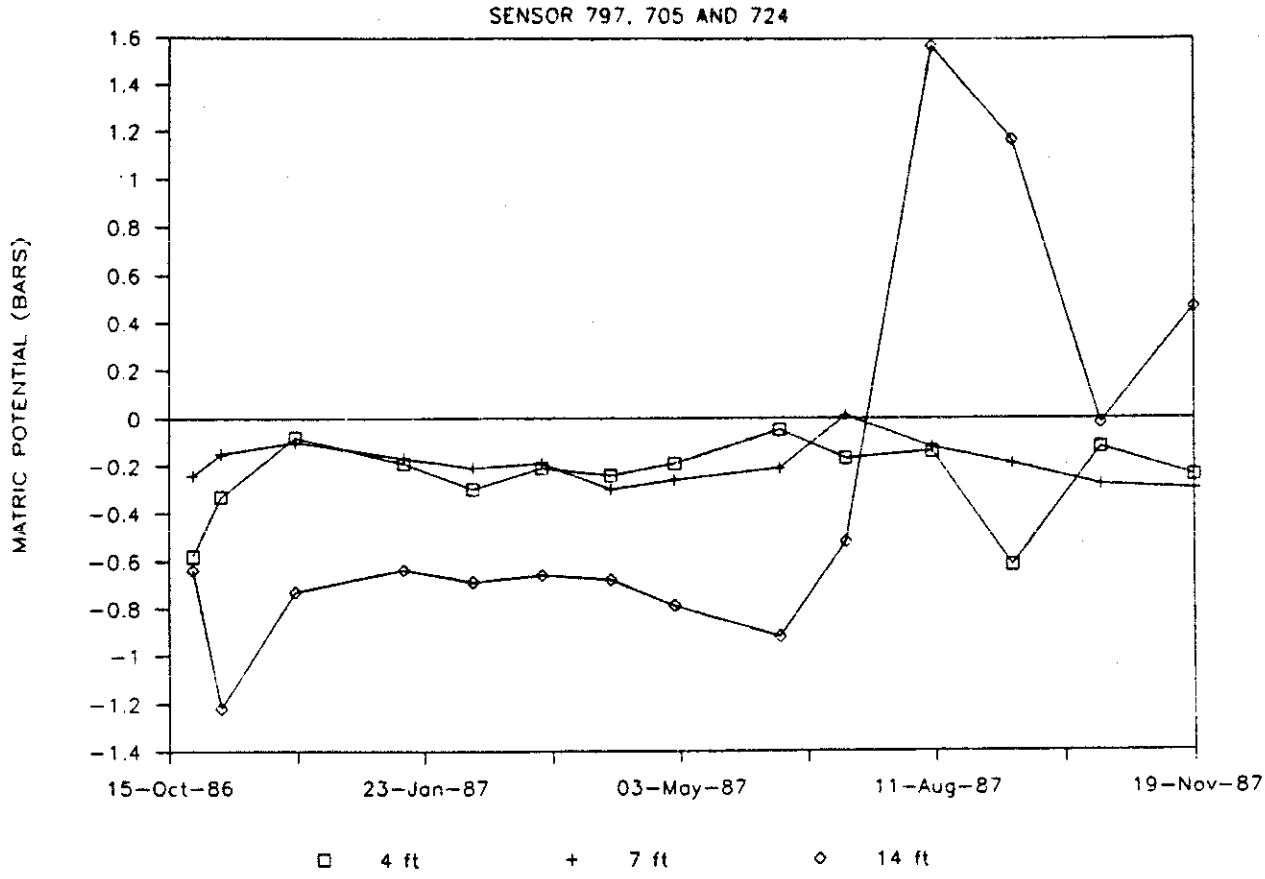

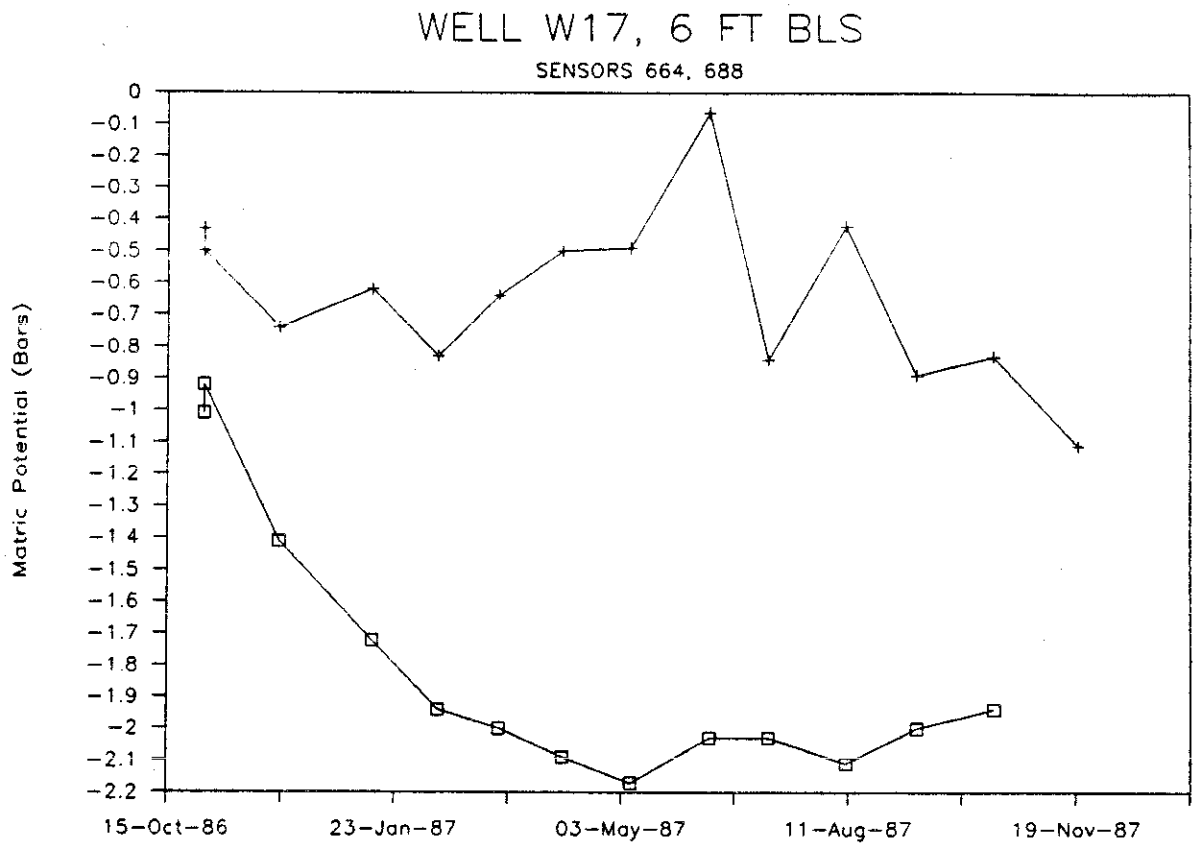
WELL W17, 6 FT BLS
SENSORS 664, 688
Matric Potential (Bars)
0
-0.1
-0.2
-0.3
-0.4
-0.5
-0.6
-0.7
-0.8
-0.9
-1
-1.1
-1.2
-1.3
-1.4
-1.5
-1.6
-1.7
-1.8
-1.9
-2
-2.1
-2.2
15-Oct-86
23-Jan-87
03-May-87
11-Aug-87
19-Nov-87

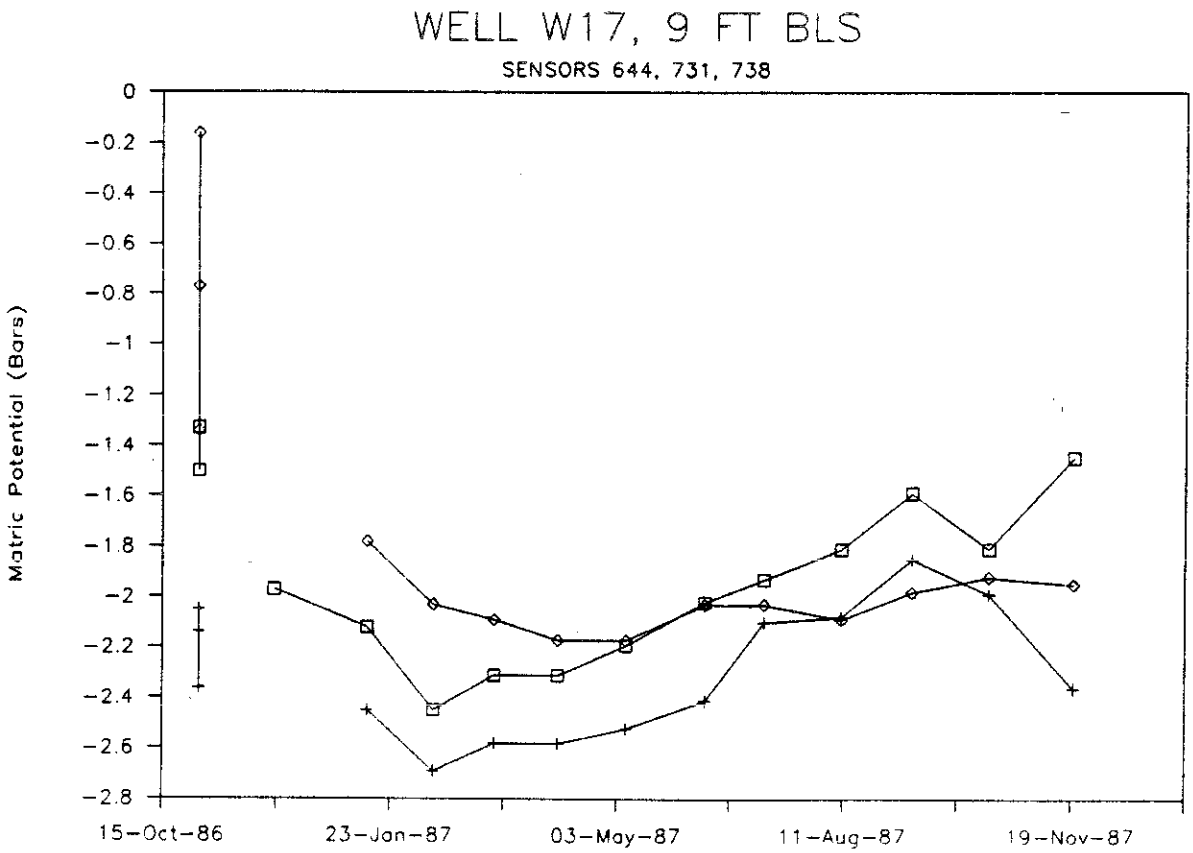
WELL W17, 9 FT BLS
SENSORS 644, 731, 738
Matric Potential (Bars)
0
-0.2
-0.4
-0.6
-0.8
-1
-1.2
-1.4
-1.6
-1.8
-2
-2.2
-2.4
-2.6
-2.8
15-Oct-86
23-Jan-87
03-May-87
11-Aug-87
19-Nov-87

WELL W18, 10 FT BLS

SENSORS 681, 706, 730

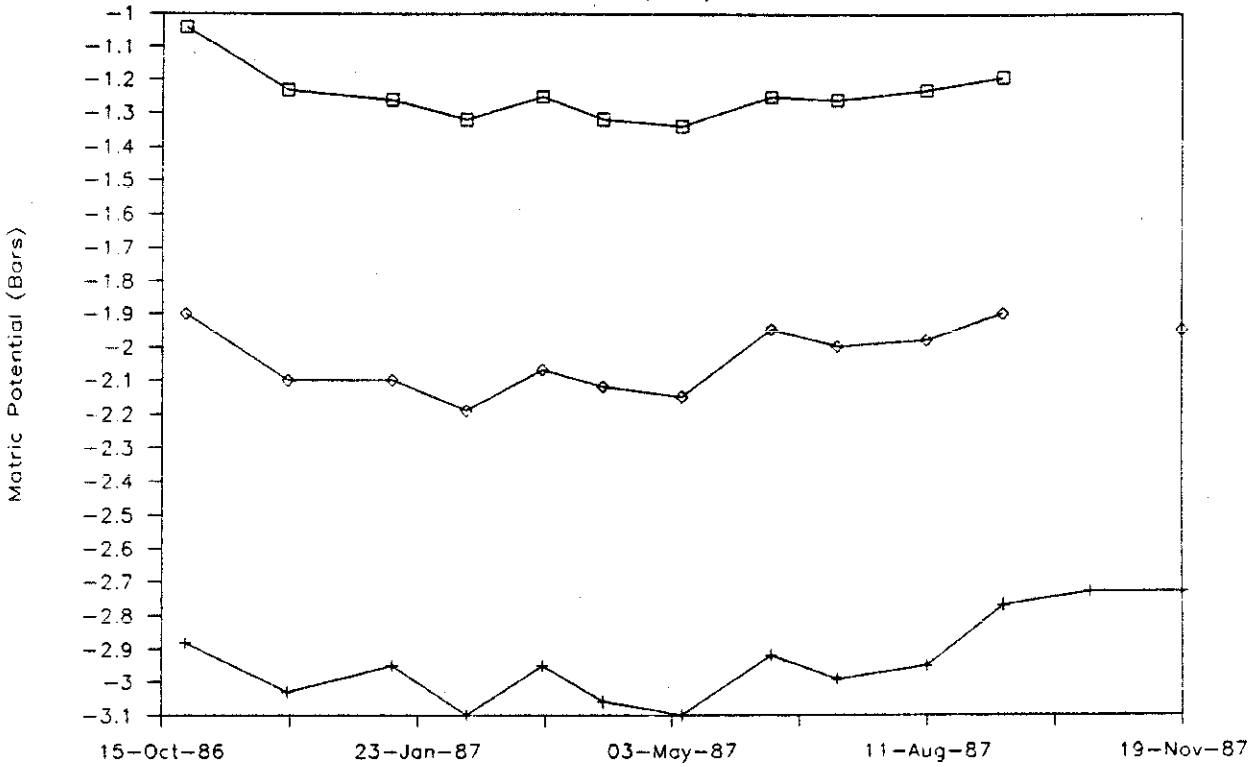

WELL W18, 16 FT BLS

SENSORS 557, 673, 686

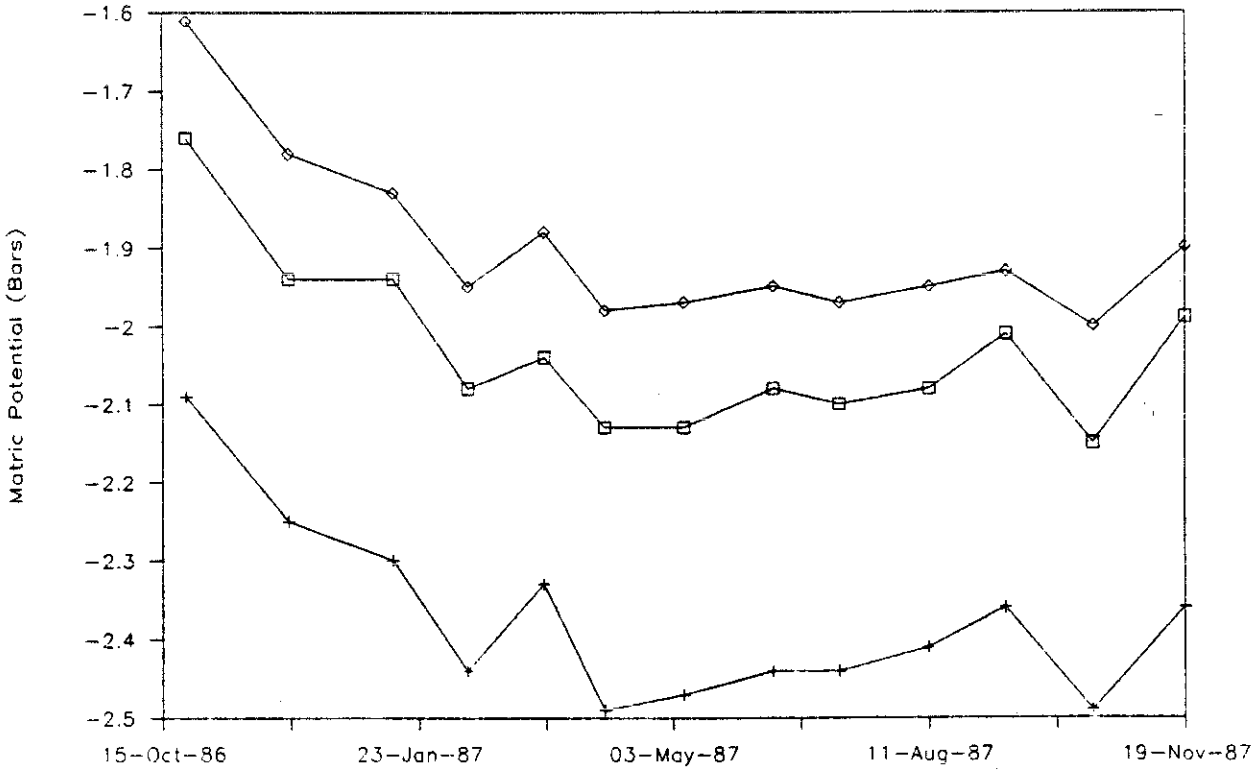

WELL W13, 3 FT BLS

SENSORS 658, 753, 761

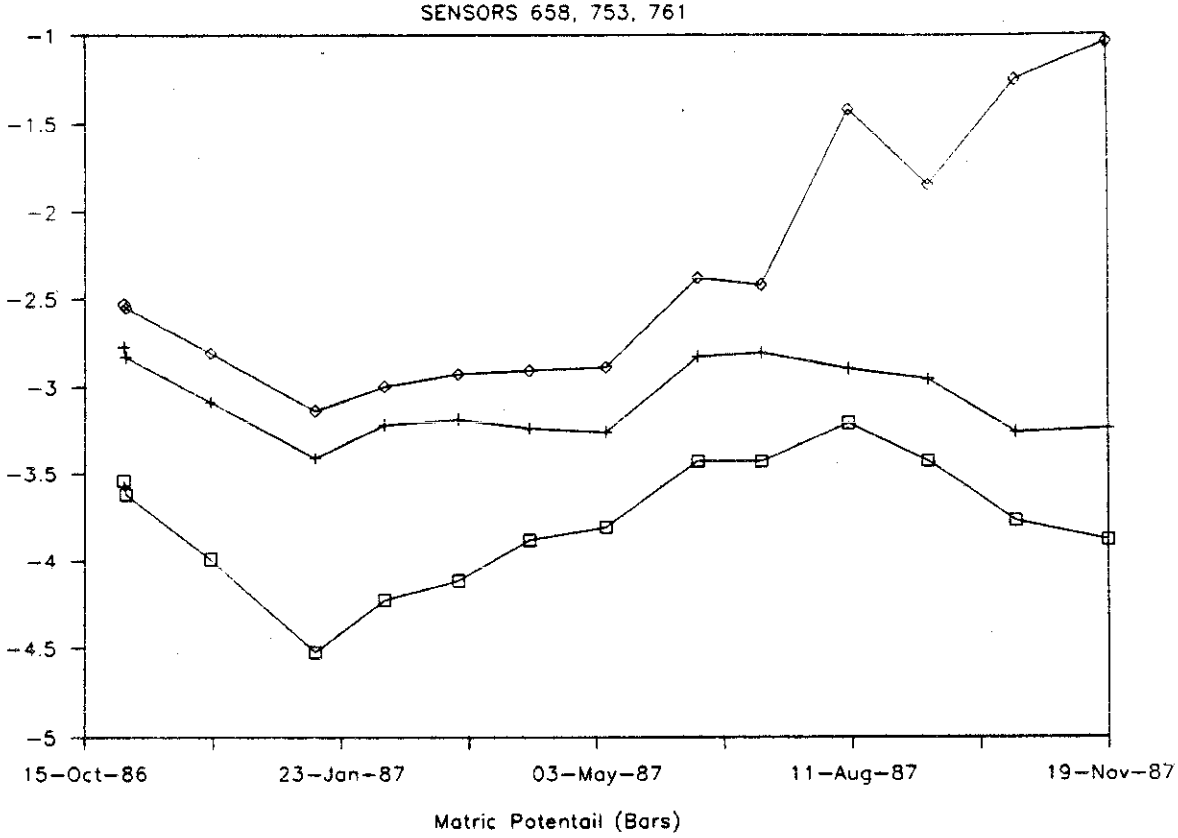

WELL W13, 6 FT BLS

SENSORS 035, 696, 707

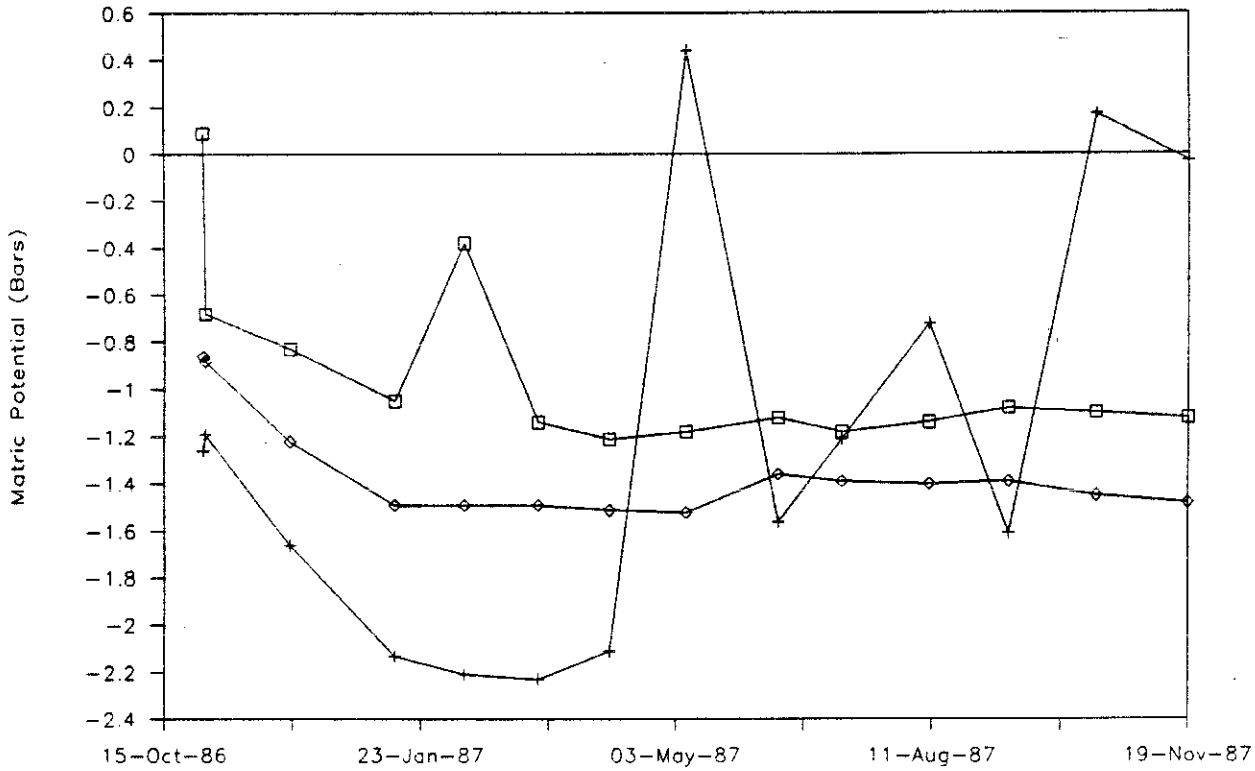

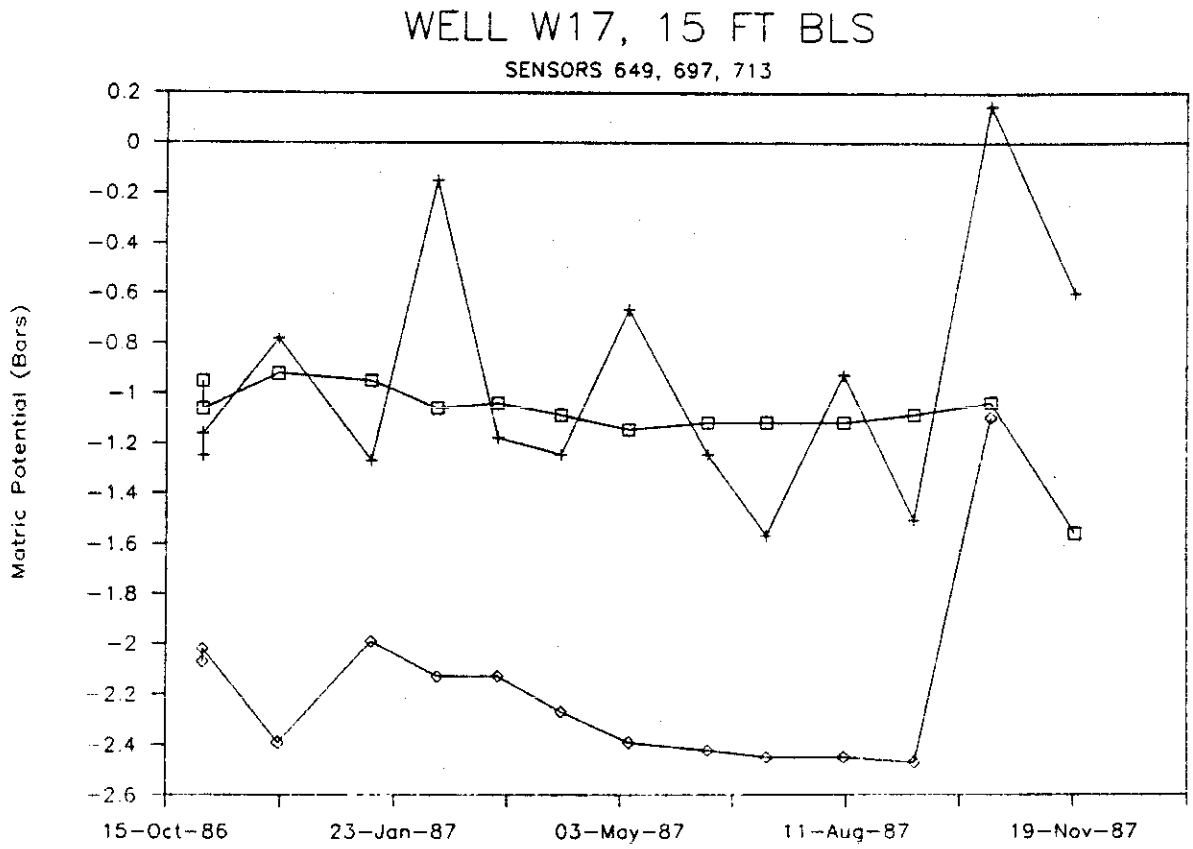
WELL W17, 15 FT BLS
SENSORS 649, 697, 713
Matric Potential (Bars)
0.2
0
-0.2
-0.4
-0.6
-0.8
-1
-1.2
-1.4
-1.6
-1.8
-2
-2.2
-2.4
-2.6
15-Oct-86
23-Jan-87
03-May-87
11-Aug-87
19-Nov-87

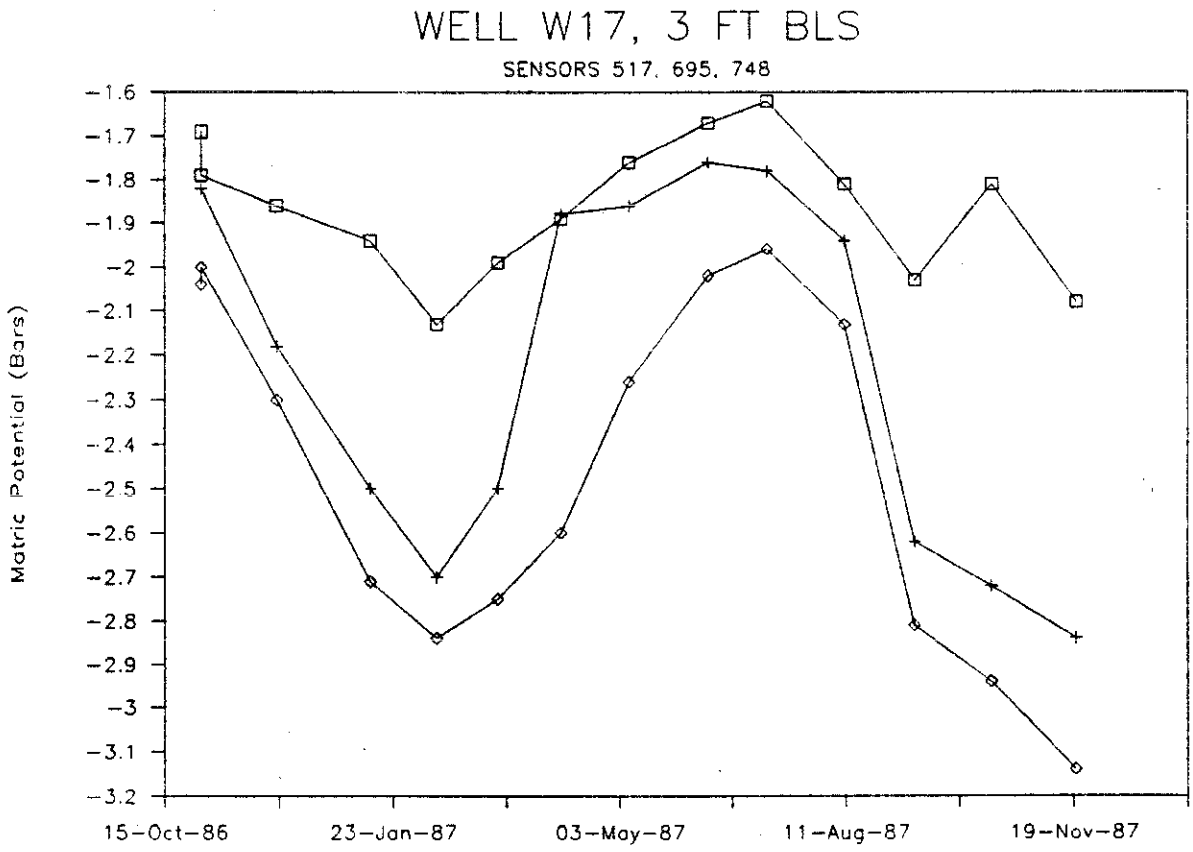
WELL W17, 3 FT BLS
SENSORS 517, 695, 748
Matric Potential (Bars)
-1.6
-1.7
-1.8
-1.9
-2
-2.1
-2.2
-2.3
-2.4
-2.5
-2.6
-2.7
-2.8
-2.9
-3
-3.1
-3.2
15-Oct-86
23-Jan-87
03-May-87
11-Aug-87
19-Nov-87

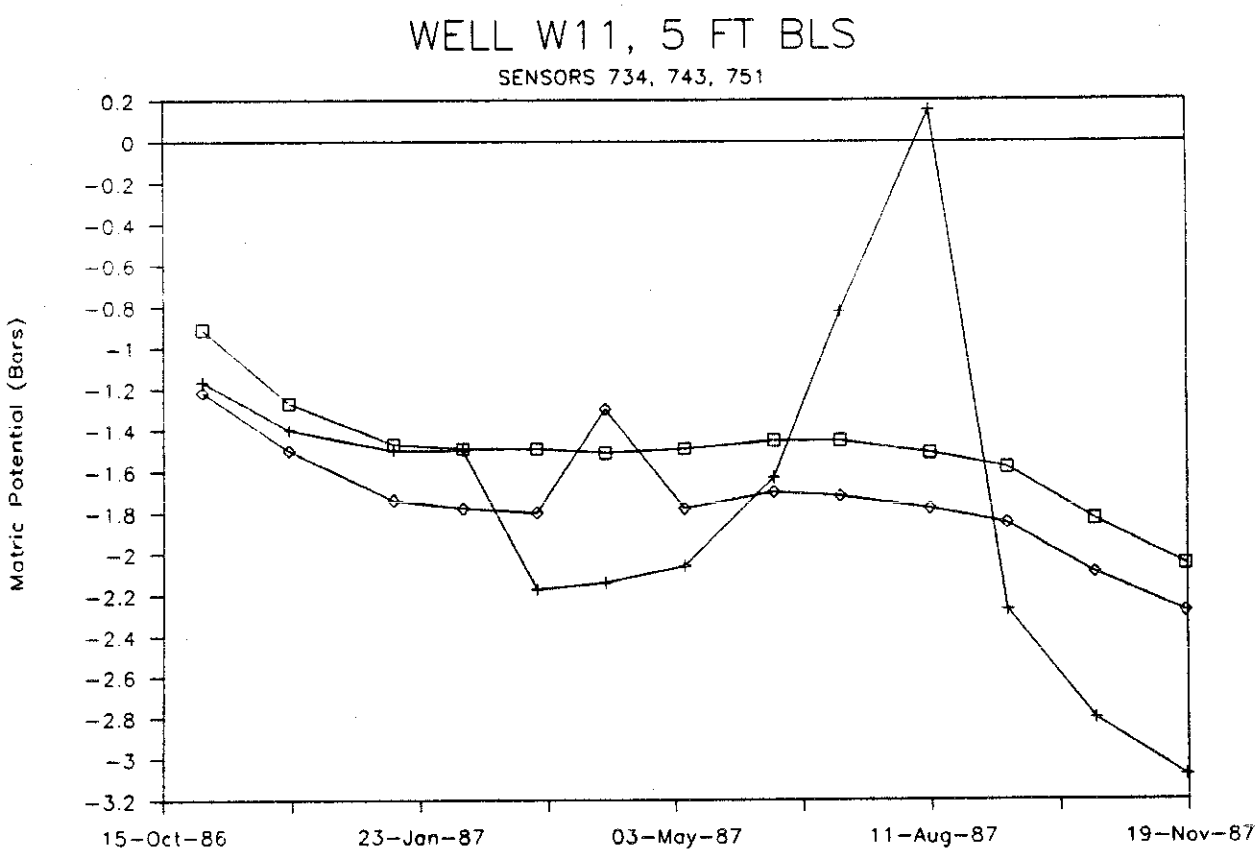
WELL W11, 5 FT BLS
SENSORS 734, 743, 751
Matric Potential (Bars)
0.2
0
-0.2
-0.4
-0.6
-0.8
-1
-1.2
-1.4
-1.6
-1.8
-2
-2.2
-2.4
-2.6
-2.8
-3
-3.2
15-Oct-86
23-Jan-87
03-May-87
11-Aug-87
19-Nov-87

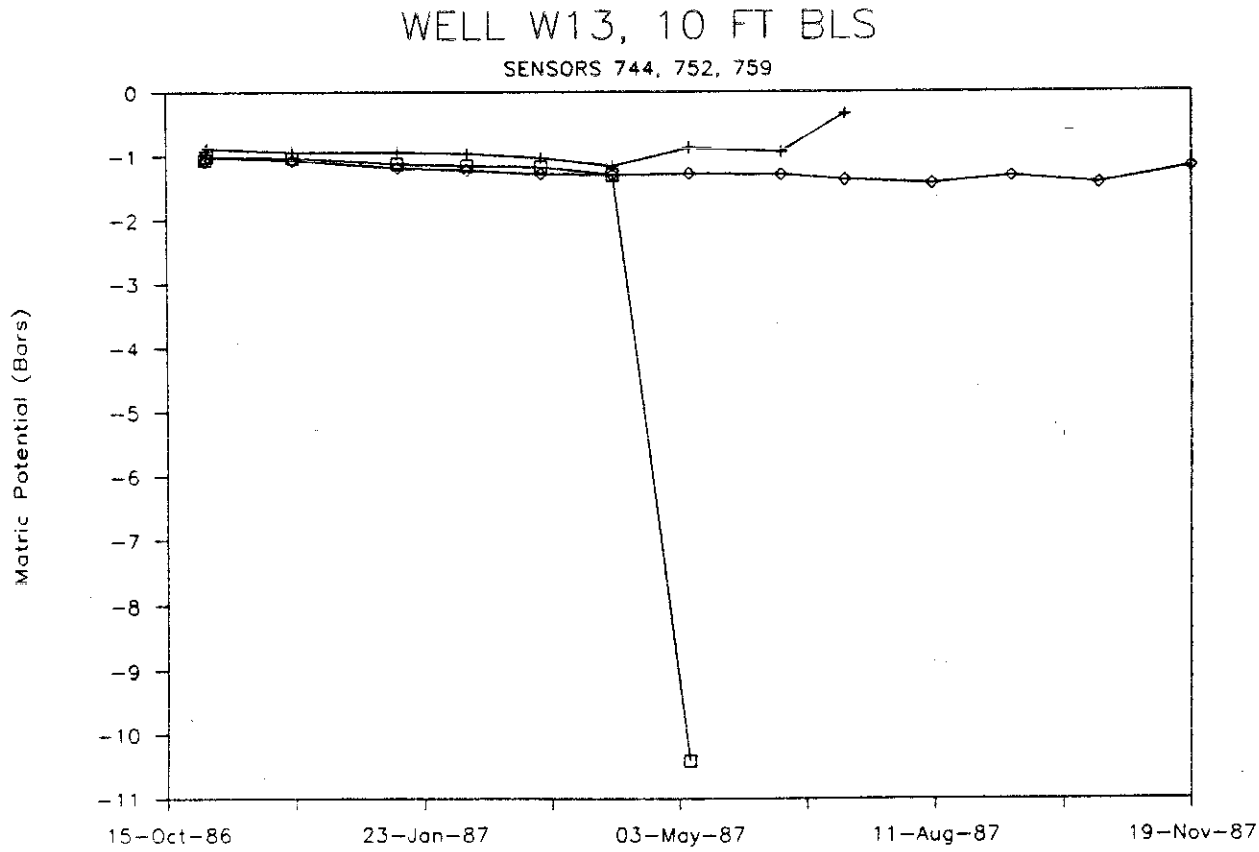
WELL W13, 10 FT BLS
SENSORS 744, 752, 759
Matric Potential (Bars)
0
-1
-2
-3
-4
-5
-6
-7
-8
-9
-10
-11
15-Oct-86
23-Jan-87
03-May-87
11-Aug-87
19-Nov-87

WELL W13, 13 FT BLS

SENSORS 684, 694, 745

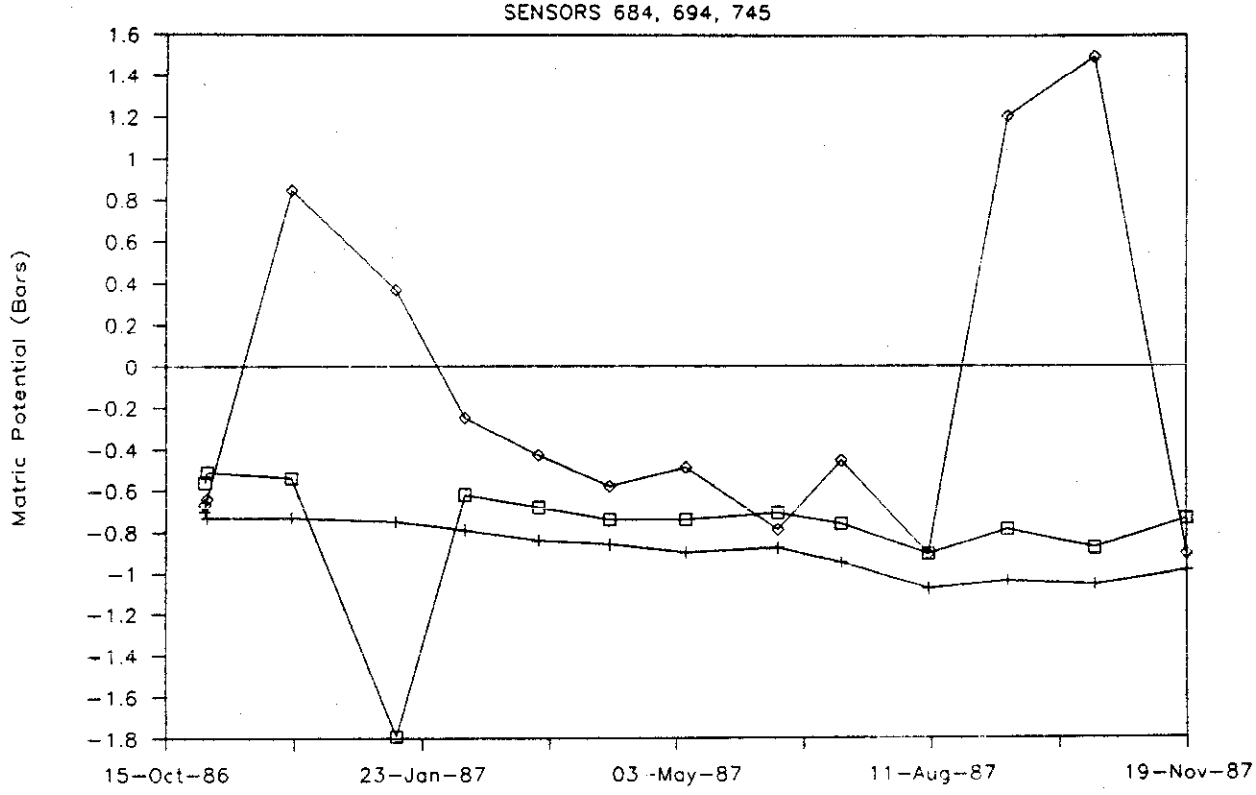

WELL W13, 17 FT BLS

SENSORS 749, 750, 763

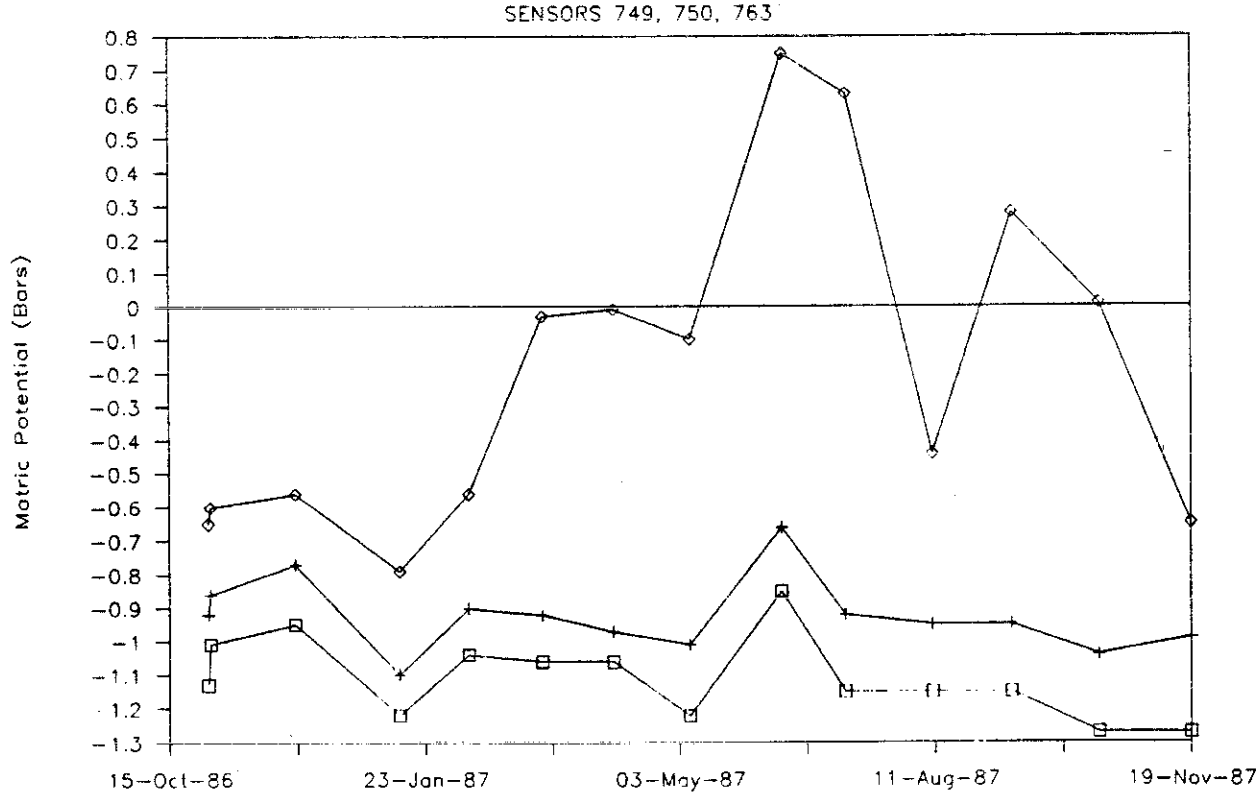

APPENDIX H
PSYCHROMETER DATA

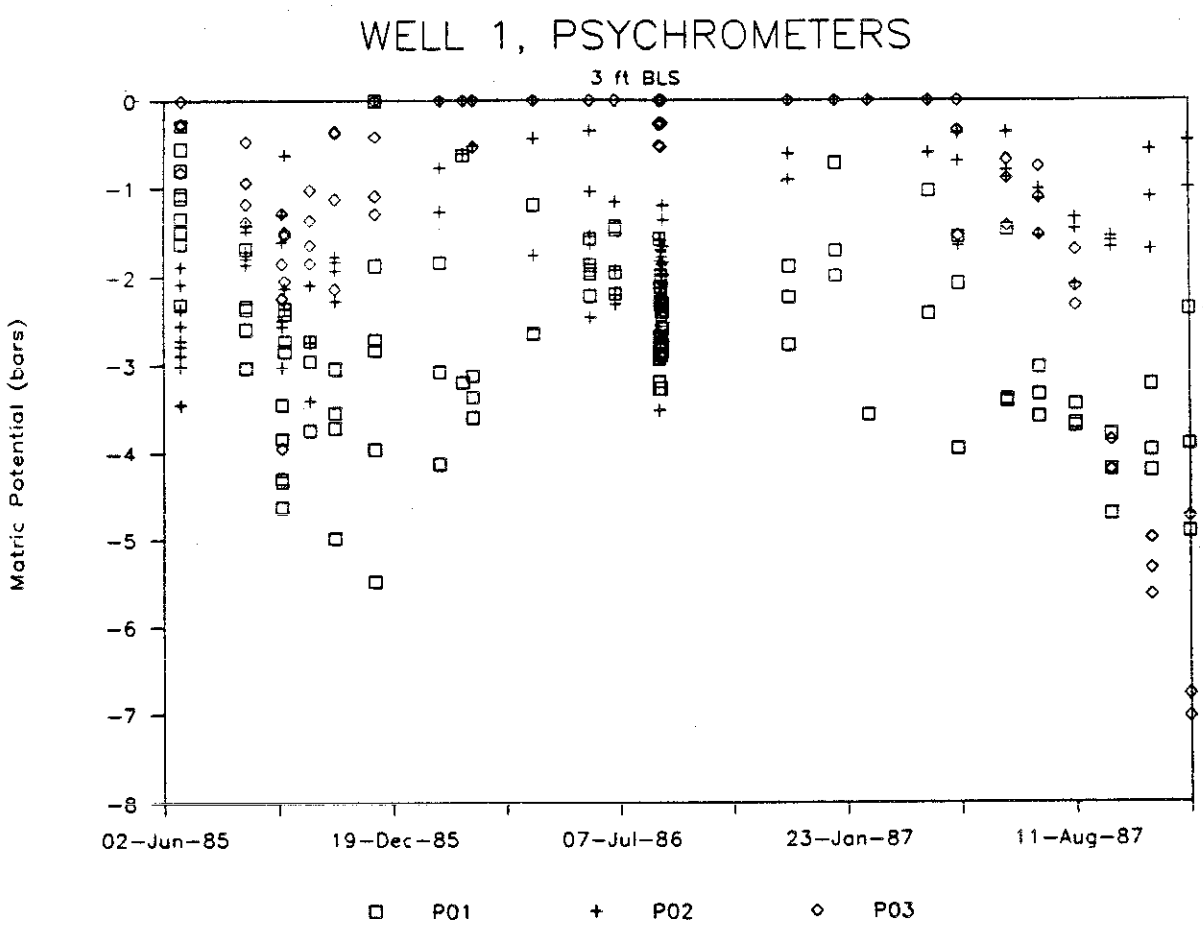
WELL 1, PSYCHROMETERS
3 ft BLS
Matric Potential (bars)
0
-1
-2
-3
-4
-5
-6
-7
-8
02-Jun-85
19-Dec-85
07-Jul-86
23-Jan-87
11-Aug-87
P01
P02
P03

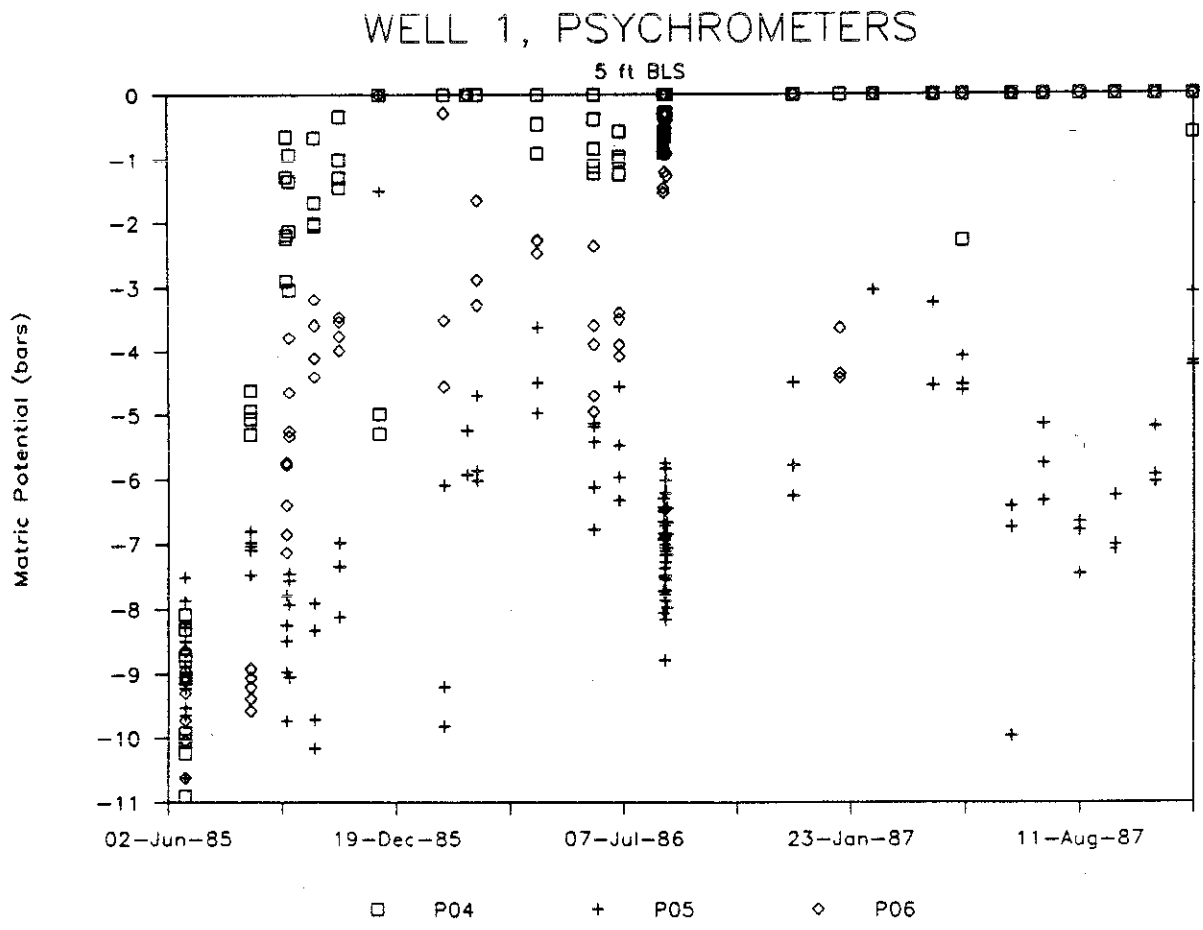
WELL 1, PSYCHROMETERS
5 ft BLS
Matric Potential (bars)
0
-1
-2
-3
-4
-5
-6
-7
-8
-9
-10
-11
02-Jun-85
19-Dec-85
07-Jul-86
23-Jan-87
11-Aug-87
P04
P05
P06

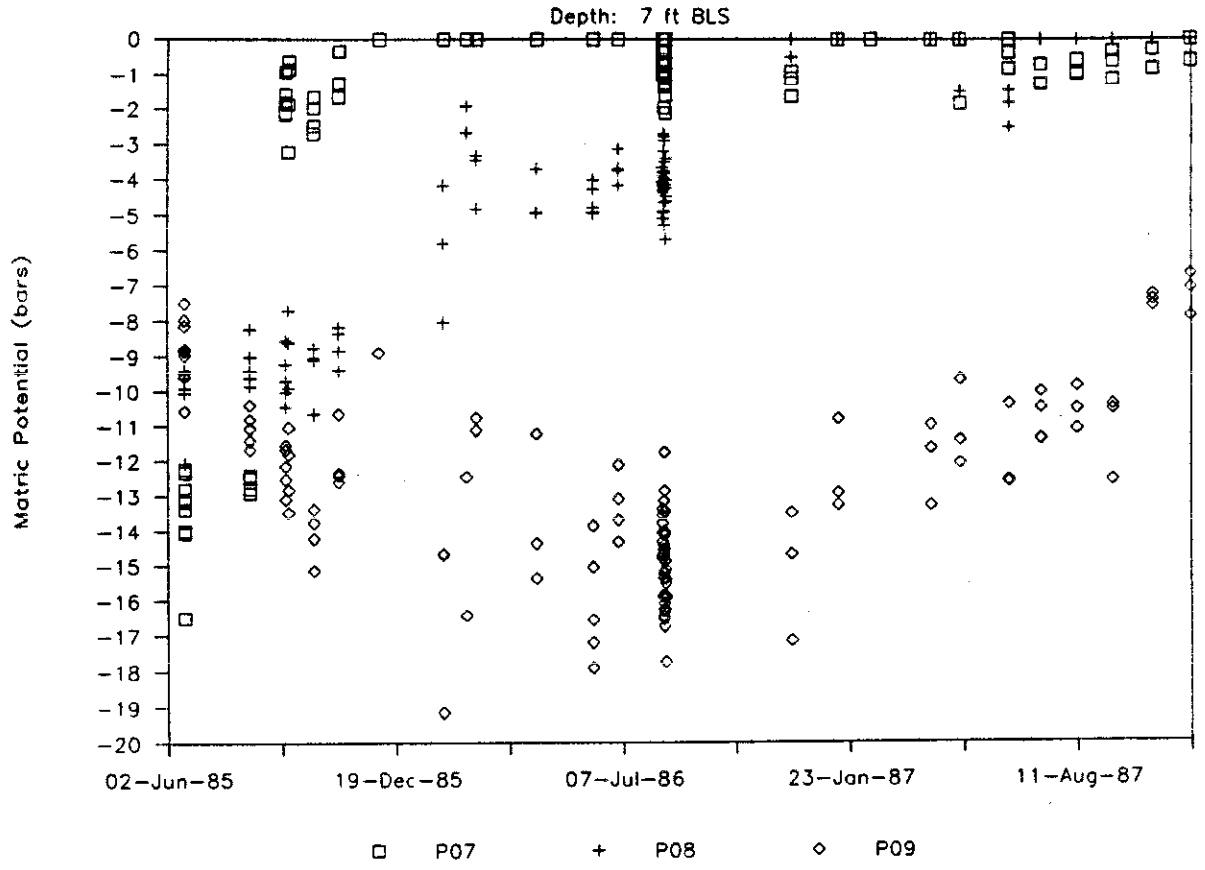
WELL 1, PSYCHROMETERS
Depth: 7 ft BLS
Matric Potential (bars)
0
-1
-2
-3
-4
-5
-6
-7
-8
-9
-10
-11
-12
-13
-14
-15
-16
-17
-18
-19
-20
02-Jun-85
19-Dec-85
07-Jul-86
23-Jan-87
11-Aug-87
P07
P08
P09

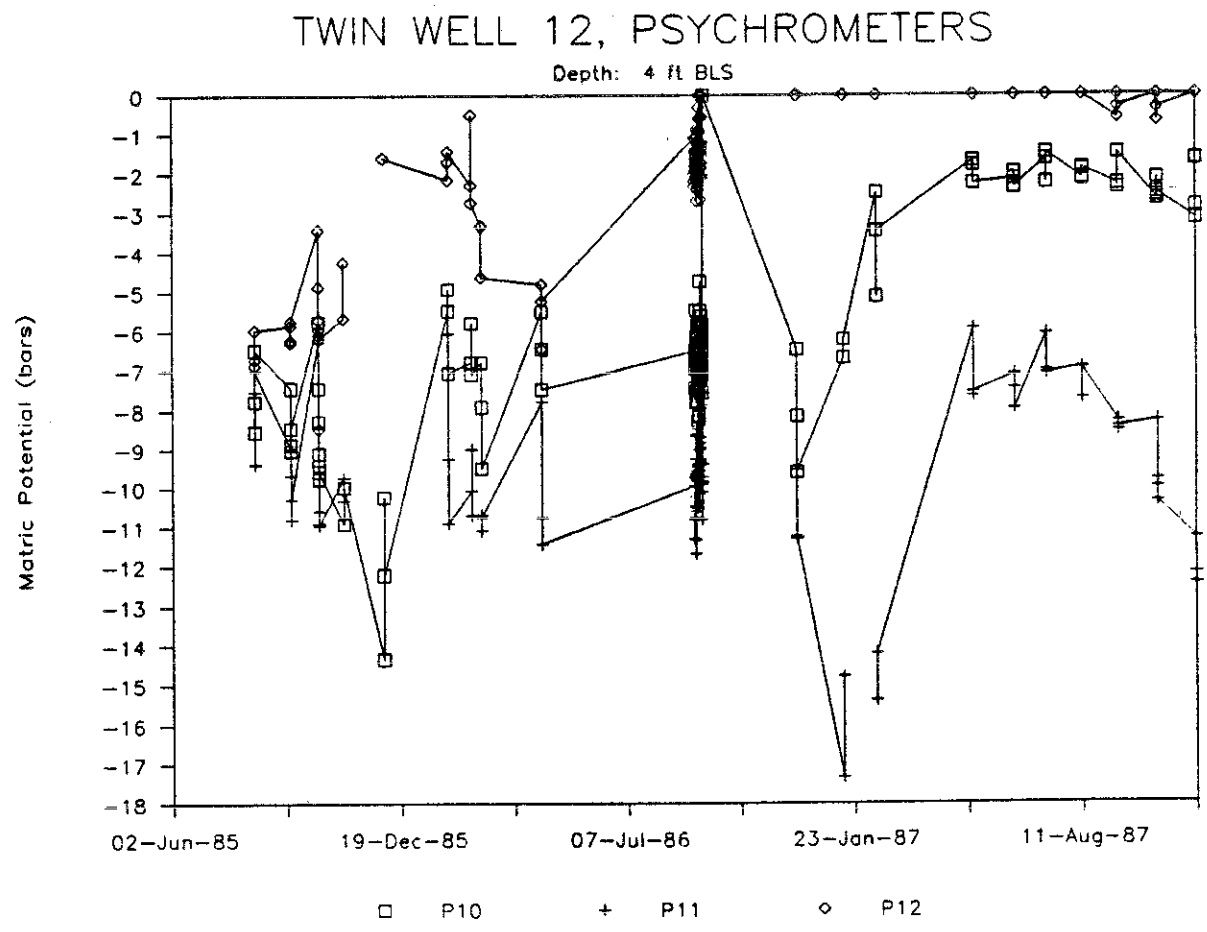
TWIN WELL 12, PSYCHROMETERS
Depth: 4 ft BLS
Matric Potential (bars)
0
-1
-2
-3
-4
-5
-6
-7
-8
-9
-10
-11
-12
-13
-14
-15
-16
-17
-18
02-Jun-85
19-Dec-85
07-Jul-86
23-Jan-87
11-Aug-87
P10
P11
P12

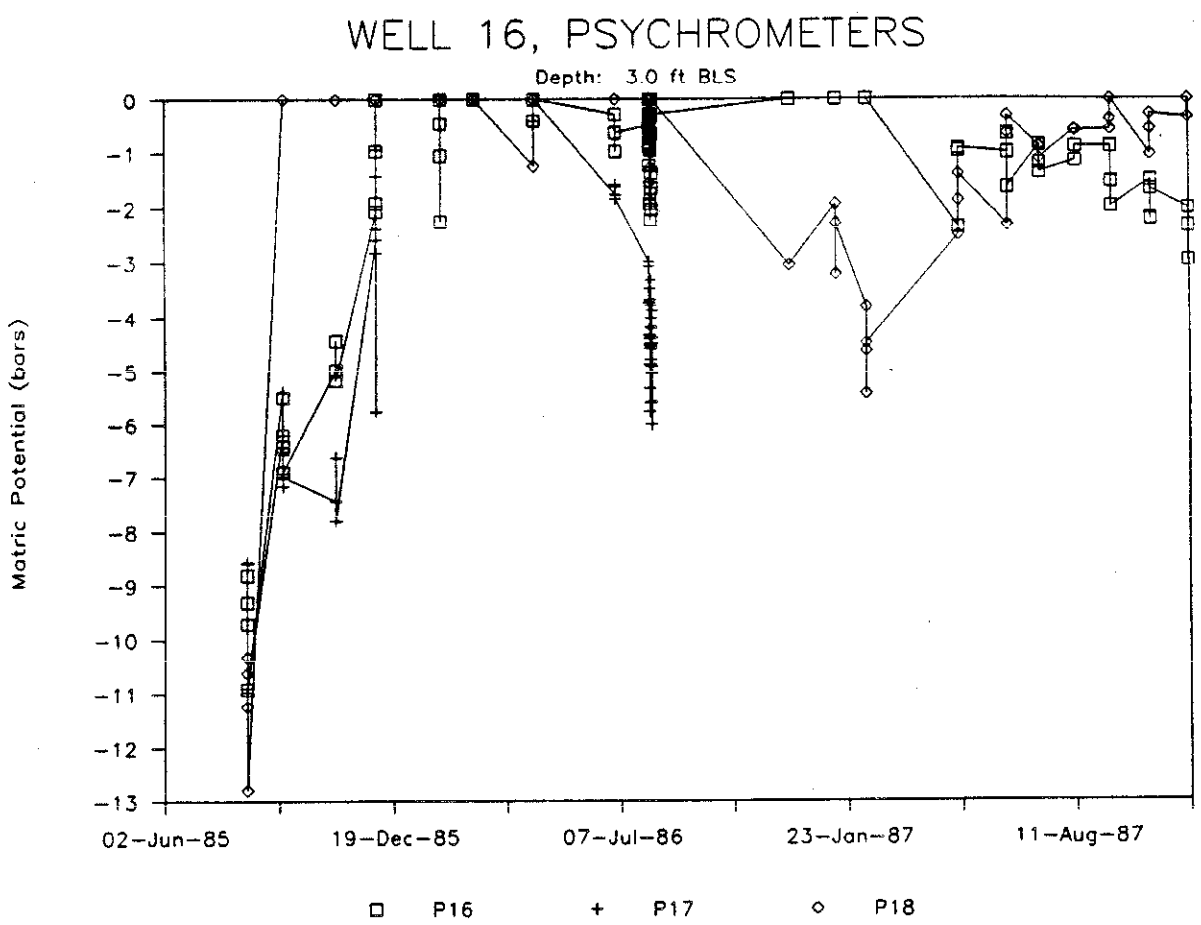
WELL 16, PSYCHROMETERS
Depth: 3.0 ft BLS
Matric Potential (bars)
0
-1
-2
-3
-4
-5
-6
-7
-8
-9
-10
-11
-12
-13
02-Jun-85
19-Dec-85
07-Jul-86
23-Jan-87
11-Aug-87
P16
P17
P18

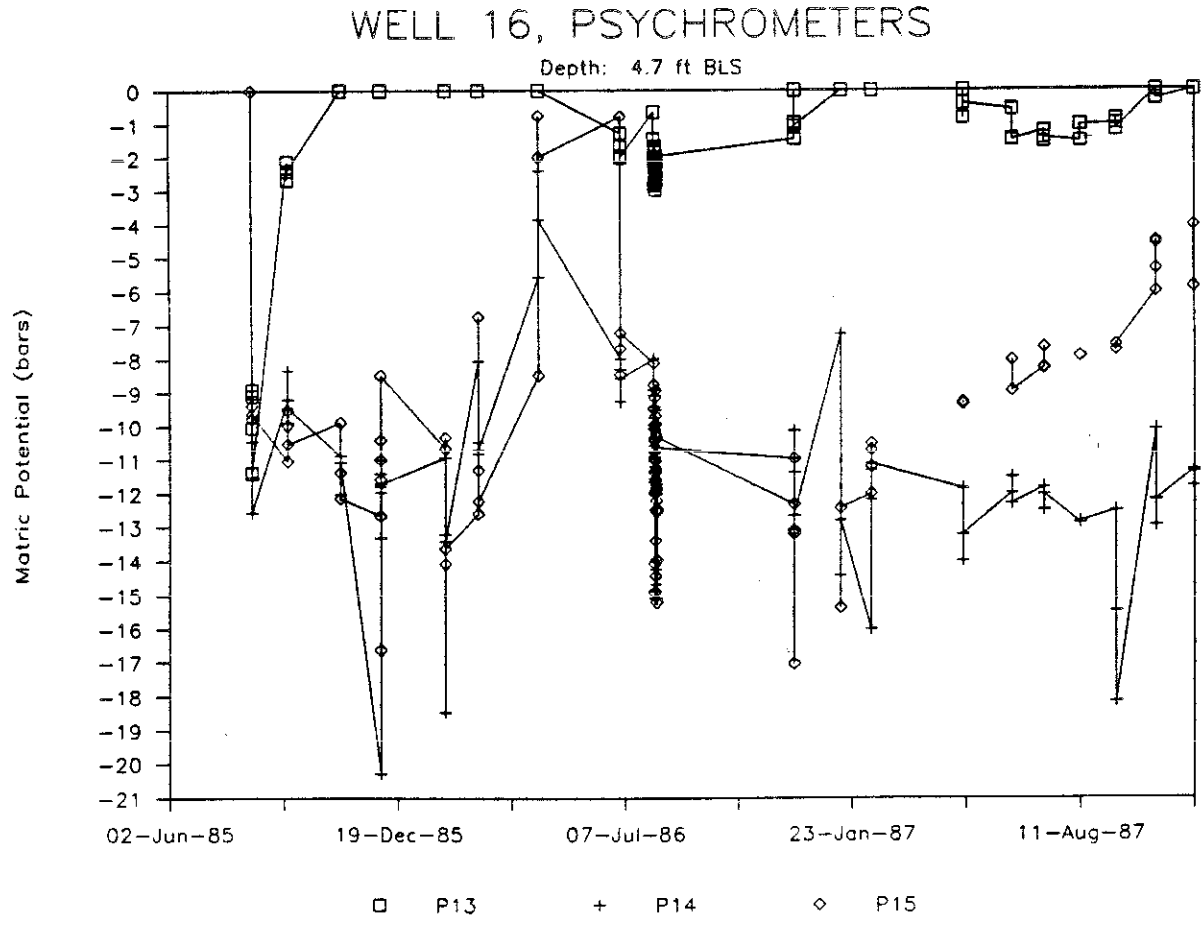
WELL 16, PSYCHROMETERS
Depth: 4.7 ft BLS
Matric Potential (bars)
0
-1
-2
-3
-4
-5
-6
-7
-8
-9
-10
-11
-12
-13
-14
-15
-16
-17
-18
-19
-20
-21
02-Jun-85
19-Dec-85
07-Jul-86
23-Jan-87
11-Aug-87
P13
P14
P15

WELL 18, PSYCHROMETERS

Depth: 2 ft BLS

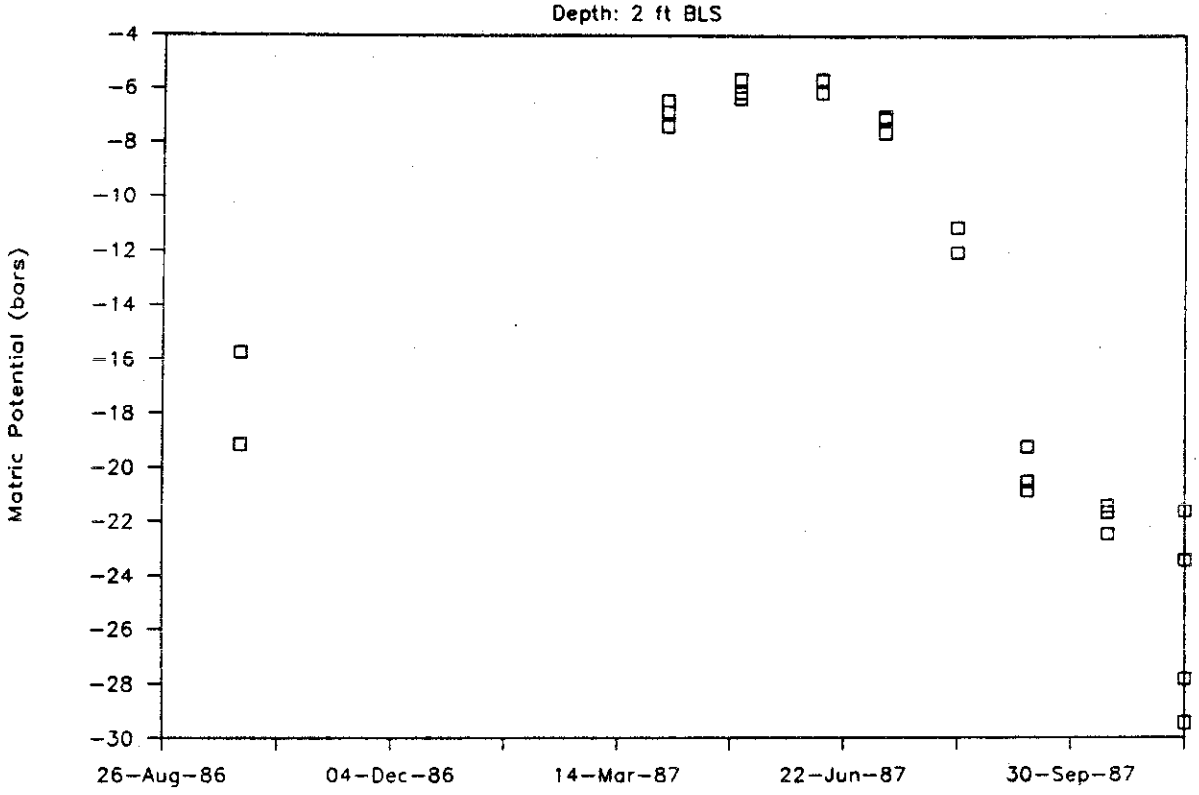

□ P50

WELL 18, PSYCHROMETERS

Depth: 3 ft BLS

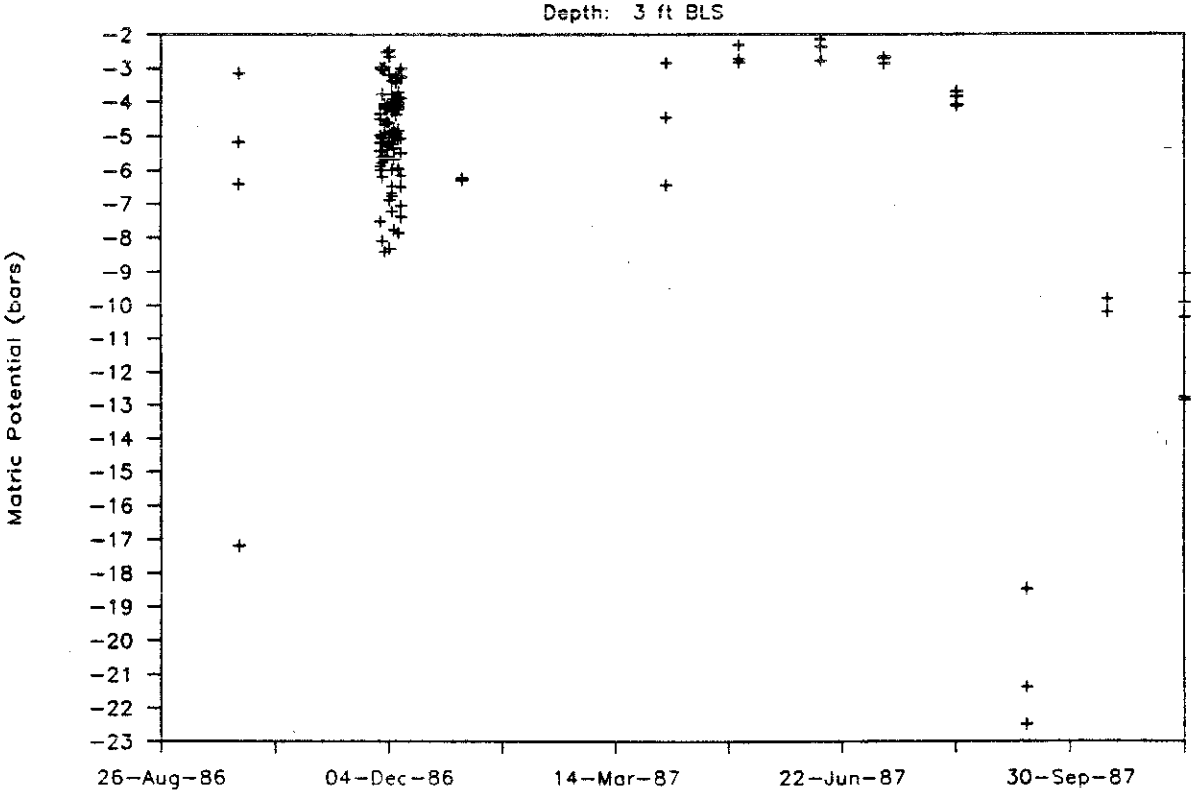

\+ P51

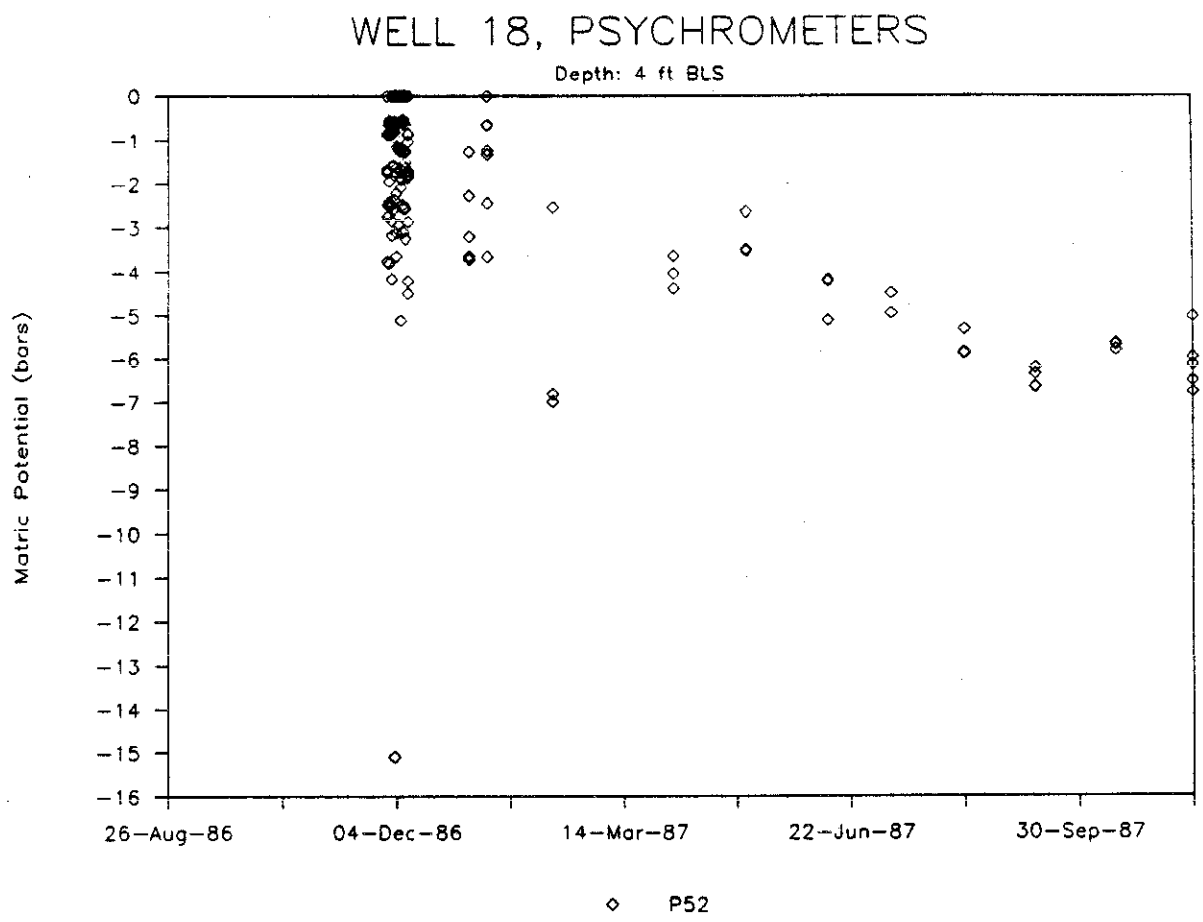
WELL 18, PSYCHROMETERS
Depth: 4 ft BLS
Matric Potential (bars)
0
-1
-2
-3
-4
-5
-6
-7
-8
-9
-10
-11
-12
-13
-14
-15
-16
26-Aug-86
04-Dec-86
14-Mar-87
22-Jun-87
30-Sep-87
P52

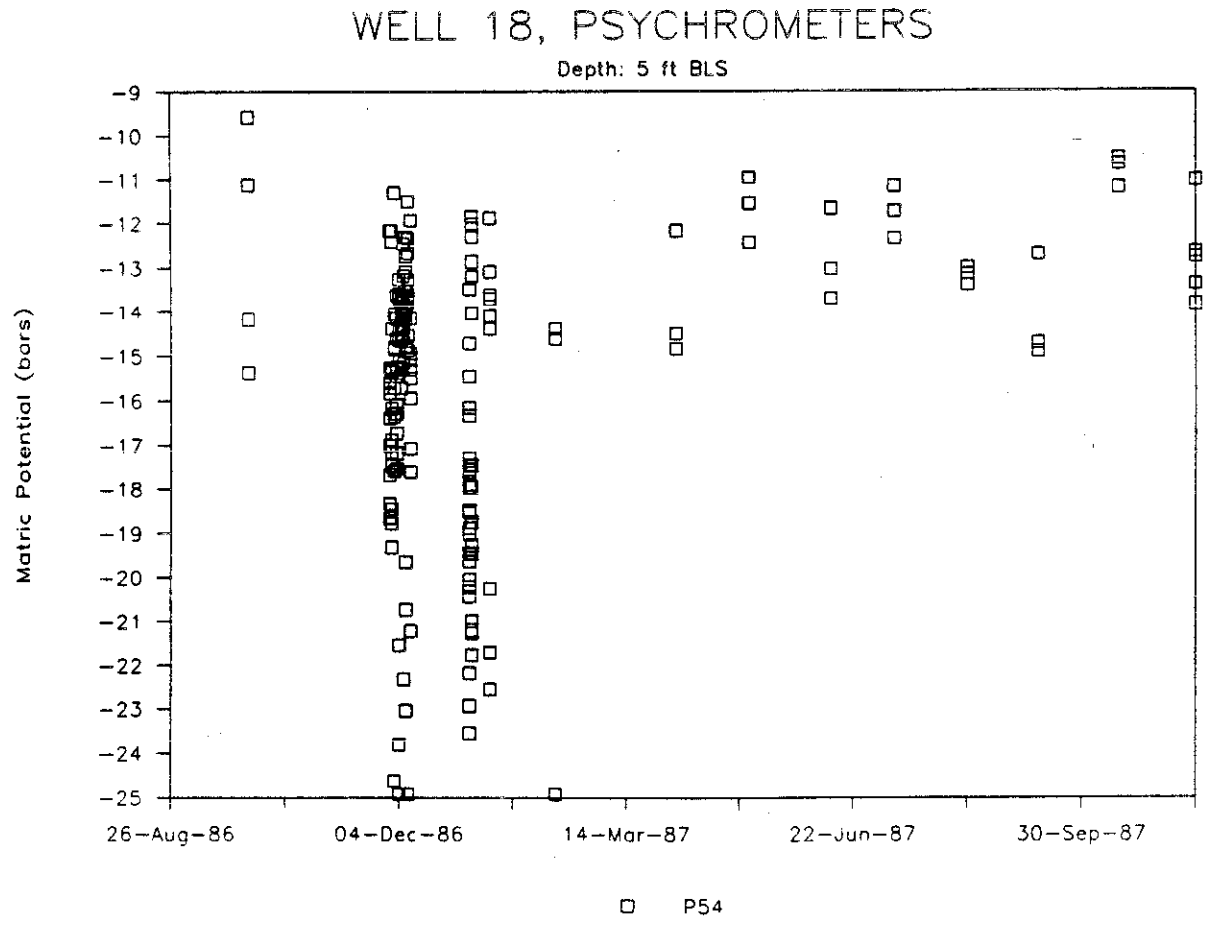
WELL 18, PSYCHROMETERS
Depth: 5 ft BLS
Matric Potential (bars)
-9
-10
-11
-12
-13
-14
-15
-16
-17
-18
-19
-20
-21
-22
-23
-24
-25
26-Aug-86
04-Dec-86
14-Mar-87
22-Jun-87
30-Sep-87
P54

WELL 18, PSYCHROMETERS

Depth: 6 ft LBS

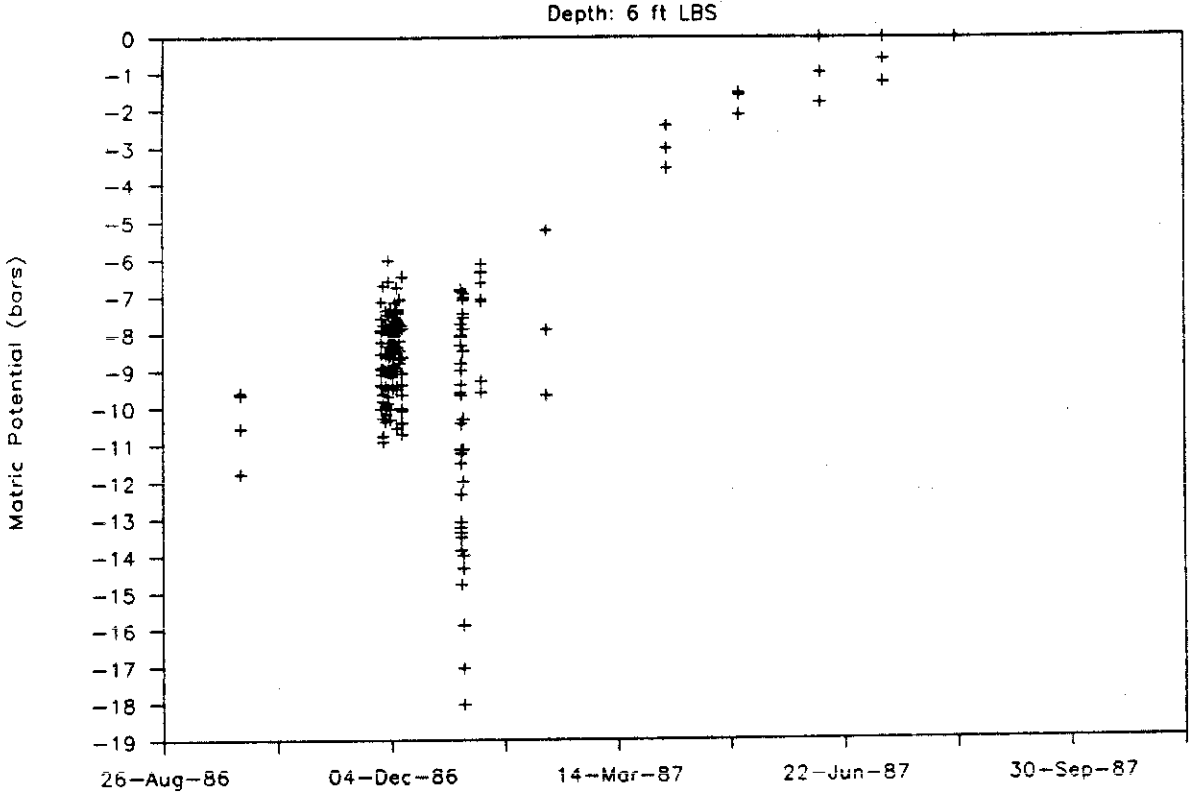

+ P55

WELL 18, PSYCHROMETERS

Depth: 7 ft BLS

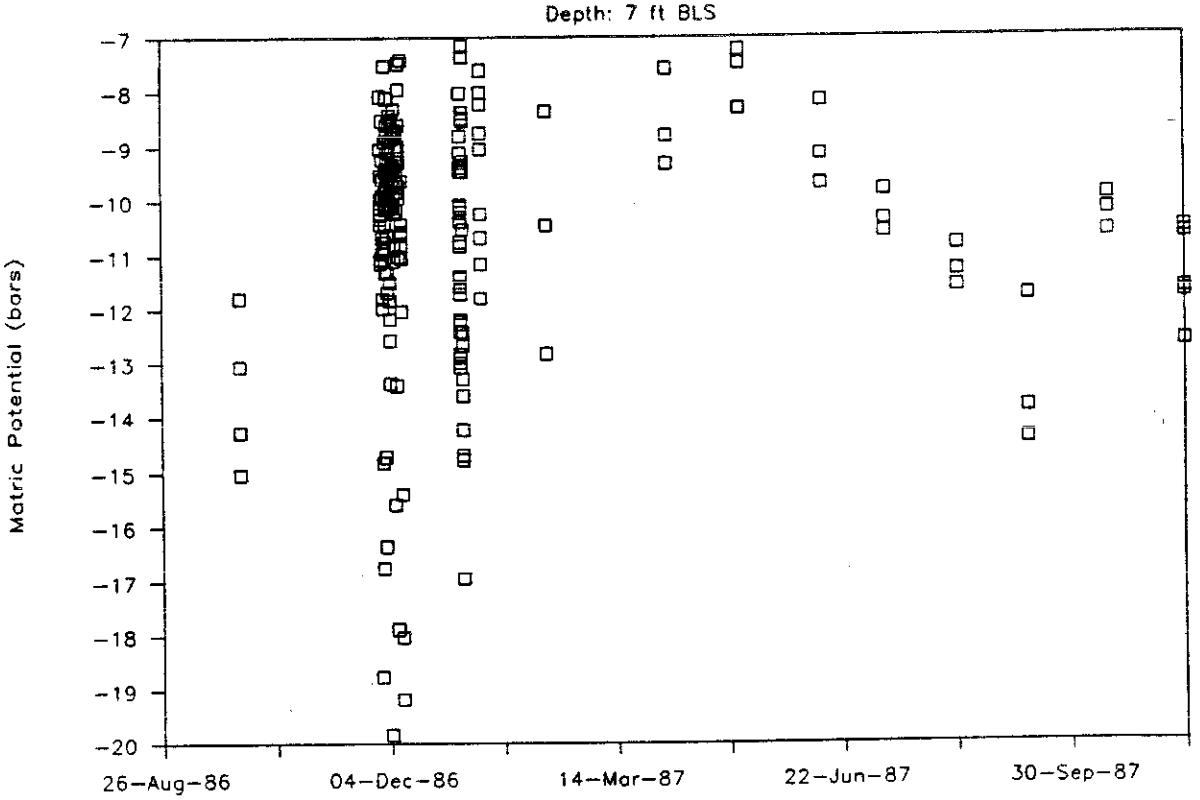

□ P56

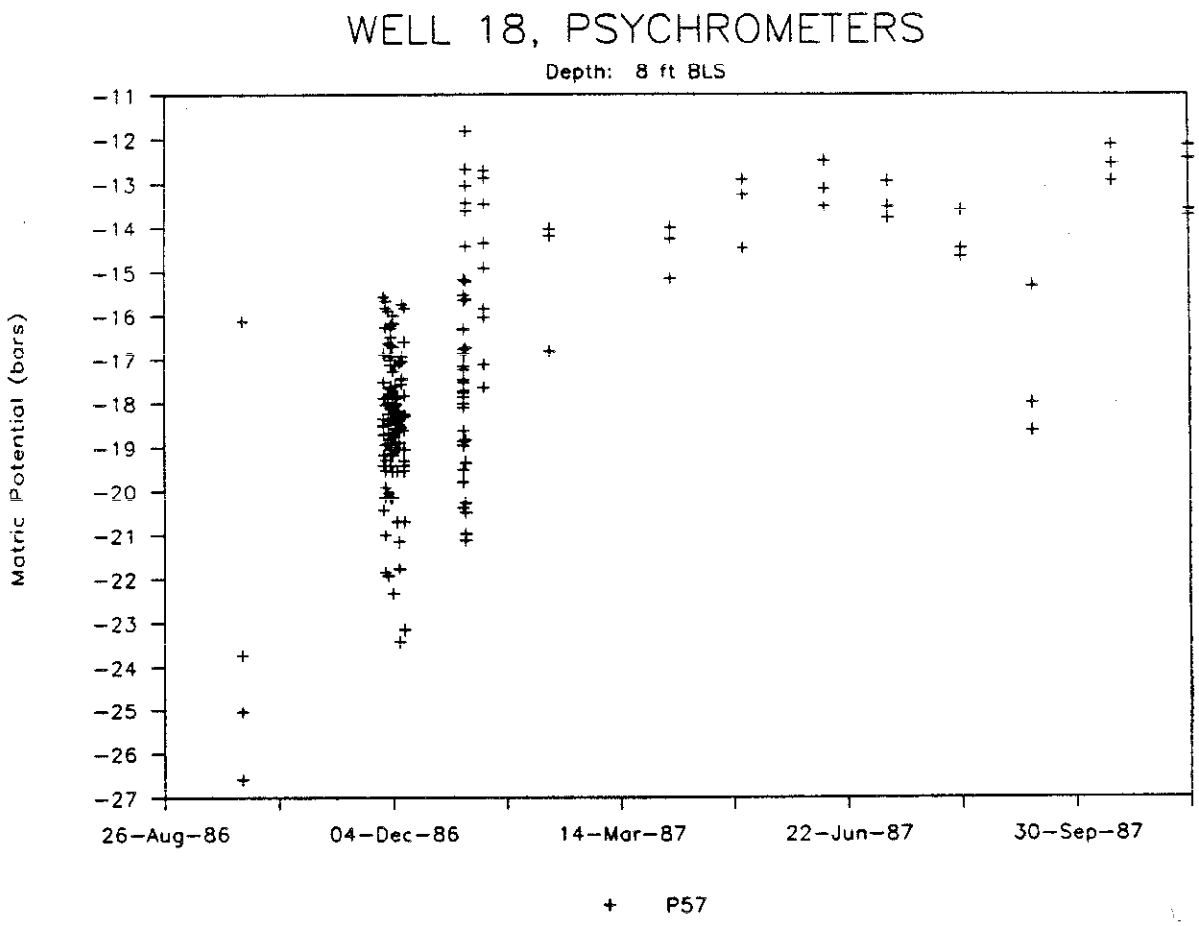
WELL 18, PSYCHROMETERS
Depth: 8 ft BLS
Matric Potential (bars)
-11
-12
-13
-14
-15
-16
-17
-18
-19
-20
-21
-22
-23
-24
-25
-26
-27
26-Aug-86
04-Dec-86
14-Mar-87
22-Jun-87
30-Sep-87
+ P57

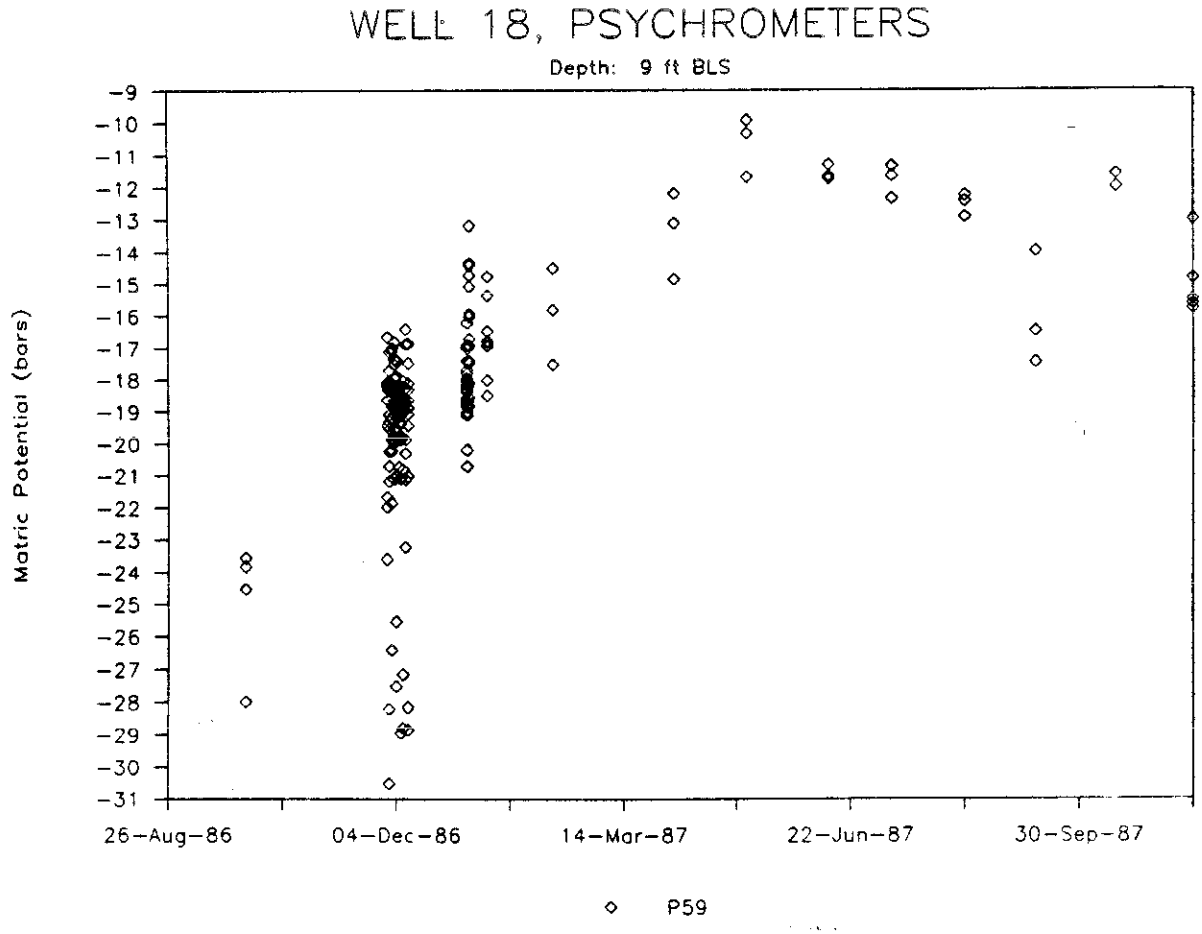
WELL 18, PSYCHROMETERS
Depth: 9 ft BLS
Matric Potential (bars)
-9
-10
-11
-12
-13
-14
-15
-16
-17
-18
-19
-20
-21
-22
-23
-24
-25
-26
-27
-28
-29
-30
-31
26-Aug-86
04-Dec-86
14-Mar-87
22-Jun-87
30-Sep-87
◇ P59

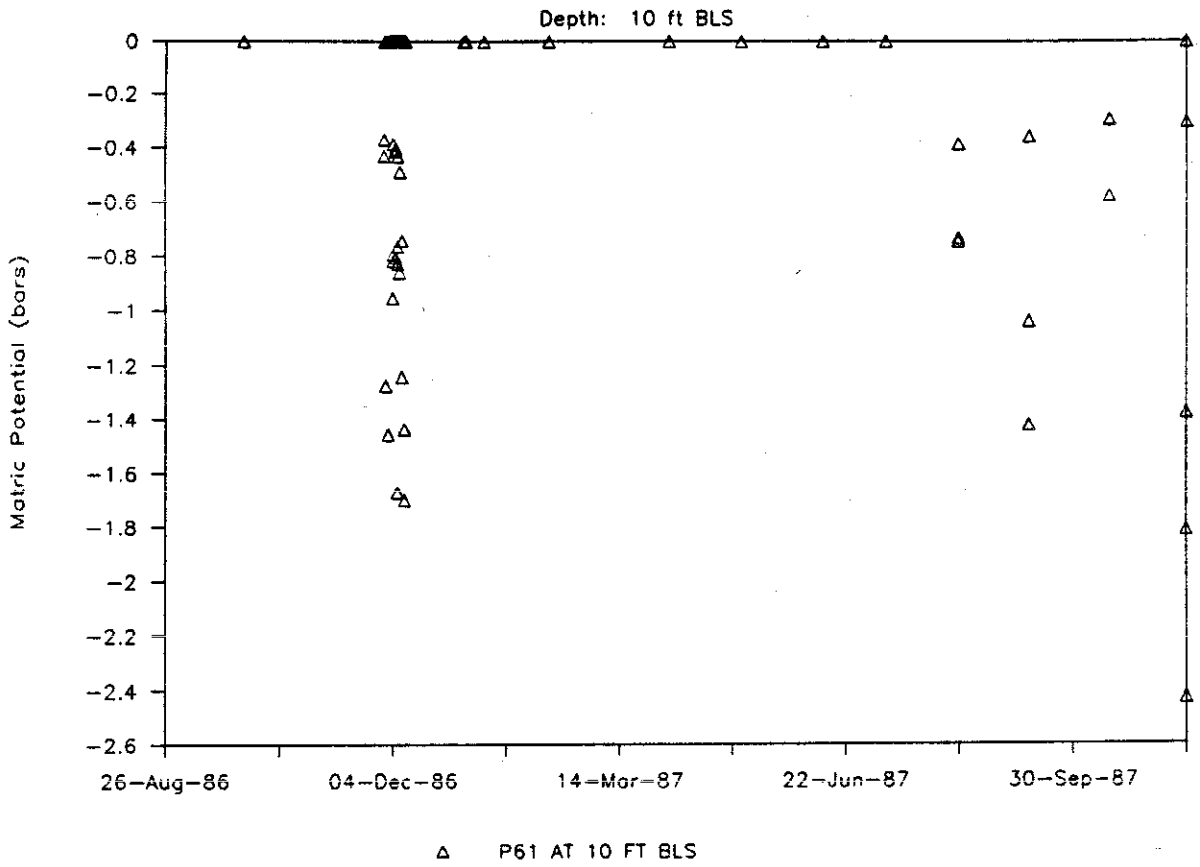
WELL 18, PSYCHROMETERS
Depth: 10 ft BLS
Matric Potential (bars)
0
-0.2
-0.4
-0.6
-0.8
-1
-1.2
-1.4
-1.6
-1.8
-2
-2.2
-2.4
-2.6
26-Aug-86
04-Dec-86
14-Mar-87
22-Jun-87
30-Sep-87
P61 AT 10 FT BLS

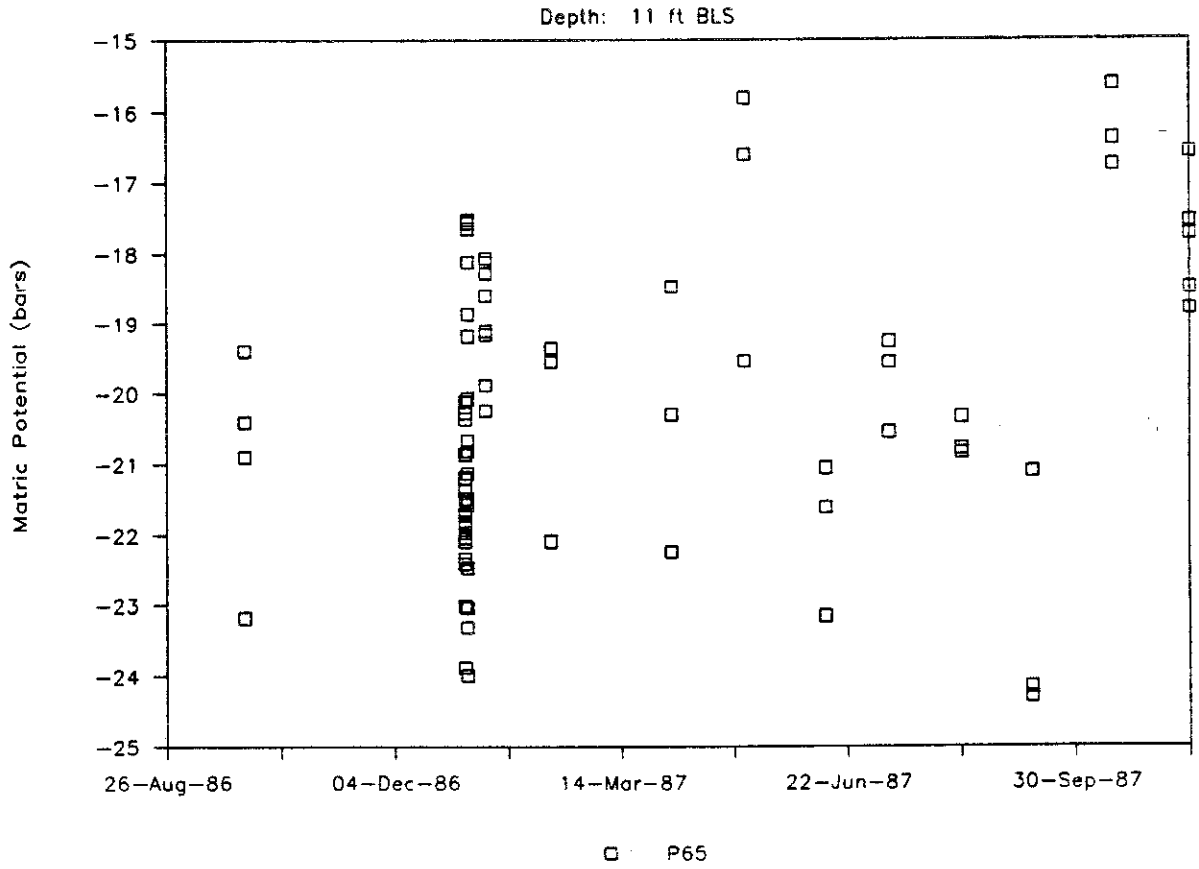
WELL 18, PSYCHROMETERS
Depth: 11 ft BLS
Matric Potential (bars)
-15
-16
-17
-18
-19
-20
-21
-22
-23
-24
-25
26-Aug-86
04-Dec-86
14-Mar-87
22-Jun-87
30-Sep-87
P65

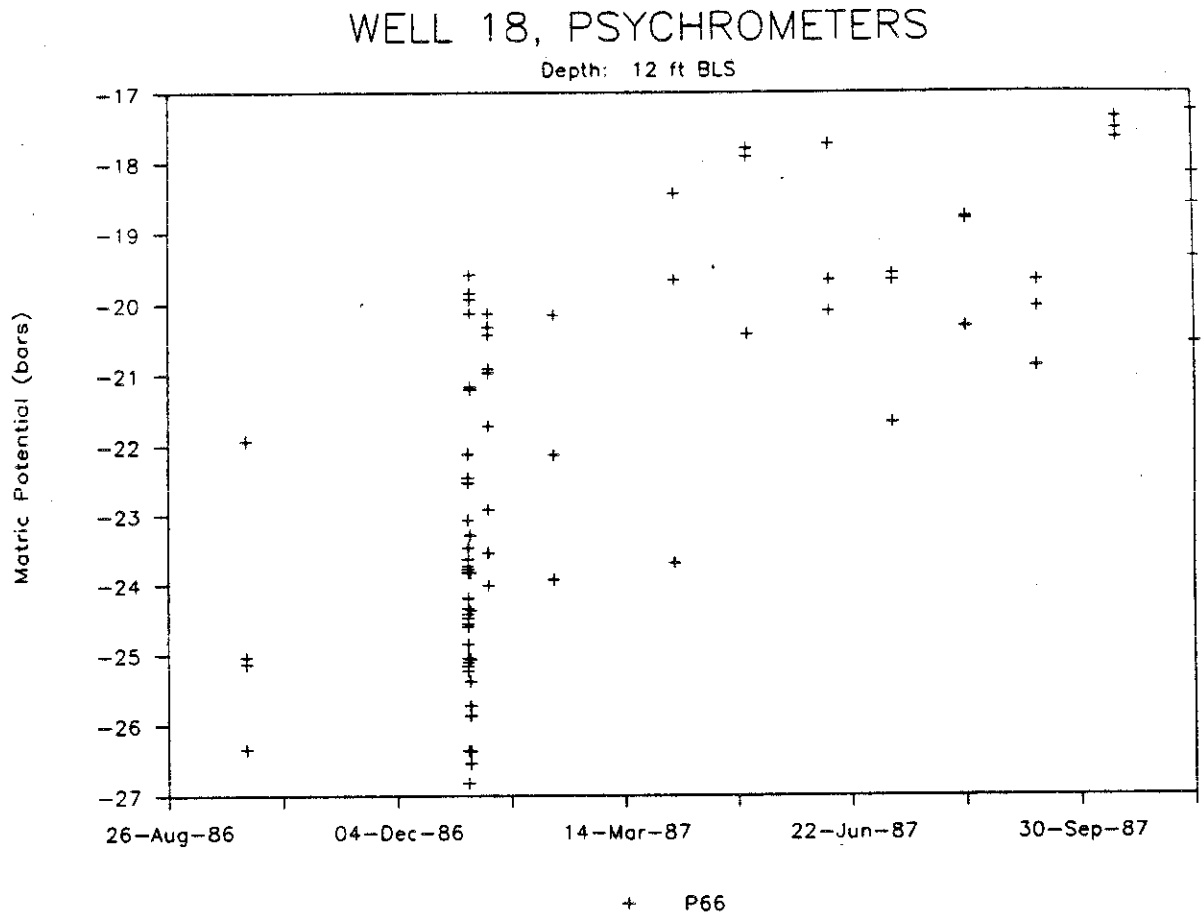
WELL 18, PSYCHROMETERS
Depth: 12 ft BLS
Matric Potential (bars)
-17
-18
-19
-20
-21
-22
-23
-24
-25
-26
-27
26-Aug-86
04-Dec-86
14-Mar-87
22-Jun-87
30-Sep-87
+ P66

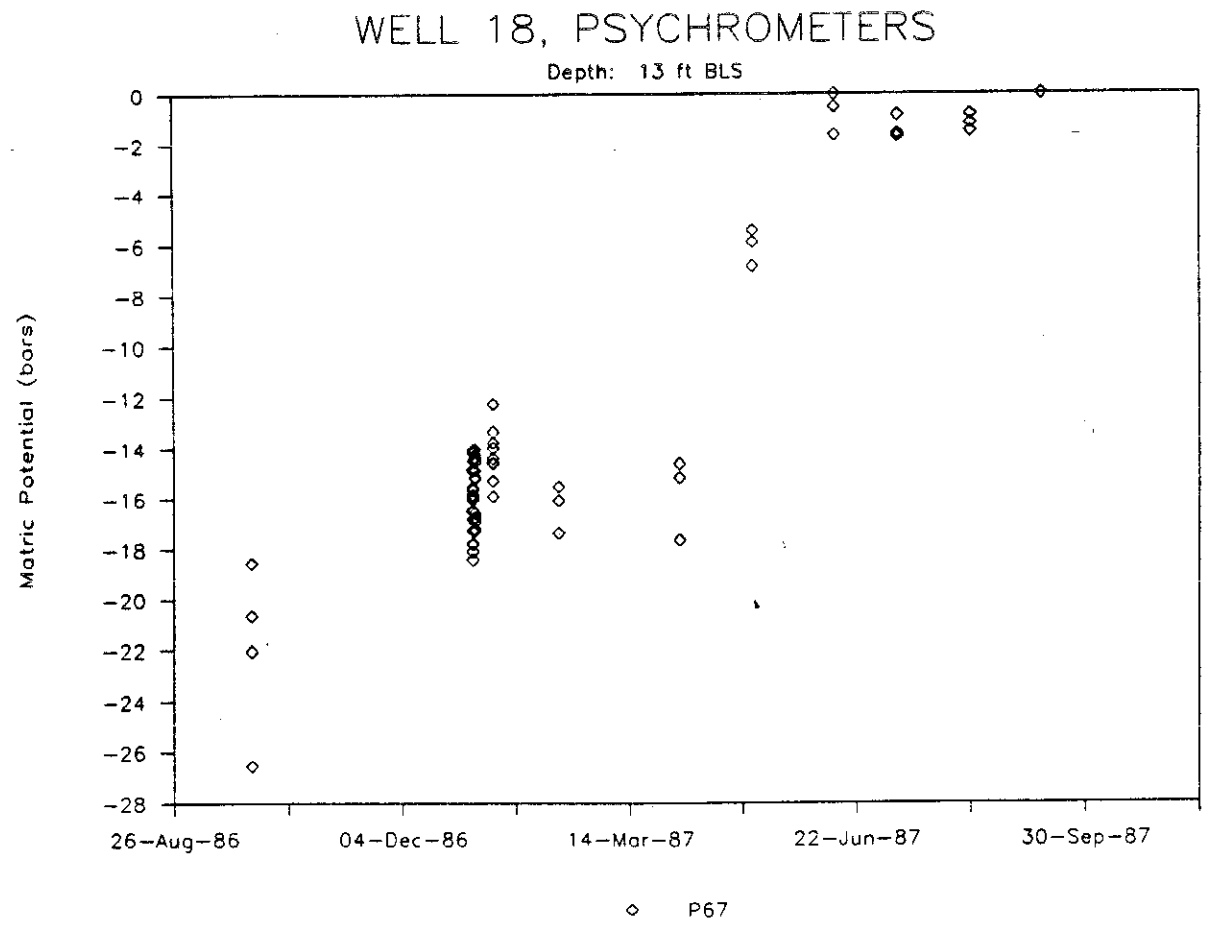
WELL 18, PSYCHROMETERS
Depth: 13 ft BLS
Matric Potential (bars)
0
-2
-4
-6
-8
-10
-12
-14
-16
-18
-20
-22
-24
-26
-28
26-Aug-86
04-Dec-86
14-Mar-87
22-Jun-87
30-Sep-87
◇ P67

WELL 18, PSYCHROMETERS

Depths: 14 ft BLS

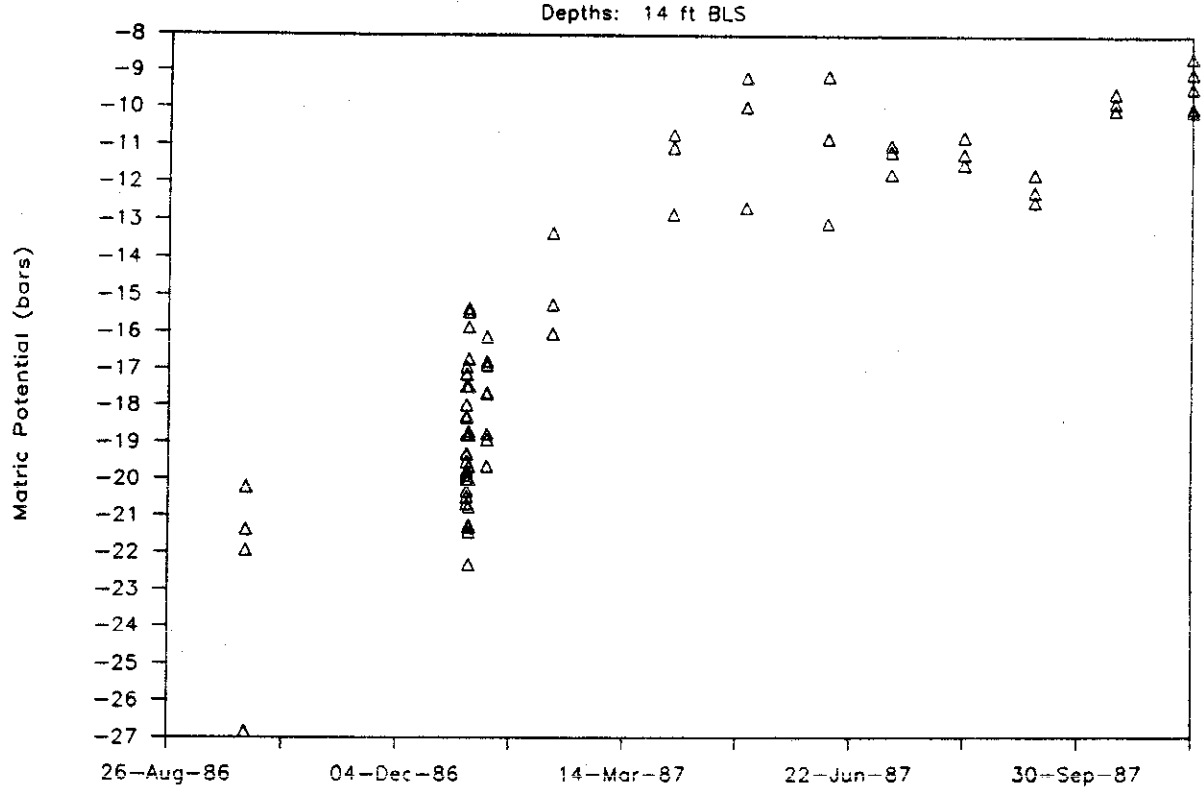

△ P68

WELL 18, PSYCHROMETERS

Depth: 15 ft BLS

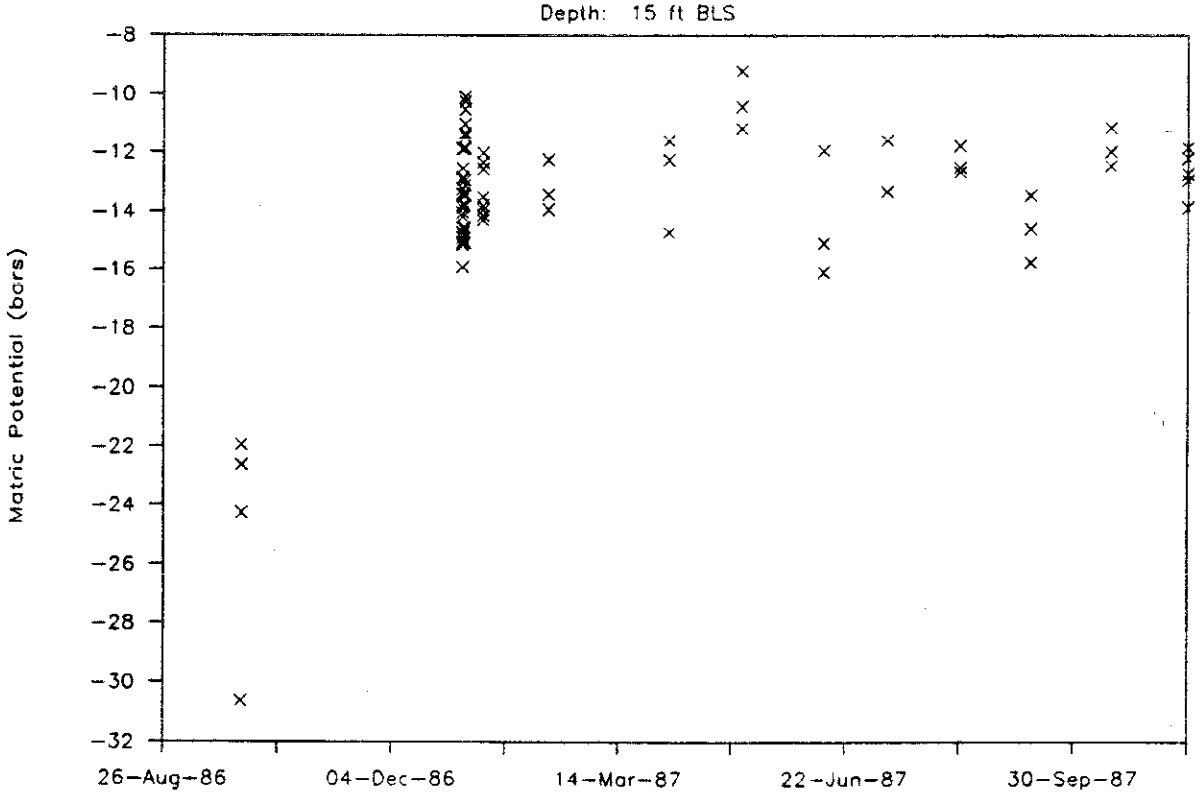

× P69

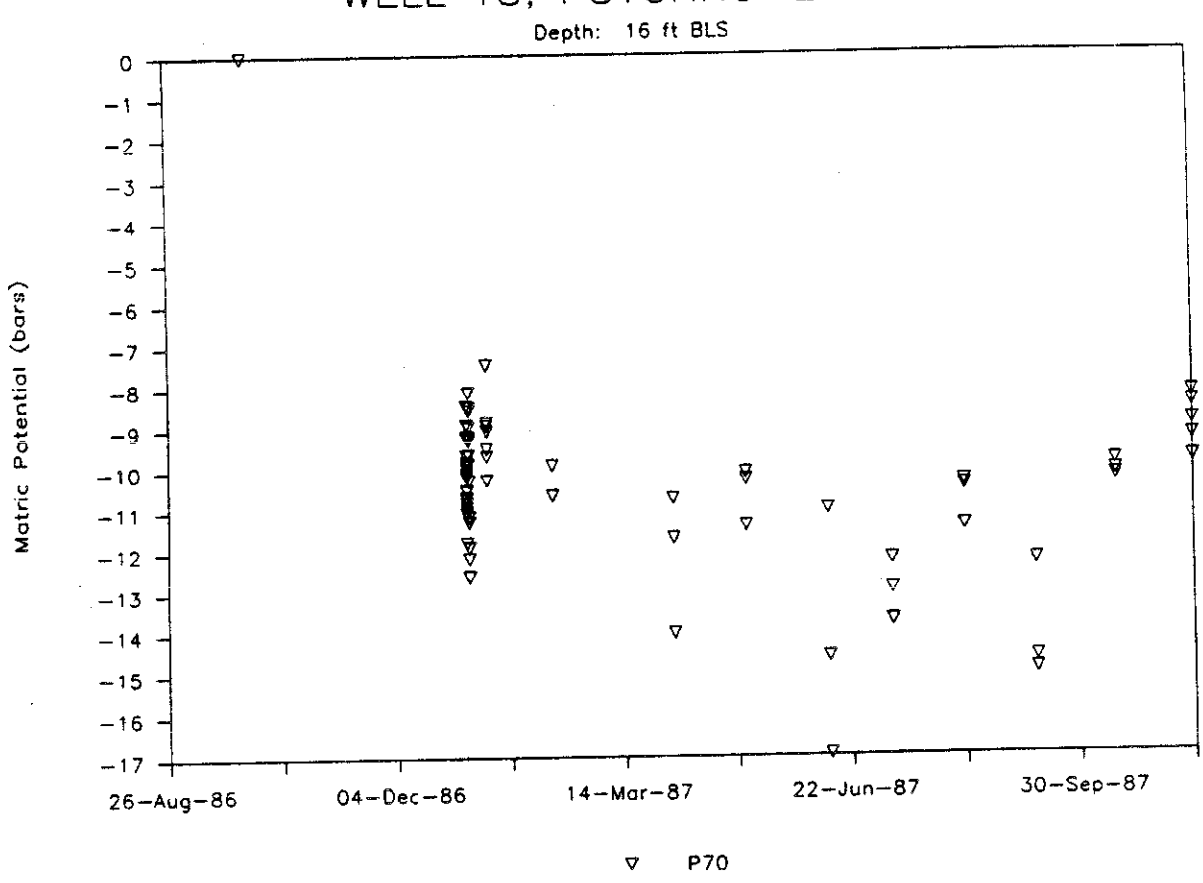
WELL 18, PSYCHROMETERS
Depth: 16 ft BLS
Matric Potential (bars)
0
-1
-2
-3
-4
-5
-6
-7
-8
-9
-10
-11
-12
-13
-14
-15
-16
-17
26-Aug-86
04-Dec-86
14-Mar-87
22-Jun-87
30-Sep-87
P70

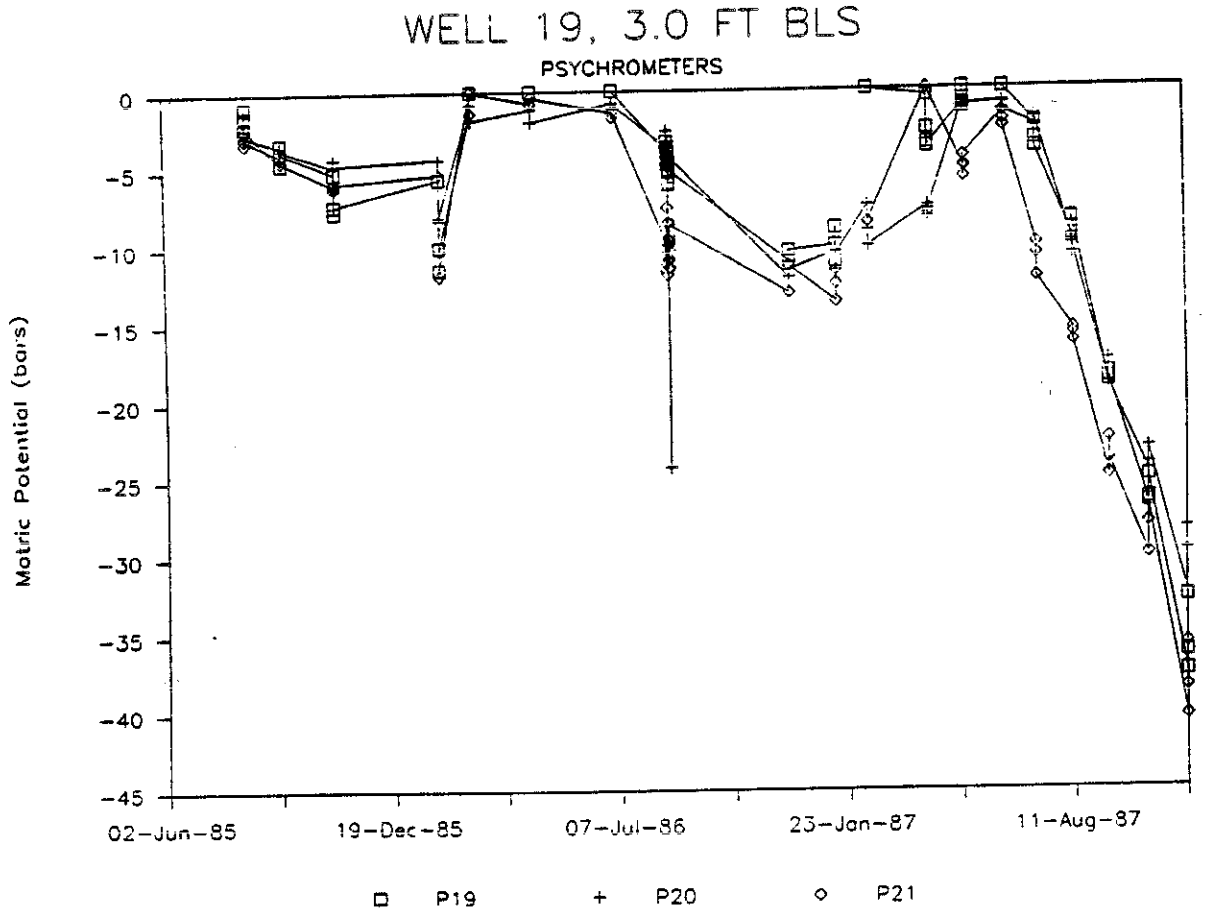
WELL 19, 3.0 FT BLS
PSYCHROMETERS
Matric Potential (bars)
0
-5
-10
-15
-20
-25
-30
-35
-40
-45
02-Jun-85
19-Dec-85
07-Jul-86
23-Jan-87
11-Aug-87
P19
P20
P21

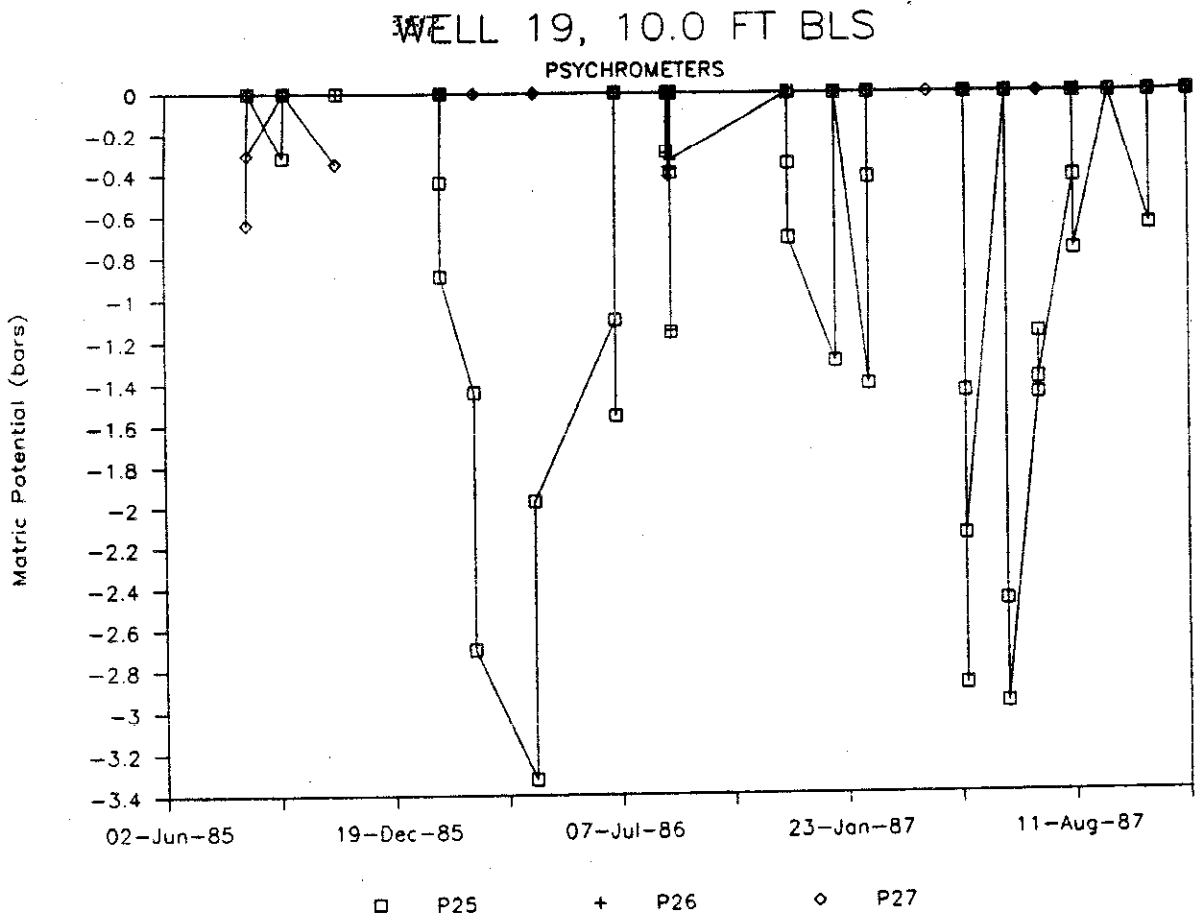
WELL 19, 10.0 FT BLS
PSYCHROMETERS
Matric Potential (bars)
0
-0.2
-0.4
-0.6
-0.8
-1
-1.2
-1.4
-1.6
-1.8
-2
-2.2
-2.4
-2.6
-2.8
-3
-3.2
-3.4
02-Jun-85
19-Dec-85
07-Jul-86
23-Jan-87
11-Aug-87
P25
P26
P27

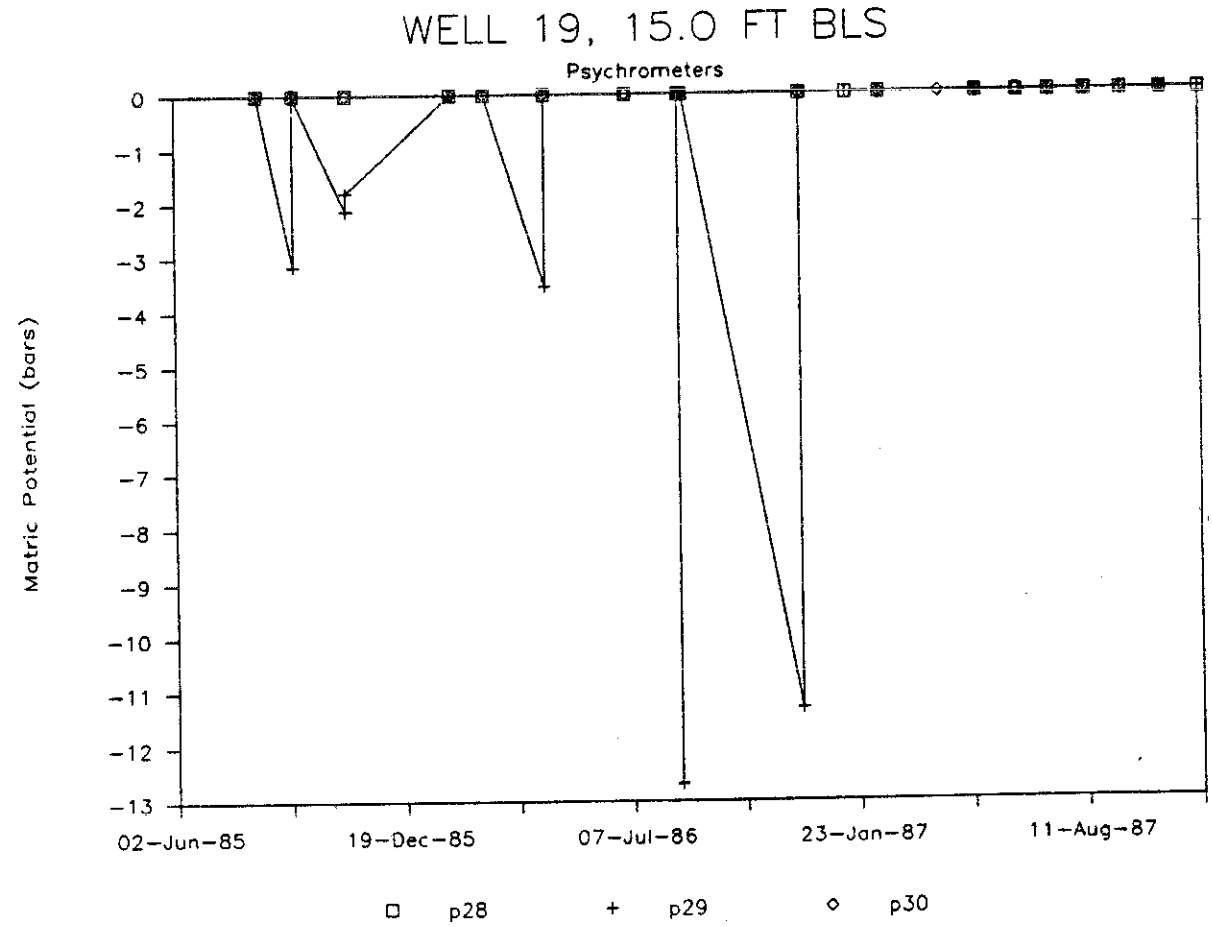
WELL 19, 15.0 FT BLS
Psychrometers
Matric Potential (bars)
0
-1
-2
-3
-4
-5
-6
-7
-8
-9
-10
-11
-12
-13
02-Jun-85
19-Dec-85
07-Jul-86
23-Jan-87
11-Aug-87
p28
p29
p30

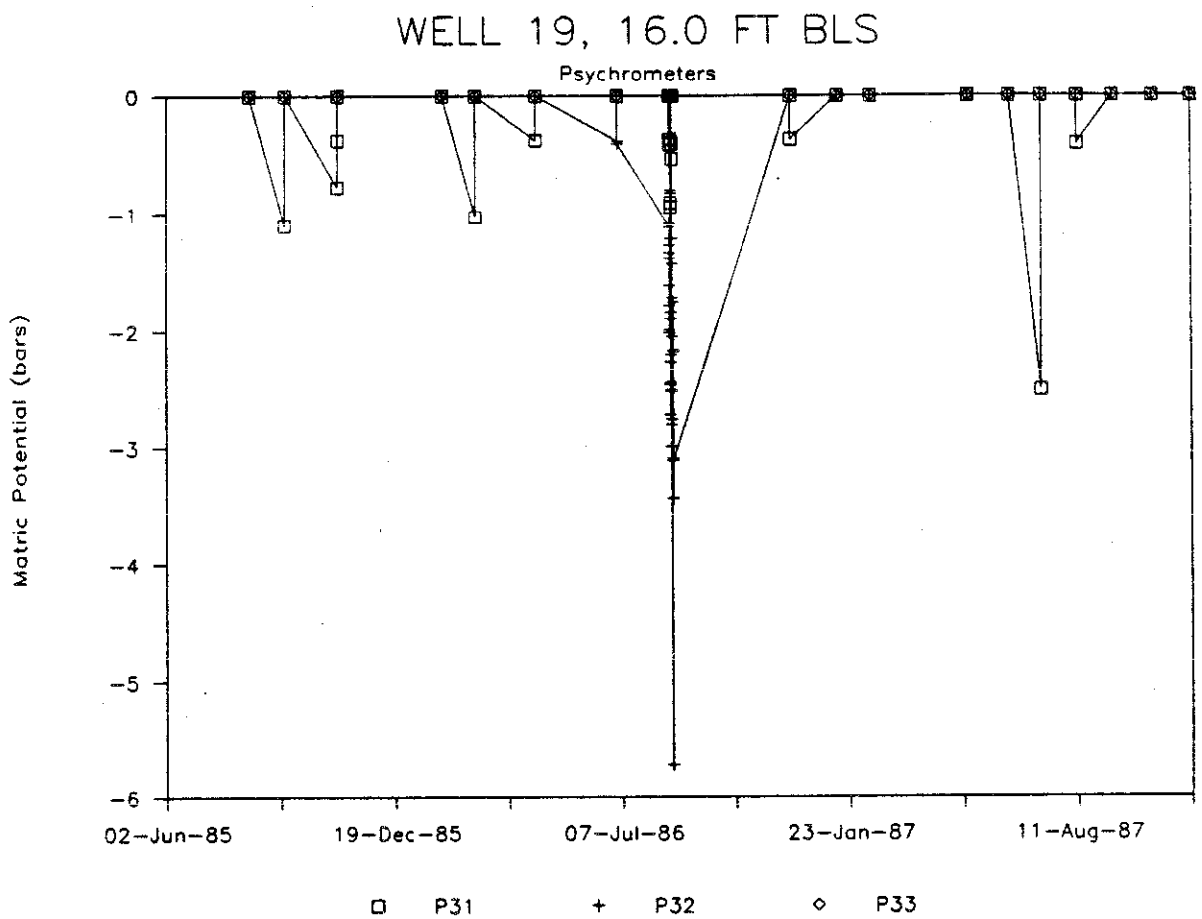
WELL 19, 16.0 FT BLS
Psychrometers
Matric Potential (bars)
0
-1
-2
-3
-4
-5
-6
02-Jun-85
19-Dec-85
07-Jul-86
23-Jan-87
11-Aug-87
P31
P32
P33

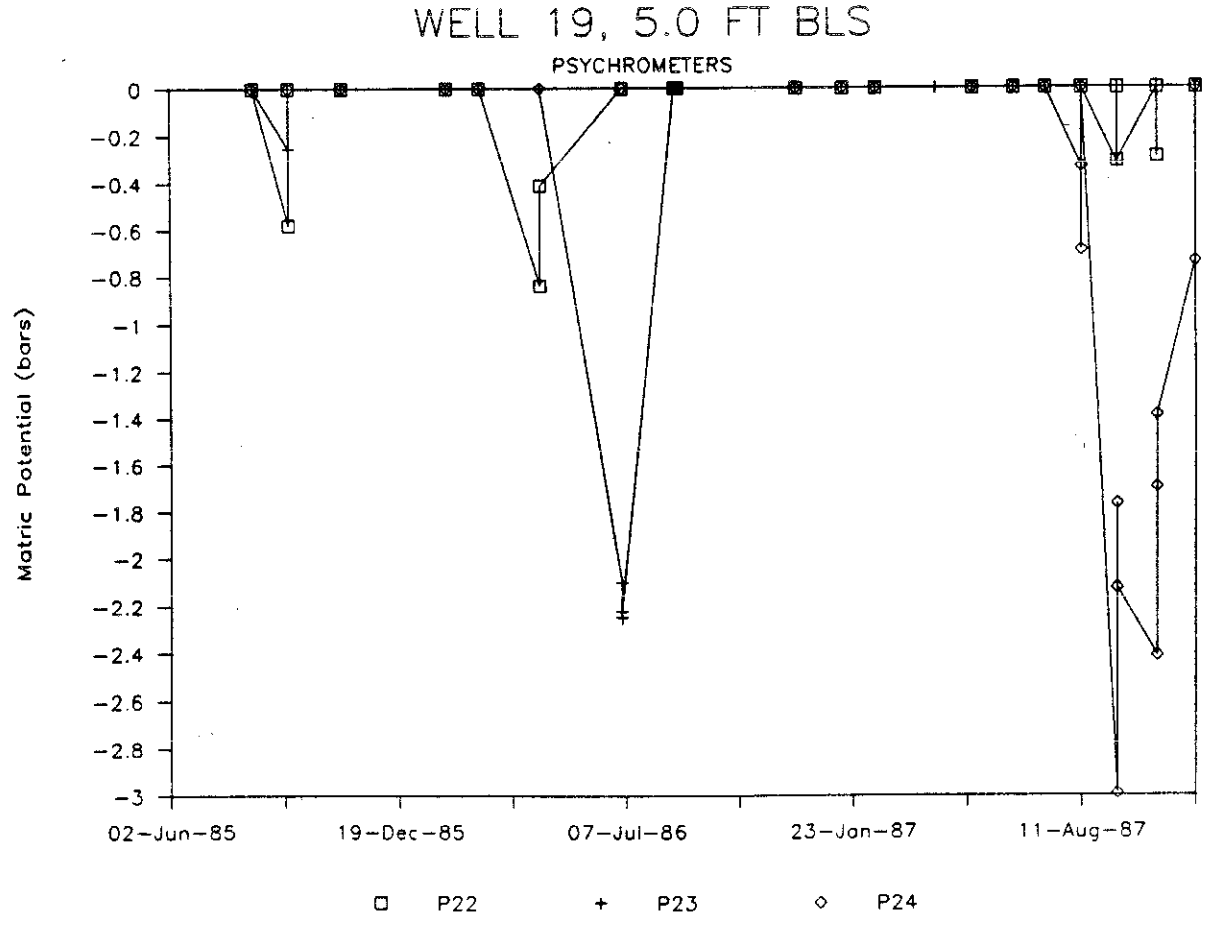
WELL 19, 5.0 FT BLS
PSYCHROMETERS
Matric Potential (bars)
0
-0.2
-0.4
-0.6
-0.8
-1
-1.2
-1.4
-1.6
-1.8
-2
-2.2
-2.4
-2.6
-2.8
-3
02-Jun-85
19-Dec-85
07-Jul-86
23-Jan-87
11-Aug-87
P22
P23
P24

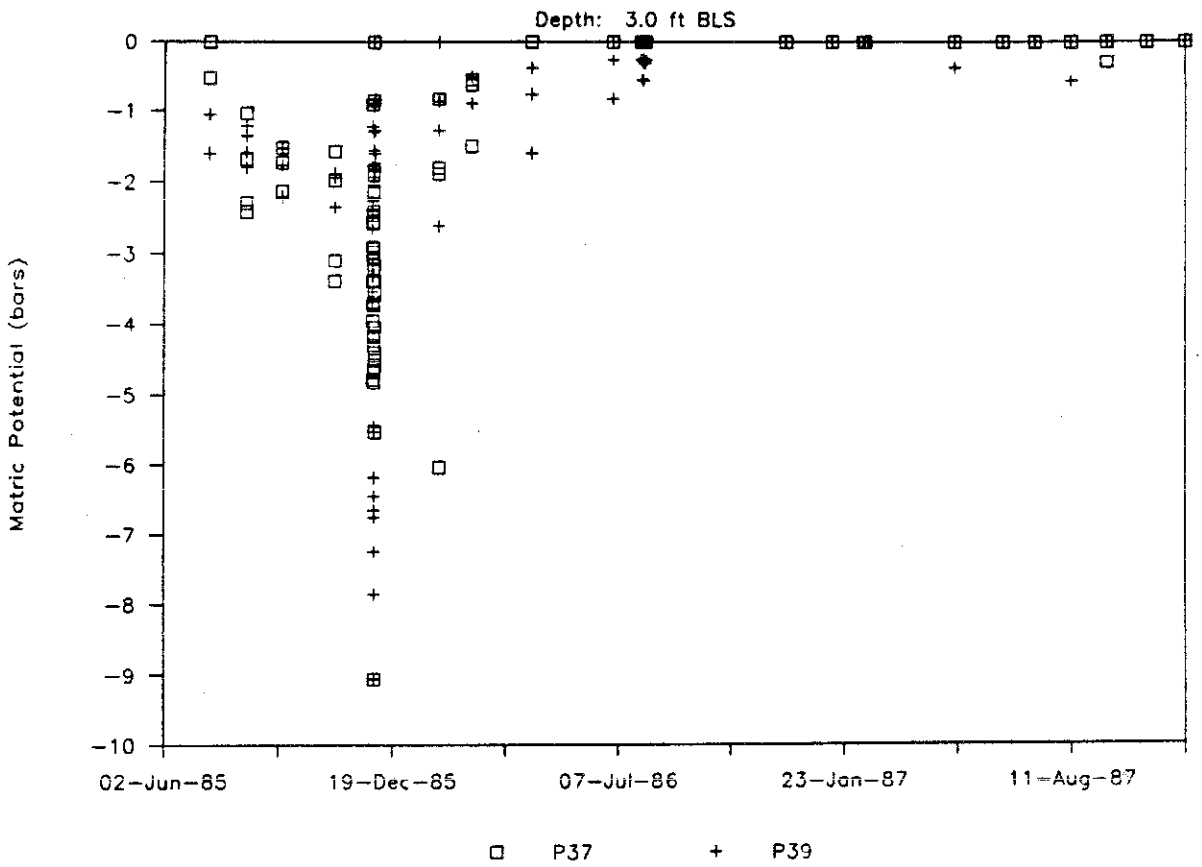
WELL 22, PSYCHROMETERS
Depth: 3.0 ft BLS
Matric Potential (bars)
0
-1
-2
-3
-4
-5
-6
-7
-8
-9
-10
02-Jun-85
19-Dec-85
07-Jul-86
23-Jan-87
11-Aug-87
P37
P39

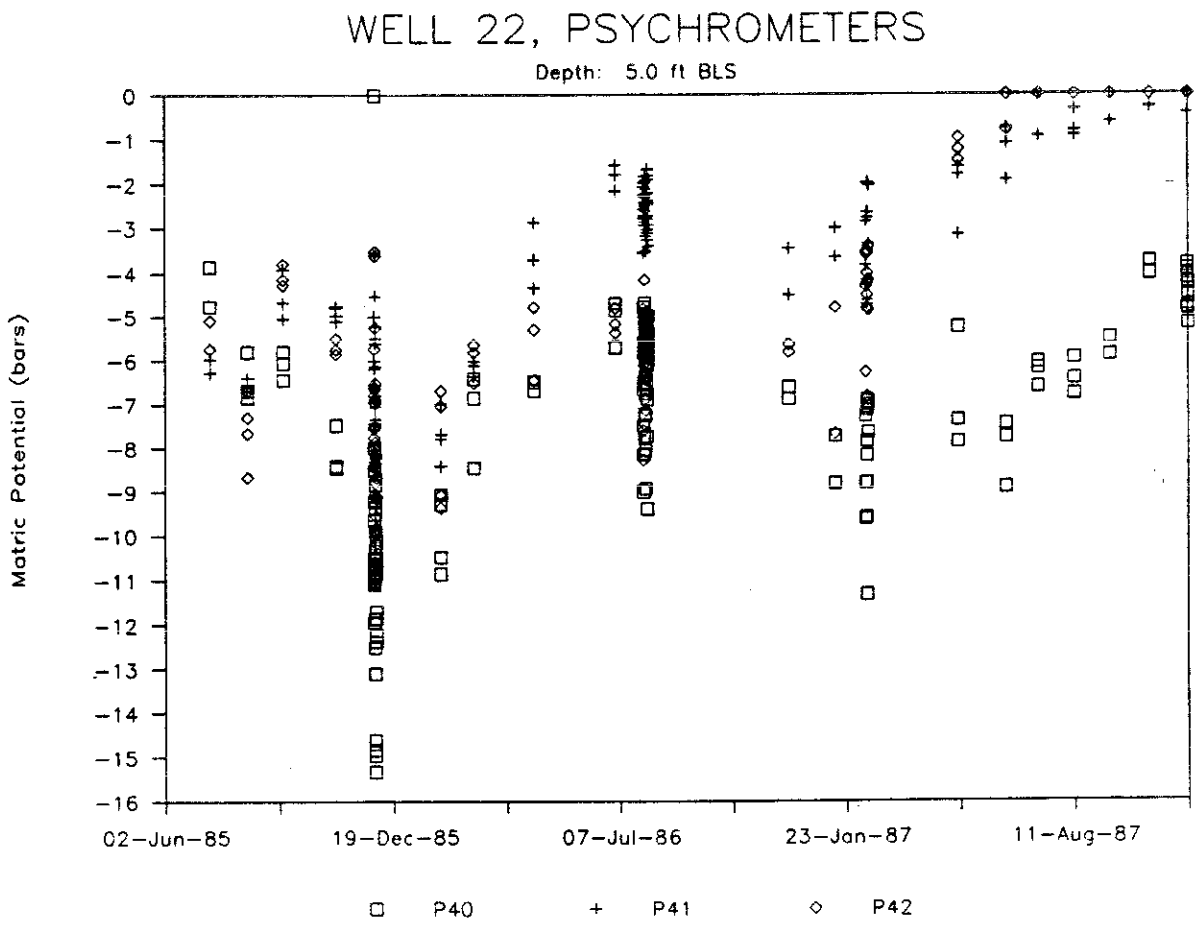
WELL 22, PSYCHROMETERS
Depth: 5.0 ft BLS
Matric Potential (bars)
0
-1
-2
-3
-4
-5
-6
-7
-8
-9
-10
-11
-12
-13
-14
-15
-16
02-Jun-85
19-Dec-85
07-Jul-86
23-Jan-87
11-Aug-87
P40
P41
P42

WELL 22, PSYCHROMETERS

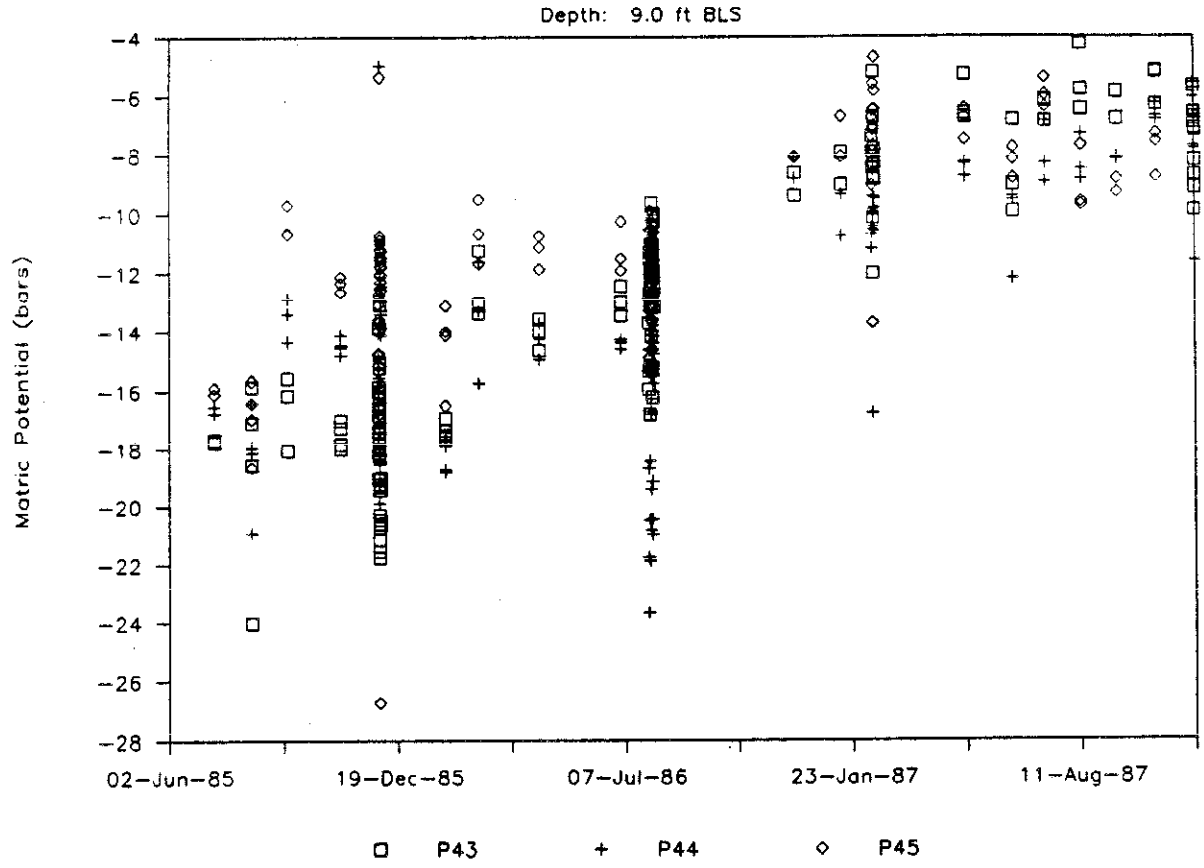

APPENDIX I
NEUTRON ACCESS PROBE DATA

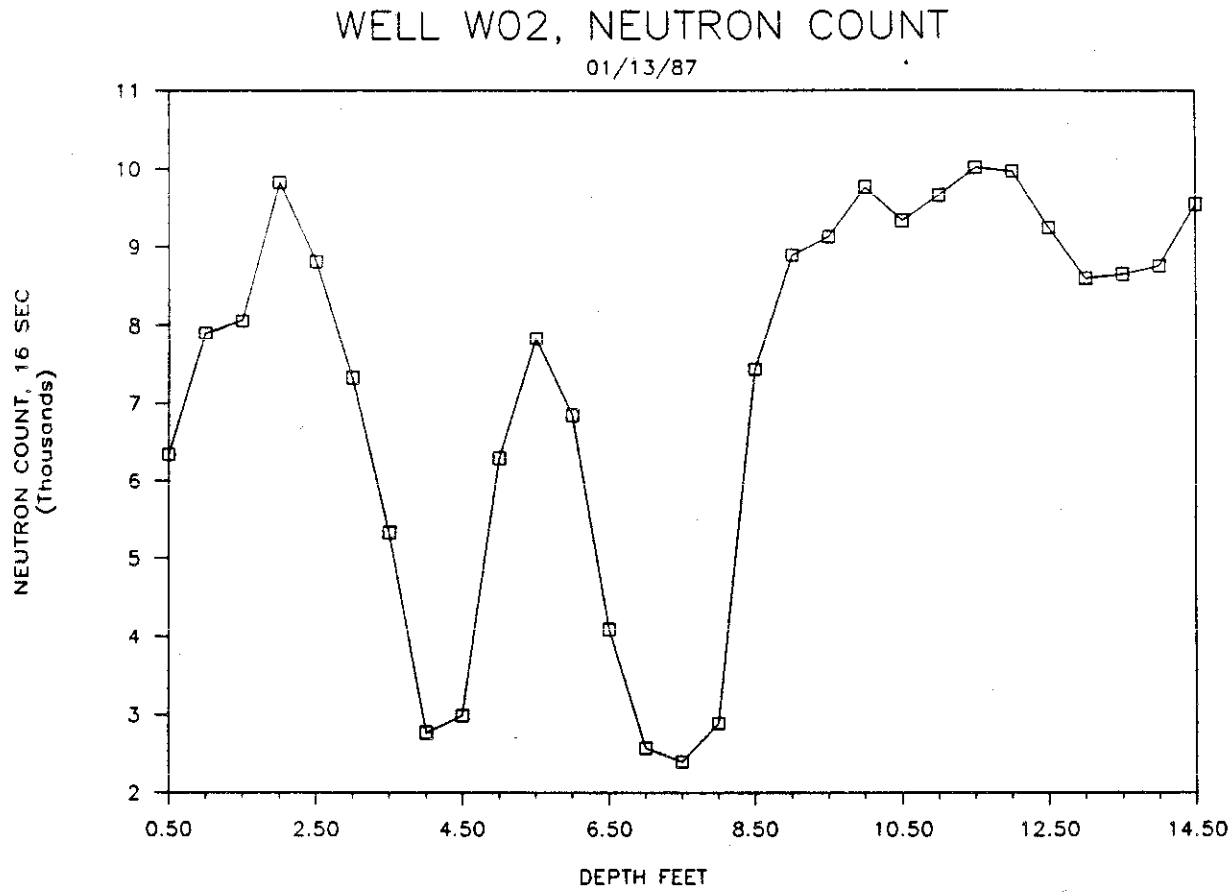
WELL W02, NEUTRON COUNT
01/13/87
NEUTRON COUNT, 16 SEC
(Thousands)
11
10
9
8
7
6
5
4
3
2
0.50
2.50
4.50
6.50
8.50
10.50
12.50
14.50
DEPTH FEET

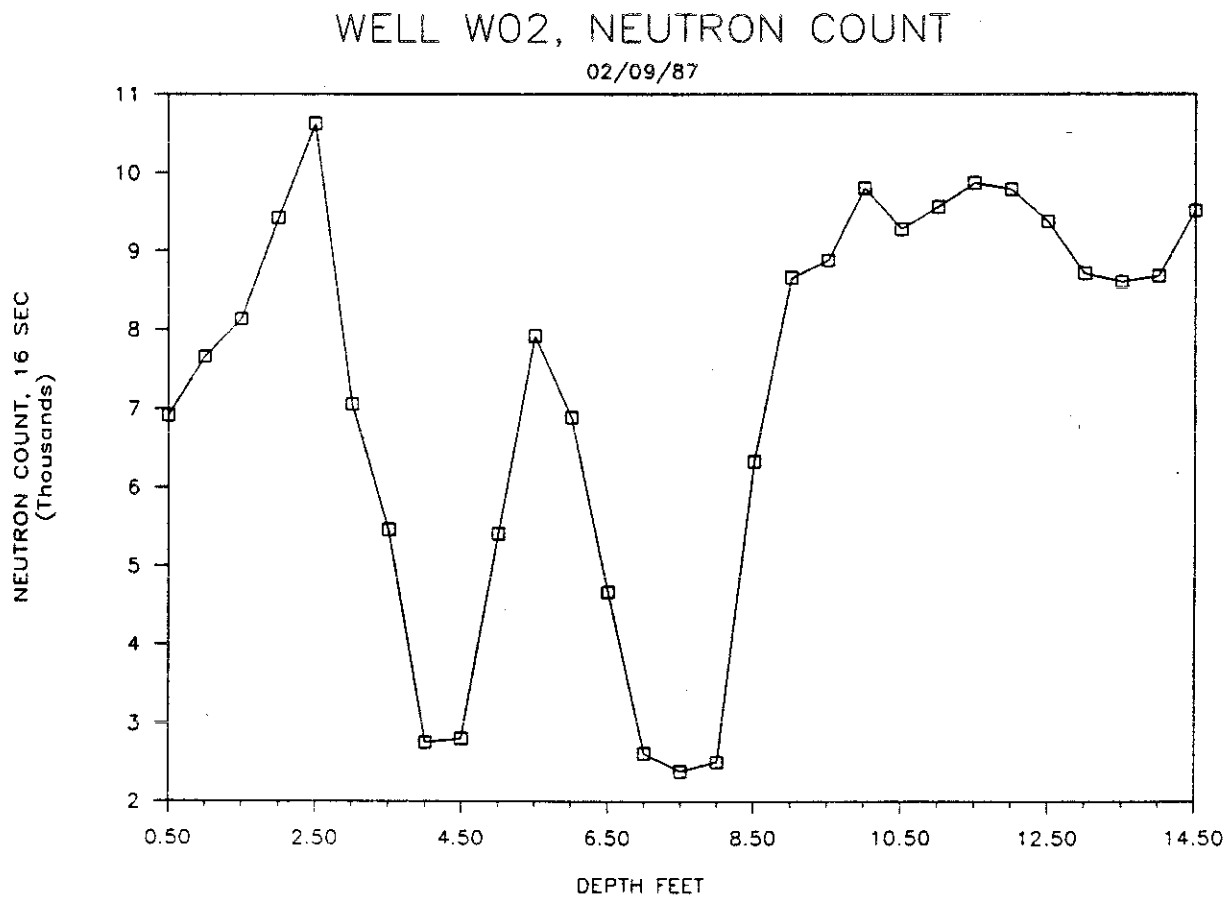
WELL W02, NEUTRON COUNT
02/09/87
NEUTRON COUNT, 16 SEC
(Thousands)
11
10
9
8
7
6
5
4
3
2
0.50
2.50
4.50
6.50
8.50
10.50
12.50
14.50
DEPTH FEET

WELL W02, NEUTRON COUNT

03/10/87

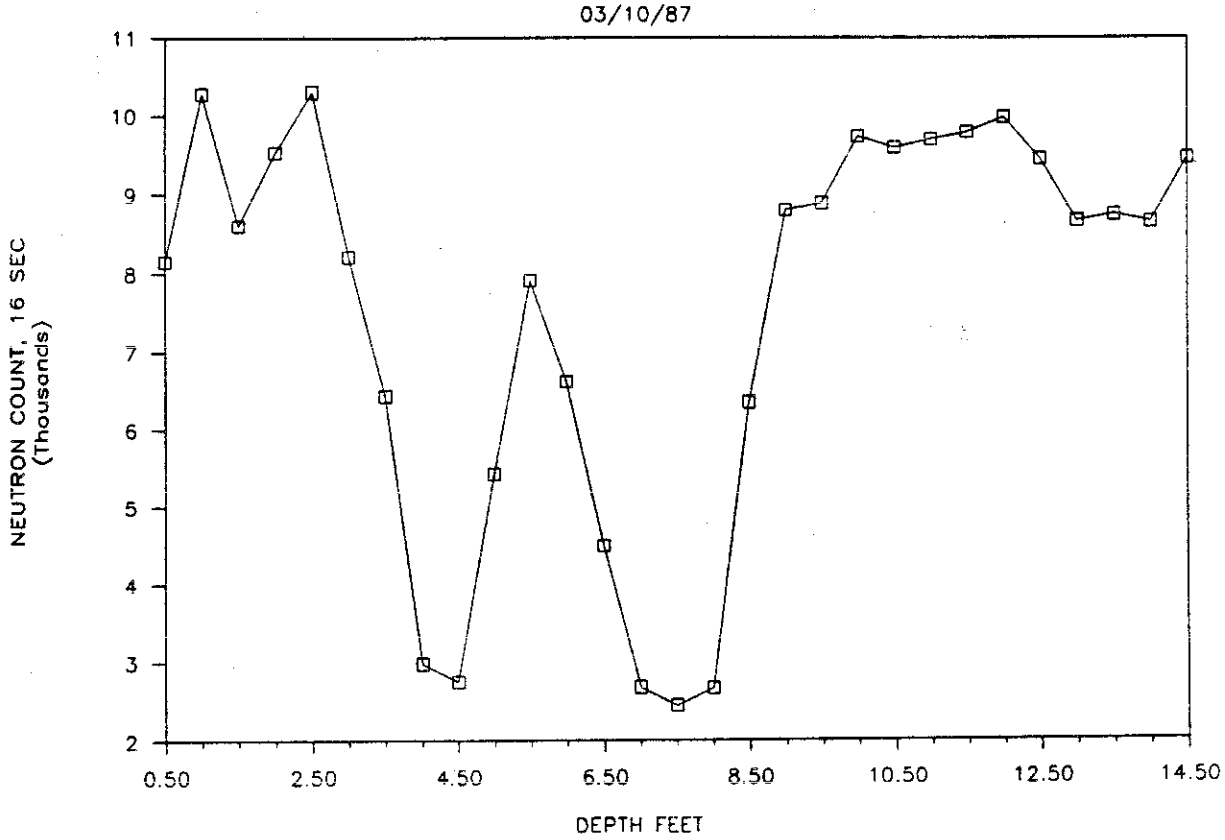

WELL W02, NEUTRON COUNT

04/08/87

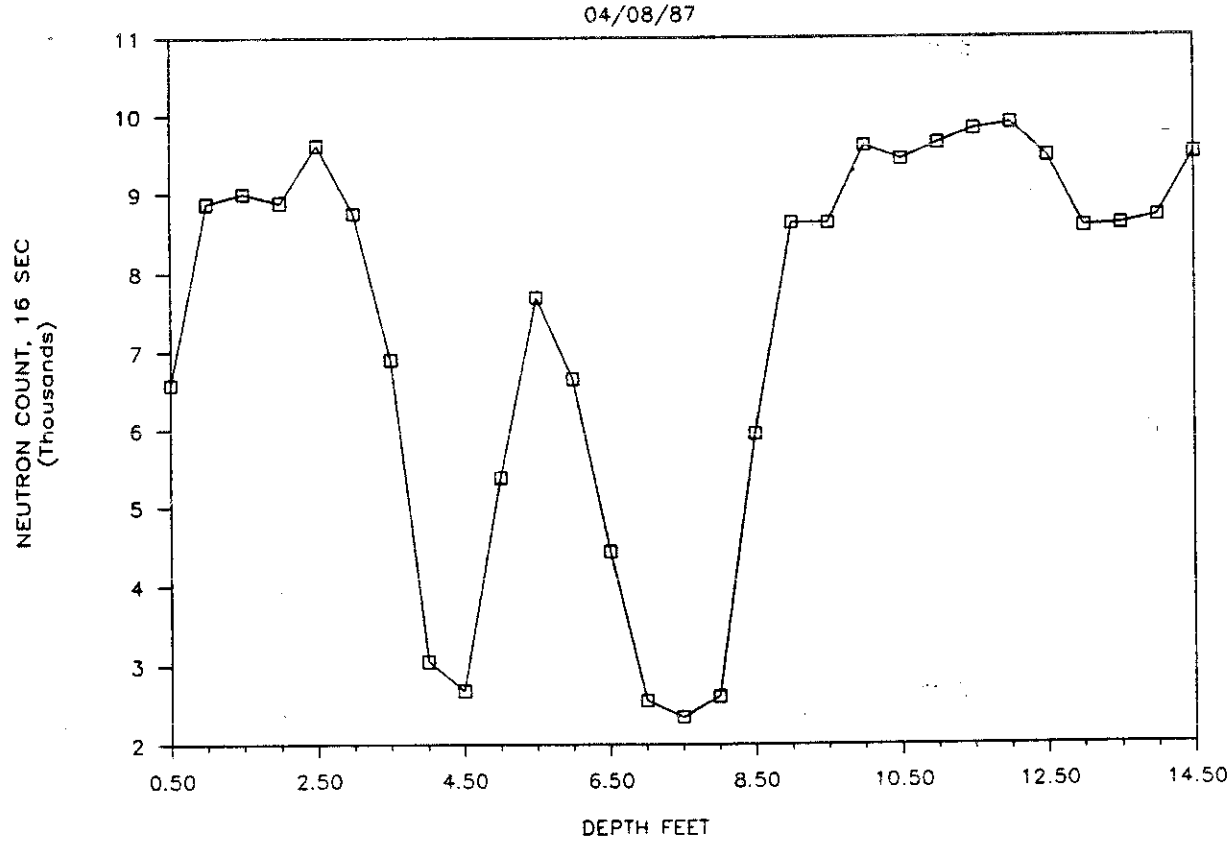

WELL W02, NEUTRON COUNT

05/07/87

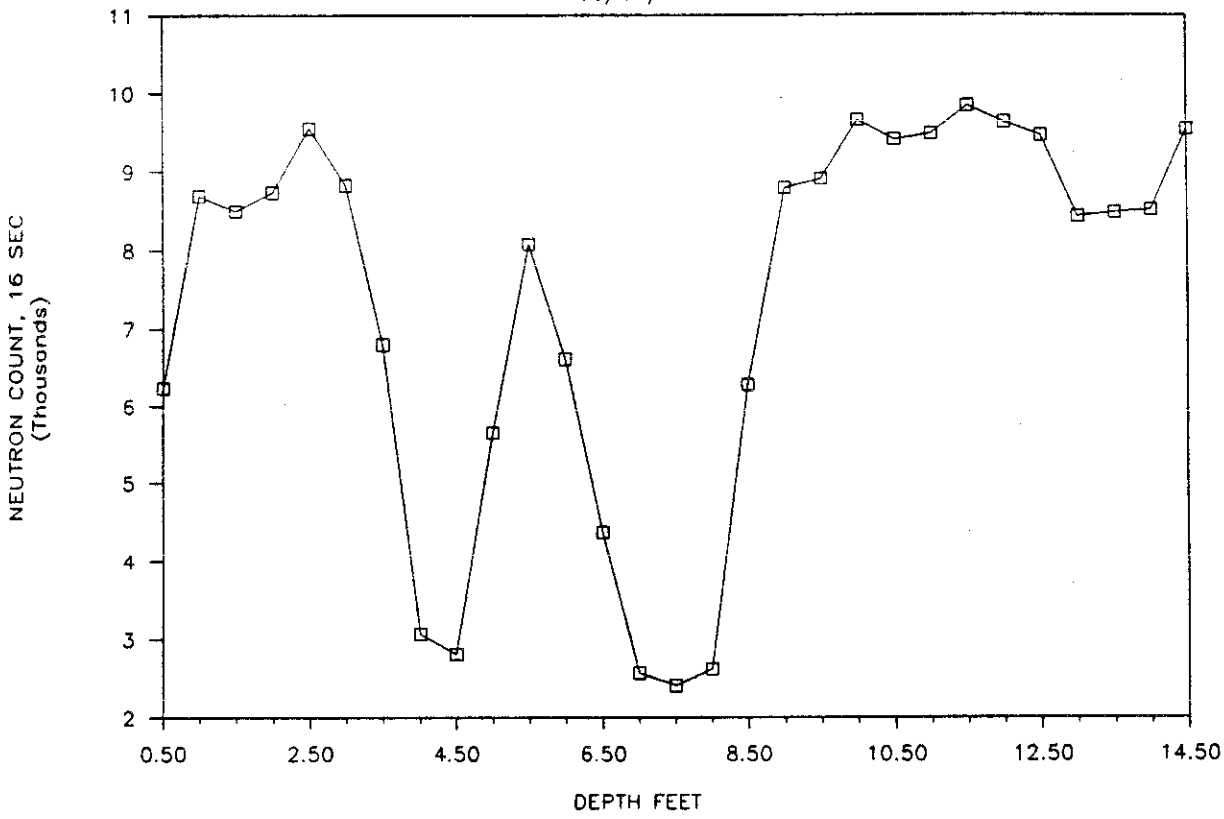

WELL W02, NEUTRON COUNT

06/17/87

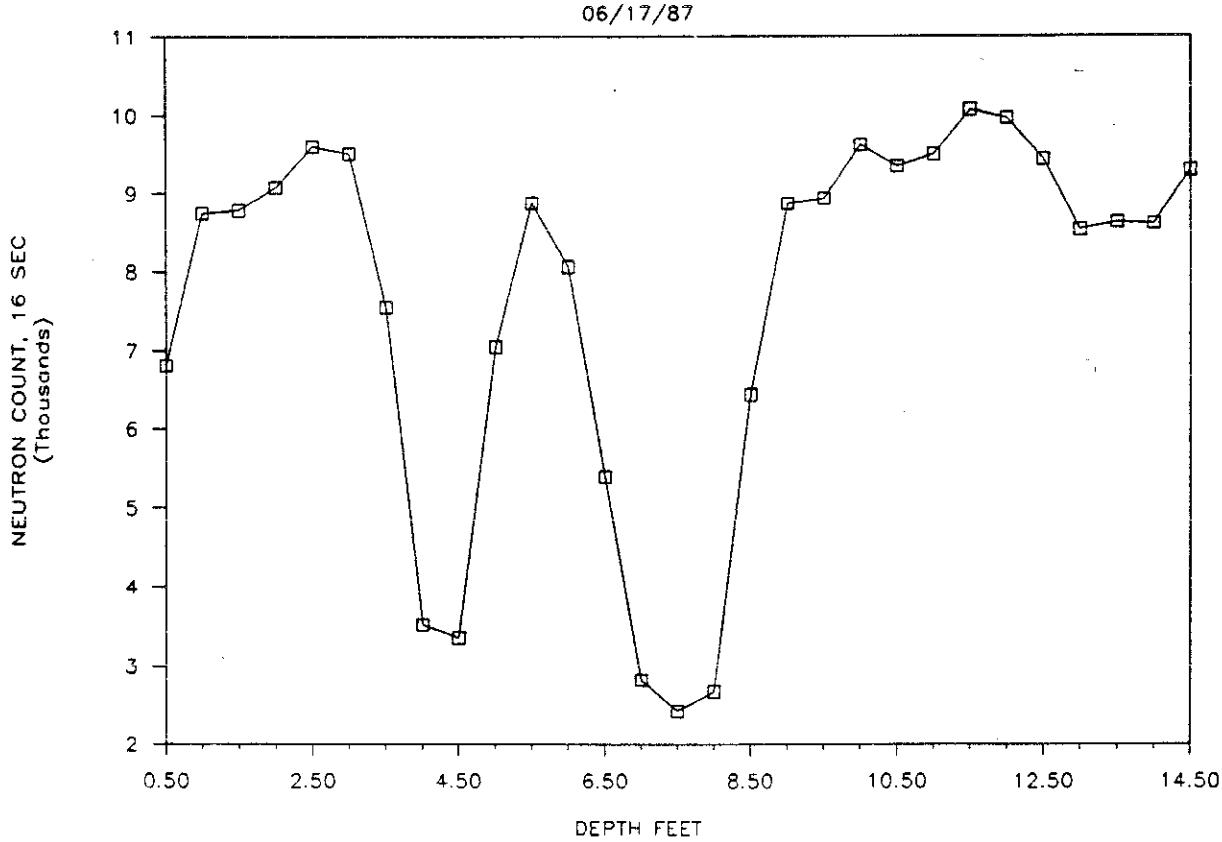

WELL W02, NEUTRON COUNT

07/16/87

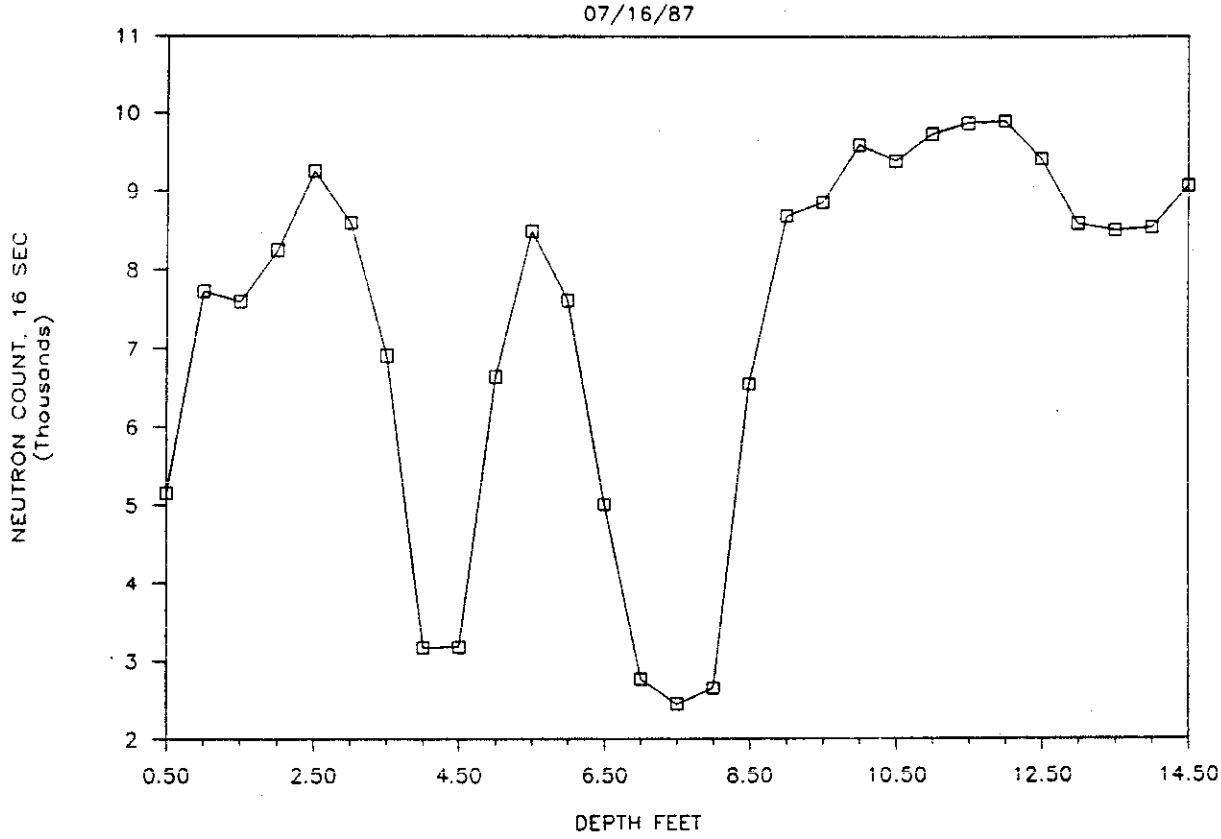

WELL W02, NEUTRON COUNT

08/25/87

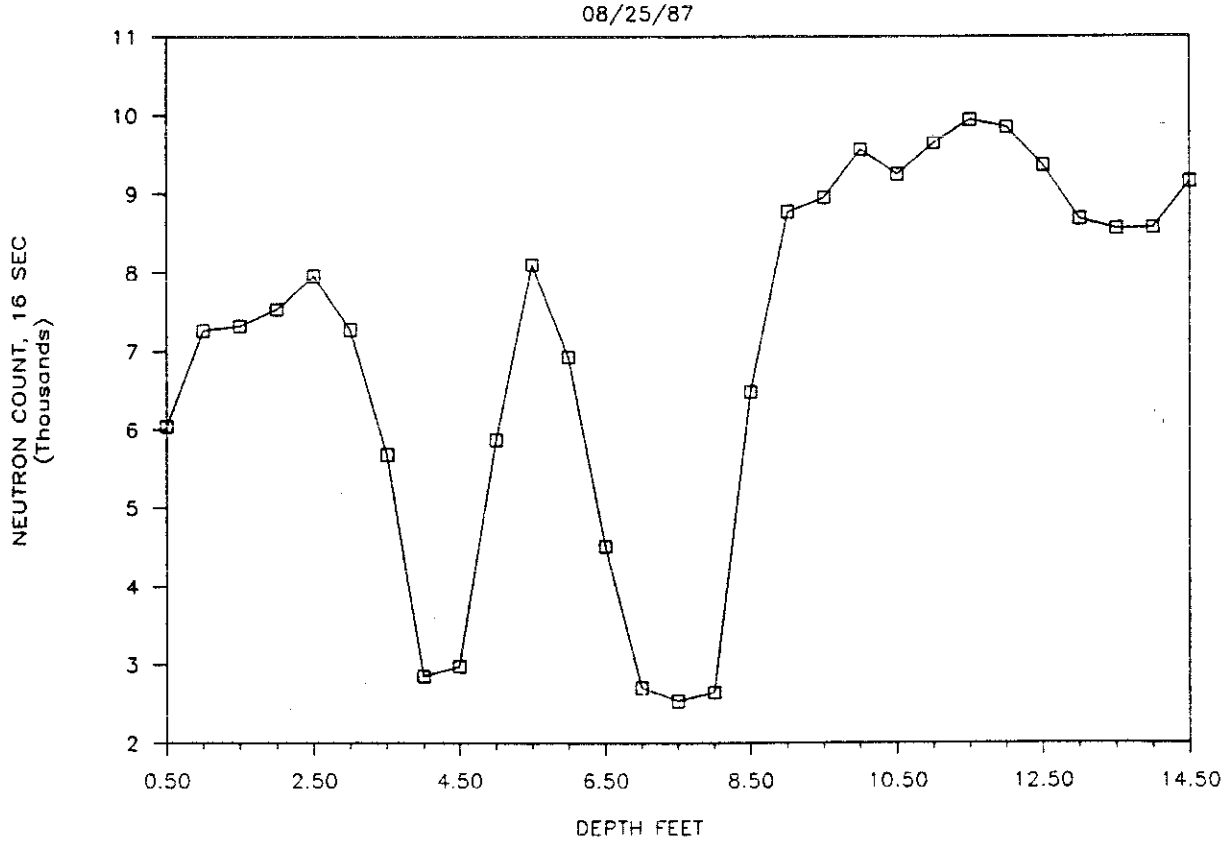

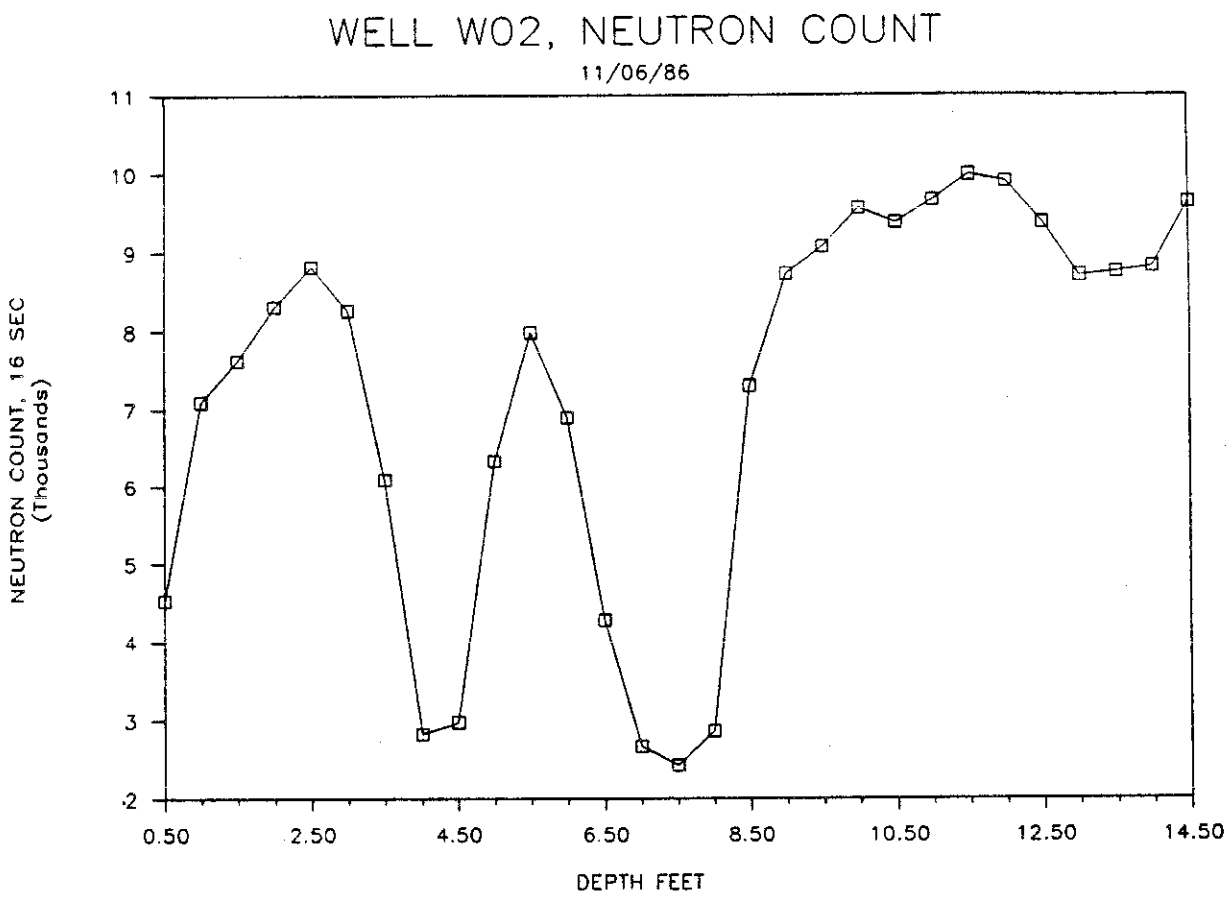
WELL W02, NEUTRON COUNT
11/06/86
NEUTRON COUNT, 16 SEC
(Thousands)
11
10
9
8
7
6
5
4
3
-2
0.50
2.50
4.50
6.50
8.50
10.50
12.50
14.50
DEPTH FEET

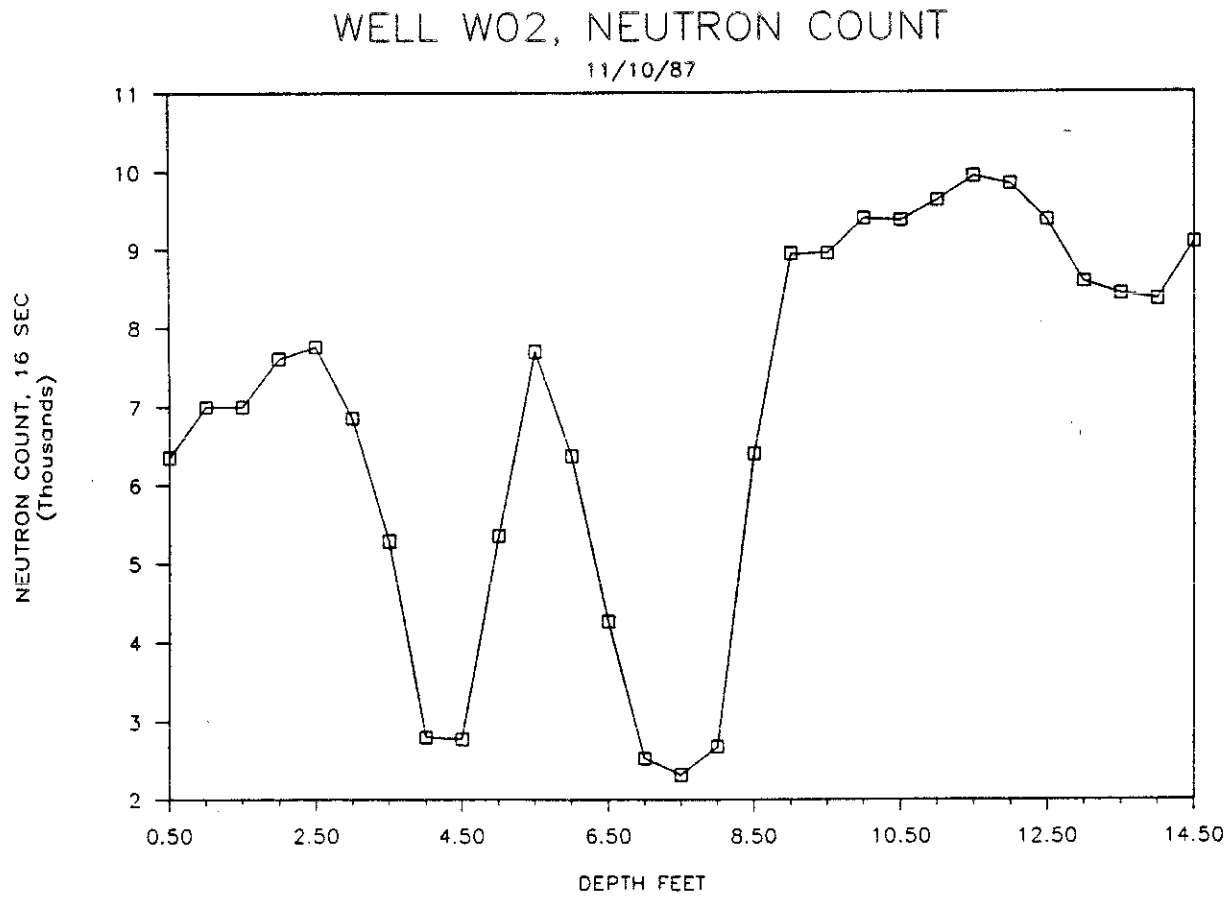
WELL W02, NEUTRON COUNT
11/10/87
NEUTRON COUNT, 16 SEC
(Thousands)
11
10
9
8
7
6
5
4
3
2
0.50
2.50
4.50
6.50
8.50
10.50
12.50
14.50
DEPTH FEET

WELL W02, NEUTRON COUNT

12/03/86

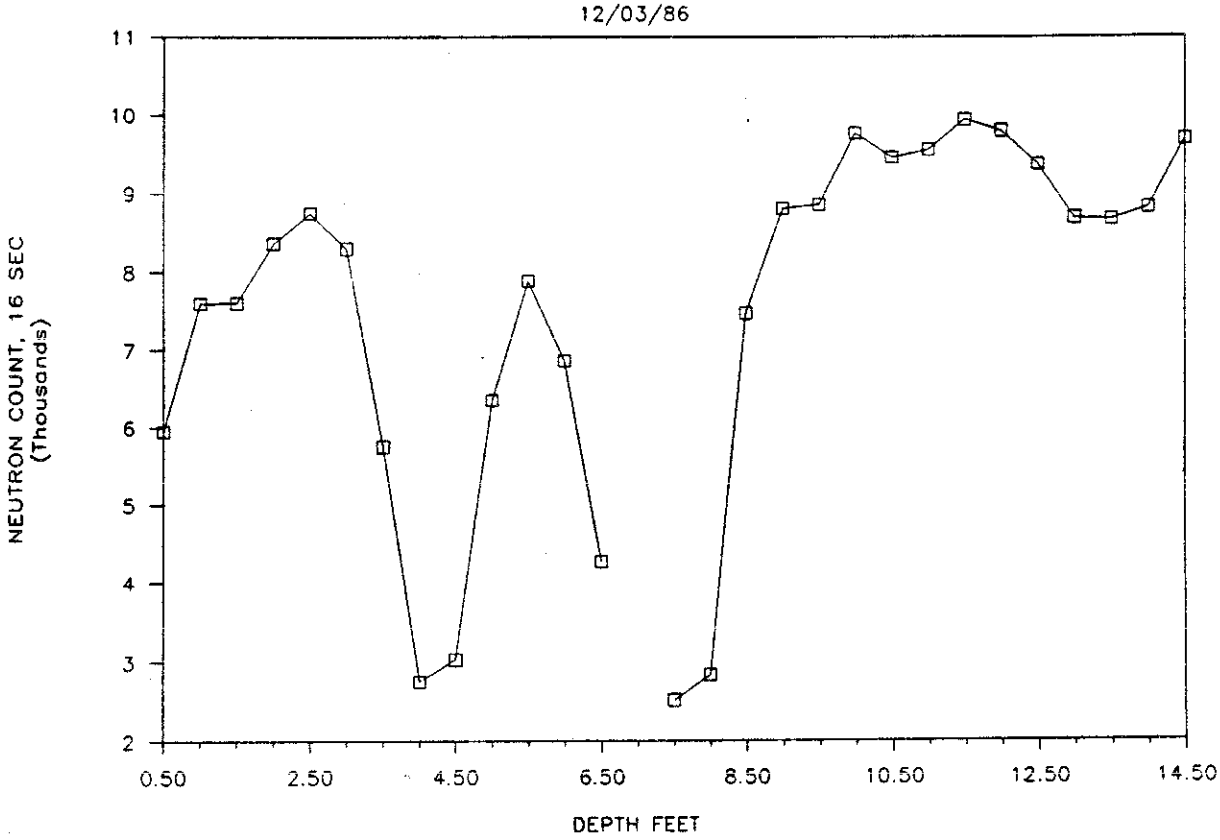

WELL W02, NEUTRON COUNT

11/86 TO 11/87

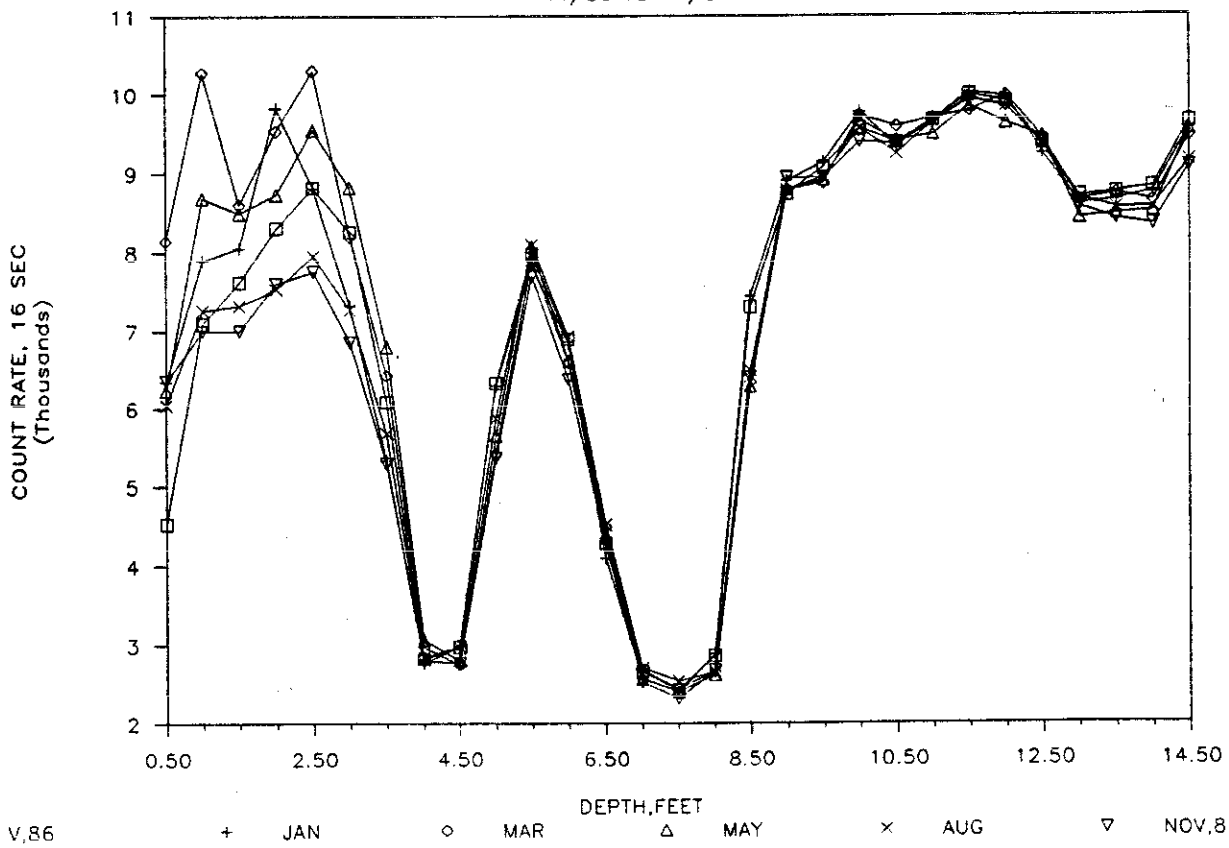

V,86 + JAN ◇ MAR △ MAY × AUG ▽ NOV,87

WELL W06, NEUTRON COUNT

01/13/87

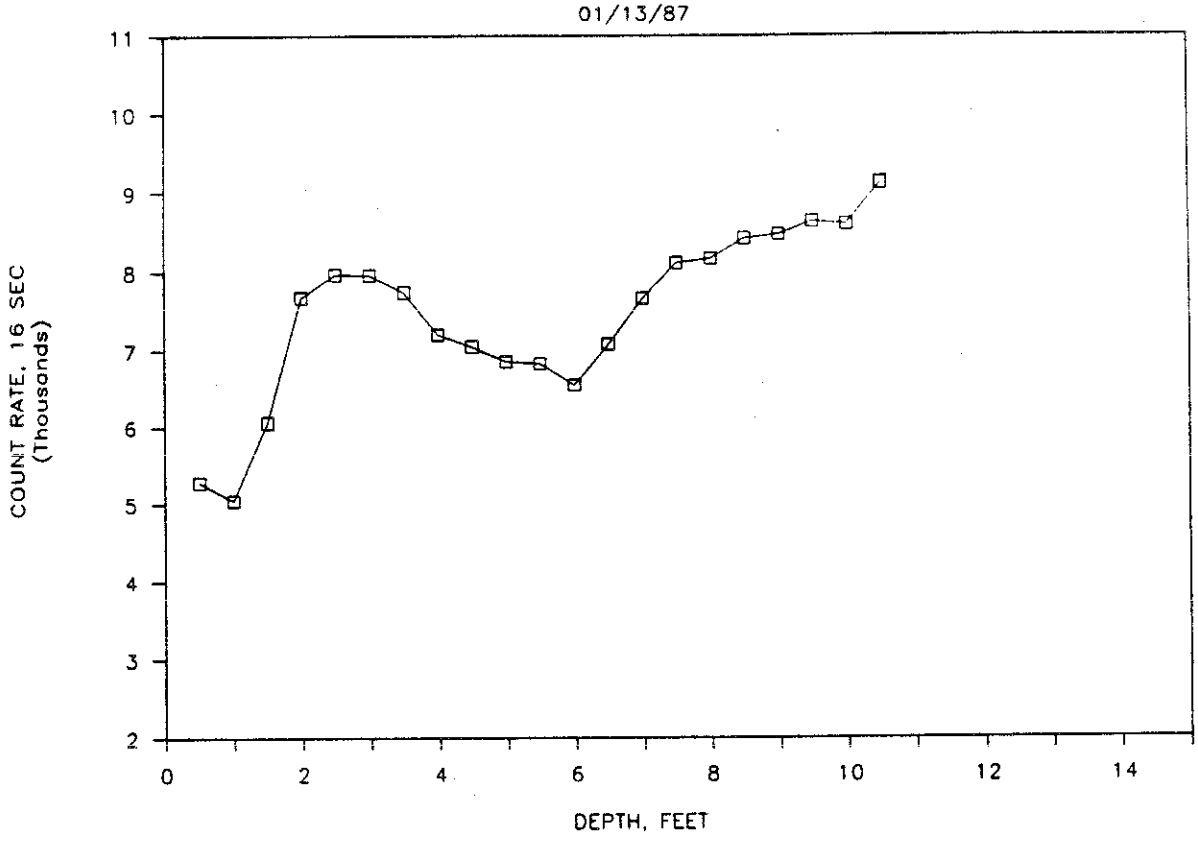

WELL W06, NEUTRON COUNT

03/10/87

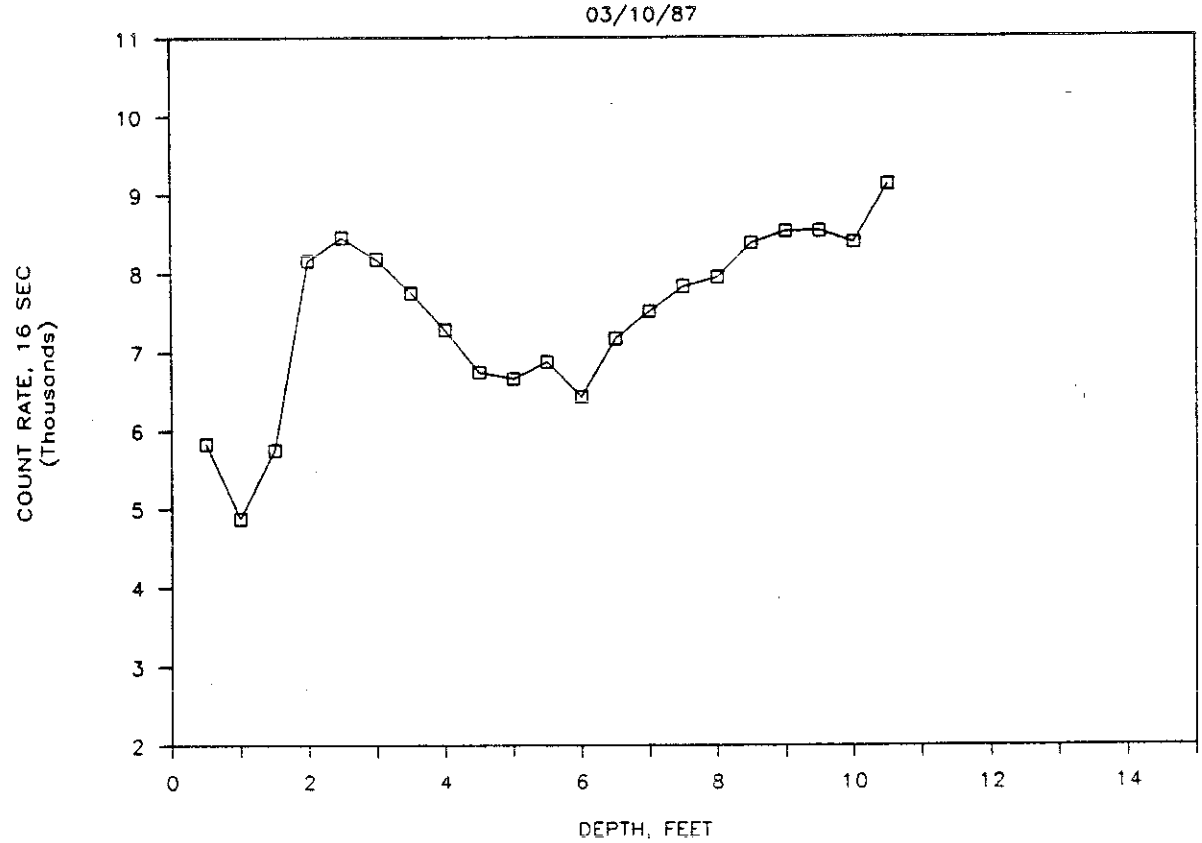

WELL W06, NEUTRON COUNT

04/08/87

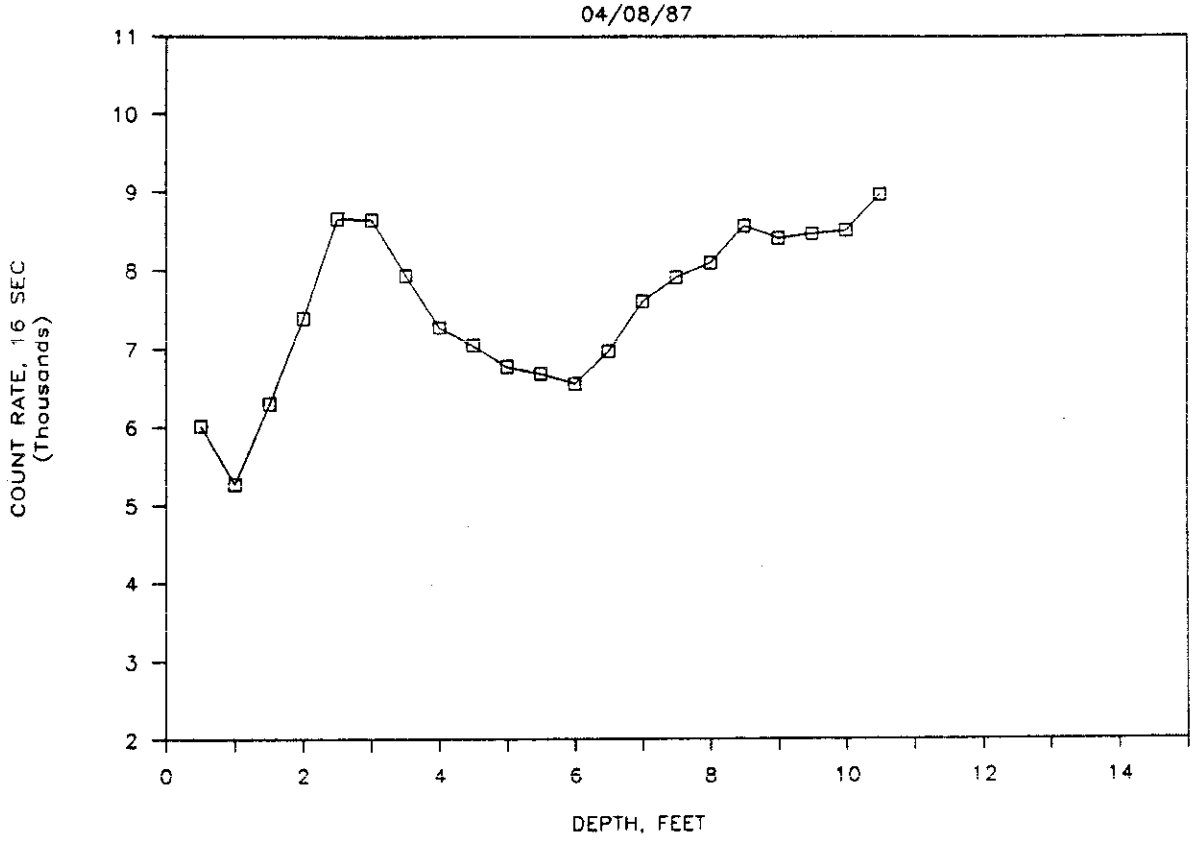

WELL W06, NEUTRON COUNT

05/07/87

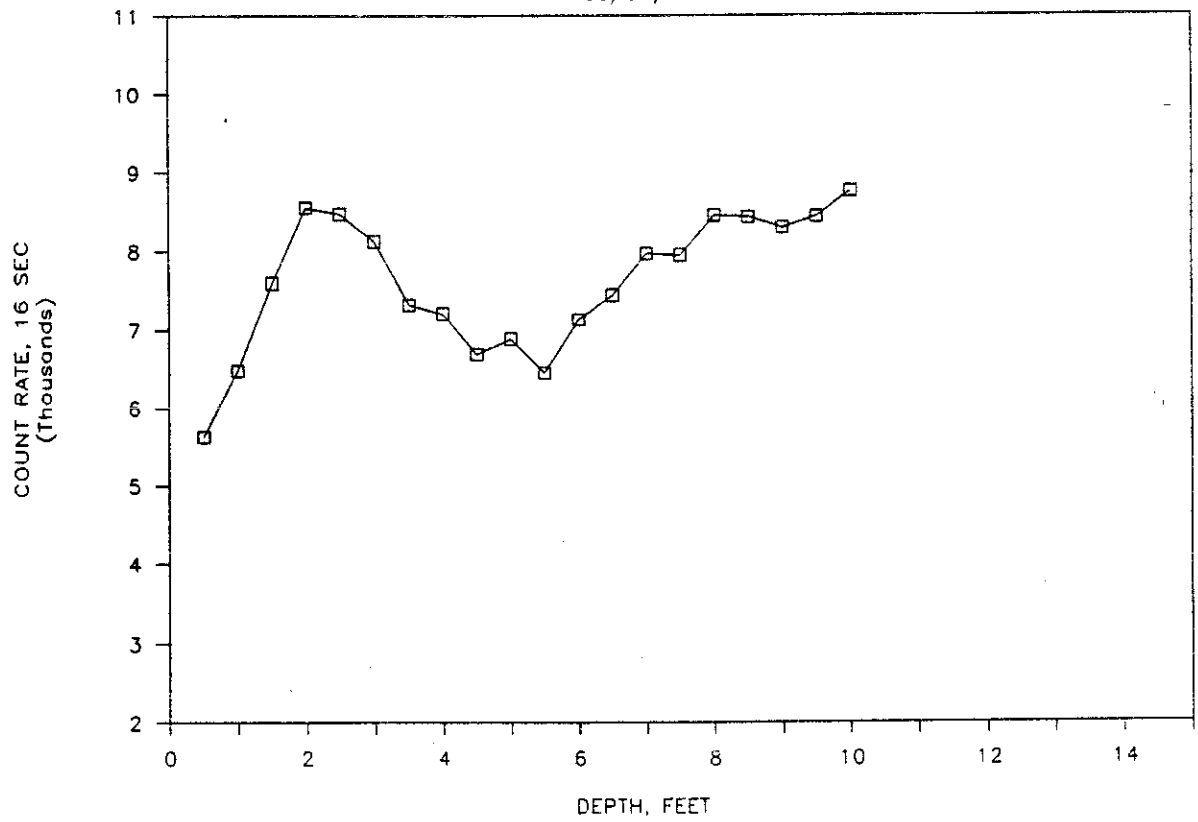

WELL W06, NEUTRON COUNT

06/17/87

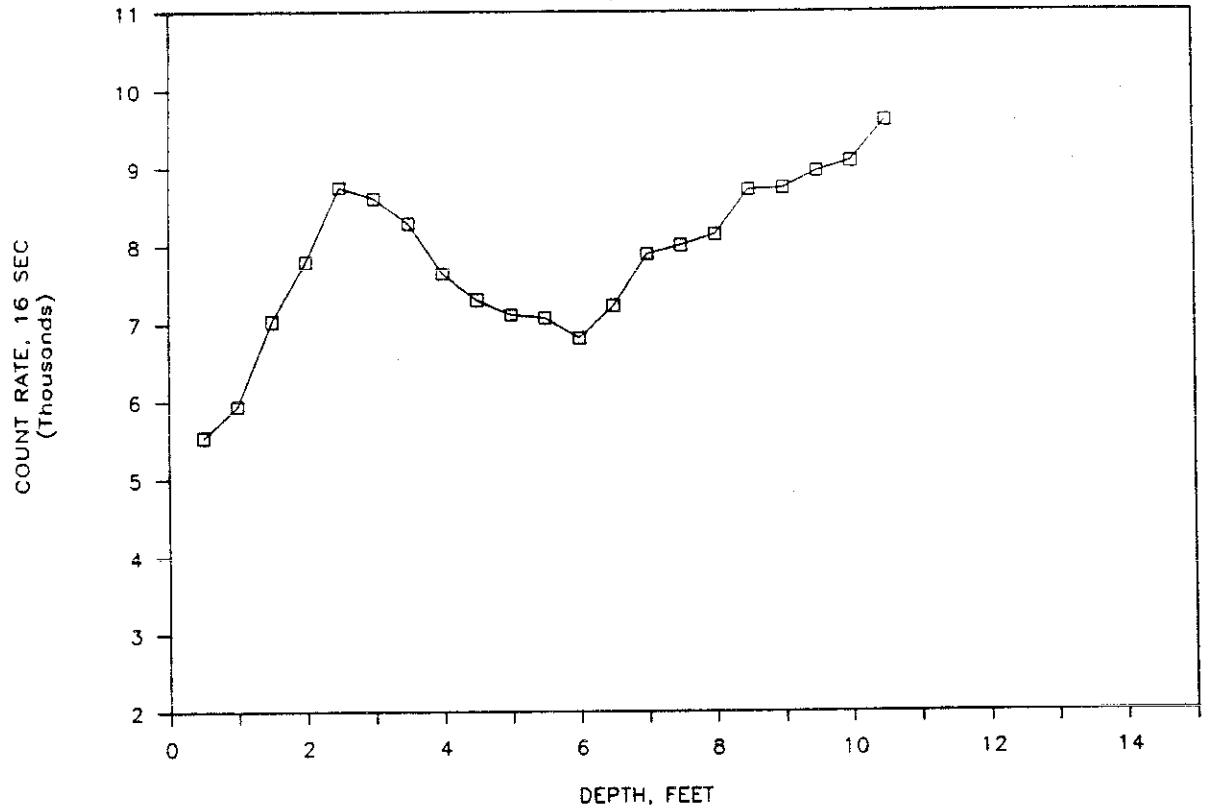

WELL W06, NEUTRON COUNT

07/17/87

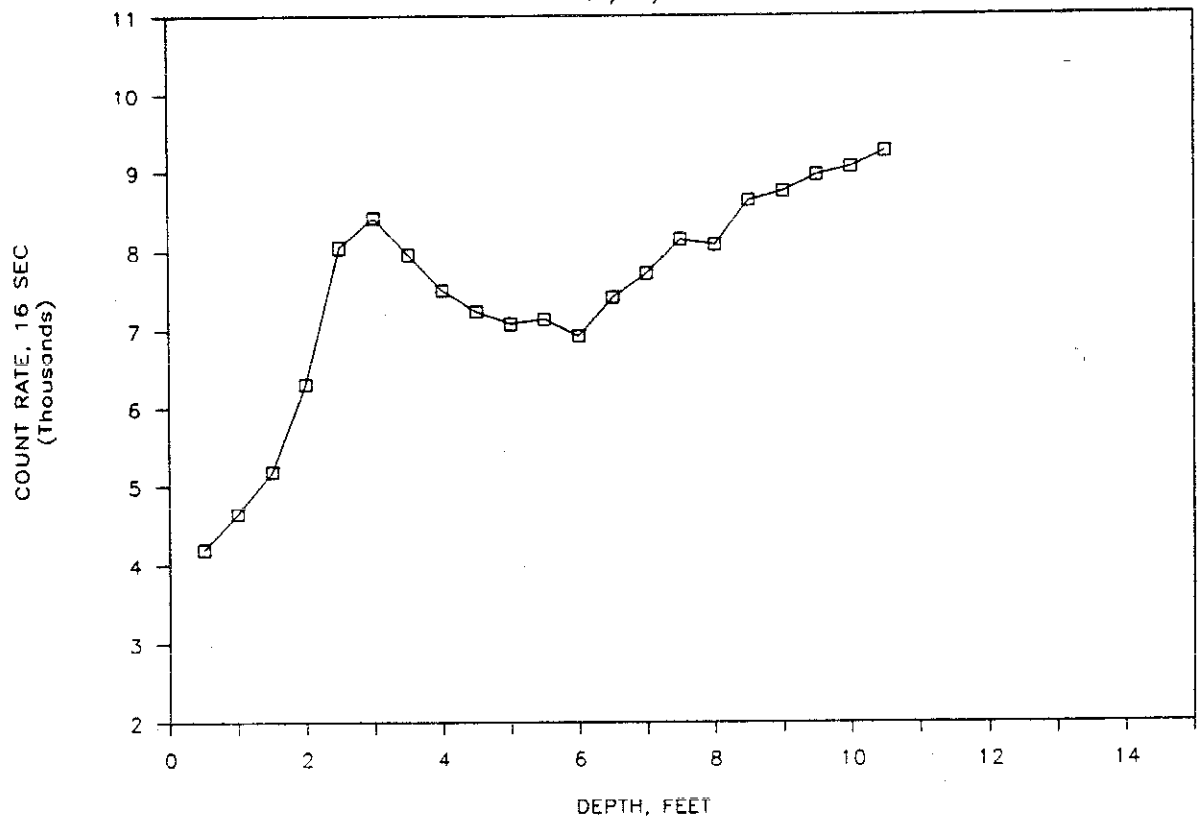

WELL W06, NEUTRON COUNT

08/25/87

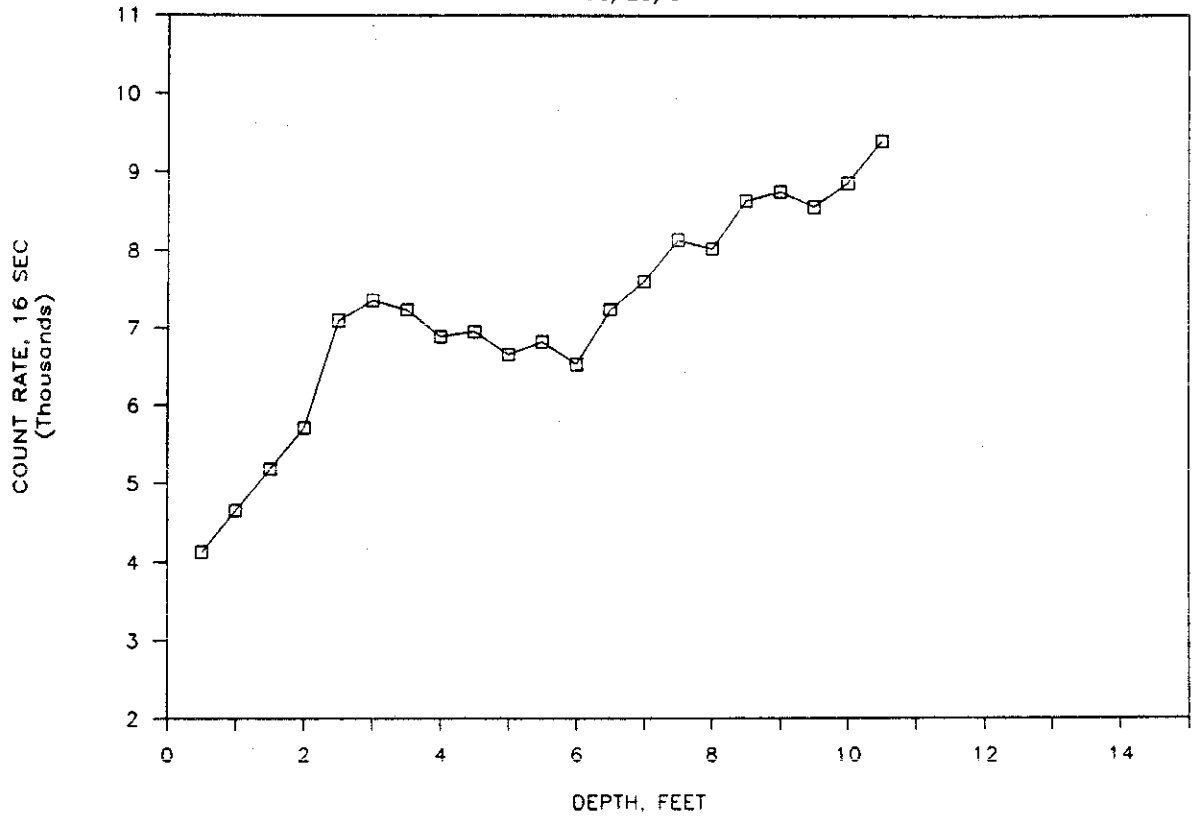

WELL W06, NEUTRON COUNT

02/09/87

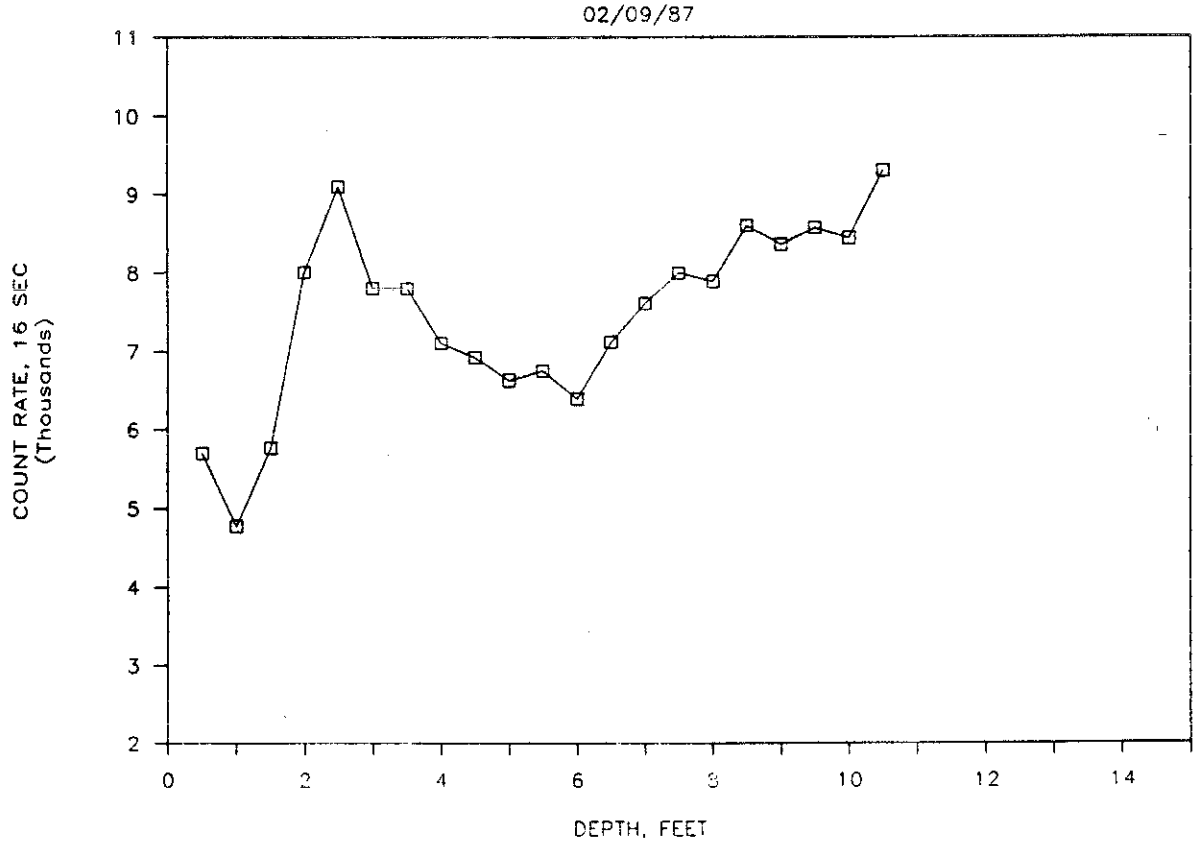

WELL W06, NEUTRON COUNT

11/06/86

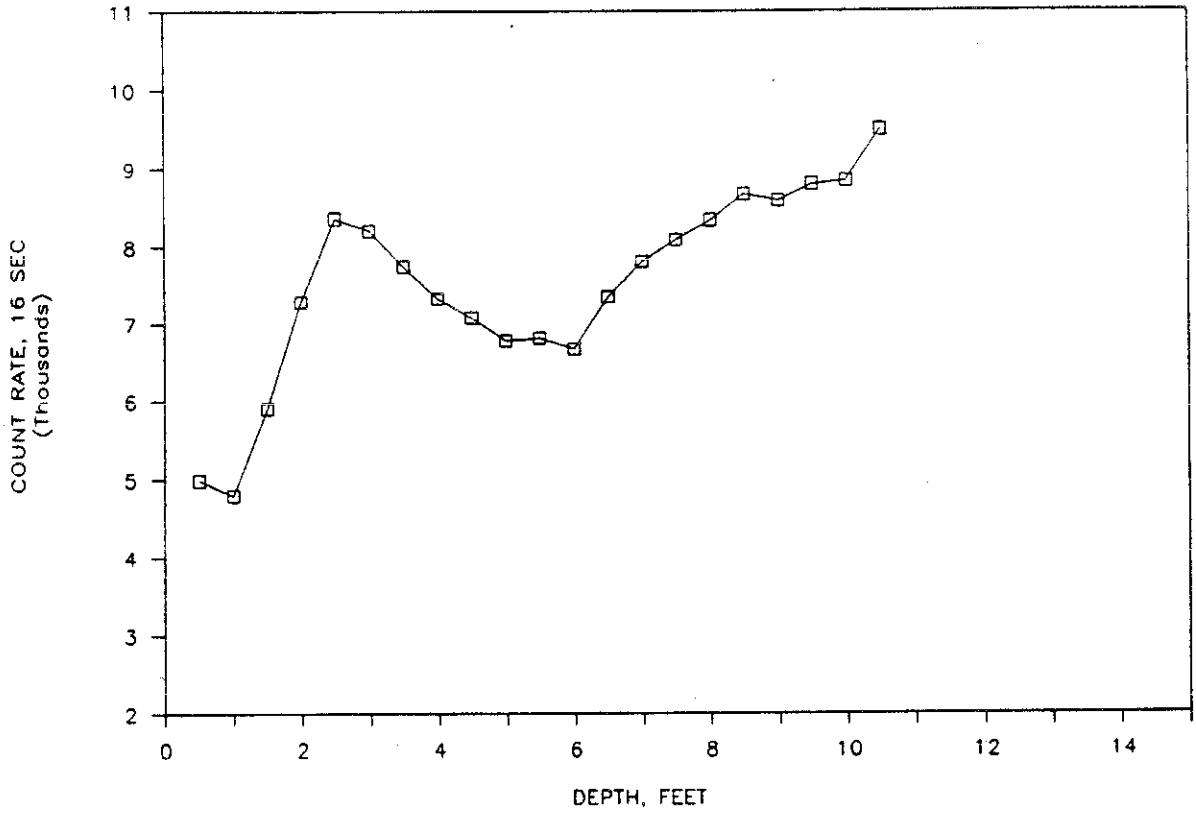

WELL W06, NEUTRON COUNT

11/10/87

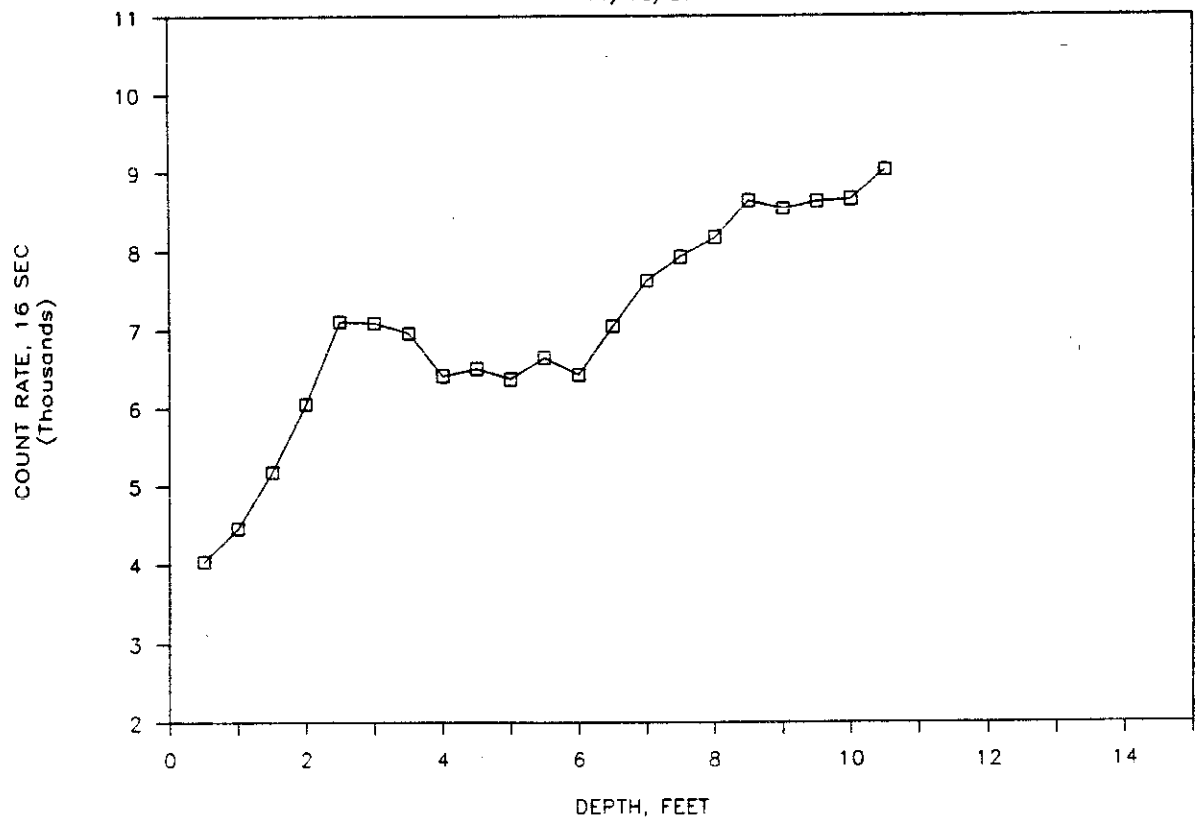

WELL W06, NEUTRON COUNT

12/03/86

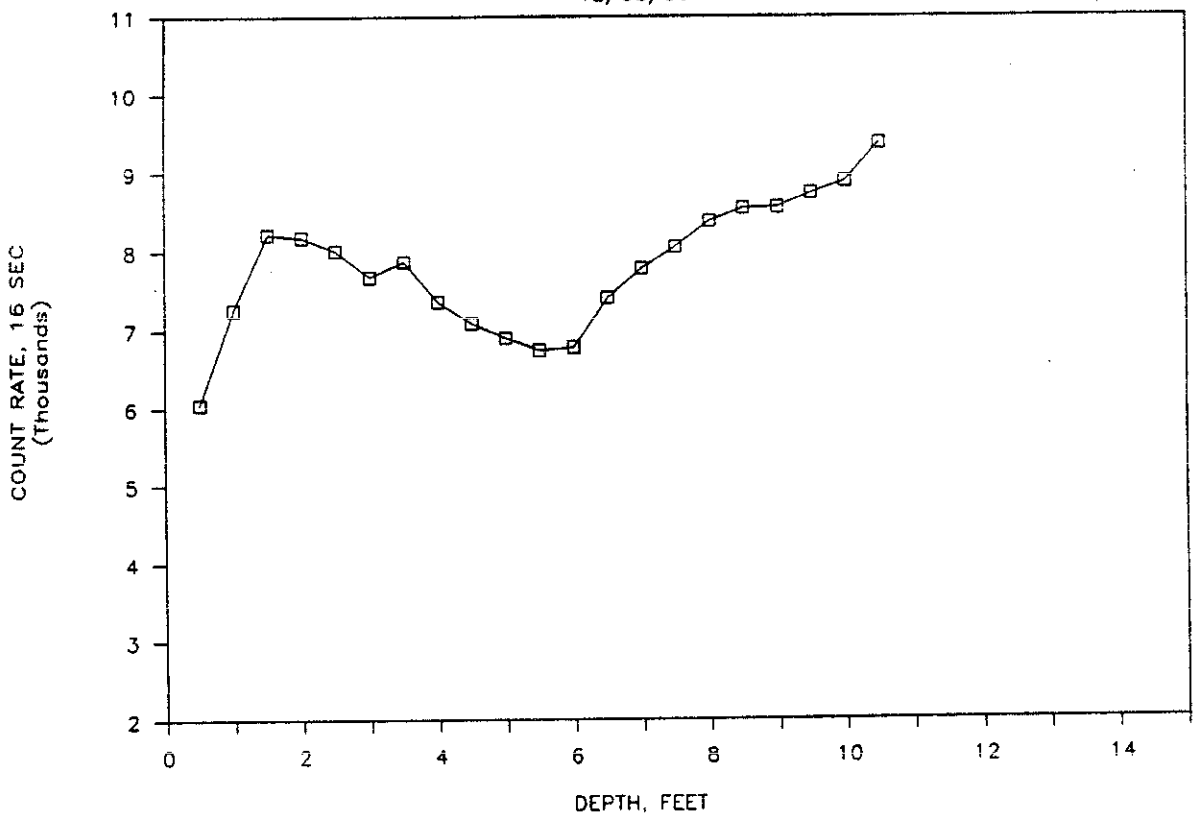

WELL W06, NEUTRON COUNT

11/86 TO 11/87

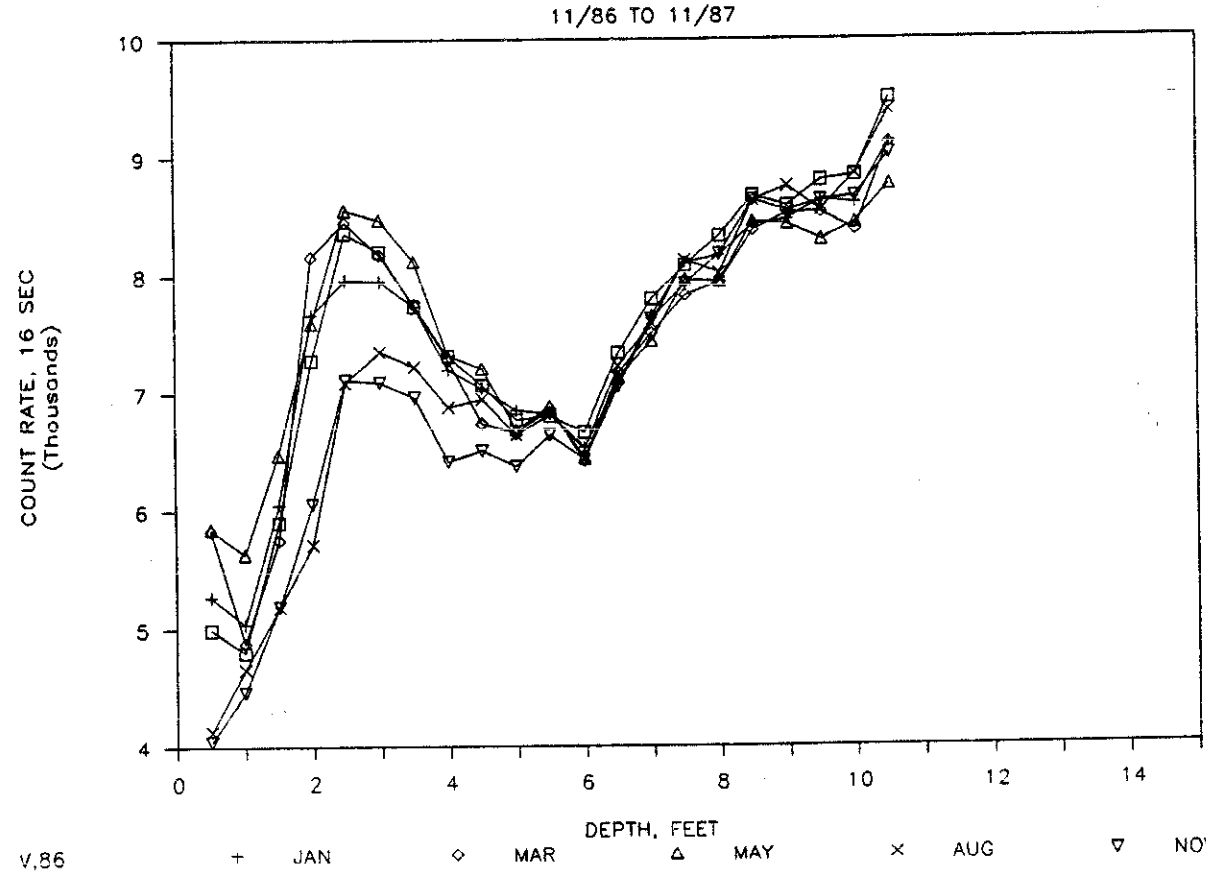

V,86 + JAN ◇ MAR △ MAY × AUG ▽ NOV,87